

A Thesis Submitted for the Degree of PhD at the University of Warwick

Permanent WRAP URL:

<http://wrap.warwick.ac.uk/79441>

Copyright and reuse:

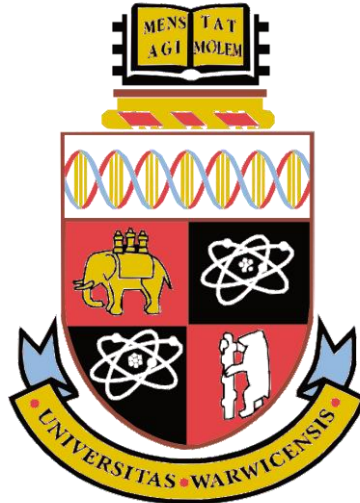
This thesis is made available online and is protected by original copyright.

Please scroll down to view the document itself.

Please refer to the repository record for this item for information to help you to cite it.

Our policy information is available from the repository home page.

For more information, please contact the WRAP Team at: wrap@warwick.ac.uk



**Characterisation of Glyoxalase 1 Mutant
Mouse and Glyoxalase 1 Copy Number
Alteration**

By

Alaa Abdulrahman M Shafie

A thesis submitted in partial fulfilment of the requirements for the
degree of

Doctor of Philosophy in Medicine

Warwick Medical School, University of Warwick

March 2016

Contents

List of Tables	7
List of Figures	9
Acknowledgement	12
Acknowledgments of specific scientific contributions	13
Declaration	14
Abstract	15
Abbreviation and Symbols	17
1.Introduction and background	23
1.1. Copy number variation	23
1.1.1. Mechanisms producing gene copy number changes	30
1.1.2. Measurement of copy number variation	32
1.1.3. Copy number variation of Glyoxalase 1	32
1.1.3.1. Mice with increased <i>Glo1</i> copy number	32
1.1.3.2. Human subjects with increased glyoxalase 1 copy number	35
1.1.4. Animal models with genetically increased Glo1	36
1.1.4.1. Transgenic mice and rats.....	36
1.1.5. Animal models with genetically-controlled decreased glyoxalase 1	38
1.1.5.1. Glyoxalase 1 deficient mice	38
1.1.5.2. Glyoxalase 1 deficient human subjects	40
1.1.5.3. Lexicon Glo1 mutant mouse	40
1.1.5.3.1. The gene trapping technique for production of a gene knockout mice	41
1.2. Embryonic stem cells	43
1.2.1. Characterization of mouse embryonic stem cells.....	43
1.2.2. Metabolic characteristics of mouse embryonic stem cells	44
1.3. Glycation.....	47
1.3.1. Physiological glycation of proteins.....	48
1.3.2. Quantitation of protein glycation, oxidation and nitration adducts.....	49
1.3.3. Dicarbonyl glycation of protein	49
1.3.4. Dicarbonyl glycation of DNA.....	51
1.4. Glyoxalase System.....	51
1.4.1. History of glyoxalase system	53
1.4.2. Glyoxalase 1.....	56
1.4.2.1. Kinetic characteristics and molecular properties	56
1.4.2.2. Genetics.....	61
1.4.2.3. Change of glyoxalase 1 expression and activity in health and disease	62

1.4.3. Glyoxalase 2.....	69
1.4.3.1. Kinetic characteristics, molecular properties, genetics and polymorphisms.....	69
1.4.4. Glyoxalases in perspective - transcriptome and proteome-wide study of expression..	72
1.4.5. Other putative glyoxalase enzymes.....	74
1.4.6. Metabolism of methylglyoxal by aldoketo reductases.....	74
1.4.7. Glyoxalase system metabolite.....	75
1.4.7.1. Methylglyoxal.....	75
1.4.7.1.1. Measurement of dicarbonyls.....	76
1.4.7.1.2. Methylglyoxal in diabetes.....	77
1.4.7.2. S-D-Lactoylglutathione.....	78
1.4.7.3. D-Lactate.....	79
1.5. Aim and objectives.....	81
1.5.1. Aim.....	81
1.5.2. Objectives.....	83
2. Materials and methods.....	86
2.1. Materials.....	86
2.1.1. Glyoxalase 1 mutant and wild type control mice.....	86
2.1.2. Human and murine cells.....	86
2.1.3. Enzymes.....	87
2.1.4. Substrates and co-factors.....	87
2.1.5. Antibodies and primers.....	88
2.1.6. Other reagents and consumables.....	89
2.1.7. Analytical kits.....	90
2.1.8. Chromatographic materials.....	91
2.1.9. Analytical standards.....	91
2.1.9.1. Calibration standards for protein damage marker analysis.....	91
2.1.9.2. Dicarbonyl calibration standards.....	91
2.1.10. Instrumentations and software.....	92
2.2. Methods.....	93
2.2.1. Animal experimentation.....	93
2.2.1.1. Tissue collection.....	96
2.2.1.2. Tissue homogenisation.....	96
2.2.2. Cell culture.....	97
2.2.2.1. Mouse embryonic stem cells.....	97
2.2.2.2. Human leukaemia 60 cells.....	98
2.2.2.3. Cell culture experimentation.....	98
2.2.2.4. Collection of cell samples.....	101

2.2.2.5. Cell viability measurement	101
2.2.3. Glyoxalase 1 copy number alteration in clinical dicarbonyl stress - end stage renal disease	101
2.2.4. Analytical Methods	102
2.2.4.1. Assay of total protein by the Bradford method	102
2.2.4.2. Activity of glyoxalase 1	103
2.2.4.3. Activity of glyoxalase 2	103
2.2.4.4. Assay of methylglyoxal reductase activity.....	104
2.2.4.5. Western Blot	104
2.2.4.6. Assay of D-lactate	105
2.2.4.7. Assay of L-lactate	106
2.2.4.8. Assay of D-glucose	107
2.2.5. LC-MS/MS methods.....	108
2.2.5.1. Protein glycation, oxidation and nitration adducts.....	108
2.2.5.2. Creatinine	116
2.2.5.3. Assay of methylglyoxal.....	118
2.2.6. Molecular biology methods	120
2.2.6.1. DNA extraction and purification.....	120
2.2.6.2. RNA extraction and purification.....	121
2.2.6.3. Reverse transcription.....	121
2.2.6.4. Mutant mice genotyping	121
2.2.6.4.1. Polymerase chain reaction	122
2.2.6.4.2. Quantitative real time PCR (qPCR).....	123
2.2.6.5. Analysis of gene mRNA expression	124
2.2.6.5.1. Gene mRNA expression analysis by SYBR green	124
2.2.6.5.2. Gene mRNA expression analysis by Taqman method.....	125
2.2.6.6. Gene copy number analysis by Taqman method	126
2.2.6.7. Microarray-based comparative genomic hybridisation.....	127
2.2.6.8. PCR–restriction fragment length polymorphism	130
2.2.7. Statistical analysis.....	131
3. Results	132
3.1. Glyoxalase 1 mutant mice.....	132
3.1.1. Genotyping.....	132
3.1.2. Glo1 activity of tissues of Glo1 (+/-) mutant mice and C57BL/6-UoW wild-type controls at 3 months of age	133
3.1.3. Glo1 activity of tissues of Glo1 (+/-) mutant mice and wild-type controls at 7 months of age.....	133
3.1.3.1. Liver.....	134

3.1.3.2. Other tissues	134
3.1.4. <i>Glo1</i> mRNA of kidney and liver of <i>Glo1</i> (+/-) mutant mice and wild-type sibling controls at 7 months of age	135
3.1.5. <i>Glo1</i> protein of liver of <i>Glo1</i> (+/-) mutant mice and wild-type sibling controls at 7 months of age	136
3.1.6. Glyoxalase 2 activity of liver of <i>Glo1</i> (+/-) mutant mice and wild-type controls at 7 months of age	137
3.1.7. Methylglyoxal and D-lactate contents of liver tissue of <i>Glo1</i> (+/-) mutant mice and wild-type controls at 7 months of age	137
3.1.8. Methylglyoxal reductase activity in liver cytosolic extract of <i>Glo1</i> (+/-) mutant mice and wild-type controls at 7 months of age	137
3.1.9. Effect of gender on glyoxalase-related variables in pooled <i>Glo1</i> (+/-) mutant mice and wild-type controls	138
3.1.10. Urinary excretion of protein glycation free adducts, oxidation free adducts and related amino acids of <i>Glo1</i> (+/-) mutant mice and wild-type sibling controls at 3 months of age	140
3.1.11. Protein glycation and oxidation adduct residue contents of cytosolic protein extracts of mouse liver of mutant <i>Glo1</i> (+/-) mice and wild-type sibling controls	141
3.1.12. <i>Glo1</i> copy number of liver, kidney, brain and pancreas in <i>Glo1</i> (+/-) mutant mice and wild-type controls at 7 months of age	144
3.1.13. Inheritance study of the <i>Glo1</i> duplication in <i>Glo1</i> (+/-) mutant mice and wild-type controls	146
3.1.13.1. Inheritance study – mouse mating and family offspring, no 1	147
3.1.13.2. Inheritance study – mouse mating and family offspring, no 2	149
3.1.13.3. Inheritance study – mouse mating and family offspring, no 3	151
3.1.14. Evaluation of Taqman copy number assay for <i>Glo1</i> gene	154
3.1.15. Characterization of <i>Glo1</i> mutation in <i>Glo1</i> mutant mice	155
3.1.15.1. Comparative genomic hybridisation microarray of <i>Glo1</i> mutant mice and sibling wild-type controls	156
3.1.15.2. Expression of duplicated genes in <i>Glo1</i> mutant mice	158
3.2. Mouse embryonic stem cells (ESCs)	161
3.2.1. Characterisation of the glyoxalase system in ESCs under normal and low oxygen conditions	161
3.2.1.1. Growth and viability of mouse ESCs <i>in vitro</i>	162
3.2.1.2. Activity and expression of glyoxalase 1 in murine ESCs <i>in vitro</i>	162
3.2.1.3. Flux of formation of D-lactate in ESC cultures under 20% oxygen and 3% oxygen atmosphere <i>in vitro</i>	164
3.2.1.4. Net flux of formation of L-Lactate by murine ESCs cultured under 20% oxygen and 3% oxygen atmosphere <i>in vitro</i>	164
3.2.1.5. Consumption of D-glucose by murine ESCs cultured under 20% oxygen and 3% oxygen atmosphere <i>in vitro</i>	165
3.2.2. Effect of cell permeable <i>Glo1</i> inhibitor on cell growth and <i>Glo1</i> copy number of ESCs <i>in vitro</i>	167

3.2.2.1. Effect of cell permeable Glo1 inhibitor on ESCs growth <i>in vitro</i>	167
3.2.2.2. Effect of cell permeable Glo1 inhibitor on <i>Glo1</i> copy number of ESCs <i>in vitro</i>	169
3.2.3. Effect of MG on growth and <i>Glo1</i> copy number of ESCs <i>in vitro</i>	170
3.2.3.1. Effect of MG on growth of ESCs <i>in vitro</i>	170
3.2.3.2. Effect of MG on <i>Glo1</i> copy number of murine ESCs <i>in vitro</i>	171
3.2.3.3. Effect of treatment of murine ESCs with 200 μ M MG for 3, 6 and 12 days <i>in vitro</i> on <i>Glo1</i> mRNA	176
3.2.3.4. Effect of treatment of murine ESCs with 200 μ M MG for 3, 6 and 12 days <i>in vitro</i> on <i>Glo1</i> protein	176
3.2.3.5. Effect of treatment of murine ESCs with 200 μ M MG for 3, 6 and 12 days <i>in vitro</i> on <i>Glo1</i> activity.....	177
3.2.3.6. Effect of treatment of ESCs <i>in vitro</i> with 200 μ M MG every 6 h for 24 h on cell viability and <i>Glo1</i> copy number.....	179
3.2.3.7. Effect of treatment of ESCs <i>in vitro</i> with 200 μ M MG for 3 and 12 days on <i>Glo1</i> copy number under 3% oxygen atmosphere	180
3.2.4. Effect of silencing of <i>Glo1</i> on the cell growth and <i>Glo1</i> expression and activity of ESCs <i>in vitro</i>	181
3.2.4.1. Effect of silencing of <i>Glo1</i> on the cell growth of ESCs <i>in vitro</i>	181
3.2.4.2. Effect of silencing of <i>Glo1</i> on <i>Glo1</i> protein of ESCs <i>in vitro</i>	183
3.2.4.3. Effect of MG and silencing of <i>Glo1</i> on the growth of ESCs <i>in vitro</i>	185
3.3. Effect of MG on the growth and <i>GLO1</i> copy number of human leukaemia cells <i>in vitro</i>	186
3.4. <i>GLO1</i> copy number in clinical end stage renal disease	188
4. Discussion.....	190
4.1. Importance of advancing understanding of the glyoxalase system in biomedical research	190
4.2. Lexicon Glyoxalase 1 mutant mouse	193
4.2.1. Genotyping and evidence for <i>Glo1</i> copy number alteration induced by gene Gene trapping	193
4.2.2. Glyoxalase pathway metabolism - evidence for normal homeostasis.....	198
4.2.3. <i>Glo1</i> activity – effect of ageing.....	199
4.3. Glyoxalase 1 copy number alteration in mouse embryonic stem cells	200
4.4. Other studies of glyoxalase 1 copy number alteration	203
5. Conclusion and Further work.....	205
5.1. Conclusion	205
5.2. Further work.....	206
6. Bibliography	207
Appendix.....	236
List of presentations and publications derived from this project.....	237

List of Tables

Table 1.1: Examples of CNVs and genomic disorders.	29
Table 1.2: Copy number variation of human and mouse glyoxalase 1.	36
Table 1.3: Studies with mice and rats overexpressing glyoxalase 1.	38
Table 1.4: Studies with glyoxalase 1 deficient mice.	39
Table 1.5: Advantages and disadvantages of gene trapping methods to produce knockout mice.	42
Table 1.6: Characteristics of human glyoxalase 1.	59
Table 1.7: Effect of ageing on glyoxalase 1 expression and activity.	63
Table 1.8: Concentration of methylglyoxal-derived hydroimidazolone in mammalian tissue and extracellular proteins.	76
Table 1.9: Concentration of methylglyoxal in tissues from human, laboratory animal and plant origin and cultured mammalian cells.	78
Table 2.1: Characteristics of end stage renal failure patients and healthy controls.	102
Table 2.2: Protocol for enzymatic hydrolysis using CTC-PAL automated sample processor.	110
Table 2.3: Protocol for preparation of calibration standard solutions from cocktails of normal and stable isotopic standards for assay of protein glycation, oxidation and nitration adduct residues of liver protein extracts.	110
Table 2.4: Analyte content of calibration standard solutions for assay of protein glycation, oxidation and nitration adduct residues of liver protein extracts.	111
Table 2.5: Protocol for preparation of calibration standard solutions from cocktails of normal and stable isotopic standards for assay of protein glycation, oxidation and nitration free adducts of urine.	112
Table 2.6: Analyte content of calibration standard solutions for assay of protein glycation, oxidation and nitration free adducts of urine.	113
Table 2.7: Elution profile for LC-MS/MS analysis of protein glycation, oxidation and nitration adducts (Acquity-Xevo-TQS™ system).	114
Table 2.8: Chromatographic retention times and MRM detection conditions for detection of glycation, oxidation and nitration adducts by stable isotopic dilution analysis tandem mass spectrometry (Acquity-Xevo-TQS™ system).	115
Table 2.9: Elution profile for creatinine assay.	116
Table 2.10: Detection of creatinine by positive ion multiple reaction monitoring.	117
Table 2.11: Preparation of calibration standards for creatinine assay.	117
Table 2.12: Calibration standards for dicarbonyl assay.	119
Table 2.13: Preparation of calibration standards from stock solutions.	119

Table 2.14: Chromatographic elution profile in the MG assay.....	119
Table 2.15: Mass-spectrometric multiple reaction monitoring detection of dicarbonyls. ...	120
Table 2.16: PCR programme used for genotyping.....	122
Table 2.17: qPCR protocol.	123
Table 2.18: Taqman PCR reaction mix component.	125
Table 2.19: PCR protocol of Taqman gene expression assay.....	126
Table 2.20: Component of Taqman copy number assay PCR reaction mix.	127
Table 2.21: PCR protocol of Taqman copy number assay.....	127
Table 2.22: Components of the digestion master mix.....	128
Table 2.23: Components of the labelling master mix.	128
Table 2.24: Expected yield and specific activity after labelling and purification with the SureTag complete DNA labelling kit.	129
Table 2.25: Hybridization master mix for microarray.	129
Table 2.26: PCR protocol for A111E genotyping.....	131
Table 3.1: Glo1 activity in brain, heart, kidney, pancreas, skeletal muscle, spleen and liver tissue of C57BL/6-UoW and Glo1 (+/-) and mice.	133
Table 3.2: Glo1 activity in liver, brain, skeletal muscle, heart, kidney, pancreas and spleen of Glo1 (+/-) mutant mice and wild-type siblings at 7 months of age.	135
Table 3.3: Relative mRNA content of <i>Glo1</i> in liver and kidney tissue of Glo1(+/-) mutant mice and wild-type sibling controls at 7 months of age.	136
Table 3.4: Glyoxalase 2 activity, D-lactate and MG content and methylglyoxal reductase activity in liver of Glo1 (+/-) mice and wild-type sibling control mice at 7 months of age.	137
Table 3.5: Summary of comparison between male and female mice for glyoxalase-related variables.....	139
Table 3.6: Urinary excretion of protein glycation and oxidation free adducts of Glo1(+/-) mutant mice and wild-type sibling controls at 3 months of age.....	140
Table 3.7: Protein glycation and oxidation adduct residue contents of liver protein of mutant Glo1(+/-) mice and wild-type sibling controls.	142
Table 3.8: Protein glycation and oxidation adduct residue contents of liver protein of male and female mice.....	143
Table 3.9: Summary of the qPCR genotyping and Taqman copy number assays for mouse breeding pair 1.....	148
Table 3.10: Summary of the qPCR genotyping results and Taqman copy number assay for the second family.....	149
Table 3.11: Summary of the qPCR genotyping results and Taqman copy number assay for the third family.	152

Table 3.12: Characterization of ESCs under under 20% oxygen and 3% oxygen atmosphere <i>in vitro</i>	166
Table 3.13: Effect of treatment of murine ESCs with 200 μ M MG for 3, 6 and 12 days <i>in vitro</i> on copy number of <i>Glo1</i> and surrounding genes.	172
Table 3.14: Effect of treatment of ESCs <i>in vitro</i> with 200 μ M MG for 3, 6 and 12 days on <i>Glo1</i> mRNA content.....	176
Table 3.15: Effect of treatment of 200 μ M MG for 1 day with dose every 6 hours on ESCs <i>in vitro</i>	179
Appendix A: Primers sequences	236
Appendix B: Taqman gene expression assay.....	236
Appendix C: TaqMan copy number assay.....	236

List of Figures

Figure 1.1: Lexicon qPCR analysis of the absent transcript in the (<i>Glo1</i> ^{-/-}) mouse	41
Figure 1.2: Mechanisms of formation of early glycation adducts and advanced glycation endproducts from glucose, glycolytic intermediates and lipid peroxidation.....	47
Figure 1.3: Molecular structure of the physiologically reactive glycating dicarbonyls 3-DG, glyoxal and methylglyoxal.....	50
Figure 1.4: The Glyoxalase system.....	51
Figure 1.5: Structure and catalytic mechanism of glyoxalase 1.....	60
Figure 1.6: Human <i>GLO1</i> gene.....	61
Figure 1.7: S-p-bromobenzylglutathione cyclopentyl diester structure	68
Figure 1.8: An example of how activation of the NF- κ B system via RAGE may conflict with the Nrf2 system to down regulate GLO1 expression.	69
Figure 1.9: Structure and catalytic mechanism of glyoxalase 2.....	71
Figure 1.10: Reaction of methylglyoxal with arginine residues to form hydroimidazolone MG-H1.	75
Figure 2.1: Insertion cassette in mouse <i>Glo1</i> gene.	93
Figure 2.2: Study1. Summary of mice and tissues analysed.....	94
Figure 2.3: Study 2. Summary of mice and tissues analysed.....	95
Figure 2.4: Study 3. Summary of mice and analysis performed.	95
Figure 2.5: Study 4. Summary of mice inheritance study outcome and analysis performed.	96
Figure 2.6: Summary of <i>in vitro</i> experiments of <i>Glo1</i> CNV induction.	99
Figure 2.7: Summary of <i>in vitro</i> experiments of ESCs transfection with <i>Glo1</i> siRNA.....	99
Figure 2.8: Summary of <i>in vitro</i> experiments of embryonic stem cells grown under a 3% oxygen environment.....	100
Figure 2.9: Typical calibration curve for assay of D-lactate.....	106
Figure 2.10: Typical calibration curve for assay of L-lactate.	107

Figure 2.11: The coupled enzyme reactions of the glucose assay.	107
Figure 2.12: Typical calibration curve for assay of D-glucose.	108
Figure 2.13: Typical calibration curves for arginine and MG-H1 in stable isotopic dilution analysis LC-MS/MS.	111
Figure 2.14: Calibration curve of creatinine.	118
Figure 2.15: Derivatization used in the dicarbonyl assay.	118
Figure 2.16: Genotyping of wild-type and knockout gene.	122
Figure 2.17: Typical calibration curve for qPCR.	124
Figure 2.18: Dissociation curve of <i>Glo1</i> primers.	125
Figure 2.19: Determination of the digested DNA size in 0.8% agarose gel.	128
Figure 3.1: Electrophoresis results for PCR analysis of <i>Glo1</i> mutant and wild-type control mice.	132
Figure 3.2: <i>Glo1</i> activity of liver of <i>Glo1</i> (+/-) mutant mice, wild-type sibling mice (WT) and wild-type “C57BL/6-UoW” mice.	134
Figure 3.3: <i>Glo1</i> protein in liver tissue of <i>Glo1</i> (+/-) mutant mice and wild-type controls at 7 months of age.	136
Figure 3.4: Assay of <i>Glo1</i> copy number by the Taqman method in liver tissue of <i>Glo1</i> (+/-) mutant and sibling wild-type control mice at 7 months of age.	144
Figure 3.5: Assay of <i>Glo1</i> copy number by the Taqman method in kidney tissue of <i>Glo1</i> (+/-) mutant and sibling wild-type control mice at 7 months of age.	145
Figure 3.6: Assay of <i>Glo1</i> copy number by the Taqman method in brain tissue of <i>Glo1</i> (+/-) mutant and sibling wild-type control mice at 7 months of age.	145
Figure 3.7: Assay of <i>Glo1</i> copy number by the Taqman method in pancreas tissue of <i>Glo1</i> (+/-) mutant and sibling wild-type control mice at 7 months of age.	145
Figure 3.8: qPCR and Taqman copy number assay for inheritance studies.	147
Figure 3.9: Pedigree of inheritance study - mouse mating and family offspring, no 1.	148
Figure 3.10: Taqman copy number assay for <i>Glo1</i> gene in wild-type, <i>Glo1</i> (+/+) ^{<i>Gt(·)1Lex</i>} and <i>Glo1</i> (+/+) ^{<i>Gt(·)2Lex</i>} mutant mice.	150
Figure 3.11: Pedigree of inheritance study - mouse mating and family offspring, no 2.	150
Figure 3.12: Taqman copy number assay for <i>Glo1</i> mutant allele in offspring of breeding of <i>Glo1</i> (+/+) ^{<i>Gt(·)1Lex</i>} mutant mice.	151
Figure 3.13: Pedigree of inheritance study - mouse mating and family offspring, no 3.	153
Figure 3.14: Evaluation of Taqman copy number assay for <i>Glo1</i> gene.	155
Figure 3.15: SurePrint G3 aCGH results of one mouse of each genotype.	158
Figure 3.16: Relative mRNA level of genes duplicated in liver tissue of wild-type mice and <i>Glo1</i> ^{<i>Gt(·)1Lex</i>} and <i>Glo1</i> ^{<i>Gt(·)2Lex</i>} genotypes.	160
Figure 3.17: Growth of murine ESCs under 20% oxygen and 3% oxygen atmosphere <i>in vitro</i>	162
Figure 3.18: Activity of glyoxalase 1 of ESCs cultured under 20% oxygen and 3% oxygen atmosphere <i>in vitro</i>	163
Figure 3.19: <i>Glo1</i> protein content of ESCs cultured under 20% oxygen and 3% oxygen atmosphere <i>in vitro</i>	163

Figure 3.20: Flux of D-lactate formation by ESCs cultured under 20% oxygen and 3% oxygen atmosphere <i>in vitro</i>	164
Figure 3.21: Net formation of L-lactate by ESCs cultured under 20% oxygen and 3% oxygen atmosphere <i>in vitro</i>	165
Figure 3.22: Glucose consumption of ESCs cultured under 20% oxygen and 3% oxygen atmosphere <i>in vitro</i>	166
Figure 3.23: Effect of BrBzGSHCP ₂ on ESCs growth and viability <i>in vitro</i>	168
Figure 3.24: Effect of BrBzGSHCP ₂ on murine ESCs growth and <i>Glo1</i> copy number <i>in vitro</i>	169
Figure 3.25: Effect of MG on ESCs growth and viability <i>in vitro</i> cultured under 20% oxygen atmosphere.....	171
Figure 3.26: Effect of MG on ESCs growth and viability <i>in vitro</i> cultured under 3% oxygen atmosphere.....	171
Figure 3.27: Effect of treatment of 200 µM MG for 3 days on copy number of <i>Glo1</i> and the surrounding genes in ESCs <i>in vitro</i>	173
Figure 3.28: Effect of treatment of 200 µM MG for 6 days on copy number of <i>Glo1</i> and the surrounding genes in ESCs <i>in vitro</i>	174
Figure 3.29: Effect of treatment of 200 µM MG for 12 days on copy number of <i>Glo1</i> and the surrounding genes in ESCs <i>in vitro</i>	175
Figure 3.30: Effect of treatment of 200 µM MG for 3, 6 and 12 days on Glo1 protein content in ESCs <i>in vitro</i>	177
Figure 3.31: Effect of treatment of 200 µM MG for 3, 6 and 12 days on Glo1 activity in ESCs <i>in vitro</i>	178
Figure 3.32: Effect of treatment of 200 µM MG for 3 days on <i>Glo1</i> copy number of ESCs <i>in vitro</i> under 3% oxygen atmosphere.....	180
Figure 3.33: Effect of treatment of 200 µM MG for 12 days on <i>Glo1</i> copy number of ESCs <i>in vitro</i> under 3% oxygen atmosphere.....	180
Figure 3.34: Effect of silencing of <i>Glo1</i> on the growth of ESCs <i>in vitro</i>	182
Figure 3.35: Effect of silencing of <i>Glo1</i> on <i>Glo1</i> mRNA of ESCs <i>in vitro</i>	183
Figure 3.36: Effect of silencing of <i>Glo1</i> on Glo1 protein of ESCs <i>in vitro</i>	184
Figure 3.37: Effect of silencing of <i>Glo1</i> on Glo1 activity of ESCs <i>in vitro</i>	185
Figure 3.38: Effect of MG with on the growth ESCs <i>in vitro</i> with prior silencing of <i>Glo1</i>	186
Figure 3.39: Effect of MG on the growth of HL60 cells <i>in vitro</i>	187
Figure 3.40: Effect of MG on the <i>GLO1</i> copy number of HL60 cells <i>in vitro</i>	187
Figure 3.41: Taqman copy number assay for <i>GLO1</i> gene in the DNA of end stage renal failure patients, controls and NCL-H522 cell line.....	188
Figure 3.42: Specimen genotyping results for C419A SNP in <i>GLO1</i> gene.....	189



Acknowledgement

First and foremost all praise is due to almighty Allah; the most beneficial and the most merciful, for endowing me with health, patience, strength and knowledge to complete this project.

I thank Taif University, Kingdom of Saudi Arabia for the financial support and my PhD scholarship. Also, I thank the Saudi Arabian Cultural Bureau in London for their supervision through my academic studies in UK.

I would like to express my special appreciation and thanks to my supervisor Dr Naila Rabbani, who has been a tremendous mentor for me. I appreciate her training, efforts and encouragement to help me shaping my research skills. I thank Dr Rabbani for always being there for any of my questions and for the motivation to help me work independently. This thesis would not have been possible without her supervision. I would also like to express my deepest thanks and appreciation to Professor Paul Thornalley for his contribution of time, guidance, enthusiasm, inspiration and immense knowledge in research that kept me motivated. His insights, suggestions and valuable feedback contributed greatly to this thesis. I would also like to thank all the past and present members of the Protein Damage and Systems Biology Research Group for their support and friendship during my PhD. It has been a great pleasure to work with such friendly and inspiring colleagues. Thank you everyone for brightening up the long research hours. The University of Warwick has been an excellent place to learn and develop my research capabilities.

A special thanks to my family. Words cannot express how grateful I am to my mother, father, mother-in law, father-in-law for all of the sacrifices that they have made on my behalf. Their prayer for me was what sustained me thus far. I would also like to thank all of my sisters, brothers and friends who supported me in writing and incited me to strive towards my goal.

At the end I would like express appreciation to my beloved wife and colleague Dr Amal Ashour who spent sleepless nights with me and was always my support in the moments when there was no one to answer my queries. This PhD

would not have been possible without her moral and emotional support. Also, warmest thanks to my lovely daughters Maria and Reema who sacrificed a lot of time to give me chance to reach my goal.

Acknowledgments of specific scientific contributions

I acknowledge and thank the following people for assistance with my PhD research:

- Dr Naila Rabbani for primary supervision, advice and guidance on the development of the project and related hypotheses, design of experimental plan, analysis and the interpretation of results, and discussion.
- Professor Paul J Thornalley for supplementary supervisory support and performing tissue measurements of methylglyoxal.
- Dr Daniel Zehnder for gaining ethical approval, recruiting patients with renal failure and healthy controls and collecting peripheral venous blood samples with consent for the study.
- Dr Guy Barker for advice on the selection of DNA microarray, sample processing, data extraction, evaluation and interpretation.
- Dr Mingzhan Xue for technical advice and optimised protocols for measurement of *Glo1* mRNA and protein.
- Dr Attia Anwar for technical assistance in LC-MS/MS instrument setup and operation for running samples in the analysis of methylglyoxal, protein glycation and oxidation adducts and urinary creatinine.
- Dr Cindy Shirley, the IMKC project leader at Lexicon Pharmaceuticals, for providing genotyping primer sequence and in-house pilot data.
- Samantha Dixon, the manager of the Biological Services Unit (University of Warwick) and her team of technicians for assistance with breeding and maintenance of *Glo1* mutant and wild-type mice and collection of tissues, blood and urine therefrom.

All other project work was performed by myself, specifically, development of the study hypothesis, design of the experimental programme, performing the experiments, data collection and interpretation of the results, discussion and conclusions arising from the experimental outcomes and writing up this thesis.

Declaration

I am aware of the University regulations governing plagiarism and I declare that all the work presented in this thesis, unless otherwise specifically stated, was original research performed by myself under the supervision of Dr Naila Rabbani. None of this work has been previously submitted to any other degree. All sources of information have been acknowledged by means of reference.

Alaa Abdulrahman M Shafie

Abstract

Glyoxalase 1 (Glo1) of the glyoxalase system catalyses the metabolism of the reactive dicarbonyl metabolite, methylglyoxal, and thereby prevents potentially damaging glycation of protein and DNA. Glo1 is hypothesised to be a potential factor in the development of vascular complication of diabetes, such as diabetic nephropathy. The induction of diabetes in mice deficient in Glo1 provides a pre-clinical *in vivo* model to test this hypothesis. Glo1 mutant mice with putative Glo1 deficiency produced by the International Mouse Knockout Consortium (IMKC) were acquired from the European Mutant Mouse Archive. The initial aim of this study was to study the exacerbation of diabetic nephropathy by Glo1 deficiency in streptozotocin-induced diabetic mice, with an initial objective to confirm Glo1 deficiency in the IMKC Glo1 mutant mouse and subsequent objectives contingent on this. The preliminary studies were unable to confirm Glo1 deficiency in this mouse model and so a revised aim was to characterise the mechanism of compensatory Glo1 expression in the mutant mouse and explore similar occurrence in similar precursor mouse embryonic stem cells (ESCs) and related clinical application.

Genotyping of Glo1 mutant mouse offspring by PCR revealed only heterozygotes and wild-type (WT) littermates, and no homozygotes without *Glo1* wild-type alleles. Studies of the Glo1 mutant mouse revealed levels of Glo1 activity, protein and mRNA identical to those of wild-type control siblings. Other components of the glyoxalase system were also analysed – activity of glyoxalase 2, concentrations of methylglyoxal (MG) and D-lactate, and tissue protein content and urinary excretion of MG-derived glycation adduct MG-H1 and found no significant change in Glo1 mutant mice, with respect to WT controls. This suggested a functionally normal Glo1 and glyoxalase system in Glo1 mutant mice. Therefore, Glo1 mutant mice have a mutated *Glo1* gene but with compensatory Glo1 expression identical to that of WT control. This provided a possible explanation for the unexpected normal phenotype of Glo1 mutant mice reported in the IMKC project.

To explore the mechanism of compensatory Glo1 expression, *Glo1* copy number was quantified by Taqman® method, normalizing response to transferrin receptor protein-1 (*Tfrc*). Glo1 mutant mice had 3 copies of *Glo1* in all tissues analysed with amplification extending from 3'-end of exon 1 to the 5'-end of exon 6. Taqman copy number assay was established to detect and quantify mutant

Glo1^{Gt(·)Lex} and WT alleles. Most mutant mice contained two copies of *Glo1* and one mutant copy of *Glo1*^{Gt(·)Lex} – *Glo1*(+/+)Gt(·)1Lex. In some cases, however, 2 copies of both *Glo1* and mutated *Glo1*^{Gt(·)Lex} – *Glo1*(+/+)Gt(·)2Lex were found. Inheritance studies suggested a simple Mendelian inheritance with a WT allele accompanying the *Glo1*^{Gt(·)Lex} mutant allele on arms of chromosome 17 such that *Glo1* deficiency was prevented. This was indeed observed throughout the all breeding of the *Glo1* mutant mice.

I hypothesised that *Glo1* copy number increase may have arisen in the mutant mice during gene trapping by copy number alteration (CNA) induced by increased methylglyoxal concentration, or dicarbonyl stress, in mouse ESCs. To explore and model this, mouse ESCs were cultured with exogenous 200 µM MG under atmospheres containing 20% oxygen - typical of most cell culture conditions, and 3% oxygen - typical of ESCs oxygen exposure *in vivo*. Incubation of ESCs for 12 days with MG induced CNV increase of *Glo1* by up to 16% in both 20% and 3% oxygen atmospheres. Increase in *Glo1* CNV at day 12 with MG treatment was associated with an increase in *Glo1* protein. Therefore, functional low level CNA of *Glo1* was induced by exposure to high levels of exogenous MG. No evidence was found for *Glo1* CNA with dicarbonyl stress induced by *Glo1* silencing or cell permeable *Glo1* inhibitor.

Finally, I hypothesised that *GLO1* CNA may occur in clinical dicarbonyl stress, a severe example of which is patients with renal failure receiving haemodialysis - associated with *ca.* 5-fold increase in plasma MG concentration. DNA of peripheral mononuclear cells from healthy subjects and patients with renal failure receiving hemodialysis renal replacement therapy were examined. Human *GLO1* copy number was not significantly different between the patients and the control subjects. This requires further investigation in this case and other examples of clinical dicarbonyl stress.

From these studies I conclude that the IMKC *Glo1* mutant mouse does not exhibit the *Glo1* deficiency; rather, it maintains wild-type levels of *Glo1* expression through *Glo1* copy increase likely induced during gene trapping. Dicarbonyl stress in mouse ESCs *in vitro* induced low level *Glo1* copy number increase – a model of *Glo1* CNA in putative gene trapping associated dicarbonyl stress. It is unclear if *GLO1* CNA occurs clinically. These findings reveal that focussed copy number

alternation of *GLO1* may provide a protective response to dicarbonyl stress in some circumstances.

Abbreviation and Symbols

µg	microgram
µl	microlitre
µM	micromolar
17-AAG	17-allylamino-17-demethoxy-geldanamycin
3-DG	3-deoxyglucosone
3DG-H	<i>N</i> _δ -[5-hydro-5-(2,3,4-trihydroxybutyl)-4-imidazolone-2-yl]ornithine
3-NT	3-nitrotyrosine
AASA	α-aminoadipic acid semialdehyde
aCGH	array comparative genomic hybridization
ACTB	β-Actin
AD	alzheimer's disease
AF	attachment factor
AGEs	advanced glycation endproducts
AICAR	5-aminoimidazole-4-carboxamide ribonucleotide
AKRs	aldoketo reductases
Akt	serine/threonine-specific protein kinase (also known as protein kinase B)
AMDCC	animal models of diabetic complications consortium
AMP	5'-adenosine monophosphate
AMY1	salivary amylase gene
ANOVA	analysis of variance
AP-2α	activating enhancer binding protein 2 alpha
ApoB	apolipoprotein B
ApoE	apolipoprotein E
APP	amyloid precursor protein
AR	aldose reductase
ARE	antioxidant response element
ARI	aldose reductase inhibitor
ATP	adenosine triphosphate
BAC	bacterial artificial chromosome
Bar	bialaphos resistance gene
bp	base pair
BrBzGSHCp ₂	bromobenzylglutathione cyclopentyl diester
BSA	bovine serum albumin
BTBD9	bric-a-brac (BTB) domain containing 9
<i>C. elegans</i>	<i>Caenorhabditis elegans</i>
C4	complement component 4A
C57BL/6	C57BL/6 strain of laboratory mice

C57BL/6J	C57BL/6 strain of laboratory mice genetically homogenous with the C57BL/6 strain stock of Jackson Laboratories (Mainem USA)
C57BL/6-UoW	C57BL/6 control strain colony maintained at University of Warwick
C6ORF102	chromosome 6 open reading frame 102
C6ORF64	chromosome 6 open reading frame 64
CALBINDIN-D9K	vitamin-D-dependent, calcium-binding protein
CCL3L1	chemokine (C-C motif) ligand 3-like 1
cDNA	complementary deoxyribonucleic acid
CEL	N_{ϵ} -(1-carboxyethyl)lysine
CGH	comparative genomic hybridization
CKD	chronic kidney disease
CMA	N_{ω} -carboxymethyl-arginine
CMC	S -carboxymethylcysteine
CMdG	N_2 -carboxymethyl-deoxyguanosine
CML	N_{ϵ} -carboxymethyl-lysine
CMT1A	charcot marie tooth disease type 1A
CNA	copy number alteration
CNC	copy number change
CNV	copy number variation
CREB	cAMP response element-binding protein
Ct	cycle threshold
CVD	cardiovascular disease
CYP2D6	cytochrome P450, 2D6 isoform
DB	1,2-diaminobenzene
DCP	dicarbonyl proteome
del	deletion
DETAPAC	diethylenetriaminepenta-acetic acid
dG	deoxyguanosine
DGV	database of genomic variants
DHAP	dihydroxyacetone phosphate
DM	diabetes mellitus
D-MEM	dulbecco's modified eagle medium
DN	diabetic nephropathy
DNA	deoxyribonucleic acid
DNAHC8	dynein, axonemal, heavy chain 8
dRFU/dT	the derivative of relative fluorescence divided by the derivative of temperature
dsDNA	double-stranded DNA
DT	dityrosine
dup	duplication
E2F	E2 transcription factor
E2F4	E2 transcription factor 4
EC ₅₀	median effective concentration

ECL	enhanced chemiluminescence
EDTA	ethylenediaminetetra -acetic acid
ESCs	embryonic stem cells
ESRD	end stage renal disease
F3K	fructosamine-3-kinase
FA	formic acid
FBS	fetal bovine serum
FGF	fibroblast growth factor-4
FISH	fluorescence <i>in situ</i> hybridisation
Fkbp5	FK506-binding protein 5
FL	N _ε -fructosyl-lysine
G6P	glucose-6-phosphate
GA3P	glyceraldehyde-3-phosphate
GABA _A	gamma-aminobutyric acid A
GC ₅₀	median growth inhibitory concentration
GFAT	glutamine fructose-6-phosphate amidotransferase
GFOGER	glycine-phenylalanine-hydroxyproline-glycine-glutamine-arginine peptide
GFP	glomerular filtration rate
G-H1	glyoxal-derived hydroimidazolone, N _δ -(5-hydro-4-imidazolone-2-yl)ornithine
Glo1	glyoxalase 1
Glo2	glyoxalase 2
GLP1R	glucagon-like peptide 1 receptor
GLUT-1	glucose transporter -1
GOLD	glyoxal-derived lysine dimer 1,3-di(N _ε -lysino) imidazolium
GRE	glucocorticoid responsive element
GSA	glutamic semialdehyde
GSH	glutathione, reduced form
GSK3b	glycogen synthase kinase 3-beta
GSSG	glutathione, oxidised form
H-2	histocompatibility 2
HAEC	human aortal endothelial cell
HAGH	hydroxyacylglutathione hydrolase
Hb _{A1C}	glycated haemoglobin
HBPC-GSH	S-(N-hydroxy-N-bromophenylcarbamoyl)glutathione
HD	haemodialysis
HEPES	4-(2-hydroxyethyl) piperazine-1-ethanesulfonic acid
HER2	human epidermal growth factor receptor
HIF1 α	hypoxia-inducible factor 1 α
HIV/AIDS	human immunodeficiency virus/acquired immunodeficiency syndrome
HL60	human leukaemia 60
HMEC-1	human dermal microvascular endothelial cell line
HMM	hidden markov model
HPLC	high performance liquid chromatography

HRE	hypoxia response element
HSP90	heat shock protein 90
IMKC	international mouse knockout consortium
inv	inversion
IRE	insulin response element
iRNA	interfering ribonucleic acid
kb	kilobase
KCNK16	potassium channel, subfamily, member 16
KCNK17	potassium channel, subfamily, member 17
KCNK5	potassium channel, subfamily, member 5
kDa	kiloDalton
KSR	knockout serum replacement
LC-MS/MS	liquid chromatography-tandem mass spectrometry
LDL	low density lipoprotein
LDLR	low density lipoprotein receptor
LIF	leukaemia inhibitory factor
LPA	lipoprotein-a
LRP1b	low density lipoprotein receptor-related protein 1B
LTR	long terminal repeat
Mb	megabases
MDR	multidrug resistance
MeCN	acetonitrile
MEF	irradiated mouse embryonic fibroblasts
MetSO	methionine sulfoxide
MG	methylglyoxal
MG-H1	methylglyoxal-derived hydroimidazolone, <i>N</i> _δ -(5-hydro-5-methyl-4-imidazolone-2-yl)ornithine
MLPA	multiplex ligation-dependent probe amplification
mM	millimolar
mmHg	millimeter of mercury (unit of pressure)
MOLD	methylglyoxal-derived lysine dimer 1,3-di(<i>N</i> _ε -lysino)-4-methylimidazolium
MRE	metal responsive element
MRM	multiple reaction monitoring
mRNA	messenger ribonucleic acid
mTOR	mechanistic target of rapamycin
mU	milliunit
MYC	proto-oncogene C-myc
NAD ⁺	nicotinamide adenine dinucleotide, oxidised form
NADH	nicotinamide adenine dinucleotide, reduced form
NADPH	nicotinamide adenine dinucleotide phosphate, reduced form
NANOG	homeobox transcription factor Nanog
NCI-H522	human non-small cell lung cancer cell line
NEAA	non-essential amino acids

NER	nucleotide excision repair
NFK	N-formylkynurenine
NF-κB	nuclear factor-kappa β
nmol	nanomole
NO	nitric oxide
NRES	national research ethics service
Nrf2	nuclear factor 2 (nuclear factor-erythroid 2 p45 subunit related factor 2)
nt	nucleotide
NV	non-viable cell count
O ₂ ⁻	superoxide anion
OCT3/4	octamer-binding transcription factor-3/4
OMIM	online mendelian inheritance in man
PCA	perchloric acid
PCR-RFLP	PCR-restriction fragment length polymorphism
pI	isoelectric point
pmol	picomole
PMP22	peripheral myelin protein 22
pO ₂	partial pressure of oxygen
PRT	paralogue ratio test
qPCR	quantitative polymerase chain reaction
rad51	recombination A-like protein
RAGE	receptor for advanced glycation endproducts
Rai1	retinoic acid induced 1 gene
recA	recombinase A
RF	renal failure
RGD	arginine-glycine-aspartate peptide
Rn 18s	18S ribosomal ribonucleic acid
RNA	ribonucleic acid
ROS	reactive oxygen species
RPMI	roswell park memorial institute
SDS	sodium dodecylsulphate
SDS-PAGE	sodium dodecyl sulfate polyacrylamide gel electrophoresis
SfaNI	restriction enzyme
shRNA	short hairpin ribonucleic acid
siRNA	small interfering ribonucleic acid
SLG	S-D-lactoylglutathione
SNCA	synuclein, alpha
SNP	single nucleotide polymorphism
SOD1	copper-zinc superoxide dismutase
SOD2	mitochondrial manganese superoxide dismutase
SOX2	sex determining region Y-box 2
SOX9	sex determining region Y-box 9
SpBrBzGSH	S-p-bromobenzylglutathione
Ss	serum substance

ssDNA	single-stranded DNA
STZ	streptozotocin
TBS	tris-buffered saline
TCA	trichloroacetic acid
TERT	telomerase reverse transcriptase
TFRC	transferrin receptor protein 1
THF	tetrahydrofuran
TK	thymidine kinase
tri	triplication
U	unit
UNG	uracil-N glycosylase
UTF1	undifferentiated embryonic cell transcription factor 1
UTR	untranslated region
UV	ultraviolet
VMN2R112	vomeronasal 2, receptor 112
WB	western blotting
WT	wild-type
YES1	yamaguchi sarcoma viral oncogene homolog 1
ZFP206	C2H2 zinc finger transcription factor

1. Introduction and background

1.1. Copy number variation

Development of techniques for complete and detailed sequencing of organism genomes has revealed genetic rearrangements in many different locations throughout the genome within a species. Genetic rearrangements may be inversions, duplications, insertions and deletions. They result in changes in the physical arrangement of genes and chromosomes. Cytogeneticists have observed variations in chromosome structure when studied by light microscopy. Change in chromosome structure involves: aneuploidy - abnormal chromosome number, translocations – movement of part of a chromosome to a new chromosomal location, deletions and insertions, fragile sites, and Y chromosome size variation (Feuk et al., 2006). One of the earliest structural variations reported was the duplication of the *Bar* gene in *Drosophila*, which was linked to a phenotype where the eye field of affected flies was narrowed, compared with wild-type flies (Bridges, 1936).

A major contribution to genetic variations comes from deletions and replication of DNA sequences. These genetic arrangements are called copy number variations (CNVs). They are a key component of genomic diversity, and may be compared along with single nucleotide polymorphisms (SNPs) as major causes of genomic diversity. Indeed, CNVs account for approximately 10-fold greater total nucleotide content than total SNPs (Zarrei et al., 2015). CNV was defined as a DNA segment of one kilobase (kb) or larger which is present at variable copy number in comparison with a reference genome (Redon et al., 2006). The size of CNVs is now typically defined as larger than 50 bp to 3 Mb (MacDonald et al., 2014). Smaller elements are referred to as insertions or deletions. Copy-number polymorphism is a term applied to a CNV that occurs in more than 1% of the population (Feuk et al., 2006). CNV is a source of substantial diversity of gene expression and phenotype (Choy et al., 2010, Schrider and Hahn, 2010). Some CNVs have not shown any influence on phenotype, however, many others have been linked with a characteristic phenotype. Host interaction with additional environmental or genetic factors may influence detectable phenotypic effect of CNVs (Redon et al., 2006).

CNVs as a genetic diversity have been found in all human populations as well as in many other mammalian species (Freeman et al., 2006). This genetic diversity is a major driving force in evolution, especially in the rapid evolution that has occurred, and continues to occur, within the human (Bailey and Eichler, 2006). A complete catalogue of 55 CNV studies of the human genome was performed by the Database of Genomic Variants (DGV) which has collected and curated 2,391,408 CNVs comprising 202,431 CNV regions in the human genome (MacDonald et al., 2014). Among 125 distinct human populations, 14,467 autosomal CNVs and 545 X-linked CNVs were identified (Sudmant et al., 2015). In this study, deletions exhibit stronger selective pressure and were better phylogenetic markers of population relationships than duplication polymorphisms. In addition, 1036 population stratified copy number variable regions were identified, 295 of which intersect coding regions and 199 of which exhibit extreme signatures of differentiation. Furthermore, there were 571 loci that segregate in the human population and another 2026 loci of fixed 2 copies in all human genomes (Sudmant et al., 2015). Analysis of CNV regions showed that they were unevenly distributed in the genome and among chromosomes. The susceptibility of any chromosome region to CNV varied from 1.1% to 16.4% for gains and from 4.3% to 19.2% for losses. For gains, chromosome 22 and the Y chromosome showed the highest proportion of variability, followed by chromosomes 16, 9 and 15. Chromosomes 3 and 18 showed the lowest proportion of variability. For losses, the highest proportion of variable sequence was in chromosomes 19 and 22 and the Y chromosome. The lowest proportion was found in chromosomes 5, 8 and chromosome 18. CNVs were unevenly distributed within the chromosomes. The pericentromeric and subtelomeric regions had a high proportion of CNVs (Zarrei et al., 2015).

In the laboratory mouse genome, the copy number content was analysed to 10 kb resolution. Over 1,300 CNV regions were identified and span 3.2% (85 Mb) of the genome. Most of the identified regions were less than 10 kb in length and presented in more than one mouse strain (Cahan et al., 2009). More recently, Pezer *et al* applied a read depth approach to genome resequencing data and bioinformatics analyses with experimental validation using droplet digital PCR to detect CNVs ≥ 1 kb in wild-caught mice belonging to four different populations of *Mus musculus domesticus*. In total, 1863 transcription units appear to be completely encompassed

within CNVs in at least one individual when compared to the reference assembly. In addition, 179 of these CNVs show population-specific copy number differences, and 325 are subject to complete deletion in multiple individuals (Pezer et al., 2015). Comparing this result with Cahan *et al.*, the difference between both studies appears to be due to the depth of the analyses as Cahan *et al.* used 10 kb resolution whereas Pezer *et al.* used 1 kb resolution.

CNVs typically lie outside of coding sequences and ultra-conserved regulatory elements. These elements are sequences of at least 200 bp that are conserved across mammalian species - including human, mice, and rat populations (Bejerano et al., 2004). The greatest enrichment areas for CNVs of the functional categories were those genes involved in cell adhesion, responses to chemical stimuli and the sensory perception of smell (Bejerano et al., 2004, Nguyen et al., 2006). The exons of all genes were more variable than the genome average, with exons of non-coding genes the highest proportion of CNV sequence. Exons of many constrained gene sets - particularly those associated with diseases or other health-altering phenotypes - were less variable than the genome average (Zarrei et al., 2015). In agreement with this, Li *et al.* (2011) found significantly higher number of structural variants in untranslated regions. Protein-coding exon regions had fewer variants than introns (Li et al., 2011).

The biological impact of changes in gene copy number depends on whether such changes produce related change in gene expression. There may be compensatory mechanisms that ensure wild-type levels of expression irrespective of gene copy number. These mechanisms, collectively called dosage-compensation mechanisms, are known and exist for sex chromosomes which vary in copy number between sexes (Disteche, 2006). Gene copy number proportional expression of whole chromosomal or segmental aneuploidies has been observed in fission yeast, budding yeast, arabidopsis, trisomic mouse embryonic fibroblasts, partially trisomic mouse tissues, and human trisomies (Pavelka et al., 2010, Huettel et al., 2008, Kahlem et al., 2004, Upender et al., 2004, Stingele et al., 2012). Most CNVs, however, result in a corresponding change in gene expression. In humans and mice, 85% – 95% of CNVs are associated with changes in expression of the affected genes (Stranger et al., 2007, Henrichsen et al., 2009). In these organisms, the change in protein production was due to related change in mRNA levels. In human cells, quantitative proteomic analyses showed that changes in gene copy number result in

changes in protein levels in the majority of CNVs (Stranger et al., 2007, Stingele et al., 2012). However, some proteins do not show concomitant increase in protein levels with gene copy number. This is often due to the protein being a component of large complexes of multiple proteins without similar change of CNV. Excess unassembled protein subunit may be susceptible to degradation and therefore protein concentration does not increase with increased CNV (Stingele et al., 2012). Additional copies of genes may also provide redundancy that allows some copies to evolve new or modified functions or expression patterns while other copies maintain the original function (Inoue and Lupski, 2002). The non-homologous recombination events that underlie changes in copy number also allow generation of new combinations of exons between different genes by insertion, deletion or translocation (Zhang et al., 2009) so that proteins might acquire new domains, and hence new or modified activities.

CNV changes may have adverse effects on fitness. The degree of effect scales with the size of the alteration. Segmental and whole chromosome aneuploidies lead to severe developmental abnormalities or death of the organism in all species analysed (Torres et al., 2008). These types of CNVs are rare and they are under strong negative selection (Itsara et al., 2010). Small DNA sequence deletions and insertions are widespread in the human genome, indicating their likely minor impact on fitness (Girirajan et al., 2011). Rare CNV change in regions that are generally copy number stable tend to have adverse effects on fitness (Zarrei et al., 2015). Copy number stable genes are typically involved in cell proliferation and cell signalling, as well as those involved in regulation of protein phosphorylation. These findings reflect the functional sensitivity of the products of these genes to dosage effects, particularly during embryonic development, also the potential of these genes as tumour suppressor genes or oncogenes (Futreal et al., 2004).

CNVs caused by genomic rearrangements can produce phenotypic changes by effects of gene dosage, gene interruption, gene fusion, positional effects, unmasking of recessive alleles or functional polymorphism, and potential transvection effects (Lupski and Stankiewicz, 2005). CNVs involving dosage-sensitive genes can alter gene expression levels and cause consequent clinical phenotypes. For example, *PMP22*, encoding peripheral myelin protein, is located within the 1.4 Mb CMT1A region at 17p12. The duplication of this region can lead to Charcot Marie Tooth disease by *PMP22* overexpression, whereas deletion can

result in Hereditary neuropathy with pressure palsies by PMP22 under-expression (Lupski and Chance, 2005). When the breakpoint of an insertion, deletion, or tandem duplication is located within a functional gene, it may interrupt the gene. This causes a loss of function by inactivating a gene. For example, interruption of red-green opsin genes function alters the genes encoding red and green visual pigments causing colour blindness (Nathans et al., 1986).

Gene fusion is caused by genomic rearrangements between different genes or their regulatory sequences can generate a mutation or gain of function. This mechanism is prominent among cancers associated with somatic chromosomal translocations (Lifton et al., 1992). For example, genes encoding steroid 11 β -hydroxylase and aldosterone synthase on chromosome locus 8q are candidate genes for glucocorticoid remediable aldosteronism. These two genes have 95% identity and non-allelic homologous recombination causes gene fusion between them, segregating with glucocorticoid remediable aldosteronism in a large extended family (Lifton et al., 1992).

CNV may cause regulatory sequence removal or alteration and thereby affect expression or regulation of a gene beyond the CNV region. This is called a position effect (Kleinjan and van Heyningen, 2005). For example, mutations in *SOX9* lead to campomelic dysplasia, but it was reported that two balanced translocations, with breakpoints mapping to approximately 900 kb upstream and 1.3 Mb downstream of *SOX9* can also cause the disease (Velagaleti et al., 2005). Alteration of one allele may unmask another recessive allele or functional polymorphism. For example, the activity of the plasma coagulation factor XII (Hageman factor) in patients with the common Sotos syndrome deletion is predominantly determined by the functional polymorphism of the remaining hemizygous coagulation factor XII allele (Kurotaki et al., 2005). Pairing of alleles on homologous chromosomes influences the gene expression by a mechanism called transvection. This effect is mediated via deletion of regulatory elements required for communication between alleles. For example, studies of mouse models of Smith-Magenis syndrome showed that the penetrance of craniofacial anomalies (a major clinical manifestation of Smith-Magenis syndrome) was modified by the 590 kb genomic sequence surrounding *Rai1* in which potential transvection may exist (Yan et al., 2007).

Initially CNV was thought to be pathogenic and limited to rare genomic disorders (Lee and Scherer, 2010, Emanuel and Shaikh, 2001). However, CNVs present in all phenotypically normal individuals reported to date (Sebat et al., 2004, Iafrate et al., 2004, Armengol et al., 2009). It has been attributed to a number of susceptibility of common and complex diseases (Gonzalez et al., 2005, Aitman et al., 2006), neuropsychiatric diseases (Rovelet-Lecrux et al., 2005, Cook Jr and Scherer, 2008), and notably, cardiovascular diseases (Norton et al., 2011, Prakash et al., 2010).

Changes in the copy number of specific genes can have a marked impact on cellular and organismal fitness. For example, human studies suggest that 15% of neurodevelopmental disorders and other diseases are due to large, rare CNVs resulting in imbalance of few genes (Malhotra and Sebat, 2012). For example, duplication of *SNCA* gene is associated with Parkinson's disease (Singleton et al., 2003), duplication of *GSK3b* gene is associated with bipolar disorder (Lachman et al., 2007), and low-copy amplification of the *C4* gene is associated with systemic lupus erythematosus (Yang et al., 2007). Deletions and amplifications of individual genes are major drivers of tumorigenesis. For example, amplification of the oncogene *Myc* is thought to be a driving factor in human acute myeloid leukaemia (Jones et al., 2010). Copy number increase of *APP* gene is located in chromosome 21 and has been found to be duplicated in familial forms of early onset Alzheimer's disease. This is found in Down syndrome where this is trisomy of chromosome 21 (Kingsbury et al., 2006).

CNVs are likely to contribute to unexplained genetic variation in metabolic diseases. It is probable that both rare and common CNVs contribute to susceptibility to metabolic diseases. For example, CNVs in the low-density lipoprotein receptor *LDLR* gene underlie a substantial portion of disease in patients with heterozygous familial hypercholesterolaemia (Wang et al., 2005). In addition, a common CNV in *LPA* encoding apolipoprotein-a is the primary determinant of plasma lipoprotein-a concentrations - a risk factor for atherosclerosis (Shia et al., 2011). Interestingly, the severity of phenotype found in heterozygous familial hypercholesterolaemia patients was significantly associated with the type of mutation. The patients with nonsense mutations or CNVs in *LDLR* had higher untreated LDL cholesterol levels than patients with no detected abnormality or with missense mutations in *LDLR* or *APOB*. This example of phenotype-genotype correlation further underlines the potential for

large effects due to a CNV within a gene that encodes an important metabolic protein (Pollex and Hegele, 2007). More examples of CNVs associated with diseases are given in Table 1.1.

Table 1.1: Examples of CNVs and genomic disorders.

Phenotype	OMIM	Locus	CNV	References
Spinocerebellar ataxia type 20	608687	11q12	dup	(Knight et al., 2008)
Adult-onset leukodystrophy	169500	<i>LMNB1</i>	dup	(Padiath et al., 2006)
food allergy susceptibility	607667	10q21	dup	(Li et al., 2015)
food allergy susceptibility	605104	16p13.3	dup	(Li et al., 2015)
Mental retardation	300534	Xp11.22	dup	(Froyen et al., 2008)
Mental retardation	300706	<i>HUWE1</i>	dup	(Froyen et al., 2008)
Pelizaeus-Merzbacher disease	312080	<i>PLP1</i>	del/dup/tri	(Combes et al., 2006, Lee et al., 2006)
Progressive neurological symptoms (MR+SZ)	300260	<i>MECP2</i>	dup	(del Gaudio et al., 2006)
Alzheimer disease	104300	<i>APP</i>	dup	(Rovelet-Lecrux et al., 2006)
Autism	611913	16p11.2	del/dup	(Weiss et al., 2008)
Type 2 diabetes	254268	<i>1p13.3</i>	dup	(Dajani et al., 2015)
non-alcoholic fatty liver disease	64328	13q11	dup	(Zain et al., 2015)
Hemophilia A	306700	Xq28/ <i>F8</i>	inv/del	(Antonarakis et al., 1995)
Ichthyosis	308100	<i>STS</i>	del	(Shapiro et al., 1989)
Crohn disease	266600	<i>HBD-2</i>	copy number loss	(Fellermann et al., 2006)
Pancreatitis	167800	<i>PRSS1</i>	tri	(Le Maréchal et al., 2006)
Parkinson disease	168600	<i>SNCA</i>	dup/tri	(Fuchs et al., 2007)
Psoriasis	177900	<i>DEFB</i>	copy number gain	(Hollox et al., 2008)
Schizophrenia	612001	15q13.3	Del	(Stone et al., 2008)
Systemic lupus erythematosus	152700	<i>FCGR3B</i>	copy number loss	(Aitman et al., 2006)

Dup; duplication, del; deletion, tri; triplication, inv; inversion, OMIM; Online Mendelian Inheritance in Man at <http://omim.org/>

Maintenance of some CNVs in a subset of the human population may be due to selective advantage, particularly those present at relatively high minor allele frequency. For example, unusual high copy numbers of *CYP2D6* and *CCL3L1* genes are associated with increased drug metabolism (Eichelbaum et al., 2006) and decreased susceptibility to HIV/AIDS (Gonzalez et al., 2005) respectively. However, their frequencies suggest that most CNVs have been subject to selection leading to their elimination and low prevalence (Sebat et al., 2004). Another example is positive selection of increased CNV of human salivary amylase (*AMY1*) – encoding the enzyme responsible for starch hydrolysis. *AMY1* copy number is correlated positively with salivary amylase protein levels. Mean *AMY1* copy number was increased in populations with high-starch diets, compared to those with a low-starch

diet. This is likely due to higher *AMY1* copy number and protein improving the digestion of starchy foods and acting as buffer against the fitness-reducing effects of intestinal disease (Perry et al., 2007).

CNV changes are more complex in cancer. The contribution of gene-dosage changes of many genes is increased by the variability of a changing genetic make-up in many cancers. However, some specific aneuploidies could be targeted in therapy. For example, trisomy 8 is frequently observed in patients with acute myeloid leukaemia and associated with poor survival rate when present together with other genetic aberrations (Wolman et al., 2002). Drugs that target cells with amplified chromosome 8 may aid in the treatment of this disease. Genomic instability in cancers also leads to loss or polymorphism of many genes which could provide additional therapeutic targets (Nijhawan et al., 2012). Compounds that specifically inhibit the proliferation of cell lines with aneuploidy have been found and appear to exaggerate the general stress phenotypes associated with whole-chromosome copy number changes (Tang et al., 2011). For example, AICAR, an agonist of the stress-activated AMP kinase, and HSP90 inhibitor 17-AAG which display antitumor efficacy in HER2-positive breast cancer (Tang et al., 2011). Therefore, targeting the cell stress associated with aneuploidy could be developed as cancer drug targets.

Recent efforts to map CNVs in healthy populations have defined their distribution, frequency and size. Many of the identified CNVs overlap genes with important functions in metabolic pathways. The overlap of CNVs that were found in control datasets with functional candidate genes or genes with previous evidence of association with metabolic syndrome presents an important subset for future CNV association studies (Tang and Amon, 2013).

1.1.1. Mechanisms producing gene copy number changes

Mechanisms of copy number change have been studied in model organisms, notably *Drosophila melanogaster*, *Escherichia coli* and *Saccharomyces cerevisiae*. These findings show similar characteristics as CNVs in human and primate genomes and improved the understanding of the processes that lead to chromosomal structural change. Insights were thereby also gained into a potential major driving force of human evolution (Hastings et al., 2009a). Although extrapolation from one organism to another is not always reliable, it has proved very successfully in the study of processes acting on DNA. Almost all DNA repair mechanisms acting in humans

were first described in model organisms, particularly bacteria (Friedberg et al., 2005).

Changes in copy number involve changes in the structure of the chromosomes. These occur by two general mechanisms: homologous and non-homologous recombination. Homologous recombination requires extensive DNA sequence identity of approximately 50 bp in *Escherichia coli* (Lovett et al., 2002) and up to 300 bp in mammalian cells (Liskay et al., 1987). Most of homologous recombination mechanisms require a strand exchange protein - recA in prokaryotes and rad51 in eukaryotes. The reason for this dual requirement is that an early step in most homologous recombination pathways is the recA/rad51-catalysed invasion of homologous duplex sequence by the 3' end of single strand DNA (ssDNA); that is, the 3' end replaces the equivalent strand of the duplex. Non-homologous recombination mechanisms use only microhomology or no homology (Hastings et al., 2009b). Mutation rates of CNVs can vary widely at different loci in the genome, likely reflecting the differences in CNV formation mechanism and local or regional genome architecture inciting genomic instability (Hastings et al., 2009b).

CNVs can arise both somatically and meiotically, as shown by the finding that repeated sequences in different organs and tissues from the same individual can vary in copy number (Piotrowski et al., 2008) and that identical twins can have different CNVs, respectively (Bruder et al., 2008). Most common distribution areas of CNVs are three categories of genes which are enriched for structural variants including: genes that are involved in immunity and cell-cell signalling, genes encoding proteins involved in interaction with the environment, such as immune response and perception of smell and retrovirus and transposition related protein coding genes (Bejerano et al., 2004, Nguyen et al., 2006). Dosage-sensitive genes are under-represented in regions affected by CNVs (Schuster-Böckler et al., 2010). Genes which are more evolutionarily conserved appear to have fewer CNVs (Li et al., 2011).

Risk for new CNVs is increased by exposures to mutagens and by inherited genetic predisposition. There are at least two distinct pathways involved in the formation of most disease-associated CNVs: unequal meiotic recombination and replication errors (Arlt et al., 2012). Chemical agents that stress or disrupt replication induce a high frequency of CNVs in human cells. These agents include the polymerase inhibitor aphidicolin, the ribonucleotide reductase inhibitor, and

hydroxyurea which are commonly used in the treatment of sickle cell disease and other disorders. This provides experimental evidence supporting replication error models for the origin of CNVs (Arlt et al., 2012).

1.1.2. Measurement of copy number variation

The discovery of CNVs was a consequence to the introduction of new genomic technologies enabling high resolution analysis of genomic DNA. CNVs can be detected and analysed by different technologies, both at the genome-wide scale and the locus specific level. The main genome-wide scale screening methods includes array comparative genomic hybridization (aCGH), single nucleotide polymorphism (SNP) array, fluorescence *in situ* hybridisation (FISH) and next generation sequencing approaches. The main locus specific approaches include multiplex ligation-dependent probe amplification (MLPA), quantitative polymerase chain reaction (qPCR) and paralogue ratio test (PRT).

In this work, I focus on studying copy number variation of glyoxalase 1 (*Glo1*) of the glyoxalase system - specifically for *Glo1* in mice, mouse embryonic stem cells and human *GLO1* in a clinical study of healthy human subjects and patients with renal failure. Characteristics of the Glyoxalase system will be discussed in detail in section 1.4.

1.1.3. Copy number variation of Glyoxalase 1 (*Glo1*)

1.1.3.1. Mice with increased *Glo1* copy number

In the mouse, *Glo1* is located in chromosome 17 at locus 17 a3.3, *ca.* 3 centimorgans from the Ss locus of the H-2 histocompatibility region (Meo et al., 1977). Murine *Glo1* CNV was firstly reported among inbred mouse strains (Williams et al., 2009). They analysed gene copy number in mice strain using a Hidden Markov Model (HMM) approach and Affymetrix exon arrays. This assigns probabilities to hybridisation probes for three states: duplicated, deleted or ground, relative to the C57BL/6 reference strain. The use of the HMM model and a large number of exon-specific probes provided high power to detect large copy number changes of known genes but small or intergenic copy number changes were less likely detected. A total of 68 gene duplications and 47 deletions were identified in 71 inbred mouse strains. A 475 kb tandem duplication on chromosome 17 (30,174,390–

30,651,226 Mb; mouse genome build 36) that included *Glo1* and complete and partial copies of other genes. In this duplication, *Glo1* and dynein, axonemal, heavy chain 8 (*Dnahc8*) were fully duplicated. Presence of the duplication is associated with increased *Glo1* expression. Other genes were partially duplicated – Bric-a-brac (BTB) domain containing 9 (*Btbd9*) and glucagon-like peptide 1 receptor (*Glp1r*). A PCR-based strategy was developed and used to detect the gene duplication. The duplication was detected in 23 strains out of 71 inbred strains tested of various outbred and wild-type mice. *Dnahc8* expression is confined to the principal piece of the sperm tail and polymorphisms may be linked to male infertility (Samant et al., 2005). *Btbd9* is known to be involved in protein-protein interactions. Polymorphisms at this locus have been reported to be associated with susceptibility to Restless Legs Syndrome and may also be associated with Tourette's Syndrome (Moore et al., 2013). Increased *Glp1r* expression and signaling potentiates glucose-dependent insulin secretion from pancreatic islet β -cells, regulates gastric emptying and central nervous system linked regulation of glucose homeostasis (Koole et al., 2013).

Deep sequencing of chromosome-17 in C57BL/6 and A/J mice, without and with gene duplication, confirmed complete duplication of *Glo1* and *Dnahc8* and partial duplication of *Btbd9* (1 - 7 of 13 exons) and *Glp1r* (1 - 5 of 13 exons). In A/J mice, there were 36 other gene copy increases and 10 deletions on chromosome 17 (Sudbery et al., 2009).

Williams *et al.* found the 475 kb duplication including *Glo1* was associated with an increased anxiety phenotype. This compared with a previous report (Hovatta et al., 2005) where *Glo1* overexpression was linked to an anxiety phenotype. This phenotypic association was questionable as the reverse association, decreased *Glo1* expression with an anxiety phenotype, had been found in other in-bred strains of mice (Kroemer et al., 2005). This suggested the finding by Hovatta and co-workers may have been an artefact of in-breeding in the line of mice used. These conflicting observations made without either group attempting to explain the discordant findings was noted by Thornalley (Thornalley, 2006). This association of *Glo1* duplication and increased expression was drawn into further doubt by the inadvertent cross-breeding the 475 kb duplication into mice in *Fkbp5* knockout studies without a demonstrable anxiety phenotype. *Glo1* protein and mRNA were elevated in association with *Glo1* duplication in *Fkbp5* $-/-$ mouse. *Fkbp5* and *Glo1* are approximately 2 Mb apart on chromosome 17. *Fkbp5* deletion was constructed in

129SvJ embryonic stem cells, and the resulting mice were then crossed with C57BL/6 animals; 129SvJ mice carry the *Glo1* gene duplication but C57BL/6 mice do not. The wild-type *Fkbp5* allele originating from C57BL/6 mice is usually co-inherited with a single copy of *Glo1*, whereas the knockout *Fkbp5* allele originating from 129SvJ mice is co-inherited with two copies of *Glo1* (Kollmannsberger et al., 2013). The duplication in this model may be a response for the deletion in a nearby gene, which is due to “flanking allele problem”. This is a common phenomenon in gene knockout via homologous recombination, especially when crossing different background strains. It could be avoided, for example, by genome editing with engineered nucleases or by using inducible gene knockout techniques (Crusio et al., 2009). Further recent evidence came from a genome-wide study of CNV associations with the anxiety phenotype in mice which did not link *Glo1* CNV with anxiety (Brenndörfer et al., 2014). Other gene copy number change within the 475 kb duplication may have contributed to the anxiety phenotype. Interestingly, when transgenic mice were produced with bacterial artificial chromosomes (BAC) with overexpression of *Glo1* by 2, 4 and 5-fold, only mice with 4-fold and 5-fold increase in *Glo1* expression displayed decreased time in the centre of the open-field anxiety test; mice with 2-fold increase in *Glo1* expression did not exhibit the anxiety phenotype (Distler et al., 2012). Currently the link of *Glo1* duplication is uncertain following these conflicting findings.

In attempts to substantiate *Glo1* duplication, increased *Glo1* expression and related decreased methylglyoxal (MG) to dysfunctional brain metabolism and anxiety, MG concentration in brain tissue of mice has been estimated at *ca.* 170 – 360 μM (Hambusch et al., 2010) and 5 μM MG (Distler et al., 2012). Both appear to be overestimates as assay of mouse content of MG by interference-free assay methodology gave estimates of 0.3 and 1.5 μM brain stem/midbrain and cortex (Kurz et al., 2011). Acid stable peroxidase in brain tissue led to MG formation from the derivatizing agent, 1,2-diamino benzene, used in the assay if not blocked by sodium azide (Thornalley and Rabbani, 2014). Lower estimates also were in agreement of a mathematical model of MG formation in the mouse brain (Rabbani and Thornalley, 2014c). MG was found to agonise the GABA_A receptor in primary cerebellar granule neurons with a median effective concentration EC₅₀ of 10.5 μM . MG agonism at the GABA_A receptor was proposed as mediator of sedation to explain increased *Glo1* CNV with an anxiety phenotype (Distler et al., 2012). MG

concentration in mouse brain tissue is *ca.* 7-fold lower than this (Kurz et al., 2011) and only approached the EC₅₀ value with dosing of 300 mg/kg MG (Distler et al., 2012) – similar to doses that have previously produced acute toxicity (Conroy, 1979). The evidence linking *Glo1* duplication, increased Glo1 protein and putative decreased sedation effect of brain MG cannot be sustained on current evidence. Further investigations are required.

Shortly after the report of *Glo1* duplication by Williams *et al.*, *Glo1* CNV was reported as part of genome-wide CNV analysis in all sites tested including hematopoietic stem cells and progenitors, hypothalamus and adipose tissue. Analysing the CNV content with density of 10 kb resolution, over 1,300 CNV regions were found spanning 3.2% (85 Mb) of the murine genome. Most CNVs were less than 10 kb in length and mapped outside of the transcribed regions of genes. Six hundred CNVs were associated with gene expression. Only 3 genes were found with increased expression of 2 – 4 fold in all sites. One of these was *Glo1*. The copied region was from 30,172,971 - 30,654,177 (*ca.* 0.5 Mb) (Cahan et al., 2009), a similar location and size to that reported tandem duplication by Williams *et al.* (Williams et al., 2009).

BALB/cJ mice lacked *Glo1* duplication whereas BALB/cByJ mice have *Glo1* duplication and express approximately 10- fold higher levels of Glo1 protein on a similar genetic background. These strains were used to study development of diabetic neuropathy where BALB/cByJ mice showed resistance to diabetic neuropathy development compared to BALB/cJ mice (Jack et al., 2012).

1.1.3.2. Human subjects with increased glyoxalase 1 copy number

CNV of human *GLO1* was first detected by Redon *et al.* in constructing a first-generation CNV map of the human genome by studying 270 subjects from four populations with ancestry in Europe, Africa or Asia. A total of 1,447 CNV regions were found covering 12% of the genome. *GLO1* was the only gene found in a copied region of *ca.* 122 kb. There were 5 copy number increases, suggesting *GLO1* CNV prevalence of *ca.* 2% (Redon et al., 2006). *GLO1* CNV was confirmed in the human population (Wong et al., 2007) and also found in other primates (Perry et al., 2008).

Increased *GLO1* copy number has recently been found in human tumour cell lines and primary human tumours. The minimum common copy number increase region was *ca.* 1 Mb and it contained 8 genes: *GLO1*, *DNAH8*, *GLP1R*, *C6ORF64*,

KCNK5, *KCNK17*, *KCNK16* and *C6ORF102*. The increased copy number was generally functional – associated with increased *GLO1* protein and activity but weak correlation between copy number and expression suggested that not all copies have normal functionality. In a survey of 520 human tumours, increased *GLO1* copy number had a prevalence of 8%. The highest prevalence was in breast cancer (19%), small cell lung cancer (16%) and non-small cell lung cancer (11%) (Santarius et al., 2010). Increased expression of *GLO1* is associated with multidrug resistance (MDR) in cancer chemotherapy and thereby increased *GLO1* copy number is a mechanism by which human tumours may be MDR from the earliest stages of tumour carcinogenesis (Sakamoto et al., 2000). It has been previously proposed that increased *GLO1* expression is required in tumours with high flux Embden-Meyerhof glycolysis for protection from the toxic challenge of associated high flux of MG formation (Thornalley et al., 2010). Studies on *GLO1* copy number variation are summarised in Table 1.2.

Table 1.2: Copy number variation of human and mouse glyoxalase 1.

Species	CNV		
	Locus	Length (bp)	Reference
Human	6p21.2512 (38,696,947-38,819,063)	122,116	(Redon et al., 2006)
	6p21.2	ca. 1Mb	(Santarius et al., 2010)
	6p21.2 (38,753,034 – 38,908,635)	155,116	(Wong et al., 2007)
Mouse	17 a3.3 (30,174,390 - 30,651,226)	476,836	(Williams et al., 2009)
	17 a3.3 (30,172,971 - 30,654,177)	481,206	(Cahan et al., 2009)

1.1.4. Animal models with genetically increased *Glo1*

1.1.4.1. Transgenic mice and rats

Glo1 transgenic mice and rats were produced by Inagi and co-workers. Human *GLO1* cDNA was cloned into the pBsCAG-2 vector to be overexpressed under control of the cytomegalovirus enhancer/chicken β -actin promoter. The vector was microinjected into one pronucleus of fertilised C57BL/6 eggs and transferred into the oviduct of pseudopregnant mice for development. Of 96 founders, 15 had *Glo1* transgene detected and two were successfully bred to C57BL/6. Six mice were

used to create two independent *Glo1* transgenic mouse lines. Both lines transmitted the transgene to their progeny and litter sizes, haematological, biochemical and tissue histological characteristics were normal. Human GLO1 protein was detected in all tissues and GLO1 activity was increased 2 – 50 fold but unexpectedly not increased in red blood cells (Inagi et al., 2002). *Glo1* transgenic Wistar rats were prepared similarly (Kumagai et al., 2009).

Distler *et al.* produced *Glo1* overexpression mouse by using a bacterial artificial chromosome (BAC). This BAC contained *Glo1* gene and its cis-regulatory elements as well as partial copies of two additional genes, *Dnahc8* and *Btbd9*. The transcriptional start sites of these flanking genes were obtained using recombinogenic engineering (Copeland et al., 2001) by inserting ampicillin and kanamycin cassettes into the first exons of each gene, respectively. Therefore, this BAC should express *Glo1* only. Using the BAC modification method, 3 lines of transgenic mice on a C57BL/6J background were generated. BAC copy number was measured in each line using (qPCR): transgenic lines had 2, 8, and 10 copies of the BAC. These mice were healthy, fertile, and did not display any grossly discernible behavioural or physical abnormalities. In order to confirm that the BAC dose-dependently increased *Glo1* mRNA and protein in the transgenic mice, *Glo1* mRNA expression was measured using qPCR. The transgenic mice showed a copy number-dependent increase in *Glo1* mRNA in the brain and peripheral tissues. Also, there was a copy number-dependent increase in *Glo1* protein in the brain, which was measured by immunoblot. In addition, the specificity of the process was confirmed by using gene-expression microarrays. The microarray result showed overexpression of *Glo1* but there were no other changes in gene expression; particularly, there was no increased expression of *Dnahc8* or *Btbd9* (Distler et al., 2012).

Glo1 transgenic mice and rats have been employed in studies of abnormal physiological state and disease mechanism where dysfunctional MG metabolism is suspected; for example, the development of vascular complications of diabetes, renal senescence, anxiety and obesity – Table 1.3.

Table 1.3: Studies with mice and rats overexpressing glyoxalase 1.

Study	Outcome	Reference
Diabetic nephropathy	Glo1 overexpression prevented diabetic nephropathy	(Giacco et al., 2014) (Brouwers et al., 2014)
Diabetic retinopathy	Glo1 overexpression prevented diabetic retinopathy	(Berner et al., 2012)
Diabetic neuropathy	Glo1 overexpression prevented diabetic neuropathy	(Bierhaus et al., 2012)
Diabetic atherosclerosis in apolipoprotein E deficient background	No effect of Glo1 overexpression on atherosclerotic plaque development	(Geoffrion et al., 2014) (Hanssen et al., 2014)
Diabetic angiogenesis	Overexpression of Glo1 corrected the diabetes angiogenesis deficiency	(Ceradini et al., 2008) (Vulesevic et al., 2014)
Age-related endothelial dysfunction	Overexpression of Glo1 decreased age-related endothelial dicarbonyl and oxidative stress, altered phosphorylation of endothelial nitric oxide synthase, and attenuated endothelial dysfunction.	(Jo-Watanabe et al., 2014)
Renal senescence	Glo1 overexpression delays renal senescence	(Ikeda et al., 2011)
Renal ischemia-reperfusion injury	Glo1 overexpression exerts renoprotective effects in renal ischemia-reperfusion injury via a reduction in MG accumulation in tubular cells	(Kumagai et al., 2009)
Cardiovascular disease – post-myocardial reperfusion injury	Glo1 overexpression protects against post-myocardial reperfusion injury	(Blackburn et al., 2013)
Anxiety phenotype	Four – five fold over-expression of Glo1 was linked to increased anxiety	(Distler et al., 2012)

1.1.5. Animal models with genetically-controlled decreased glyoxalase 1

1.1.5.1. Glyoxalase 1 deficient mice

Brownlee and co-workers created mice deficient in Glo1 by viral transfection of C57BL/6 mice to express short hairpin *Glo1* iRNA. Short oligonucleotides with a target sequence to mouse Glo1 from nucleotide 235 to 255 in a hairpin sequence

with restriction enzyme cohesive end sequences prepared and cloned into the pSilencer 1.0-U6 vector (Ambion). Fragments, including the mouse U6 promoter and inserts, were subcloned into FUGW lentiviral vector. Lentiviral particles were produced from the recombined plasmids. shRNA lentivirus was injected into the perivitelline space of single-cell C57BL/6 mouse embryos. After incubation of 4 – 6 h, embryos were implanted into pseudopregnant females and were carried to term. Mice whose genome contained a single copy of the insert were identified by Southern blotting and used to establish founder lines. *Glo1* mRNA and protein levels were determined by qPCR and Western blotting and further confirmed by measurement of Glo1 activity. Heterozygous offspring of founder were 14 and had a 45 – 65% decrease in Glo1 activity of tissue. These mice were bred and used in subsequent experiments (El-Osta et al., 2008). Glo1 deficient mice have been employed in studies of abnormal physiological state and disease mechanism where dysfunctional MG metabolism is suspected e.g. inflammatory signalling of the aortic endothelium, proteasomal activity of kidney, diabetic nephropathy and diabetic atherosclerosis – Table 1.4.

Table 1.4: Studies with glyoxalase 1 deficient mice.

Study	Outcome	Reference
Inflammatory signalling of the aortic endothelium	Glo1 deficiency produced increased inflammatory signalling by the NF-kB system in normoglycaemia, similar to that of wild-type mice in transient hyperglycaemia	(El-Osta et al., 2008)
Proteasomal activity of kidney	Non-diabetic Glo1 deficient mice and STZ diabetic Glo1 deficient mice had impaired proteasomal activity	(Queisser et al., 2010)
Diabetic nephropathy	Increased urinary albumin excretion in non-diabetic state which was further exacerbated by STZ-diabetes	(Giacco et al., 2014)
Diabetic atherosclerosis in apolipoprotein E deficient background	No effect of atherosclerotic plaque development	(Geoffrion et al., 2014)

1.1.5.2. Glyoxalase 1 deficient human subjects

A patient with renal failure and very low GLO1 activity had a high occurrence of CVD events (Miyata et al., 2001). The cause of the GLO1 deficiency was unknown.

Deep sequencing of *GLO1* derived from peripheral blood or post-mortem brain tissue was performed in 1761 patients with schizophrenia and 1921 control subjects. A rare frameshift mutation in the *GLO1* gene was found that produced a truncated peptide, non-functional expression product. Only heterozygous inheritance was found with *GLO1* activity *ca.* 50% of normal healthy controls. Homozygous inheritance of the mutation is therefore considered embryonically lethal. There was a high frequency of severe schizophrenia in the heterozygous *GLO1* mutant individuals. To date, only 3 individuals with this mutation have been identified (Arai et al., 2010). In these subjects, decreased GLO1 activity was associated with decreased glomerular filtration rate (Ikeda et al., 2011).

1.1.5.3. Lexicon Glo1 mutant mouse

Glo1 mutant mice were produced by the International Mouse Knockout Consortium (IMKC). The IMKC is a consortium founded in 2007 to mutate all protein-coding genes in the mouse using a combination of gene trapping and gene targeting in C57BL/6 mouse ESCs (International-Mouse-Knockout-Consortium, 2007). Genes to be prioritised for targeted could be proposed to the Wellcome Trust UK in their “Access to mutant mouse resources” programme, 2007 – 2010, who then made the mutant mouse available free-of-charge to the successful proposal applicant. Professor Paul J Thornalley and Dr Naila Rabbani applied successfully to this scheme in 2007 and the IKMC accordingly produced and delivered the Glo1 mutant mouse. The IMKC mutant mouse targeted to *Glo1* was produced by gene trapping, with retroviral insertion of vector VICTR48 between exons-1 and -2 of *Glo1* gene in chromosome 17 of 129SvEv^{Brd} strain derived mouse ESCs and bred in a C57BL/6J background. The vector insertion site was in GST_4497_D9 OmniBank®.

Lexicon Pharmaceuticals, Inc., USA evaluated the expression of *Glo1* in several tissue and they claimed that mRNA of *Glo1* is completely absent - Figure 1.1. There was also the suggestion of increased blood glucose concentration in heterozygotes and homozygotes with respect to wild-type controls (Lexicon, 2007). Wild-type and heterozygotes sample sizes were small (n = 4), with homozygote

samples size, n = 8. Re-analysis by ANOVA indicated no significant change of blood glucose with genotype.

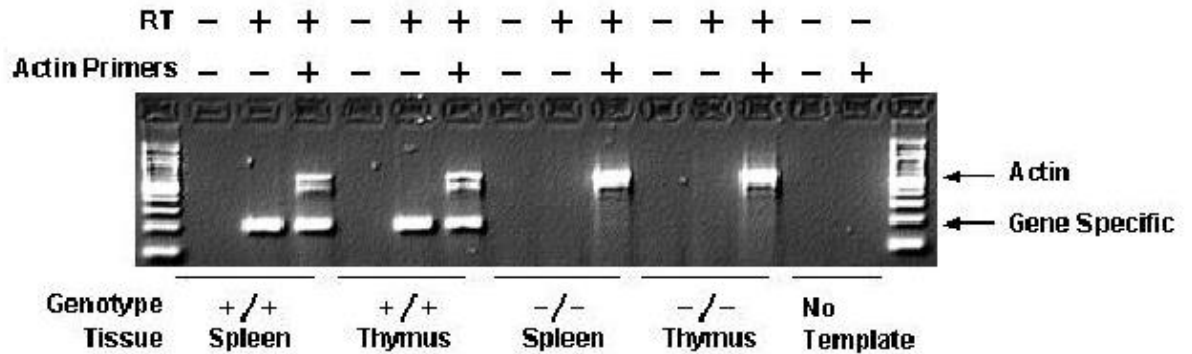


Figure 1.1: Lexicon qPCR analysis of the absent transcript in the (Glo1^{-/-}) mouse. (Provided by Dr Cindy Shirley, the IMKC project leader at Lexicon Pharmaceuticals).

The Lexicon Glo1 mutant mouse is the genetically modified mouse used in this project. It was produced by gene trapping technique and so in the following section I describe the technique of gene trapping as background for later interpretation of the experimental results of genome analysis.

1.1.5.3.1. The gene trapping technique for production of a gene knockout mice

In the gene trapping technique, DNA fragments are inserted to nucleus and are designed to be inserted randomly to any gene. The DNA fragments prevents RNA splicing mechanisms, which thereby prevents expression of the encoded protein and achieves knockout the function of mutated gene (Kile and Hilton, 2005). The advantage of gene trapping is that it is a high throughput technique and many genes may be disrupted. A single vector can be used to mutate a large number of genes in a limited number of experiments – Table 1.5. Gene trapping has been successfully applied to create a large collection of mutant mouse ESCs over the last 20 years - see International Gene Trap Consortium, www.genetrap.org. It is estimated that gene trapping can cover up to 60% of all mouse genes (Friedel et al., 2007).

In the gene trapping technique, mutated ESCs are grown in the laboratory for several days and then injected into mouse embryos. The embryos are implanted into a female mouse uterus and allowed to develop to term to produce mouse pups. These pups have the gene knockout in some tissues, which were derived from the modified

ESCs (Kile and Hilton, 2005). However, they also have tissues which contain heterozygous mutant cells. These mice are partly knockout because they have heterozygous knockout of the targeted gene in some tissues only. To produce homozygous knockout mice, crossbreeding of the deficient mice is required (Nagy, 2000).

Table 1.5: Advantages and disadvantages of gene trapping methods to produce knockout mice. Summarised from (Kile and Hilton, 2005).

	Advantages	Disadvantages
Gene trapping	No need to know the DNA sequence of the target gene. A single vector can be used in high throughput capacity. More than one gene can be knockout in one process.	Lacks efficiency as not every successful insertion of DNA fragments will lead to gene knockout. Lentgthy process to find out the knockout genes in ESCs. As it is random process, it is difficult to target some genes due to statistics or the gene might be inactive in ESCs, so there will be no marker indicating that the target gene is knockout.

Gene trapping and the related technique of gene targeting were the techniques used by the IMKC to produce knockout mice. Approximately 50,000 alleles have now been mutated in the mouse genome by these techniques (Czechanski et al., 2014). These modifications have been created by the IMKC and by individual investigators around the world which have created null and/or conditional null alleles for many genes in the mouse genome (Bradley et al., 2012). In addition to the knockout process, ESCs are also used for basic research such as pluripotency and the development of therapies based on stem cell as the starting material for directed differentiation of defined and enriched cell types *in vitro* (Bradley et al., 2012). Mouse ESCs used in these techniques are also a valuable model in the studies herein when seeking to model the metabolic effects of Glo1 knockdown in ESCs and in the production of Glo1 knockout mice by gene trapping. In the next section, I describe growth and metabolic characteristics of mouse ESCs as background to my studies.

1.2. Embryonic stem cells

ESCs are pluripotent stem cells which are at the epiblast lineage of the blastocyst. They therefore have the developmental potential to differentiate into any one of the three primary germ layers including mesoderm, definitive endoderm and ectoderm. The main defining features of ESCs are this developmental pluripotency combined with a high capacity for self-renewal *in vitro*. Mouse ESCs are derived from embryo's stage of pre-implantation (Evans and Kaufman, 1981). ESCs were originally derived and maintained on feeder layers. However, now it has been established that they could also be maintained in feeder layer free culture conditions in which the media are supplemented with leukaemia inhibitory factor (LIF). The activation of the LIF pathway appears to be required for self-renewal of ESCs (Williams et al., 1988).

The progenitor cells that give rise to ESCs reside in epiblast of the late blastocyst at 4 – 5 days post fertilization. ESCs express several factors associated with pluripotency including OCT3/4 and NANOG. In addition, ESCs have the capacity to populate the germline after microinjection into/or combination with host embryos, which makes ESCs essential tools for genetic engineering (Bradley et al., 1992).

1.2.1. Characterization of mouse embryonic stem cells

There are some important criteria which need to be fulfilled before a cell line qualifies to be an ESC line from mammals. In mouse, the criteria for validating the stem cell nature of ESC lines are cell morphology, expression of surface markers, biochemical markers, transcriptional factor expression, the ability to differentiate into various cell and tissue types and participation in embryonic development. Extended proliferative capacity and pluripotency while maintaining a normal karyotype are important features of ESCs (Evans and Kaufman, 1981).

ESCs are relatively small cells, with an intracellular volume two to three fold smaller than that of normal mammalian cells. The rate of cell division of ESCs is more rapid than the fastest growing cancer cell lines and they do not develop into senescence (Wang et al., 2011). ESCs grow in colonies, which have a characteristic morphology. These cells usually proliferate in tight round shaped colonies with smooth edges. The morphology of ESCs has two important traits including relatively

small amount of cytoplasm and exhibition of faster proliferation rate in a given population of cells (Evans and Kaufman, 1981). Recently, there are several reports regarding the karyotyping of the ESCs in long term culture. This has been studied by G-banding with most ESCs exhibiting a normal complement of chromosomes. Studying of several ESC lines reveals normal karyotype at passages ranging from 24 - 140 (Buzzard et al., 2004).

ESC pluripotency may be confirmed by assessing the expression of a set of transcriptional factors. OCT4, a Pou-domain transcription factor, was identified when it was expressed in unfertilized oocytes, ESCs and primordial germ cells (Schöler et al., 1989). More recently, it has been identified that overexpression of NANOG protein is capable of maintaining cytokine-independent self-renewal in ESCs (Mitsui et al., 2003). In addition, SOX2 is a transcription factor that forms a trimeric complex with OCT4 on DNA. It controls the expression of a number of genes involved in embryonic development such as YES1, FGF4, UTF1 and ZFP206 and it is critical for early embryogenesis and for embryonic stem cell pluripotency (Masui et al., 2007). These proteins are the most widely known markers of pluripotency both *in vivo* and *in vitro*. The expression of these proteins is common in all pluripotent cell types that can be maintained *in vitro* as well as across those species from which ESCs have been derived.

1.2.2. Metabolic characteristics of mouse embryonic stem cells

Metabolism of many types of stem cell shows high importance of anaerobic glycolysis, and regulation of stem cell function by bioenergetic signaling, the Akt–mTOR pathway, glutamine metabolism and fatty acid metabolism (Ito and Suda, 2014). Metabolic analyses of purified stem cells and their progeny have shown that the metabolic profile of the stem cells differs from that of committed progenitors. Unlike their progeny, the stem cells accumulate high levels of fructose-1,6-bisphosphate and have high pyruvate kinase activity, indicative of high flux of anaerobic glycolysis. They also have low levels of phosphoenolpyruvate but increased levels of pyruvate. Stem cells rely heavily on anaerobic glycolysis to support ATP production (Simsek et al., 2010) and the activity of oxidative phosphorylation is relatively low in cultured stem cells. ATP synthesis seems to be decoupled from O₂ consumption by the mitochondrial electron transport chain and is more dependent on glycolysis. It has been suggested that mitochondrial oxidation

operates both to recycle NAD^+ and to deploy tricarboxylic acid cycle metabolites for the generation of fatty acids and amino acids (Shyh-Chang et al., 2011).

In amino acid metabolism of ESCs, threonine has a crucial role (Wang et al., 2009). ESCs have extremely high levels of the threonine catabolizing enzyme L-threonine dehydrogenase relative to differentiated cells. L-Threonine dehydrogenase converts threonine to glycine and acetyl-coenzyme A. Glycine is then used by the mitochondrial enzyme glycine decarboxylase to generate the folate one-carbon pool to promote nucleotide synthesis and rapid proliferation of ESCs. L-Threonine dehydrogenase also increases the synthesis of S-adenosylmethionine, leading to a high ratio of S-adenosylmethionine /S-adenosylhomocysteine and high levels of trimethylation of histone H3 lysine 4 which is also thought to contribute to the maintenance of pluripotency and the proliferation of ESCs (Wang et al., 2011).

ESCs show increased activity in the pentose phosphate pathway which supports high flux nucleotide synthesis for cell proliferation. Further major functions of the pentose phosphate pathway are to produce NADPH which is necessary for the regeneration of glutathione for cell protection against oxidative stress and to act as an alternative pathway to glycolysis (Ito and Suda, 2014). Recently, studies have identified a HIF1 α -induced reciprocal metabolic switch between the pentose phosphate pathway and glycolysis. Expression of pentose phosphate pathway enzymes and glucose flux throughout both the pentose phosphate pathway and the tricarboxylic acid cycle are reduced under hypoxia, whereas glycolysis enzymes are upregulated (Ito and Suda, 2014).

ESCs are remarkably resistant to potential genotoxic stress. There are multiple pathways that may contribute to this resistance: cellular antioxidant defence, the activity of a verapamil-sensitive multidrug efflux pump, DNA strand break repair and heat shock protein expression. In addition, the ability to maintain low peroxide levels and antioxidant capacity decrease very early during differentiation, with concomitant decreased expression of antioxidant and chaperone genes. This suggests that very high resistance to oxidative and proteotoxic stresses is maintained in pluripotent ESCs (Saretzki et al., 2004).

ESC survival, proliferation, maintenance of the cell phenotype and bioenergetics are affected by the partial pressure of oxygen, pO_2 , in the local environment. Culturing the cells at a high pO_2 exposes the cells to higher concentrations of reactive oxygen species (ROS) which damages proteins, lipids and nucleic acids and can lead to senescence and cell death (Saretzki et al., 2004). Many cell types have a higher growth rate at $pO_2 < 142$ mmHg, including early embryos of both humans and mice. In contrast, providing too little oxygen can be harmful and lead to apoptotic or necrotic cell death (Powers et al., 2008). Embryonic development takes place in a low pO_2 environment, and hypoxia inducible factor-1 α (HIF1 α), a transcription factor regulating the metabolic response to low oxygen concentration, has been shown to play an important role in directing morphogenesis in the embryo and placenta (Zhou et al., 2012). Stem cell culture is often performed at pO_2 levels much higher than that of the embryo *in vivo*. It is cultured typically in a humidified atmosphere consisting of 95% air and 5% CO_2 that results in a gas phase pO_2 of 20% of 152 mmHg. The oxygen environment of ESCs *in vivo* is much lower and with a pO_2 of approximately 3% (Simon and Keith, 2008). When ESCs were cultured at pO_2 levels similar to that experienced physiologically, they consumed more glucose and produced more lactate compared to those maintained at pO_2 of 20%. ESCs cultured at pO_2 of 20% also express decreased functional markers, OCT4, SOX2 and NANOG, than those maintained at lower pO_2 of 5%. This suggests that environmental pO_2 regulates energy metabolism and is intrinsic to the self-renewal of ESCs (Forristal et al., 2013). Culturing ESCs at reduced pO_2 favours self-renewal, while increased pO_2 favours differentiation and maturation (Powers et al., 2008). In this project, I will be studying the metabolism of MG by the glyoxalase system. Since MG is formed mainly by the degradation of triosephosphates in anaerobic glycolysis, characteristics of the ESC glyoxalase pathway – particularly flux of MG formation - may likely depend on the pO_2 of culture conditions where a low pO_2 of 3% may model most closely the ESC conditions and metabolic status *in vivo*.

In this project, I focus on the role of protein glycation by methylglyoxal in disease processes where my initial focus is on the disease setting where evidence of involvement is most well-developed – vascular complications of diabetes. The process of protein glycation in physiological systems is now described as background to the project.

1.3. Glycation

Protein glycation is the non-enzymatic reaction of proteins with saccharides and saccharide derivatives to form one or more glycation adducts. It occurs by a series of complex sequential and parallel reactions called the Maillard reaction (Thornalley, 2005b). Glycation of proteins by glucose occurs by reaction between N-terminal and lysine side chain free amino groups of proteins and the aldehyde group of the open chain form of glucose forming Schiff's base (Thornalley, 2008). The Schiff's base undergoes further rearrangement to form a stable Amadori product or fructosamine (Bookchin and Gallop, 1968). This is the early glycation stage of the glycation process and the early glycation adducts are Schiff's base and fructosamine. The Amadori intermediate product undergoes further rearrangements to form more stable irreversible compounds called advanced glycation endproducts (AGEs) (Rabbani and Thornalley, 2012c) - Figure 1.2.

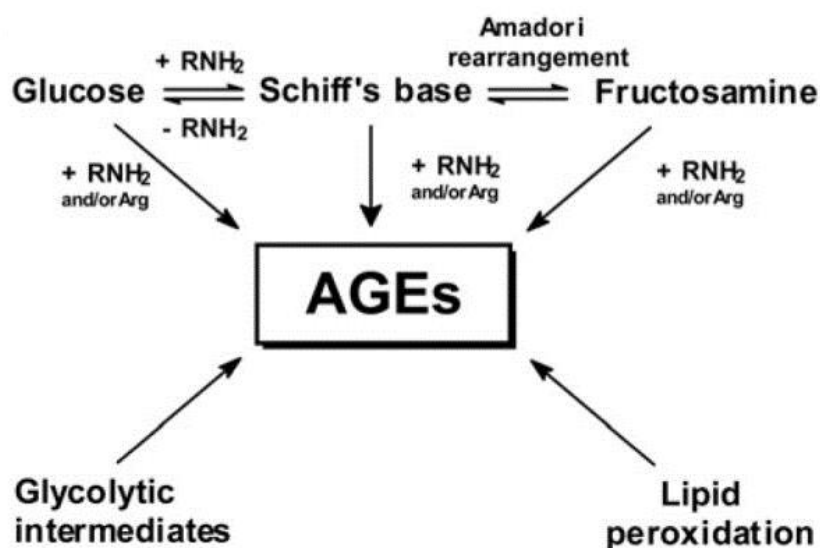


Figure 1.2: Mechanisms of formation of early glycation adducts and advanced glycation endproducts from glucose, glycolytic intermediates and lipid peroxidation (Rabbani and Thornalley, 2008).

The term AGE was first used in 1986 to refer to brown fluorescent pigments that cross link protein (Cerami, 1986). This is, however, contradictory; it is known that AGEs are formed in both early and advanced stages of glycation (Rabbani and Thornalley, 2012c). When glucose is not attached to a protein, the glucose may degrade to form α -oxoaldehydes. The α -oxoaldehydes are potent glycating agents which can form AGEs directly. In addition, the Schiff's base intermediate may also

degrade through non-Amadori rearrangement pathways to form AGEs. Glycolytic intermediates and lipid peroxidation may also form AGEs via production of α -oxoaldehydes. Thus, AGEs may be formed where Amadori intermediate is not a precursor as well as by glucose in both pre-Amadori and post-Amadori product reactions (Rabbani and Thornalley, 2012c).

Important AGEs quantitatively are hydroimidazolones derived from arginine residues modified by MG, glyoxal and 3-deoxyglucosone (3-DG): N_{δ} -(5-hydro-5-methyl-4-imidazolone-2-yl)ornithine (MG-H1), N_{δ} -(5-hydro-4-imidazolone-2-yl)ornithine (G-H1) and N_{δ} -[5-hydro-5-(2,3,4-trihydroxybutyl)-4-imidazolone-2-yl]ornithine (3DG-H) and related structural isomers. Other significant AGEs are: N_{ϵ} -(1-carboxyethyl)lysine (CEL), N_{ϵ} -carboxymethyl-lysine (CML), N_{ω} -carboxymethyl-arginine (CMA), S-carboxymethylcysteine (CMC), MG-derived lysine dimer 1,3-di(N_{ϵ} -lysino)-4-methylimidazolium salt (MOLD), glyoxal-derived lysine dimer 1,3-di(N_{ϵ} -lysino)imidazolium salt (GOLD) and the other protein cross links pentosidine and glucosepane (Rabbani and Thornalley, 2008).

1.3.1. Physiological glycation of proteins

Glycation of proteins is a continuous damaging process of the proteome in the living systems. Protein glycation is increased in diabetes due to increased glucose and other saccharides derivatives in plasma and at the sites of vascular complications. Metabolic dysfunction in vascular cells leads to increased formation of α -oxoaldehydes. This results in further damage in hyperglycaemia. AGEs have been found to accumulate at sites of vascular complications *in vivo* (Thornalley et al., 2003b). These AGEs may cause diabetic complications through impairment of protein function and protein-protein and enzyme substrate interactions by AGE residue formation and by increasing resistance to proteolysis of extracellular matrix proteins (Rabbani and Thornalley, 2012c).

Glycation free adducts are the main form in which protein glycation adducts are cleared from cells. In the cultured cells, the glycation free adducts increase in the culture medium with time, also, *in vivo* they are released into plasma and other body fluids to be eventually excreted in the urine. Glycation free adducts are filtered from plasma in the kidney and have high renal clearance (Ahmed and Thornalley, 2007).

1.3.2. Quantitation of protein glycation, oxidation and nitration adducts

The analysis of protein glycation, oxidation and nitration adducts requires the quantitation of multiple trace amounts of glycated, oxidised and nitrated amino acids (fmol – pmol) in the presence of 10^3 - 10^6 fold excess of related unmodified amino acid. This is the main challenge for any analytical methodology employed. In addition, the physiological samples are unstable to pre-analytic processing particularly under high pH and temperature. Thus, there is a possibility of the formation of glycation, oxidation and nitration adduct analytes during inappropriate sample processing. Protein glycation, oxidation and nitration adducts have been assayed by fluorescence (Vishwanath et al., 1986) and immunoassay (Wu and Steward, 1991, Yamamoto et al., 1989). However, the current gold standard is quantification by stable isotopic dilution analysis liquid chromatography-tandem mass spectrometry (LC-MS/MS) (Thornalley et al., 2003b).

In the LC-MS/MS methodology, protein glycation, oxidation and nitration adduct residues are determined after comprehensive enzymatic hydrolysis and filtering the protein glycation, oxidation and nitration free adducts in ultrafiltrates from physiological fluids using typically a 3 or 12 kDa cut-off microspin filter. Other techniques like immunoassay are more practicable for high sample throughput but the protocol and the particular sample matrix should be validated to the reference LC-MS/MS method before use (Thornalley et al., 2003b).

1.3.3. Dicarbonyl glycation of protein

There are reactive dicarbonyls in the physiological systems. The reactive dicarbonyls are known also as α -oxoaldehydes. They are important reactive intermediates of Maillard reaction and redirect minor but significant part of the flux of glycation reaction intermediates to form AGEs (Thornalley, 2005a). These α -oxoaldehydes are important saccharide derivatives participating in glycation in physiological setting of mammalian metabolism. They are potent glycating agents being 200 to 20,000 times more reactive than glucose to form AGEs directly. (Thornalley, 2005a). The dicarbonyls physiological concentrations are 10,000 to 50,000 times less than glucose; however, these reactive dicarbonyls remain important precursors of AGEs. The main dicarbonyls are MG, glyoxal and 3-DG - Figure 1.3. MG is an important dicarbonyl as it has relatively high glycation

reactivity directed mainly but not exclusively to arginine residues to form MG-H1 which is the most quantitatively prevalent AGE (Thornalley, 2005a).

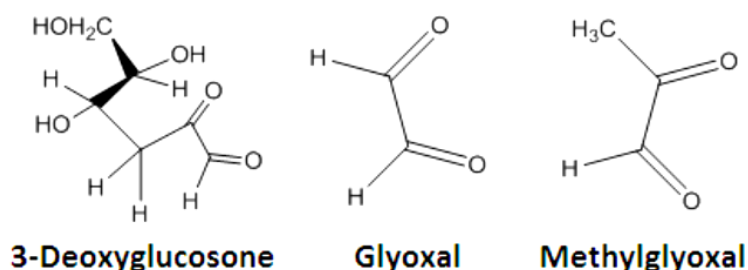


Figure 1.3: Molecular structure of the physiologically reactive glycating dicarbonyls 3-DG, glyoxal and methylglyoxal (Rabbani and Thornalley, 2008).

There are three forms of MG in aqueous solution under physiological conditions: monohydrate $\text{CH}_3\text{COCH}(\text{OH})_2$ (71%), dehydrate $\text{CH}_3\text{C}(\text{OH})_2\text{CH}(\text{OH})_2$ (28%) and the reactive unhydrated form CH_3COCHO (1%) (Dobler, 2008). AGE formation by MG causes protein modification mainly in arginine residues. This modification causes loss of side chain charge, structural derangement and function impairment (Thornalley, 2008). Examples are human serum albumin (Ahmed et al., 2005c), haemoglobin (Chen et al., 2005), type IV collagen (Dobler et al., 2006) and mitochondrial proteins (Morcos et al., 2008).

Glyoxal is formed in the physiological systems by auto-oxidation of glucose and lipid peroxidation (Thornalley, 2005a). Glyoxal targets arginine and lysine residues of proteins to form hydroimidazolone G-H1, CML, CMA and GOLD (Nangia-Makker et al., 1993, Lo et al., 1994b). Glycation of proteins by glyoxal leads to structural modification and impaired functions.

3-DG is a reactive glycating agent. The major source for 3-DG is degradation of fructoselysine to 3-DG by phosphorylation of fructosamine-3-kinase (F3K) (Beisswenger et al., 2003). 3-DG is also formed by degradation of fructose-3-phosphate formed by phosphorylation of fructose by F3K, and by glucose auto-oxidation (Thornalley, 2005a, Beisswenger et al., 2003). Elevated 3-DG levels are found in diabetes linked diabetic nephropathy (Beisswenger et al., 2003). Increased concentrations of 3-DG-derived hydroimidazolone were detected in the kidneys of diabetic patients and animals (Niwa et al., 1996, Karachalias et al., 2010). 3-DG reacts with lysine and arginine residues in proteins to form hydroimidazolones and pyrroline (Beisswenger et al., 2003, Thornalley et al., 2003b).

1.3.4. Dicarbonyl glycation of DNA

In addition to the proteins, DNA is also susceptible to glycation by MG and glyoxal. Deoxyguanosine (dG) is the most reactive nucleotide under physiological conditions (Thornalley et al., 2010). Excessive nucleotide glycation is associated with mutagenesis, cytotoxicity and DNA strand breaks (Thornalley, 1999). Nucleotide excision repair (NER) has been shown to suppress nucleotide glycation and its detrimental effects (Murata-Kamiya et al., 1998, Murata-Kamiya et al., 1999, Pischetsrieder et al., 1999).

1.4. Glyoxalase System

The glyoxalase system consists of two enzymes, glyoxalase 1 (Glo1) and glyoxalase 2 (Glo2), and a catalytic amount of reduced glutathione (GSH). The major function of these enzymes is detoxification of MG to D-lactate. The detoxification process consists of two sequential reactions: (i) the formation of S-D-lactoylglutathione (SLG) from the hemithioacetal formed non-enzymatically from MG and GSH, catalysed by Glo1; and (ii) the hydrolysis of SLG to D-lactate, catalysed by Glo2, with reformation of GSH consumed in the Glo1-catalysed step (Thornalley et al., 1989) – Figure 1.4.

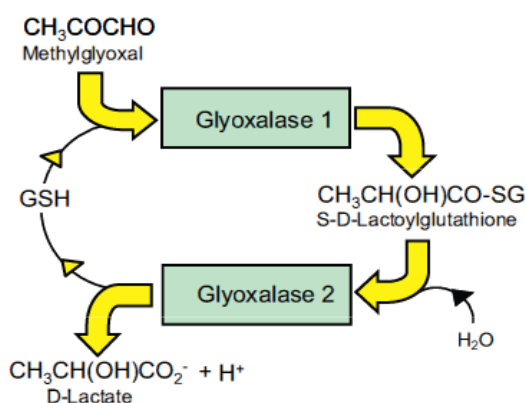
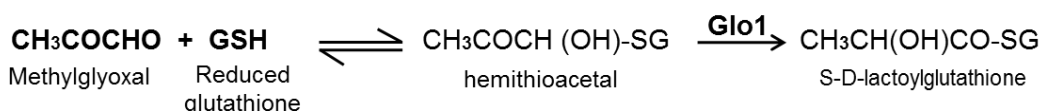


Figure 1.4: The Glyoxalase system (Rabbani and Thornalley, 2014b).

The glyoxalase system also catalyses the metabolism of other small, acyclic α -oxoaldehydes found in physiological systems: glyoxal (CHO)₂ – converted to glycolate via S-glycolylglutathione; hydroxypyruvaldehyde HOCH₂COCHO - converted to L-glycerate via S-L-glyceroylglutathione; and 4,5-dioxovalerate – converted to D-2-hydroxyglutarate via S-2-D-hydroxyglutarylglutathione (Clelland and Thornalley, 1991, Jerzykowski et al., 1973). MG is the Glo1 substrate of highest flux in physiological systems and hence the major substrate of the glyoxalase system.

The glyoxalase system has an important protective role found throughout biological life. That is, to prevent the accumulation of MG and related dicarbonyls in cells and body fluids to levels that potentially cause dysfunction and toxicity – the metabolic state of dicarbonyl stress (Xue et al., 2012, Rabbani et al., 2014b). The fundamental importance of this role is highlighted by the null mutation of *GLO1* is embryonically lethal (Arai et al., 2010). *GLO1* is a tumour suppressor gene - one of only 13 genes in genome-wide analysis (Zender et al., 2008). Inducers of GLO1 are prospective therapeutic agents for the prevention of cancer, dyslipidemia and cardiovascular disease, treatment of vascular complications of diabetes and food supplements for healthy ageing. Inhibitors of GLO1 are prospective anti-cancer and anti-microbial agents – particularly for GLO1 overexpression-linked multidrug resistance tumours and micro-organisms. The *GLO1* gene is a hotspot of copy number variation in the human and mouse genomes although the prevalence is low, 1 – 2%. Increased plasma concentration of MG associated with increased modification of protein and DNA is found in obesity, diabetes, renal failure and ageing, suggesting that dicarbonyl stress is a feature of these high prevalence abnormal physiological states and disease – of increasing importance in the current increased aged populations of Westernised countries (Rabbani et al., 2014b). Improved understanding of the function and regulation of the glyoxalase system may help characterise the role of dicarbonyl stress in disease and ageing and thereby develop improved therapeutics for prevention and treatment of disease and increase human healthspan.

1.4.1. History of glyoxalase system

The glyoxalase system was discovered in the early 20th century. It was described in the physiological system as an enzymatic process that catalyses the conversion of MG to lactate (Neuberg, 1913). Concurrently Dakin and Dudley (Dakin and Dudley, 1913) published the discovery of glyoxalase and nine further papers on glyoxalase and related studies.

Neuberg devoted himself to strengthen the role of methylglyoxal and glyoxalase in mainstream glycolysis (Neuberg, 1929). Embden opposed Neuberg's view because he found that glycolysis produced only the L-enantiomer of lactic acid whereas with addition of methylglyoxal to tissues he found both L- and D- lactic acid. Embden discovered and postulated alternative glycolytic intermediates and pathway, later confirmed by Meyerhof, which are now accepted as mainstream glycolysis in the pathway that bears their names – Embden-Meyerhof pathway (Embden et al., 1933, Meyerhof, 1933). In the 1930s – 1950s advances were made that characterised the essential aspects of the glyoxalase system that we know today. Lohmann discovered glutathione (GSH) which was a specific and essential cofactor for methylglyoxal metabolism by the glyoxalase system (Lohmann, 1932). Jowett and Quastel presented evidence that GSH and methylglyoxal combined reversibly to form a hemithioacetal substrate of the glyoxalase system (Jowett and Quastel, 1933) Yamazoye found that the hemithioacetal was converted to a novel acid-stable base-labile intermediate – now known to be S-D-lactoylglutathione (Yamazoye, 1936) Gowland-Hopkins and J Morgan found wide distribution of the glyoxalase in living organisms (Hopkins and Morgan, 1945). In 1951, Racker discovered that there are two major sequential steps in the catalysis process including GLO1 and GLO2 (Racker, 1951). In 1954, he also suggested that D-lactate was the terminal product of metabolism of MG by glyoxalase system rather than L-lactate (Racker, 1954). This was confirmed later in 1973 (Ekwall and Mannervik, 1973). In 1960, human arterial tissue were showed with decrease GLO1 activity with age (Kirk, 1960), which might be associated with increased risk of cardiovascular disease with ageing.

With the role of MG and glyoxalase in glycolysis discounted, investigators speculated on the functions of the glyoxalase system. In 1963, Szent-Gyorgyi proposed that the conflict of MG and GLO1 controlled cell growth and could be exploited for treatment of cancer. MG was hypothesised to be a growth retarding substance or “retine” and GLO1 a counter to this growth restriction effect or

“promine” (Szent-Gyorgyi et al., 1963). The discovery of many other growth factors and change of cell responsiveness to them on malignant transformation led to the redundancy and demise of this hypothesis. High concentrations of MG were toxic to tumour cells and in 1969 Vince and Wadd suggested GLO1 inhibitors may be more effective anticancer agents, producing toxicity through accumulation of endogenous MG (Vince and Wadd, 1969).

In the 1970s – 1990s, glyoxalase enzymes were purified and molecular, kinetic, mechanistic and structural characteristics identified. Distinctive molecular characteristics of mitochondrial matrix and cytosolic GLO2 were also identified, originating from one gene in mammals by mRNA splicing. This culminated with catalytic mechanisms of action and crystal structures of human of GLO1 and GLO2 (Marmstal et al., 1979, Rhee et al., 1987, Allen et al., 1993, Schimandle and Vander Jagt, 1979, Uotila, 1973, Landro et al., 1992, Cameron et al., 1997, Cameron et al., 1999, Cordell et al., 2004).

In 1972, Bonsignore *et al.* presented the first evidence that a triosephosphate, glyceraldehyde-3-phosphate, degraded non-enzymatically under physiological conditions to form MG (Bonsignore et al., 1972). In 1977, Takahashi reported that MG and other dicarbonyls reacted mainly with arginine residues of proteins and a hydroimidazolone was one molecular structure proposed for the adducts formed (Takahashi, 1977). This was later found to be predominant adduct, hydroimidazolone MG-H1 (Ahmed et al., 2002, Henle et al., 1994, Thornalley et al., 2003b).

The glyoxalase system was linked to diabetes by Thornalley in 1988 who discovered the increased formation of MG in the red blood cells which were cultured in a high glucose medium *in vitro* (Thornalley, 1988). In 1989, the increased activity of Glo1 in red blood cells and tissues of streptozotocin (STZ)-induced diabetic and obese (ob/ob) mice was reported by Thornalley and Atkins (Atkins and Thornally, 1989, Atkins and Thornalley, 1989). In the same year, the concentrations of MG, S-D-lactoylglutathione and D-lactate in blood samples were compared between healthy people and patients with diabetes, and it was reported that all three components were higher in diabetes (Thornalley et al., 1989). In 1991, *GLO1* was found to be a genetic factor linked to body mass index and a feature of the human obesity genome (Wilson et al., 1991).

In 1993, studies by Phillips and Thornalley indicated that the major source of formation of MG in mammalian metabolism is the spontaneous degradation of triosephosphates; *ca.* 0.1% glucotriose flux degraded to MG (Phillips and Thornalley, 1993). In 1994, it was reported that MG is one of the major glycating agents that forms AGEs (Lo et al., 1994b). In addition, the inhibition of MG by aminoguanidine was one of the solutions that reduced the formation of AGEs in order to prevent the development of cardio-vascular complications in diabetes (Lo et al., 1994a).

In 1998, Shinohara *et al* reported that the overexpression of GLO1 in endothelial cells *in vitro* prevented the increase of MG accumulation and formation of AGEs respectively (Shinohara et al., 1998). Abordo and colleagues noticed that there was increased accumulation of MG in the cell culture in the presence of oxidative stress and reported the accumulation of α -oxoaldehydes during oxidative stress (Abordo et al., 1999). In the same year, it was reported that the increase of plasma MG concentration in patients with type 2 diabetes is less marked with treatment by metformin, an oral hypoglycaemic agent (Beisswenger et al., 1999). Furthermore, analysis of human *GLO1* gene promoter was reported and revealed presence of an insulin response element which likely produces disturbed GLO1 expression in the diabetic state (Ranganathan et al., 1999).

Between the years 1989- 2003, several studies showed decrease in GLO1 and GLO2 activities and increase in MG- and glyoxal-derived AGEs with age in human tissues, mouse tissues and cells (McLellan and Thornalley, 1989, Dunn et al., 1989, Dunn et al., 1991, Haik Jr et al., 1994, Ahmed et al., 1997, Sharma-Luthra and Kale, 1994). In 2003, it was reported that MG-derived AGEs were major type of protein damage *in vivo* based on high flux on urinary excretion of these adducts (Thornalley et al., 2003b).

In 2006, Redon and colleagues constructed a copy number variation (CNV) map of the human genome and found that *GLO1* was a hotspot for CNV increase (Redon et al., 2006). In 2008, *Glo1* was presented as a *vitagene* for the first time by Morcos who demonstrated that overexpression of *Glo1* in *Caenorhabditis elegans* increases median and maximum lifespan by *ca.* 30% (Morcos et al., 2008). In addition, Morcos *et al.* showed that silencing of *Glo1* decreased the life span by *ca.* 50% (Morcos et al., 2008). Cahan and colleagues showed that the non-transcribed region of *Glo1* gene was an important site of functional increase of CNV in the

mouse genome resulting in 4-fold changes in expression of Glo1 (Cahan et al., 2009).

In 2010, Brouwers with co-workers showed that Glo1 overexpression prevented oxidative stress and impairment of endothelium dependent vasorelaxation in mesenteric arteries of diabetic rats. This implied to the increased MG in the diabetic state in induction of vascular dysfunction and oxidative stress (Brouwers et al., 2010, Brouwers et al., 2011). In the same year, it was showed that methylglyoxal-derived DNA imidazopurinone adducts are major markers of physiological damage to genome linked to DNA instability *in vivo* (Thornalley et al., 2010). Santarius his colleagues showed that *GLO1* gene is amplified in human tumours and linked to multidrug resistance (Santarius et al., 2010).

In 2012, a functional antioxidant-response element (ARE) was identified in the 5' -untranslated region of exon 1 of the mammalian *GLO1* gene. Nrf2 transcriptional factor (nuclear factor-erythroid 2 p45 subunit related factor 2) binds to this ARE region, increasing basal and inducible expression of GLO1. Furthermore, the expression of mRNA and protein of GLO1 as well as GLO1 activity were increased by Nrf2 Activators (Xue et al., 2012). This now provides a strategy for design and development of GLO1 inducers from dietary bioactive compounds. These compounds improve health span and synthetic GLO1 inducers for pharmaceuticals in prevention and treatment of some diseases.

The current era of investigation focus on regulation of the glyoxalase system where a role in ageing and disease, physiological stress and drug resistance and development of healthier foods and new pharmaceuticals are emerging.

1.4.2. Glyoxalase 1

1.4.2.1. Kinetic characteristics and molecular properties

Glyoxalase 1 (EC 4.4.1.5; GLO1) catalyses the isomerisation of the hemithioacetal, formed spontaneously from methylglyoxal CH_3COCHO and GSH to S-D-lactoylglutathione $\text{CH}_3\text{CH}(\text{OH})\text{CO-SG}$:



For the MG-GSH hemithioacetal and human GLO1, the K_M is 71-130 μM and the k_{cat} is $7-11 \times 10^4 \text{ min}^{-1}$. The major physiological substrate for GLO1 is MG

and this accumulates markedly when GLO1 is inhibited *in situ* by cell permeable Glo1 inhibitors and by depletion of GSH (Thornalley, 1993, Abordo et al., 1999, Thornalley et al., 1996). Other substrates are glyoxal – formed by lipid peroxidation and the fragmentation of glycated proteins, hydroxypyruvaldehyde HOCH₂COCHO and 4,5-doxoalate H-COCOCH₂CH₂CO₂H (Thornalley, 1993, Thornalley, 1998). GLO1 and the glyoxalase system prevent the accumulation of these reactive α -oxoaldehydes in cells and body fluids *in vivo* and thereby suppresses α -oxoaldehyde-mediated glycation reactions (Shinohara et al., 1998). It is a key enzymatic system of the enzymatic defence against glycation (Thornalley, 2003b, Thornalley, 2003a).

There is characteristic expression of GLO1 in all mammalian tissues (Thornalley, 1991). GLO1 activity in human tissues was 30 – 150 mU per mg protein; it was highest in the pancreas, lung, kidney and brain and lowest in the liver and adipose tissue. The specific activity of GLO1 in foetal tissue is *ca.* 3 times higher than corresponding adult tissue (Larsen et al., 1985). Glo1 activity in rat tissues was 42 – 165 mU per mg wet weight; it was highest in the liver and muscle, and lowest in the nerve and lens (Phillips et al., 1993). Glo1 activity in mouse tissues was 1 – 10 U per mg protein; it was highest in the liver, kidney and brain and lowest in the nerve and lungs (Bierhaus et al., 2012).

Human GLO1 is a dimeric protein of molecular mass 42 kDa (by sequence, 46 kDa by gel filtration chromatography), isoelectric point (pI) value 4.8 - 5.1 and contains one zinc ion per subunit. There are two active sites per protein formed by amino acid residues from each of the subunits such that the monomer is inactive. The human *GLO1* gene is diallelic, which expressed in heterozygotes. The two alleles, *GLO¹* and *GLO²*, give two similar subunits and three dimer allozymes, GLO 1-1, GLO 1-2, GLO 2-2. The difference in amino acid between the expression products of the two GLO1 alleles is only at position 111. There is an alanine residue in subunit GLO1-A and a glutamic acid residue in subunit GLO1-E (Kim et al., 1995). All human allozymes have similar mass but different charge density and/or their molecular shapes. They can be resolved by non-denaturing gel electrophoresis and by ion exchange chromatography (Thornalley, 1993).

The human GLO1 translation product contains 184 amino acids. In the post-translational process, the N-terminal methionine is removed and the N-terminal alanine thereby produced is acetylated. Cysteine residues C19 and C20 are linked by

vicinal disulfide bridge. C139 may form an intra-molecular disulfide with C61. If a mixed disulfide with GSH forms on C139 *in vitro*, enzymatic activity is inhibited (Birkenmeier et al., 2010). GLO1 activity is not affected by the oxidation state of C19/C20 and N-terminal acetylation. There is also acetylation of human GLO1 at K148 which is likely de-acetylated by cytosolic sirtuin-2 (Lundby et al., 2012, Rauh et al., 2013). The modification of GLO1 by S-nitrosylation occurs by reaction with nitric oxide (NO) on C139. The oxidative state of C19 and C20 is influential in S-nitrosylation process. The NO-responsive form of GLO1 is the basic, reduced form of GLO1 without intramolecular disulfide bonding at C19 and C20 (De Hemptinne et al., 2007). GLO1 is a substrate for calcium and calmodulin-dependent protein kinase II. It may be phosphorylated at T107 which occurred preferentially on the reduced and NO-responsive form (De Hemptinne et al., 2007).

Glo1 present in other mammalian species is similar to the human GLO1. Mammalian, bacterial and plant Glo1 enzymes is usually dimeric. However, Glo1 of the yeast (*Saccharomyces cerevisiae* and *Schizosaccharomyces pombe*) is a monomer of 32 and 37 kDa, respectively, with two copies of a segment equivalent to the monomer of human GLO1. The sequence identity of human GLO1 with Glo1 of bacterial *Pseudomonas putida* is 55% and with yeast *Saccharomyces cerevisiae* Glo1 between residues 1-182 and 183-326 is 47% (Thornalley, 2003b). This suggests that GLO1 of different origins may have arisen by divergent evolution from a common ancestor (Xue et al., 2011).

The structure of human GLO1 in complex with *S*-benzylglutathione was determined to 2.2 Å resolution – Figure 1.5. Each monomer consists of two, structurally equivalent domains. The active site is situated in the dimer interface, with the inhibitor and essential Zn²⁺ ion interacting with side chains from both subunits. The zinc binding site is two structurally equivalent residues from each domain – Gln33A, Glu99A, His126B, Glu172B and two water molecules in octahedral coordination (Cameron et al., 1997).

The mechanism proposed for the reaction catalysed by GLO1 is that the isomerisation of MG-GSH hemithioacetal to *S*-D-lactoylglutathione - involves base-catalysed shielded-proton transfer from C1 to C2 of the hemithioacetal, bound in the active site, to form an enediol intermediate and rapid ketonisation to the thioester product. Both *R*- and *S*-forms of the hemithioacetal are bound in the active site of GLO1 and are therein deprotonated; the subsequent reprotonation of the putative

enediol intermediate occurs stereospecifically to form the *R*-2-hydroxyacyl-glutathione derivative. It has been proposed that Glu172 is the catalytic base for the *S*-substrate enantiomer and Glu99 the catalytic base for the *R*-substrate enantiomer. Both reaction mechanisms form *cis*-enediol intermediate coordinated directly to the Zn²⁺ ion: this is deprotonated to a *cis*-enediolate by Glu-172 which then reprotonates C2 stereospecifically to form the *R*-2-hydroxyacylglutathione product (Himo and Siegbahn, 2001)– Figure 1.5. Glu111 or Ala111 is not involved in the catalytic mechanism, consistent with the allozymes of GLO1 having similar kinetic characteristics. The characteristics of human GLO1 are summarised in Table 1.6.

Table 1.6: Characteristics of human glyoxalase 1. (Rabbani et al., 2014b)

Characteristic	Glyoxalase 1
Molecular mass	46 kDa (gel filtration) or 42 kDa (sequence)
No of subunits and structure	Two. Monomers consists of 2 structurally equivalent domains with the active site in the dimer interface
pI	4.8 - 5.1
Prosthetic groups	Zn ²⁺
Reaction catalysed and kinetics	CH ₃ COCH(OH)-SG → CH ₃ CH(OH)CO-SG K _M = 192 μM, k _{cat} = 1.1 x 10 ⁵ min ⁻¹
Genetics and polymorphism	<i>GLO1</i> . Locus: 6p21.2. Polymorphism: A/E111 - <i>GLO1/GLO2</i> (common); frameshift mutation (rare). Hotspot for CNV.
Transcriptional regulatory elements	MRE, IRE, E2F4, AP-2α, ARE, HIF1α

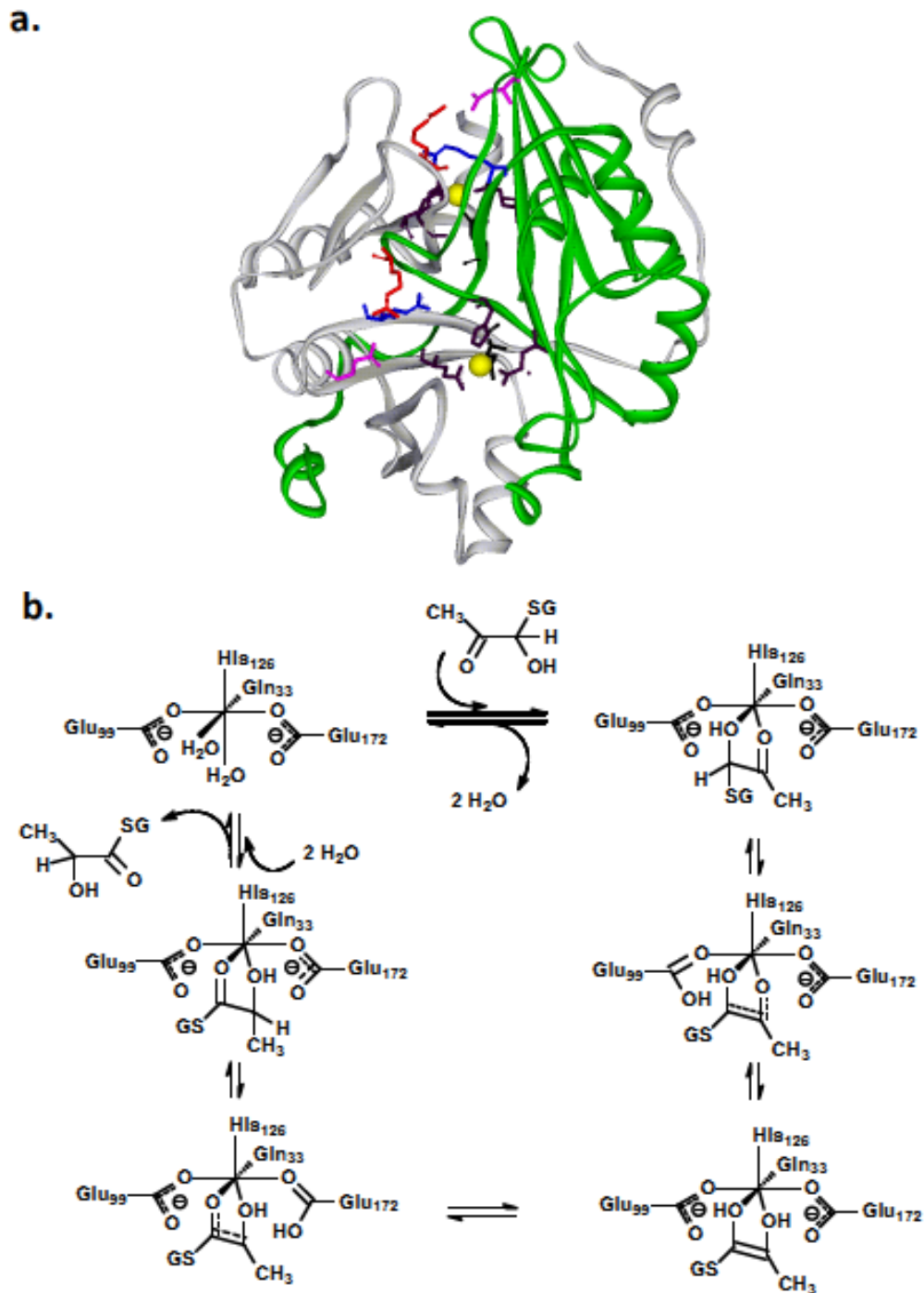


Figure 1.5: Structure and catalytic mechanism of glyoxalase 1.

a. Solid ribbon representation of the crystal structures of human glyoxalase 1 Subunits, A (grey ribbon) and B (green ribbon), Zinc ions (yellow balls) and coordinating amino acid residues Gln33A, Glu 99A, His126B and Glu172B (black sticks) and GSH moiety binding site (Arg37, Asn103 and Arg122 – blue, pink and red sticks) are shown. **b.** Catalytic mechanism of human glyoxalase 1 for the isomerisation of the R-hemithioacetal – from (Thornalley, 2003b).

1.4.2.2. Genetics

The GLO1 enzyme is produced by expression of the *GLO1* gene. Human *GLO1* is a diallelic gene inherited in a simple co-dominant manner. It is located in chromosome 6 at locus 6p21.2 (38,675,926 - 38,703,176). Gene cloning showed that *GLO1* consists of 27,251 bp (Tripodis et al., 1998). It is comprised of five introns and six exons (Gale and Grant, 2004). Bioinformatics analysis of human *GLO1* showed 70 single nucleotide polymorphisms (SNPs): 6 in the 5' UTR, 60 in introns, 3 in the 3' UTR and one within the coding sequence Ala111Glu phenotypic variation. The amino acid substitution Ala111Glu was predicted to be tolerant. A claimed association of this polymorphism with autism could not be confirmed (Junaid et al., 2004, Rehnström et al., 2008), nor association with vascular complications of diabetes (McCann et al., 1981, McLellan et al., 1994). There is a suggestion, however, that the Glu111Glu homozygote in stage 5 renal failure on hemodialysis is associated with increased prevalence of cardiovascular disease (CVD) and peripheral vascular disease (Kalousová et al., 2008). Multiple alternative transcription start sites and alternative 3' UTRs were found and ubiquitous expression of *GLO1* confirmed. Conserved regulatory regions were predicted 5' to the transcription start site and in the distal promoter, and several predicted conserved transcription regulatory elements were suggested in the 5'UTR - Figure 1.6. Six different *GLO1* transcripts were identified. None produced insertion or deletion of amino acids in the expression product. No splice variants have been reported so it is likely that *GLO1* does not display alternative exon splicing.

Murine *Glo1* is located in chromosome 17 a3.3 and consists of 19,793 bp (30,592,866-30,612,659) (Meo et al., 1977). It has a similar genomic structure to human *GLO1*.

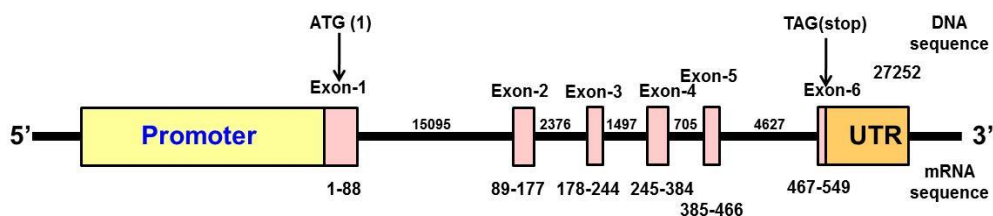


Figure 1.6: Human *GLO1* gene.

The figure shows the domain structure of the human *GLO1* gene (Yellow: promoter region, Pink: exon, Orange: untranslated region (UTR)) (Shafie et al., 2014).

Human and murine *GLO1* genes are hotspots for functional copy number increase. The human *GLO1* promoter region is 982 bp and contains several regulatory elements:

- (i) Metal responsive element (MRE) at -647 to -641 bp (TGCACTC) (Ranganathan et al., 1999).
- (ii) Insulin response element (IRE) at -849 to -842 bp (GAGGCGGG) – glyceraldehyde-3-phosphate dehydrogenase IRE-A like motif (Ranganathan et al., 1999, O'Brien et al., 2001).
- (iii) E2F – binding to transcription factor E2F4 (Conboy et al., 2007),
- (iv) Activating enhancer binding protein 2 alpha (AP-2 α) (Orso et al., 2010).
- (v) Antioxidant response element (ARE) (Xue et al., 2012).

IRE and MRE functionalities were validated in reporter assays where insulin and zinc chloride exposure produced a 2-fold increased transcriptional response (Ranganathan et al., 1999). Similar functional activities were shown for E2F, AP-2 α and ARE. Promoter analysis suggests also a glucocorticoid responsive element (GRE) at -368 to -363 bp (Ranganathan et al., 1999) and a functional *GLO1* hypoxia response element (HRE) is at -131 to -125 bp (TGACTCA) (Xue and Thornalley, P.J., unpublished). Functional activity was not found for the GRE (Ranganathan et al., 1999) but was found for the HRE where hypoxia decreased expression of *GLO1* (Zhang et al., 2012).

1.4.2.3. Change of glyoxalase 1 expression and activity in health and disease

GLO1 expression and activity are modified in ageing and disease. There was a marked decline of *Glo1* expression and activity in *Caenorhabditis elegans* with age. Overexpression of *Glo1* increased median and maximum lifespan whereas *Glo1* silencing decreased median and maximum lifespan. There was little change in *Glo1* activity during the lifespan of mice, except for an increase in *Glo1* activity of the kidney with age. *Glo1* activity of rat tissues decreased with age, however, there was further decreased by hypoxia in young rats. Glyoxalase activity was decreased in arterial tissues with age and in lens, brain and age-fractionated red blood cells – Table 1.7.

Table 1.7: Effect of ageing on glyoxalase 1 expression and activity.

Species	Effect on glyoxalase	Reference
<i>Caenorhabditis elegans</i>	Decrease 90% from young (1 day) to old (12 days). Overexpression of Glo1 increased median lifespan by 29% and maximum lifespan by 32% and Glo1 silencing decreased median lifespan by 52% and maximum lifespan by 36%.	(Morcos et al., 2008)
Mice	Glo1 activity varied little (5 – 10%) in liver and spleen and increased in kidney to maximum level at 24 months.	(Sharma-Luthra and Kale, 1994)
	Glo1 activity decreased in liver and lung of old (25 months) versus young (2 months) rats. Hypoxia decreased Glo1 activity in liver and lung of young rats but increased Glo1 activity in liver of old rats. Hyperoxia increased Glo1 activity of the liver.	(Amicarelli et al., 1997)
Rats	Glo1 protein decreased in skeletal muscle of old (18 and 30 months) versus young (7 months) rats	(Piec et al., 2005)
Human subjects	Glyoxalase1 activity decreased 30 – 50% in thoracic aorta and pulmonary artery from age 10 – 80 years.	(Kirk, 1960)
	Age-dependent decrease in GLO1 activity and protein of lens	(Haik Jr et al., 1994, Mailankot et al., 2009)
	GLO1 activity decreased <i>ca.</i> 20% in old, high density fraction of red blood cells.	(McLellan and Thornalley, 1989)
	GLO1 activity tends to decrease >55 years old in brain.	(Kuhla et al., 2006)

GLO1 has been studied most intensively in diabetes in relation to suppression of increased MG concentration in hyperglycaemia and the link of this to the development of microvascular complications of diabetes (nephropathy, retinopathy and neuropathy) and macrovascular complications (cardiovascular disease and stroke). In experimental diabetes, there is a tissue-specific decrease in Glo1 expression and activity. In STZ induced-diabetic mice, Glo1 was down regulated in the sciatic nerve and kidney (Bierhaus et al., 2012). Glo1 expression was also decreased in the kidney of obese (db/db) diabetic mice (Barati et al., 2007) and STZ diabetic Wistar rats (Palsamy and Subramanian, 2011), and decreased in the kidney and liver of STZ diabetic Sprague-Dawley rats (Phillips et al., 1993). Glo1 expression was also decreased *ca.* 50% in STZ diabetic Ren-2 rats which overexpressing the renin-angiotensin system in extra renal tissues (Miller et al., 2010). In STZ diabetic C57BL/6 mice, Glo1 protein of peripheral nerve was decreased *ca.* 70% compared to non-diabetic controls, whereas STZ diabetic A/J mice with higher endogenous expression of Glo1 linked to *Glo1* gene duplication was not decreased compared to non-diabetic controls (Jack et al., 2011, Bierhaus et al., 2012). In contrast to this, Glo1 activity was increased 50–60% in red blood cells of STZ diabetic C57BL/6 mice, compared to non-diabetic controls (Atkins and Thornally, 1989); and Glo1 activity was increased 30 – 40% in red blood cells of patients with type 1 diabetes and patients with type 2 diabetes, compared to healthy control subjects (McLellan et al., 1994). This may suggest that red blood cell precursor cells respond to dicarbonyl stress in diabetes and upregulate Glo1 expression, carried forward during maturation lineage to red blood cells, whereas in the kidney, retina and peripheral nerve Glo1 expression and/or stability is impaired and pre-disposes these tissues to dicarbonyl stress. Patients with diabetes and microvascular complications including nephropathy, retinopathy and neuropathy had significantly higher activity of the Glo1 in red blood cells compared to patients without complications (McLellan and Thornalley, 1994). The increased activity of Glo1 appears to be a response and marker of exposure to elevated cellular MG concentration. If so, patients with vascular complications may have had higher exposure to increased MG levels than uncomplicated patients.

Overexpression of Glo1 in transgenic rats and mice prevented the development of nephropathy, retinopathy and neuropathy (Giacco et al., 2014, Berner et al., 2012, Bierhaus et al., 2012, Brouwers et al., 2014). There are also limited studies on the involvement of Glo1 in diabetes development. Administration of cell permeable Tat peptide-Glo1 fusion protein protected against the development of STZ-induced diabetes in mice (Kim et al., 2013) and studies from our group found that Glo1 activity was unchanged but MG concentration increased *ca.* 30% in the pancreas in the high fat diet-fed mouse model of insulin resistance and type 2 diabetes development (Tym A, 2014). Increasing Glo1 expression may have benefit in prevention of diabetes.

GLO1 expression and activity has been studied in neurological disorders. In Alzheimer's disease (AD), GLO1 mRNA and protein in brain cerebral cortex were moderately increased in early-stage disease and decreased in advanced disease of patients with AD, compared to age-matched controls (Kuhla et al., 2007, Chen et al., 2004). Glo1 protein was increased in the cerebellum of the 3 x Tg AD mouse model of Alzheimer's disease which expresses mutant presenelin-1-M146V, amyloid precursor protein_{swe}, and tau protein-P301L transgenes and progressively develops plaques and neurofibrillary tangles with a temporal- and region-specific profile that resembles the neuropathological progression of Alzheimer's disease (Ciavardelli et al., 2010). Increased Glo1 protein was also found in the brains of the P301L mutant tau transgenic mice model which develops neurofibrillary tangles, a histopathologic hallmark of AD and frontotemporal dementia (Chen et al., 2004). In a mouse model exploring mechanisms of Parkinson's disease, mice deficient in α -synuclein had increased Glo1 mRNA, protein and activity in the brain stem/mid brain and cortex, compared to wild-type controls. There was also increased MG concentration. This suggests that α -synuclein may have a role in regulating processes that suppress MG formation and deletion of this imposes dicarbonyl stress inducing stress responsive increased expression of Glo1 (Kurz et al., 2011).

GLO1 has also been studied in mood-affective disorders. A rare frame shift mutation of *GLO1* producing a non-functional truncated peptide and *ca.* 50% decreased Glo1 activity in heterozygotes was associated with severe Schizophrenia, although to date only 3 cases have been detected (Arai et al., 2010). *GLO1* mRNA of peripheral blood leukocytes was decreased in major depressive and bipolar disorder

patients, compared with healthy control subjects patients in remission (Fujimoto et al., 2008).

Glo1 expression has a bewildering link with anxiety. Independent research teams found decreased and increased Glo1 linked to anxiety states in mouse models (Hovatta et al., 2005, Kroemer et al., 2005). Anxiety was then linked to strains of mice with increased Glo1 expression through *Glo1* gene duplication (Williams et al., 2009) but then an independent group inadvertently introduced *Glo1* duplication into a mouse model and found no abnormal anxiety state (Kollmannsberger et al., 2013). In these and related studies brain content of MG has been often overestimated – reviewed in (Rabbani and Thornalley, 2014c) and hence there remains uncertainty on the link of Glo1 with anxious states – as reviewed (Thornalley, 2006).

There is an emerging role of GLO1 in vascular function and CVD. A large cohort study of over 90,000 cases and control studying gene expression associations genome-wide found decreased GLO1 was a driver for CVD (Mäkinen et al., 2014). Experimental inhibition of Glo1 increased atherosclerotic plaque development in ApoE deficient mice (Tikellis et al., 2014). There is an evidence that GLO1 overexpression preserves cardiac function post-myocardial infarction through increase of vascularity and prevention of cardiomyocyte apoptosis (Blackburn et al., 2013). A contributory factor to GLO1 involvement in vascular disease may be down regulation in hypoxia linked to tissue ischemia (Zhang et al., 2012). With decreased tissue oxygenation, there will also be an increased roll for anaerobic glycolysis and increased MG formation. Overexpression of GLO1 in bone marrow cells and in endothelial cells also increased angiogenesis (Ahmed et al., 2008, Vulesevic et al., 2014).

GLO1 has a historical link to cancer research through studies of Szent-Gyorgyi, Vince and others – reviewed in (Thornalley and Rabbani, 2011). Contrary to earlier views, overall human tumour cell lines do not have higher GLO1 activity than non-malignant cells *in vitro* (Ayoub et al., 1992). Some tumour cell lines had high GLO1 activity and were multidrug resistant but sensitive to the GLO1 cell permeable inhibitor, S-p-bromobenzylglutathione cyclopentyl diester BrBzGSHCP₂ (Sakamoto et al., 2000, Sakamoto et al., 2001)- Figure 1.7. Studies by Santarius *et al.* suggested that increased GLO1 expression in some human tumours is due to *GLO1* gene amplification (Santarius et al., 2010). GLO1 overexpression is also

acquired by oncogene-linked malignant transformation (Young et al., 2004) and chronic treatment with antitumor agents (Yang et al., 2008).

End-stage renal disease (stage 5 chronic kidney disease (CKD)) is where patients suffer the most profound increase in MG concentration – up to 8-fold (Agalou et al., 2002, Rabbani and Thornalley, 2012b) – yet little is known of GLO1 activity. In patients on haemodialysis, the activity of GLO1 in red blood cells was increased 21% (Mann et al., 1999). Decreased GLO1 activity in rare *GLO1* frameshift mutation heterozygote human subjects was associated with decreased glomerular filtration rate (Ikeda et al., 2011). A patient with renal failure and very low GLO1 activity had a high occurrence of CVD events (Miyata et al., 2001). In experimental studies, over expression of Glo1 in rats decreased development of renal senescence in ageing (Ikeda et al., 2011).

There are other conditions that have noticeable effects on Glo1 expression. For example, mouse ESCs showed decreased expression of Glo1 under hypertonic stress (Mao et al., 2008). In the macrophages, the inflammatory signalling of lipopolysaccharide via the Tol-4 receptor induced increased expression of GLO1 which is thought to be part of the anti-stress gene response to endotoxaemia (Du et al., 2010). This might suggest that regulation of GLO1 is part of the anti-inflammatory, anti-stress gene response.

In several diseases, therefore, GLO1 expression and activity is decreased. The mechanisms underlying this are often uncertain. The following may apply:

(i) **Down regulation by receptor for advanced glycation endproducts (RAGE)**

GLO1 down regulation was linked to activation of the receptor for advanced glycation endproducts (RAGE) which is involved in pro-inflammatory signalling and the development of vascular complications of diabetes. These findings were supported by using RAGE knockout mice which did not develop diabetic neuropathy nor neuronal deficiency of Glo1. Furthermore, when the RAGE knockout mice treated with BrBzGSHCp₂, the cell permeable Glo1 inhibitor (Figure 1.7), the mice developed diabetic neuropathy (Konrade et al., 2006). Other studies in experimental diabetic nephropathy and liver regeneration have supported a link between RAGE and Glo1 down regulation (Reiniger et al., 2010, Zeng et al., 2012).

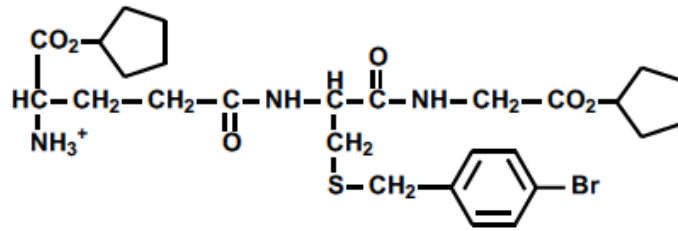


Figure 1.7: S-p-bromobenzylglutathione cyclopentyl diester structure (Thornalley and Rabbani, 2011).

(ii) Increased proteolysis of GLO1 protein

Incubation of human aortal endothelial cells in high glucose concentration media *in vitro* decreased GLO1 protein and activity without change in *GLO1* mRNA. Irshad *et al.* reproduced these findings and found that GLO1 decrease was linked to increased ubiquitination and proteolysis (Irshad Z, 2014). High glucose concentration increased the expression of RAGE and other inflammatory proteins. These elevations were normalized by GLO1 overexpression (Yao and Brownlee, 2010).

(iii) Down regulation of Nrf2 signalling

Both basal and inducible expression of GLO1 are regulated by Nrf2 (Xue et al., 2012). Therefore, physiological and disease states that impair Nrf2 signalling may likely decrease GLO1 expression and disease states that increase Nrf2 signalling may likely increase GLO1 expression. An example of decreased Nrf2 activity is inflammatory signalling by the NF- κ B system which conflicts with and counters Nrf2 signalling (Liu et al., 2008). This may occur through several mechanisms, one of which is competition for CREB binding protein by the two signalling systems (Ahmed et al., 2014) - Figure 1.8.

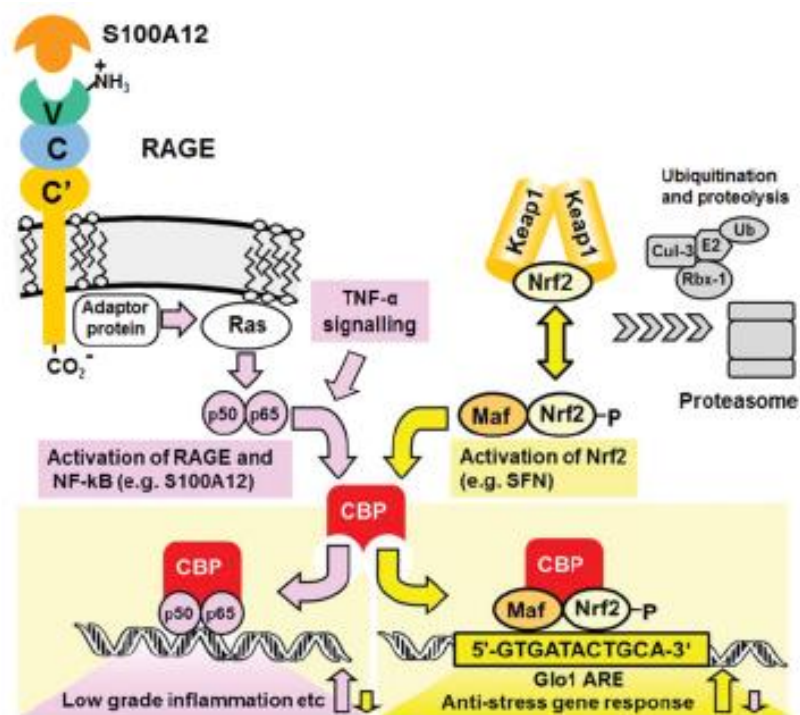


Figure 1.8: An example of how activation of the NF-κB system via RAGE may conflict with the Nrf2 system to down regulate GLO1 expression (Ahmed et al., 2014).

1.4.3. Glyoxalase 2

1.4.3.1. Kinetic characteristics, molecular properties, genetics and polymorphisms

Human GLO2 is a thiolesterase. It has broad substrate specificity for glutathione thiol esters with preference for S-2-hydroxyacylglutathione derivatives. The rate of hydrolysis of S-D-lactoylglutathione to GSH and D-lactate, catalysed by GLO2, followed Michaelis-Menten kinetics where the K_M and k_{cat} values were 146 μM and 727 s^{-1} (Clelland and Thornalley, 1991, Allen et al., 1993). There are two major isoforms of GLO2 which are mitochondrial and cytosolic form. The molecular mass of mitochondrial form is 33,806 Da (sequence) and pI of 8.3 (predicted) whereas; the molecular mass of the cytosolic one is 28,860 Da (sequence) and pI of 8.3 (Cordell et al., 2004) –Figure 1.9.

Human *GLO2* gene is called hydroxyacylglutathione hydrolase (*HAGH*) is located in chromosome 16 at band 13.3. Genetic polymorphisms of *GLO2* are extremely rare and there is usually only one phenotype expressed which is called HAGH1. However, it has been detected that there is another rare form of *GLO2* which is HAGH2 - reviewed by (Thornalley, 1993). *GLO2* contains a Fe(II) Zn(II) centres which are considered as metal ion binding sites. Metal ion binding is an important determinant of protein structure and catalytic activity – substrate hydrolysis is linked to the Zn(II) site. *GLO2* is acetylated at lys229 (Dragani et al., 1999, Limphong et al., 2009, Choudhary et al., 2009).

Human *HAGH* consists of 10 exons and is transcribed to two different mRNA species from 9 and 10 exons, respectively. The 9 exon derived transcript encodes both the mitochondrial and cytosolic GLO2 forms where GLO2 that targets mitochondria is initiated from an AUG codon in the mRNA sequence and directed to the mitochondrial matrix, whereas cytosolic GLO2 is initiated by internal ribosome entry at a downstream AUG codon. On the other hand, the transcript deriving from 10 exons has an in-frame termination codon between the two initiating AUG codons, which only encodes the cytosolic GLO2 (Cordell et al., 2004). Both forms are acetylated at lys229 (Choudhary et al., 2009).

There are two domains forming the structure of human cytosolic GLO2, which are a predominantly α -helical domain and a four-layered β -sandwich. The active site contains a binuclear metal ion binding site which has zinc (II) and iron (II) ions and a substrate binding site extending over the domain interface. In addition, there is a hydroxide ion coordinated to both metal ions, which is situated 2.9 Å from the carbonyl carbon of the substrate in a position that may act as the nucleophile during catalysis process (Cameron et al., 1999).

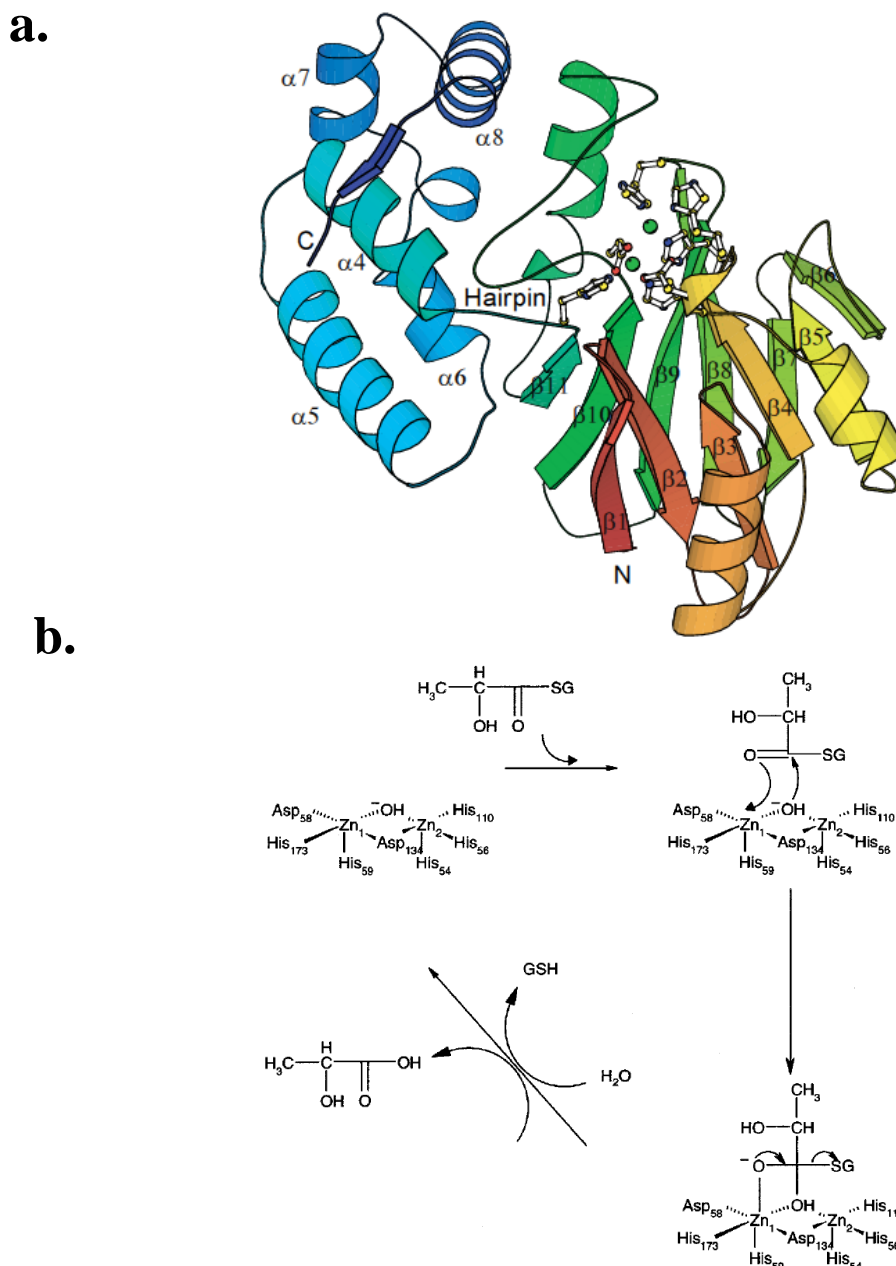


Figure 1.9: Structure and catalytic mechanism of glyoxalase 2.

a. Schematic representation of GLO2. The molecule has been colour ramped according to residue number starting with red at the N terminus and finishing with blue at the C terminus. The β strands of the first domain and the helices of the second domain have been labelled for clarity. The metal ions and the coordinating residues are represented by balls and sticks. **b.** A reaction mechanism for GLO2 proposed on the basis of the position of *S*-(*N*-hydroxy-*N*-bromophenylcarbamoyl)glutathione (HBPC–GSH) in the active site. The hydroxide ion is next to the carbonyl carbon, zinc (I) close to the carbonyl oxygen and zinc (II) near the sulphur of the HBPC–GSH. The hydroxide attacks the carbonyl carbon to form a negatively tetrahedral intermediate that may be stabilised by coordination to zinc (I). The C–S bond then breaks to yield the product. Presumably, in the apo enzyme, the sixth coordination positions of the zinc ions will be taken up by water molecules but these are not shown in the diagram (Cameron et al., 1999). (Reproduced with permission – see Appendix).

The role of GLO2 in mitochondria is uncertain as there is no mitochondrial targeting of GLO1. Mitochondrial GLO2 may be involved in delivery of GSH into mitochondria via S-D-lactoylglutathione but since GSH and S-D-lactoylglutathione had similar mitochondrial uptake kinetics and the cytosolic concentration of S-D-lactoylglutathione is usually <1% of GSH, this appears unlikely suggested by Rabbani *et al.* They further argued that GLO2 hydrolyses other acyl-GSH derivatives such as S-acetyl-GSH and S-succinyl-GSH. Recent research suggests there is significant non-enzymatic acetyl and succinyl transfer from acetyl-CoA and succinyl-CoA in mitochondria and a likely acceptor is mitochondrial GSH. GLO2 may, therefore, maintain GSH by repairing endogenous acylations where high concentrations of acetyl-CoA and succinyl-CoA in mitochondria require targeting of GLO2 to this compartment (Rabbani et al., 2014b).

1.4.4. Glyoxalases in perspective – a transcriptome and proteome-wide study of expression

The first genome-scale prediction of synthesis rates of mRNAs and proteins has been obtained by Selbach and colleagues. They simultaneously measured absolute mRNA and protein abundance and turnover by parallel metabolic pulse labelling for more than 5,000 genes in exponentially growing non-synchronized NIH3T3 mouse fibroblasts (Schwanhäusser et al., 2011). The number of copies per cell of mRNA and protein for *Glo1* and *Glo2* were: mRNA – *Glo1*, 22, *Glo2*, 16, and median of transcriptome 17; and protein – *Glo1*, *ca.* 584,000 and *Glo2*, *ca.* 61,000, and median of proteome *ca.* 50,000. The transcription rate (molecules per cell per hour) was: *Glo1*, 2.4, *Glo2*, 1.2, and median for transcription, 1.8. The translation rate (molecules protein per molecule mRNA per hour) was: *Glo1*, 750, *Glo2*, 117, and median for translation, 117. The half-lives of mRNA and protein were: mRNA – *Glo1*, 7.8 h, *Glo2*, 10.9 h, and median of transcriptome 9 h; and for protein, *Glo1*, 179 h, *Glo2*, 33 h, and median of proteome *ca.* 46 h. The view emerging from this prediction is that *Glo1* has protein abundance *ca.* 10-fold higher and half-life 4-fold higher than median value whereas *Glo2* is a protein with expression and turnover similar to the median value. The quantitative level of *Glo1* protein is in reasonable agreement with that estimated for human tissues by immunoassay of *ca.* 0.2 µg per mg protein or GLO1 is *ca.* 1/5000th of total protein (Larsen et al., 1985). GLO1 is a highly efficient enzyme and so these relatively high levels of protein probably reflect

a requirement for high *in situ* activity. GLO1 is 677 of 5028 proteins detected or in the top 13% of proteins detected by abundance (Xue et al., 2014).

GLO1 has similar abundance to that of other glycolytic enzymes such as transketolase, but lower than enzymes involved in the prevention of oxidative damage such as copper-zinc superoxide dismutase (SOD1) and mitochondrial manganese superoxide dismutase (SOD2). This is may be because of the substrate, superoxide, is more reactive than MG and a higher protein concentration is required to compete prevention of oxidative damage successfully with other proteins. Proteins which metabolise low level hydrogen peroxide, peroxiredoxins, are also found at higher copy number but they are not true catalysts –being inactivated by the substrate hydrogen peroxide and subsequently reactivated by reduction by thioredoxin. Peroxiredoxins, therefore, require high cell copy number as they are, in a sense, sacrificial targets for hydrogen peroxide-induced oxidative damage (D'Autréaux and Toledano, 2007).

There have been few comprehensive studies of the relationships between the levels of transcripts and the levels of the proteins they encode in mammals. Models from plants and yeast suggest a modest correlation. In a genetic approach in which natural variations were used to disturb both transcript levels and protein levels among inbred strains of mice, in quantifying levels of 7,185 most heritable transcripts and 486 related proteins, mRNA levels of *Glo1* had one of the strongest correlations with Glo1 protein; $r = 0.87$). Only 50% of the genes tested had significant correlation of mRNA and protein and the average correlation was $r = 0.27$ (Ghazalpour et al., 2011). This suggests that for Glo1 post-transcriptional mechanisms converting *Glo1* mRNA into protein are relatively constant – at least in the liver, and the half-life of Glo1 may be little changed in good health. Studies have indicated that GLO1 shows a moderate increase in proteolysis on activation of autophagy (Kristensen et al., 2008).

1.4.5. Other putative glyoxalase enzymes

A protein which converted MG to D-lactate without GSH cofactor and without formation of intermediate S-D-lactoylglutathione, a MG oxidoreductase, was purified from *Escherichia coli* and called “glyoxalase III” (Misra et al., 1995). This was confirmed by independent researchers, determining the specificity constant k_{cat}/K_M of $1.1 \times 10^5 \text{ M}^{-1}\text{min}^{-1}$ (Lee et al., 2012) - *ca.* 7,000 fold lower than Glo1 of *E. coli* ($7.4 \times 10^8 \text{ M}^{-1}\text{min}^{-1}$) (Clugston et al., 1998). Such low specific activity casts doubt as if this protein has significant MG metabolizing activity *in vivo*. DJ-1 isoforms were also considered as possible MG oxidoreductases, suggested by sequence analogy with glyoxalase III (Lee et al., 2012). Again, the k_{cat}/K_M for human DJ-1 was very low - *ca.* 10,000 fold lower than that of human GLO1. It is currently doubtful, therefore, that “glyoxalase III” and the DJ-1 superfamily are indeed glyoxalases and contribute significantly to MG metabolism *in vivo* (Rabbani et al., 2014b).

1.4.6. Metabolism of methylglyoxal by aldoketo reductases

MG and glyoxal is metabolised mainly by GLO1 and the glyoxalase system, with normally minor metabolism by aldoketo reductases (AKRs) and aldehyde dehydrogenases. When the glyoxalase system is impaired, AKR isoforms 1A4, 1B1 (aldose reductase) and 1B3 may metabolise MG to mainly hydroxyacetone and AKR isoforms 1B1, 1B3 and 1B8 may metabolise glyoxal to glycolaldehyde. Metabolism by AKR 1B1 may be a major fate of MG and glyoxal in the human renal medulla where high expression of AKR 1B1 outcompetes GLO1. AKRs are ARE-linked genes with expression regulated by transcription factor Nrf2 – reviewed in (Rabbani and Thornalley, 2012b). Baba and colleagues suggested that aldose reductase may play a more important role in MG metabolism than the current understanding (Baba et al., 2009). Unfortunately the observed GLO1 kinetics might be underestimated by being rate limited by hemithioacetal formation in the assay because GLO1 activity should be assayed with pre-forming the hemithioacetal substrate (Thornalley, 1993). Comparison of rates of MG metabolised by the glyoxalase pathway and aldoketo reductases *in vivo* suggests that >97% of MG metabolism is by the glyoxalase pathway except in the renal medulla where there is high expression of aldose reductase.

1.4.7. Glyoxalase system metabolite

1.4.7.1. Methylglyoxal

MG is highly reactive and potentially toxic molecule that is produced mainly as a by-product of glycolysis via the spontaneous degradation of glyceraldehyde-3-phosphate (GA3P) and dihydroxyacetonephosphate (DHAP). Other minor sources of MG formation are: from the oxidation of acetone in the metabolism of ketone bodies, the oxidation of aminoacetone in threonine catabolism and the degradation of proteins glycated by glucose. The whole body rate of formation of MG in human adults is approximately 3 mmol per day (Rabbani and Thornalley, 2012d). MG is an α -oxoaldehyde which has molecular mass of 72.0 Da. MG is highly toxic, most likely as a result of its interaction with proteins and DNA. MG reacts with arginine residues in proteins to form N δ -(5-hydroxy-5-methyl-4-imidazolone-2-yl)-ornithine (MG-H1) which considered as the most significant product accounting for more than 90% of the adducts (Rabbani and Thornalley, 2012d) - Figure 1.10. Protein contents of MG-derived hydroimidazolone in mammalian tissue and extracellular proteins are given in Table 1.8.

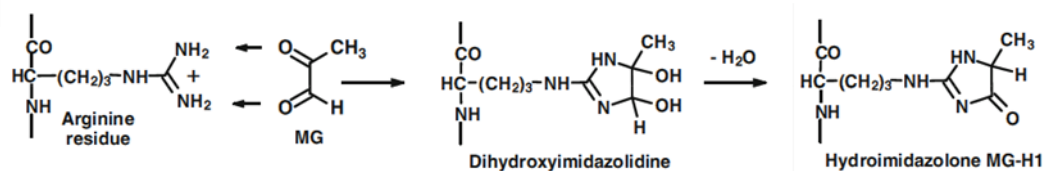


Figure 1.10: Reaction of methylglyoxal with arginine residues to form hydroimidazolone MG-H1. The figure shows the reaction of MG with arginine residues and the formation of MG-H1.

Table 1.8: Concentration of methylglyoxal-derived hydroimidazolone in mammalian tissue and extracellular proteins (mmol/mol arg).

Organism	Protein source	<i>n</i>	[MG-H1 residue]
Human	plasma protein	10	0.31 ± 0.20
	red blood cells	10	3.14 ± 0.72 (%Hb)
	peripheral lymphocytes	3	7.46 ± 1.13
	mesangial cells (<i>in vitro</i>)	3	0.60 ± 0.05
	lens protein	55	15.0 ± 1.7
	high density lipoprotein	22	1.00±0.54
Rat	plasma protein	13	1.29 ± 0.47
	aortal collagen	6	0.22 ± 0.18
	heart	7	3.43 ± 1.01
	liver	13	3.34 ± 0.32
	skeletal muscle	7	1.70 ± 0.77
	brain	7	2.73 ± 0.33
	renal glomeruli	7	2.30 ± 0.25
	retina	7	1.88 ± 0.51
	sciatic nerve	7	4.74 ± 2.74

In healthy adults, the urinary excretion of MG glycation protein adducts are *ca.* 10 µmol/day (Rabbani and Thornalley, 2012d). This indicates that only a small proportion of the MG produced physiologically acts to modify the proteome, while the majority is metabolised by the enzymatic defence systems. In patients with diabetes, there is a 15-fold increase in the MG-H1 urinary excretion, when compared to the levels of MG-H1 adducts in healthy controls (Ahmed et al., 2005b). This increase might have a great effect on the proteome modification in diabetes.

1.4.7.1.1. Measurement of dicarbonyls

Physiological concentrations of MG and related dicarbonyls have often been overestimated. For adequate sensitivity, chemical derivatization of α -oxoaldehydes is essential. The latest and most advanced method employ derivatization with 1,2-diaminobenzene, detection by LC-MS/MS and quantitation by stable isotopic dilution analysis (Rabbani and Thornalley, 2014c). Recent estimates of MG and glyoxal concentrations in human blood plasma are in the range 100–120 nM and cellular concentrations of 1–5 µM and 0.1–1 µM respectively (Dobler et al., 2006, Kurz et al., 2011). The estimates of 10 -1000 fold higher than these may be easily recorded with inadequate control of interferences during sample processing. Studies investigating the effects of glyoxal and MG on cultured cells and tissues using at concentrations of 10 folds higher than this are likely to be only of relevance for acute

intoxication and cytotoxicity. For example, the use of MG at millimolar concentrations to demonstrate the impairment of insulin signalling is unlikely to be physiologically relevant (Riboulet-Chavey et al., 2006).

1.4.7.1.2. Methylglyoxal in diabetes

Incubation of human red blood cells in short term culture *in vitro* with the presence of high glucose concentration revealed increases in the steady-state concentrations of MG as a consequence of increased flux of formation of MG – as judged by glucose concentration-dependent increase in flux of D-lactate formation. The cellular GSH, GLO1 and GLO2 activities did not change (Thornalley, 1988). In other *in vitro* studies, the human microvascular endothelial cell line (HMEC-1) and aortal endothelial cells from bovine and human were incubated in high glucose concentration media provided model of hyperglycaemia characteristic of diabetes. These studies concluded that there was decrease in the activity of GLO1 and increase in the steady-state concentrations and flux of formation of MG (Shinohara et al., 1998, Dobler et al., 2006, Yao and Brownlee, 2010). Shinohara and colleagues showed that the increased formation of AGEs was prevented by overexpression of GLO1 in endothelial cells which were cultured in high glucose concentration media (Shinohara et al., 1998).

The incubation of cells with GLUT1-dependent uptake of glucose in high glucose concentration media showed increased steady state concentrations of MG linked to increased MG formation and decreased GLO1 activity. Examples of these cells including vascular endothelial cells and lens fibre cells (Ahmed et al., 2003). The increased formation of MG occurs from increased concentrations of triosephosphates, GA3P and DHAP, with trace degradation to MG (Phillips and Thornalley, 1993). Formation of MG is a minor fate of triosephosphates, accounting for *ca.* 0.1% of glucotriose flux (Thornalley, 1988). MG concentration was increased in the blood, lens, renal medulla and cortex of diabetic rats. In the same conditions, there was a significant increase of D-lactate concentration in the blood and lens of STZ diabetic rats (Phillips et al., 1993). The concentration of MG in blood was increased 5-6 fold in patients with type 1 diabetes and 2-3 fold in patients with type 2 diabetes – Table 1.9.

Table 1.9: Concentration of methylglyoxal in tissues from human, laboratory animal and plant origin and cultured mammalian cells.

Species	Sample	Experimental condition	MG content /concentration
Human	Plasma	Healthy controls	132 ± 63 nM (n = 6)
Rat	Plasma	Sprague Dawley (male, 12 wks)	358 ± 139 nM (n = 8)
Mouse	Brain (cortex)	Strain 129S6/SvEvTac	0.30 ± 0.06 nmol/g wet weight (n = 6) [ca. 0.3 µM]
	Brain (stem/midbrain)		1.47 ± 0.16 nmol/g wet weight (n = 6) [ca. 1.4 µM]
	Liver	C57BL/6	3.26 ± 0.65 nmol/g wet weight (n = 8) [ca. 3.1 µM]
Mammalian cells in culture			
Human	Endothelial, macrovascular (aortal, primary)	Low glucose (5 mM glucose)	2.46 ± 0.20 pmol/ per 10 ⁶ cells [ca. 1.4 µM]; and culture medium, 97 ± 21 nM (n = 3)
	Endothelial, microvascular (dermal, HMEC-1 cell line)	Low glucose (5 mM glucose)	2.36 ± 0.04 pmol/ per 10 ⁶ cells [ca. 1.3 µM]; and culture medium, 121 ± 55 nM (n = 3)
	BJ fibroblast (primary)	Control + 2 µM R-sulforaphane (Glo1 inducer)	3.92 ± 0.81 pmol per 10 ⁶ cells [ca. 0.8 µM]; and culture medium, 155 ± 18 nM (n = 3) 2.53 ± 0.30 pmol per 10 ⁶ cells [ca. 0.5 µM]; and culture medium, 100 ± 19 nM (n = 3)

Data are mean ± SD. Approximate MG concentrations equivalent to estimated MG contents of tissues were deduced assuming an organ density of 1.05 g/ml and of cells from established tissue densities and cell volumes, respectively. Experiments have been repeated at least 3 times. For related sample preparation, see Supplementary methods from (Rabbani and Thornalley, 2014c).

1.4.7.2. S-D-Lactoylglutathione

SLG is formed normally in the physiological system as an intermediate of the glyoxalase system from the hemithioacetal adduct of MG and GSH, in a reaction catalysed by GLO1 (Figure 1.4) (McLellan et al., 1993). SLG is then hydrolysed to GSH and D-lactate intracellularly - catalysed by GLO2. It has poor membrane permeability and the locus of action of SLG is normally limited to the cytosol. However, if there is a leakage from cells, γ -glutamyltransferase - located on the

external surface of plasma membrane of cells - cleaves SLG to S-D-lactoylcysteinylglycine. S-D-lactoylcysteinylglycine then rearranges spontaneously to N-D-lactoylcysteinylglycine (Tate, 1975). Thornalley and co-workers demonstrated that SLG induced growth arrest and toxicity in human leukaemia cells *in vitro* (Thornalley and Tisdale, 1988).

Cellular concentrations of SLG are influenced by the activities of GLO1 and GLO2 and by the rate of formation of MG. The modification of these rates is common in several disease process particularly diabetes producing concomitant changes in SLG concentrations in the cells (McLellan et al., 1993). In human blood plasma, the concentrations of SLG was significantly higher in patients with diabetes (54.1 nmol/ml red blood cells) when compared to normal healthy controls (41.1 nmol/ml red blood cells) (Thornalley, 1993).

1.4.7.3. D-Lactate

There are two main stereoisomers of lactate formed in the human intermediary metabolism. The major stereoisomer is L-lactate. The other stereoisomer is D-lactate which is usually about 1-5% of the concentration of L-lactate. The exogenous sources of D-lactate include fermented food such as yogurt and pickles. It is also absorbed from microbial fermentation in the gut (Mortensen et al., 1991, Hove, 1998, Ewaschuk et al., 2005, De Vrese and Barth, 1991). In addition, it is formed endogenously in intermediary metabolism by the glyoxalase pathway and metabolised by mitochondrial 2-hydroxyacid dehydrogenase to pyruvate in human tissues (Thornalley, 1993). D-Lactate is efficiently metabolised in humans and has higher fractional renal clearance than L-lactate (Connor et al., 1983). Infusion of D-lactate at 1.0-1.3 mmol sodium D-lactate/kg/hr resulted in about 90% of the D-lactate being metabolised while the remaining 10% was excreted in urine (Oh et al., 1985). D-lactate concentration in blood plasma increased *ca.* 2-3 fold after meals and exercise (Ohmori and Iwamoto, 1988, Kondoh et al., 1992b).

D-Lactate is permeable to cell membranes through a specific lactate transporter, passive diffusion of the unionised conjugate acid and also by the inorganic anion transporter. It is excreted in urine and is reabsorbed actively from renal filtrate by renal tubules. In addition, it is excreted in stool and sweat (Oh et al., 1985, Kondoh et al., 1992b, Kondoh et al., 1992a).

D-Lactate can be considered as a marker of flux of MG formation in tissues where it is not metabolised such as lens fibre cells and red blood cells (Thornalley, 1993). Furthermore, the D-lactate concentration increases in cells which have glucose transporter-1 (GLUT-1) such as endothelial cells and erythrocytes when cultured in high glucose conditions, and in plasma and urine of STZ-induced diabetic rats and patients with diabetes (Thornalley, 1988, Phillips and Thornalley, 1993, Karachalias N, 2005, McLellan et al., 1994). The concentration of D-lactate level in plasma of healthy adults is in the range of 2 – 20 μ M. Higher estimates may be achieved when the analytical method does not avoid racemisation of L-lactate which is typically present in >100 fold excess over D-lactate (De Vrese and Barth, 1991, McLellan et al., 1992, Ohmori and Iwamoto, 1988, Brandt et al., 1980).

D-Lactate is measured by fluorescent endpoint enzymatic assay with D-lactic dehydrogenase. The concentration is determined by formation of NADH associated to oxidation of D-lactate to pyruvate (McLellan et al., 1992). It can also be measured by reverse phase high phase liquid chromatography (HPLC) by derivatization of the oxidation product-pyruvate with 1,2-diaminobenzene derivative (Ohmori and Iwamoto, 1988, Ohmori et al., 1991).

In experimental diabetes, urinary excretion of D-lactate increased one week after induction of diabetes in STZ rats and reached a maximum value of *ca.* 5-6 fold which was higher than healthy control after 4 weeks and remained high thereafter (Dinkova-Kostova et al., 2010). In patients with diabetes, the urinary concentration of D-lactate increased 2–3 fold, which might be used as non-invasive marker of increased MG and metabolic dysfunction linked to diabetes complication (Talasniemi et al., 2008).

1.5. Aim and objectives

1.5.1. Aim

The initial aim of this work was to study the effect of Glo1 deficiency on the development of experimental diabetic nephropathy (DN) in streptozotocin (STZ)-induced diabetic mice in a functional genomics study using Glo1 mutant mice deficient in Glo1 expression. The main study hypothesis was: *increased exposure to Glo1 substrate dicarbonyls accelerates the development of diabetic nephropathy in STZ diabetic mice*. The hypothesis would be tested by studying the effect of decreasing Glo1 activity by heterozygous genetic knockout in Lexicon Glo1 mutant mouse on the development of diabetic nephropathy in STZ-induced diabetic mice.

Supporting evidence for this hypothesis came from observations of increased plasma MG concentration in clinical and experimental diabetes and with increased formation and accumulation of MG-derived AGEs (McLellan and Thornalley, 1994, Babaei-Jadidi et al., 2004, Ahmed et al., 2005a, Karachalias et al., 2010). This led to a widely held view that increased MG or dicarbonyl stress may be a key risk factor for development of microvascular complications - including diabetic nephropathy (Thornalley, 1994, Brownlee, 2001, Rabbani and Thornalley, 2014a). Functional genomics studies with Glo1 overexpression in transgenic mice have shown prevention of diabetic microvascular complications - including diabetic nephropathy (Giacco et al., 2014, Berner et al., 2012, Bierhaus et al., 2012). Experimental diabetes is associated with down regulation of Glo1 activity in the kidney of STZ-induced diabetic mice and other models of experimental diabetic nephropathy – db/db mice and STZ-induced diabetic rats (Bierhaus et al., 2012, Barati et al., 2007, Palsamy and Subramanian, 2011). I reasoned, therefore, that if Glo1 and MG-derived AGE accumulation are risk factors for the development of diabetic nephropathy, partial ablation in heterozygous Glo1 knockout mouse with STZ-induced diabetes would exacerbate the development of diabetic nephropathy and possibly also induce nephropathy in the non-diabetic state.

To test if increased *in situ* exposure to glyoxal and MG accelerates the development of DN, the development of DN in Glo1 knockout mouse and C57BL/6J wild-type control mice with STZ-induced diabetes will be studied. STZ-induced diabetes, a model of type 1 diabetes, does not consistently show albuminuria nor severe glomerular mesangial expansion in C57BL/6J mice (Qi et al., 2005,

Nakagawa et al., 2007). Increase in renal MG-modified mitochondrial proteins is expected to induce oxidative stress and metabolic dysfunction and accelerate DN (Rosca et al., 2005). Diabetes will be induced in Glo1 knockout and wild-type controls by the Animal Models of Diabetic Complications Consortium (AMDCC) low dose STZ protocol: 50 mg/kg on 5 consecutive days (Breyer et al., 2005). If plasma glucose is more than 15 mM after 4 weeks, the mouse will be included in the study. Samples of blood and 24 h urine samples will be collected at baseline and 1, 3 and 5 months from all included mice in this study. Measurements made will be: plasma glucose, total cholesterol, HDL cholesterol, triglycerides (Hammad et al., 2003) and urinary albumin, creatinine clearance, urinary protein glycation, oxidation and nitration free adducts (Thornalley et al., 2003a). At termination, ultrastructural analysis of kidney sections will be performed by electron microscopy morphometry, reporting glomerular and tubular basement membrane thicknesses and mesangial volume (Hammad et al., 2003, Okada et al., 2003). Kidney, heart and muscle protein damage markers will be determined by quantitative proteomics. Mouse husbandry, blood and urine, sampling and nephropathy validation will be as per AMDCC protocols (Breyer et al., 2005). One kidney will be used for assay of enzyme activities: Glo1, and proteasome activities. Blood pressure will be measured non-invasively by tail-cuff method.

Following support to the host research team from the Wellcome Trust, the IMKC Glo1 mutant mouse was available for this project. I had concern, however, if this mouse model was indeed deficient in expression of Glo1. Information held on the genotype and phenotype of the mutant mouse line by the European Mutant Mouse Archive from the producer, Lexicon Pharmaceuticals Inc. (Texas, USA), indicated genotyping had been performed by non-standard analysis – assay of *Glo1* mRNA, and the phenotype was essentially that of healthy WT controls, including in putative homozygous mutants. Null mutation of *Glo1* was expected to be lethal in homozygous inheritance given the rare precedent in the human population of embryonic lethality of a *GLO1* frame shift mutation leading to expression of a functionally inactive truncated peptide (Arai et al., 2010). An initial objective of this study was therefore to establish a robust method for genotyping of the IMKC Glo1 mutant mouse and establish the required Glo1 deficiency was present. My implementation of studies towards this initial objective, however, were unable to confirm Glo1 deficiency in this mouse model and suggested compensatory Glo1

expression at WT level was present – see Results section. This explained the normal phenotype of the IMKC Glo1 mutant mouse. Proceeding with the previous aim was re-evaluated as both genotypes including Lexicon Glo1 mutant mouse and wild-types have a similar phenotype which limits the benefits of using Lexicon Glo1 mutant mouse as a Glo1 deficient mouse and a model of accelerated diabetic complication. In addition, it is interesting to further investigate the potential genetic causes behind the phenotype of Lexicon Glo1 mutant mouse, how gene trapping of Glo1 failed to produce a Glo1 deficient mouse and apply and explore the genetic causes in wider contexts.

The project aim and objectives were redeveloped. The revised aim was to characterise the compensatory Glo1 expression in the IMKC mutant mouse and explore the mechanism producing it. The latter included imposing similar metabolic conditions on precursor mouse embryonic stem cells as gene trapping of Glo1 to model the mechanism of induction of compensatory Glo1 expression and explore possible clinical translation of the findings. The revised overall study hypothesis was that *functional Glo1 deficiency in embryonic stem cells may activate a compensatory mechanism to maintain wild-type Glo1 expression and thereby prevent embryonic lethality of associated dicarbonyl stress.*

1.5.2. Objectives

Objective 1. To develop a method for genotyping of the Lexicon Glo1 mutant mouse and characterise the expression of Glo1 in heterozygous and homozygous transmission of Glo1 mutant allele

To achieve this objective, the sequence of the inserted DNA and genotyping primers used in the mouse line development was obtained from the IMKC project leader at Lexicon Pharmaceuticals and PCR and qPCR methods developed to detect and quantify WT and mutant Glo1 alleles in mouse tissue. Glo1 mutant mice were bred with wild-type controls and Glo1 genotype determined and Glo1 expression at mRNA, protein and activity levels determined in tissues. Related glyoxalase system analytes, tissue concentration of MG and tissue and urine concentrations of MG-derived glycation adducts were determined to assess the functional activity of the glyoxalase pathway in Glo1 mutant mice.

Objective 2. To identify the mechanism of compensatory expression of Glo1 in the Lexicon Glo1 mutant mouse

The mechanism of compensatory expression of Glo1 in the Glo1 mutant mouse was suggested from outcomes of Objective 1 and therefore development of the hypothesis to be tested and related experimental design to test it was contingent on this. In the event, the outcomes of objective 1 indicated a likely mechanism of compensatory expression of Glo1 was functional *Glo1* copy number alteration. The related hypothesis developed was: *functional Glo1 copy number increase is present in the Glo1 mutant mouse and the additional WT allele is co-inherited with the Glo1 mutant allele so as to maintain WT Glo1 expression and phenotype.* To tests this hypothesis and achieve this objective, copy number of *Glo1* WT and mutant alleles were quantified in several mouse tissues and the inheritance of alleles studied in mating of mutant mouse with one and two mutant alleles with WT controls studied. The extent of DNA copy number increase was determined by high intensity aCGH DNA microarray of Glo1 mutant mouse with one and two mutant alleles and WT controls.

Objective 3. To model the mechanism of Glo1 copy number alteration in mouse embryonic stem cells

Glo1 mutant mice were produced by gene trapping in mouse ESCs *in vitro*. The outcome of Objective 2 revealed that copy number increase of Glo1 produced the compensatory Glo1 expression in the Glo1 mutant mouse. I reasoned that mutation of the *Glo1* allele induced dicarbonyl stress in ESCs and this may have produced increased copy number alteration. Inducible gene copy number change is a potential mechanism to resist cytotoxic stress through increased functional copy number of protective genes (Hastings, 2007). Copy number change (CNC) occurs in replicative stress induced by polymerase inhibitor aphidicolin and ribonuclease reductase inhibitor, hydroxyurea, and also occurs in response to mutation by low-dose ionising radiation (Arlt et al., 2014, Arlt et al., 2009). Copy number changes are unfocused and occur across the human genome resembling CNV. There is no example hitherto of increased copy number change in response to exposure of high and toxic levels of an endogenous metabolite focussed and limited to the gene linked to endogenous enzymatic protection. The hypothesis developed was: *dicarbonyl stress in ESCs induces functional copy number alteration of Glo1.* To test this, ESCs

were cultured and exposed to exogenous MG and copy number of *Glo1* determined. Where *Glo1* copy number increase occurred, copy number of other genes close to the *Glo1* locus (found with increased copy number in the *Glo1* mutant mice studies of Objective 2) were assessed to determine if copy number increase in MG-induced dicarbonyl stress in ESCs *in vitro* has a similar genetic pattern as in the *Glo1* mutant mouse.

Objective 4. To study the copy number alteration of *GLO1* in clinical samples

From the previous objectives and experimental outcomes, dicarbonyl stress-induced copy number increase of *Glo1* appeared to be a viable mechanism for a protective response to counter potentially damaging dicarbonyl glycation. The occurrence of this clinically is unknown. I considered that the most likely instance of this occurring would be in clinical disease associated with most severe dicarbonyl stress. Dicarbonyl stress is most severe in patients with end stage renal disease (ESRD) receiving haemodialysis (HD). Plasma concentrations of MG are increased 5-fold with high flux of formation of dicarbonyl-derived AGEs (Rabbani and Thornalley, 2012b, Agalou et al., 2005). I developed the hypothesis that *dicarbonyl stress in ESRD patients receiving HD produces Glo1 copy number alteration*. To test this hypothesis I analysed *GLO1* copy number in peripheral blood mononuclear cells of HD patients and healthy control subjects. I collaborated with a local clinical nephrologist, Dr Daniel Zehnder, who gained ethical approval to recruit HD patients and healthy controls and collect peripheral venous blood samples with consent for the study.

These final series of studies provided a rigorous examination of the failure of gene trapping to produce a *Glo1* deficient mouse and revealed a new level of stress response of the glyoxalase system through copy number alteration.

2. Materials and methods

2.1. Materials

2.1.1. Glyoxalase 1 mutant and wild type control mice

Glo1 mutant mice were produced by Lexicon Pharmaceuticals Inc. (Houston, Texas, USA). A heterozygote breeding pair was obtained from the European Mutant Mouse Archive, Heidelberg, Germany. Wild-type control siblings of heterozygote C57BL/6 mice were produced in the Biological Services Unit, University of Warwick. Control mouse liver samples of strains C57BL/6J (stock number: 664) and DBA/1J (stock number: 670) were purchased from Jackson Laboratories (Bar Harbor, Maine, USA) via UK agent Charles River (Margate, Kent, UK).

2.1.2. Human and murine cells

Irradiated mouse embryonic fibroblasts (MEF) and mouse ESCs of C57BL/6 mouse strain were purchased from Life Technologies (Paisley, UK). Human leukaemia 60 (HL60) cells were purchased from the European Collection of Animal Cell Cultures (Porton Down, UK). Human non-small cell lung adenocarcinoma (NCI-H522) was obtained from the National Cancer Institute (Frederick, MD, USA). Dulbecco's Modified Eagle medium (D-MEM), Knockout™ D-MEM, fetal bovine serum-ES-cell qualified (FBS), 0.1% gelatin attachment factor (AF), knockout serum replacement (KSR), MEM non-essential amino acids solution (NEAA), L-glutamine, 2-mercaptoethanol, StemPro™ Accutase™ cell dissociation reagent were purchased from Life Technologies (Paisley, UK). Recombinant human leukaemia inhibitory factor (LIF) was purchased from Millipore, UK. Roswell Park Memorial Institute (RPMI) 1640 medium and fetal bovine serum was purchased from Invitrogen (Life Technologies, Paisley, UK). Phosphate buffered saline (137 mM NaCl, 2.7 mM KCl, 10 mM Na₂HPO₄, 2 mM KH₂PO₄) was provided by the preparatory services, Clinical Sciences Research Laboratories, University of Warwick (University Hospital, Coventry, UK).

2.1.3. Enzymes

Aminopeptidase, proteases, L-lactic dehydrogenase, D-lactic dehydrogenase, and other enzymes were purchased from Sigma-Aldrich. Leucine aminopeptidase (EC 3.4.11.2) was type VI from porcine kidney microsomes had a specific activity of 22 units/mg protein (1 unit of activity hydrolysed 1.0 mol of L-leucine-p-nitroanilide to L-leucine and p-nitroaniline per min at pH 7.2 and 37°C). Pepsin (EC 3.4.23.1) was from porcine stomach mucosa with a specific activity of 3460 units/mg protein (1 unit hydrolysed haemoglobin with an increase in absorbance at 280 nm of 0.001 AU per min of trichloroacetic acid-soluble products, at pH 2 and 37°C). Pronase E (EC 3.4.24.31) was type XIV from bacterial *Streptomyces griseus* with a specific activity of 4.4 units/mg protein (1 unit of activity hydrolysed casein forming 1.0 mmol of tyrosine per min at pH 7.5 and 37°C). Prolidase (EC 3.4.13.9) was from porcine kidney and had a specific activity of 145 units/mg protein, where 1 unit of activity hydrolyses 1.0 µmol of Gly-Pro per min, at pH 8 at 40°C. L-Lactic dehydrogenase (EC 1.1.1.27) was from bovine heart, type III with activity of ≥500 units/mg protein and D-lactic dehydrogenase (EC 1.1.1.28) was from *Staphylococcus epidermidis* and had activity of ≥80 units/mg lyophilised powder. SfaNI restriction enzyme was purchased from New England Biolabs, UK.

2.1.4. Substrates and co-factors

Glutathione (cat. no. G4251-10G), nicotinamide adenine dinucleotide - oxidised form NAD⁺ (cat. no. N0632-1G), β-nicotinamide adenine dinucleotide 2'-phosphate reduced tetrasodium salt hydrate NADPH (cat. no. N7505-1G), aminoguanidine hydrochloride (cat. no. 396494), sodium pyruvate (cat. no. P5280), D-lactic acid (cat. no. L0625), L-lactic acid (cat. no. L1750) and glyoxal (40% aqueous solution; cat. no. G-3140) were purchased from Sigma-Aldrich (Poole, Dorset, UK).

2.1.5. Antibodies and primers

Anti- β -actin antibody (cat. no. ab8229), anti-sex determining region Y-box 2 (SOX2) antibody (cat. no. ab97959), anti-NANOG antibody (cat. no. ab80892) and anti-OCT4 antibody (cat. no. ab19857) were purchased from Abcam, UK. Rabbit anti-human GLO1 antibody was prepared and purified in-house by previous members of the host research team as described in (Allen et al., 1993). Anti-rabbit IgG (whole molecule)–peroxidase conjugate antibody produced in goat, and non-immune IgG fraction of antiserum, buffered aqueous solution was purchased from Sigma-Aldrich, UK.

To characterise Glo1 mutant mice and for genotyping, primers suggested by Lexicon Pharmaceuticals (the Glo1 mutant mice supplier) were purchased from Invitrogen, UK. To amplify the reference gene *Rn 18s* (18S ribosomal RNA) - primer number QT01036875 was purchased from Qiagen (Manchester, UK). Two other Glo1 pairs (pair 2 and pair 3) of primers were used for genotyping of the mutation locus in Glo1 mutant mice. Genotyping of C419A SNP of *GLO1* in clinical subjects was performed using C419A genotyping primers, as described (Rinaldi et al., 2014) – see Appendix A.

Gene expression assays were performed using Taqman gene expression assay and purchased from Life Technologies, UK. The following genes were examined: bric-a`-brac tramtrack broad complex domain containing 9 (*Btbd9*), *Glo1*, dynein - axonemal, heavy chain 8 (*Dnah8*), glucagon-like peptide-1 receptor (*Glp1r*), and vomeronasal 2, receptor 112 (*Vmn2r112*). β -Actin and 18S ribosomal RNA (*Rn18s*) were used as reference genes (Appendix B). Taqman universal master mix II with Uracil-N glycosylase (UNG) was used in the transcription–polymerase chain reaction (RT-PCR) protocol.

Copy number analysis was performed using Taqman copy number assay and purchased from Life Technologies, UK. Assay of the following murine DNA was performed: *Glo1* (exon 1), *Glo1* (exon 6), *Btbd9*, *1700097n02rik* and *Dnah8*. GLO1-Vic Taqman copy number assay was designed to detect DNA straddling the inserted DNA vector and *Glo1* to differentiate the trapped copy of *Glo1* from the WT copy. Transferrin receptor protein1 (*Tfrc*) and telomerase reverse transcriptase (*Tert*) copy number assay was used as reference assay for the copy number in mouse. *GLO1* copy number assay of human DNA was referenced to *RNASE P* - Taqman copy

number reference assay – see Appendix C. The master mix was Taqman genotyping master mix from Life Technologies, UK.

2.1.6. Other reagents and consumables

Bovine serum albumin, sodium dihydrogen phosphate NaH₂PO₄, hydrochloric acid (analytical grade, 1 N; HCl), EDTA, Tween-20, diethylenetriaminepenta-acetic acid (DETAPAC), trichloroacetic acid (TCA) and β-mercaptoethanol were purchased from Sigma-Aldrich, UK. Tris(hydroxymethyl)-aminomethane (Tris base), Tris-HCl, perchloric acid, sodium chloride, potassium bicarbonate, glycine and methanol, 4-(2-hydroxyethyl) piperazine-1-ethanesulfonic acid (HEPES), sodium dodecyl sulphate (SDS) and 5x siRNA universal buffer were purchased from Fisher Scientific (Loughborough, UK). Complete lysis-M buffer was purchased from Roche, UK. Hydrazine hydrate was purchased from Fluka (Poole, Dorset, UK). Nuclease-free water was purchased from Qiagen, UK. Oligo aCGH wash buffers 1 and 2 were purchased from Agilent Technologies, UK. Mouse Cot-1 DNA was purchased from Life Technologies, UK.

Laemmli (4x) sample buffer (277.8 mM Tris-HCl, pH 6.8, 4.4% SDS, 44.4% (w/v) glycerol, 0.02% bromophenol blue), 10x Tris/glycine/SDS premixed electrophoresis buffer (25 mM Tris, 192 mM glycine, 0.1% SDS, pH 8.3), 8–16% mini-PROTEAN® TGX™ gel, Trans-Blot® Turbo™ RTA midi nitrocellulose transfer kit, 10x Tris buffered saline, precision plus protein™ dual colour standards protein ladder (10-250 kDa, for 4–20% Tris-glycine SDS-PAGE) and concentrated protein assay dye and reagents for Bradford assay – all purchased from Bio-Rad (Hemel Hempstead, UK). Photographic film was purchased from GE Healthcare (Little Chalfont, UK).

OptiMEM^(R) I reduced serum medium (1x) (liquid with L-glutamine, 2400 mg/l sodium bicarbonate, HEPES, sodium pyruvate, hypoxanthine, thymidine, trace elements, growth factors) and Lipofectamine® 2000 transfection reagent were purchased from Life Technologies, UK. ON-TARGET plus Non-targeting pool and SMART pool: ON-TARGET plus *Glo1* siRNA were purchased from Thermo Fisher Scientific Bioscience (Loughborough, UK). Biomix red, agarose, hyperladder 1 kb, bioscript reverse transcriptase, dNTP set, Oligo (dT)18, RNase inhibitor and SensiMix low-ROX kit were purchased from Biorline (London, UK).

The cell permeable Glo1 inhibitor S-p-bromobenzylglutathione cyclopentyl diester (BrBzGSHCp₂) was available in-house prepared by previous members of the host research team. It was prepared by acid-catalysed esterification of S-p-bromobenzylglutathione and purified by column chromatography as described (Thornalley et al., 1996).

All other reagents, buffers, salts, bases and acids were analytical grade and purchased from either Fisher Scientific or Sigma-Aldrich. Microplate U bottom polystyrene 96-well black and clear plate, HPLC vials, inserts and plastic supports, caps and microspin filters “Spin-X” (0.2 µm pore size) were all purchased from Fisher Scientific, UK. MicroAmp® optical adhesive film and MicroAmp® optical 96-well reaction plate were purchased from Life Technologies, UK. Amicon ultrafiltration microcentrifuge tubes and filter inserts (0.5 ml, 3 kDa and 10 kDa cut-off) were purchased from Merck-Millipore (Watford, UK). Special compressed gas mixture of 3% oxygen, 5% carbon dioxide and 92% nitrogen purchased from CK Gas Products Ltd (Leicester, UK).

2.1.7. Analytical kits

DNeasy blood & tissue kit (cat. no. 69504), all Prep DNA/RNA/protein mini kit (cat. no. 80004), RNeasy mini kit (cat. no. 74104) were purchased from Qiagen, UK. The glucose assay kit - hexokinase method (GAHK20) was purchased from Sigma-Aldrich. Enhanced chemiluminescence (ECL) reagent kit (cat. no. 34079) was purchased from Fisher Scientific, UK.

Mouse genome CNV microarray with genome-wide coverage, Agilent design identification no - 027414 SurePrint G3 unrestricted CGH 1x1M (cat. no. G4824A), SureTag DNA labelling kit (cat. no. 5190-3400), oligo aCGH/ChIP-on-chip hybridization kit (cat. no. 5188-5220) and hybridization gasket slide kit-1 microarray per slide format (cat. no. G2534-60008) were purchased from Agilent Technologies (Stockport, UK).

2.1.8. Chromatographic materials

Analytical grade methanol, acetonitrile and tetrahydrofuran (THF) - all HPLC grade, were purchased from Fisher Scientific. Trifluoroacetic acid (TFA, $\geq 99.0\%$ HPLC grade) and formic acid (FA, $\geq 98\%$) were purchased from Sigma-Aldrich. For dicarbonyl assay, the column-BEH C18, 1.7 μm particle size column (100 x 2.1 mm) fitted with a (5 x 2.1 mm) pre-column was purchased from Waters (Elstree, Herts, UK). For protein damage markers, two columns were used in series: HypercarbTM, 5 μm particle size columns - column 1, 2.1 x 50 mm, and column 2, 2.1 mm x 250 mm. For N ϵ (γ -glutamyl)lysine analysis, the column was HypercarbTM, 3 μm particle size, 150 mm x 2.1 mm. These were purchased from Fisher Scientific.

2.1.9. Analytical standards

2.1.9.1. Calibration standards for protein damage marker analysis

The standards for protein damage markers were prepared by current and previous members of host research team, as described (Thornalley et al., 2003a, Ahmed et al., 2003). [*guanidino*-¹⁵N₂]L-Arginine, 4,4,5,5-[²H₄]L-lysine and [¹³C₆]L-lysine, [methyl-²H₃]L-methionine and ring-[²H₄]L-tyrosine (all >98% isotopic purity) were purchased from Cambridge Isotope Laboratories (Andover, MA, USA). [*guanidino*-¹⁵N₂]MG-H1, [*guanidino*-¹⁵N₂]3DG-H and [*guanidino*-¹⁵N₂]G-H1 were prepared in house from [*guanidino*-¹⁵N₂]L-arginine after conversion to the N α -t-butoxycarbonyl derivative (Thornalley et al., 2003a, Meldal and Kindtler, 1986). [²H₈]MOLD was prepared from 4,4,5,5-[²H₄]L-lysine after conversion to the N α -formyl derivative (Finot and Mauron, 1969). [¹³C₆]CEL, [¹³C₆]CML and [¹³C₆]pentosidine were prepared from [¹³C₆]L-lysine after conversion to the N α -formyl derivative. The synthetic methods for the preparation, purification and characterization of all AGE calibration standards were as described for their non-isotopically substituted analogues (Ahmed et al., 2003). [methyl-²H₃]MetSO was prepared from [methyl-²H₃]L-methionine, and both [²H₆]dityrosine and 3-nitrotyrosine (3-NT) were prepared from ring-[²H₄]L-tyrosine, using the methods described in (Lapp and Dunn, 1955, Huggins et al., 1993, Sokolovsky et al., 1966).

2.1.9.2. Dicarbonyl calibration standards

Glyoxal (40% aqueous solution) from Sigma-Aldrich was used without purification. High purity MG and 3-DG were prepared in-house by the host research

team. MG was prepared by the hydrolysis of MG dimethylacetal in dilute sulphuric acid and purified by fractional distillation under reduced pressure, as described (McLellan and Thornalley, 1992). 3-DG was prepared from glucose and toluidine by method of Madson and Feather (Madson and Feather, 1981) with modifications described by Henle and Bachmann (Henle and Bachmann, 1996). The concentration of stock solutions of dicarbonyls was calibrated by conversion to 1,2,4-triazine derivatives by incubation with aminoguanidine hydrochloride and spectrophotometric detection, deducing concentrations of the 1,2,4-triazine derivatives and thereby dicarbonyl precursors from known extinction coefficients (Thornalley et al., 2000).

2.1.10. Instrumentations and software

Fusch Rosenthal haemocytometer (cat. no. 0630410) was from Marienfeld-superior (Lauda-Königshofen, Germany). The microplate reader used for enzymatic assays was a FLUOstar OPTIMA microplate reader from BMG Labtech (Aylesbury, UK). The LC-MS/MS systems used were an ultra high performance liquid chromatography (UPLC) Acquity™ system with a Quattro Premier XE or Xevo™ TQ-S tandem mass spectrometer (Waters, UK). Masslynx 4.1 software was used to integrate the data for protein damage markers. Mini-PROTEAN® tetra electrophoresis system (cat. no. 165-8005EDU), wide mini ready sub-cell GT cell (cat. no. 170-4405), Trans-Blot Turbo blotting instrument (170-4155) and PowerPac™ basic power supply (164-5050) were from Bio-Rad. ImageQuant densitometry software was from GE Healthcare. The vibra cell™ sonicator was from Jencons Scientific (Leighton Buzzard, UK). MULTI-GEN 7 homogenizer was from ProScientific (Oxford, Connecticut, USA). Hypoxia chamber (cat. no. 27310) and single flow meter (cat. no. 27311) were from Stemcell Technologies (Manchester, UK). The UVICON UV/VIS spectrophotometer was purchased from Northstar Scientific Limited (Leeds, UK). ChemiGenius² software gel image analysis was from Syngene (Cambridge, UK). Applied Biosystems™ 7500 real-time PCR machine and 7500 software v2.0.6 was from Life Technologies and the Nanodrop spectrophotometer ND-1000 was from LabTech International (Uckfield, UK).

2.2. Methods

2.2.1. Animal experimentation

The *Glo1* mutant mice are genetically-modified strain of mice derived from C57BL/6 mouse strain. A colony was maintained in the Biological Services Unit, University of Warwick, by the host research team. The mice were produced by gene trapping method – see section 1.1.5.3.1. The modification was in the chromosome 17 of the mice ESCs and the trap insertion site was in GST_4497_D9 OmniBank® using insertion trap vector VICTR48 - Figure 2.1. In most of the experiments using this mouse model, two control groups were used:

- (i) Wild type siblings produced from breeding of heterozygote of *Glo1* mutant mouse, and
- (ii) Wild type C57BL/6 mouse of the colony maintained in Biological Services Unit, University of Warwick.

In addition, extracted DNA from mouse liver samples of strains C57BL/6J (2 copies of *Glo1*) and DBA/1J (4 copies of *Glo1*) derived from reference stock of Jackson Laboratories (USA) were used as negative and positive control for *Glo1* duplication respectively.



Figure 2.1: Insertion cassette in mouse *Glo1* gene. The figure shows the exact location of the inserted trapping cassette edged with two long terminal repeat (LTR) in the first intron of *Glo1* gene.

The *Glo1* mutant mice and the control mice were housed in an environment of 19 - 23°C, 45 - 65% humidity and 12 /12 h light/dark cycle at the Biological Services Unit, School of Life Sciences, University of Warwick. Mice were kept 6 - 8 per cage with free access to food and water. All animal experimentation described in this study was conducted under the Animals (Scientific Procedures) Act 1986, UK: project licence number 80/2556, title - breeding and maintenance of genetically altered rodents.

In the animal studies, the *Glo1* gene mutation, copy number and inheritance were studied and related *Glo1* mRNA, protein and activity quantified in different tissues of the *Glo1* mutant mice, WT siblings and C57BL/6 control strain colony maintained at University of Warwick (C57BL/6-UoW). This is summarised in flowcharts below. In the initial study, Study 1, the activity of *Glo1* was measured in 7 tissues of *Glo1* mutant mouse and C57BL/6-UoW control mice at age of three months - Figure 2.2. In the second study, Study 2, *Glo1* copy number, mRNA, protein and activity of *Glo1* in *Glo1* mutant mouse and WT siblings was determined at age seven months - Figure 2.3. In the third study, Study 3, the copy number genome-wide was assessed in heterozygote siblings with 3 and 4 copies of *Glo1* (with 1 and 2 mutant *Glo1* gene, respectively) and WT siblings; *Glo1* mRNA, protein and activity and MG were also determined. Measurements were made in liver tissue of mice at age seven months - Figure 2.4. In study 4, the inheritance pattern of *Glo1* mutant gene in three families of *Glo1* mutant mice was characterised - Figure 2.5.

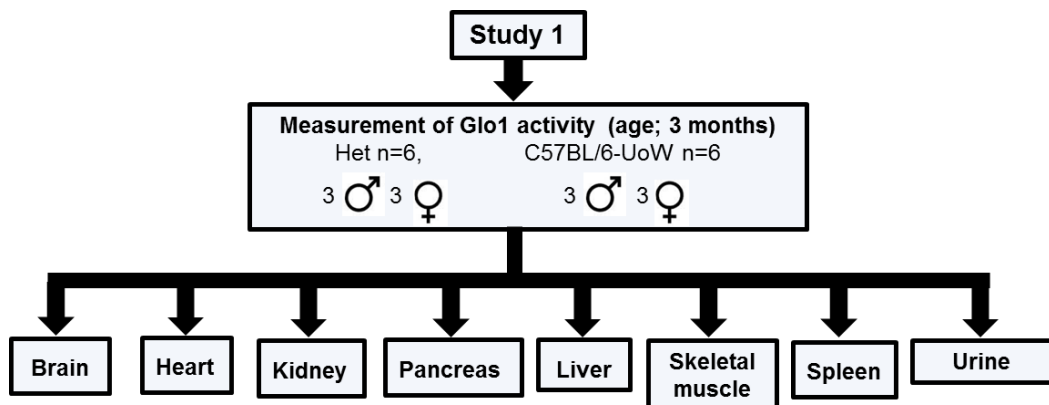


Figure 2.2: Study1. Summary of mice and tissues analysed. *Glo1* activity was measured in tissues (U/mg protein) and MG-derived glycation free adducts and related protein damage free adducts in urine (nmol/mg creatinine).

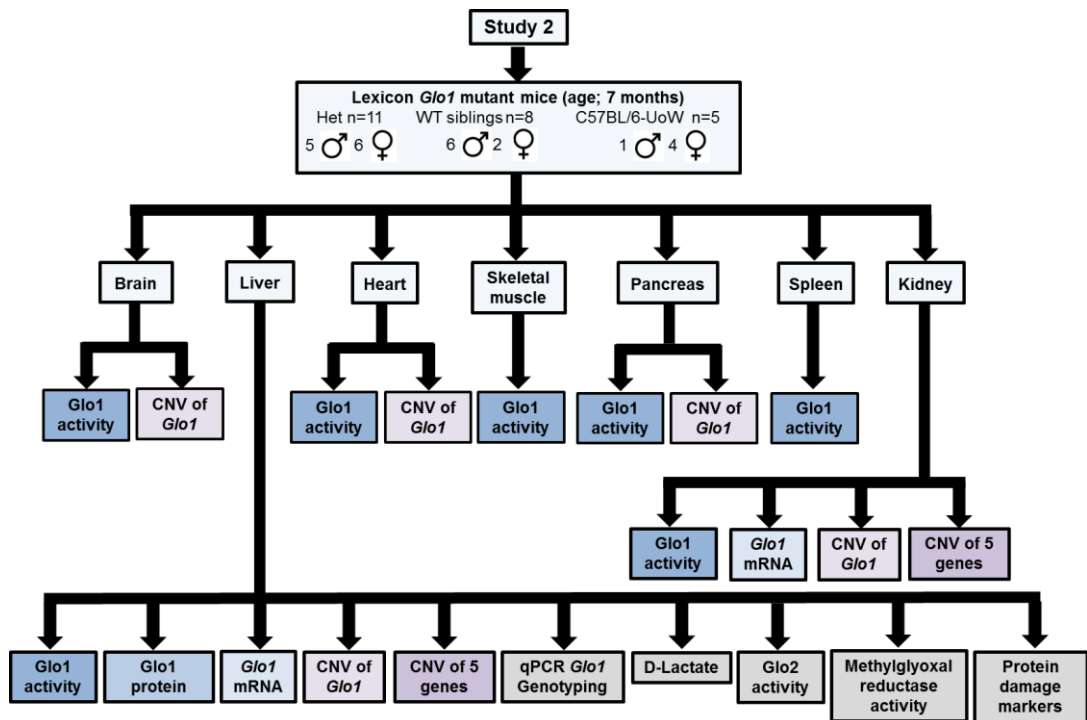


Figure 2.3: Study 2. Summary of mice and tissues analysed. Glo1 and Glo2 activity was measured in tissues (U/mg protein) and protein glycation, oxidation and nitration adduct residues of liver protein extracts (mmol/mol corresponding amino acid modified). Copy number variation was analysed in *Glo1* (exon 1), *Glo1* (exon 6), *Btd9*, *1700097n02rik* and *Dnah8* genes (5 genes).

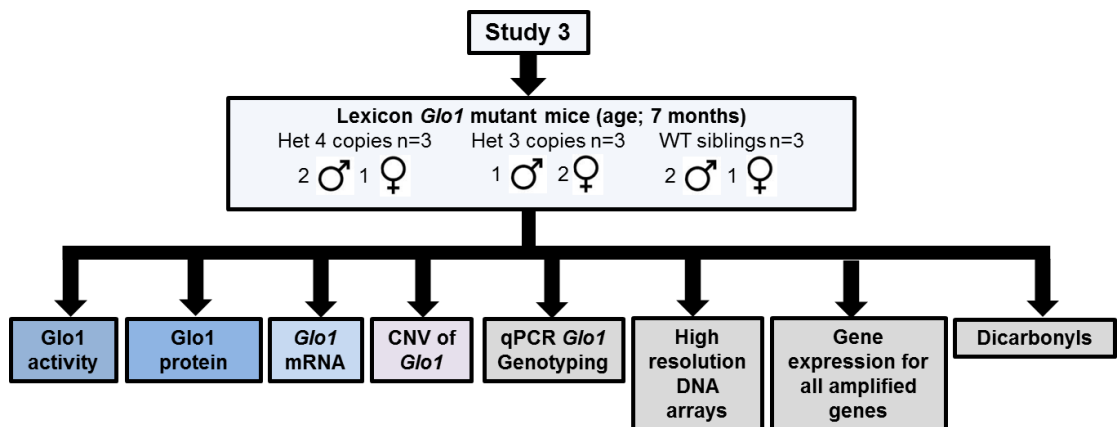


Figure 2.4: Study 3. Summary of mice and analysis performed. All measurements were made of liver tissue.

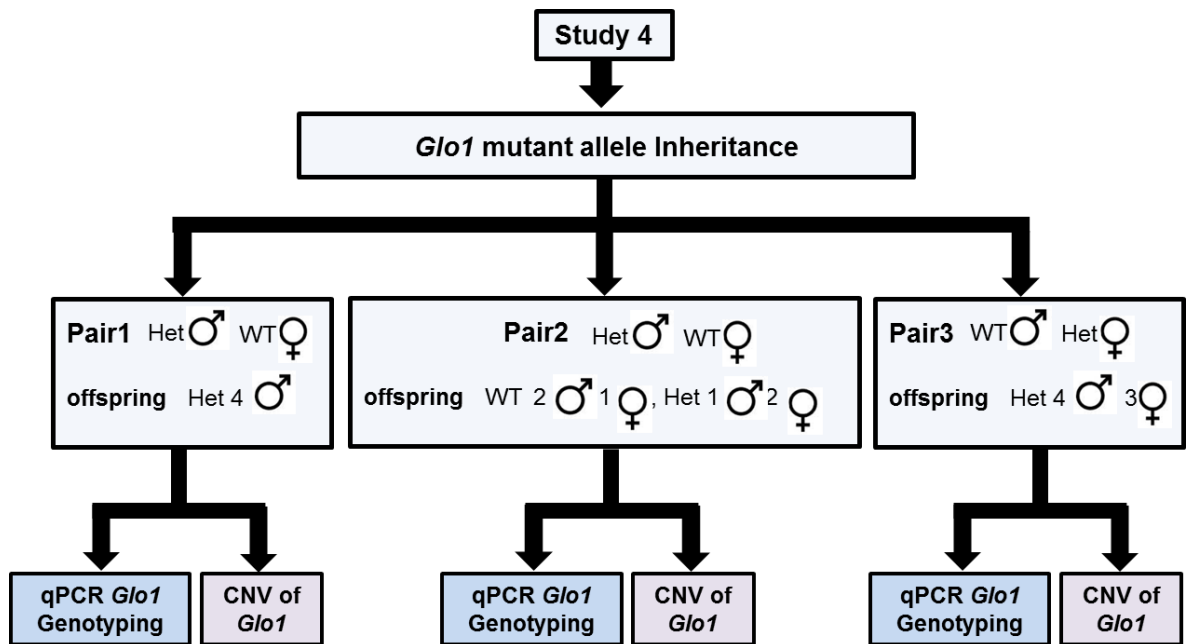


Figure 2.5: Study 4. Summary of mice inheritance study outcome and analysis performed. All measurements were made of DNA extracted from whole blood samples or ear punches.

2.2.1.1. Tissue collection

Tissues including brain, heart, liver, spleen, kidney, pancreas and skeletal muscle were collected from mice in each study group immediately after sacrifice by cervical dislocation and stored in -80°C freezer until analysis.

2.2.1.2. Tissue homogenisation

Tissue samples (*ca.* 25 mg wet weight) were transferred to chilled 1.5 ml tubes. Homogenisation buffer (10 mM sodium phosphate buffer, pH 7.4 and 4 °C; 250 µl) was added and the tissue homogenised by MULTI-GEN 7 homogenizer for 30 s - 60 s on ice. The homogenate was then centrifuged at 20,000 x g for 30 min at 4°C. The supernatant was removed and retained. Protein concentration was determined by the Bradford assay. The cytosolic extract was used to measure activities of Glo1, Glo2 and methylglyoxal reductase, protein damage markers, and was also used for Western blotting - see below. Liver tissue samples were also homogenised with 4% TCA-0.9% saline for assay of dicarbonyls – see later.

2.2.2. Cell culture

2.2.2.1. Mouse embryonic stem cells

MEF cells were cultured in high glucose D-MEM media supplemented with 10% FBS (ESC qualified). The cells were seeded over 0.1% AF at a density of 25,000 cells/cm². After 2 - 4 days, the feeder layer was ready for ESCs plating. ESCs were seeded over the feeder layer with a density of 50,000 cells/cm² and incubated at 37°C in 5% CO₂ and 95% air-water saturated atmosphere. The media used for ESCs was knockout™ D-MEM media supplemented with 15% KSR, 1% NEAA, 1% L-glutamine, 0.001% LIF and 0.00182% 2-mercaptoethanol. ESCs were incubated at 37°C in 5% CO₂ and 95% air-water saturated atmosphere. For the experiments performed under low pO₂ conditions, cells were incubated in hypoxia chamber gassed with 3% oxygen, 5% carbon dioxide and 92% nitrogen at 37°C. The ESCs media was changed every day and ESCs were passaged every 2 - 3 days when 80 - 90% confluent.

When the cells were ready for passage, medium was removed and flasks washed with PBS. Approximately 1 ml per 25 cm² StemPro Accutase solution was added to each flask and cells returned to 37°C incubator for 3 - 5 min. StemPro accutase solution was neutralised with supplemented D-MEM media. Cell pellets were diluted to required concentrations depending on cell density and added to new sterile polystyrene culture vessels over 0.1% AF and without a feeder layer. Unless otherwise mentioned, the ESCs were maintained in the conditions described above.

In the ESCs transfection experiment, Lipofectamine® 2000 was mixed with OptiMEM^(R) I reduced serum media (1:50). ON-TARGET plus Non-targeting pool or SMART pool: ON-TARGET plus *Glo1* siRNA diluted with 5x siRNA universal buffer to different concentration for optimal *Glo1* silencing and then mixed with OptiMEM^(R) I reduced serum medium. Both media were incubated for 15 min at room temperature. The media were mixed together and incubated for another 15 min. After the incubation, the mixture was added to adherent ESCs (after the passage by 24 h).

2.2.2.2. Human leukaemia 60 cells

HL60 cells were seeded in T-175 flasks in 30 ml of RPMI 1640 medium supplemented with 10% FBS with a density $1 \times 10^6/30$ ml and incubated in 37°C in 5% CO₂ and 95% air-water saturated atmosphere. Cells cultured in these conditions were passaged for four or more passages till exponential growth of cultures free of cell debris was attained. When the cells reached 80 - 90% confluence - usually within 5 days, they were then passaged to T-175 flasks with a density $1 \times 10^6/30$ ml of RPMI 1640 medium supplemented with 10% FBS.

2.2.2.3. Cell culture experimentation

Cells were grown in the following conditions:

- (i) **MG copy number alteration studies** - with varied concentrations of exogenous MG for 0.25 – 12 days with varied single or repeated treatment protocols;
- (ii) **Glo1 inhibition studies** – with varied concentrations of BrBzGSHCp₂ for 3 days, replenishing BrBzGSHCp₂ in fresh media every day in normoxia;
- (iii) **Glo1 silencing studies** – with 100 nM, 200 nM *Glo1* siRNA and non-targeting siRNA for 3 days with new dose at 36 hours, followed by incubation with exogenous MG.

To avoid phenotypic drift or differentiation of ESCs in culture, batches of new ESCs were revived from cryostorage every 3 months and cells were not used for experiments after more than 15 passages. In addition, stem cells markers including SOX2, NANOG and OCT4 were identified by Western blotting after every experiment to insure that the stem cells were not differentiated. All cell culture experiments are summarised in Figures 2.6, 2.7, 2.8.

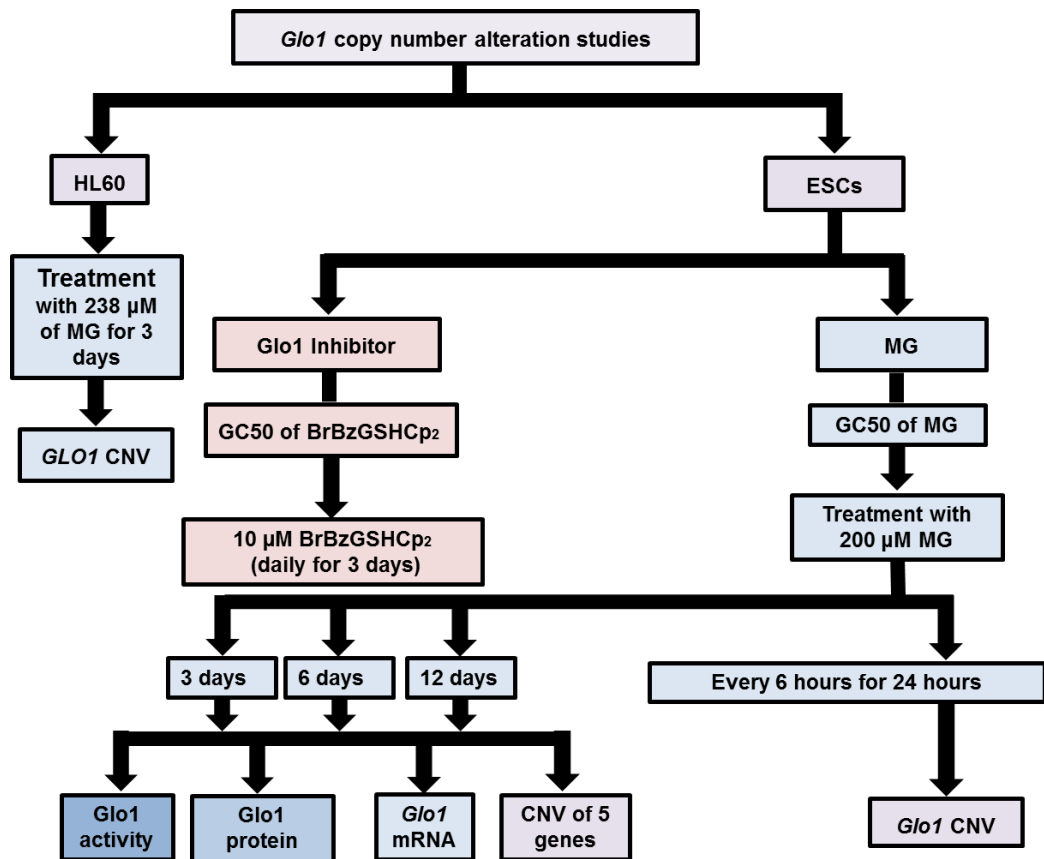


Figure 2.6: Summary of *in vitro* experiments of *Glo1* CNV induction. *Glo1* activity was measured in cells (U/mg protein). Copy number variation was analysed in *GLO1* (exon 1), *GLO1* (exon 6), *BTBD9*, *1700097N02RIK* and *DNAH8* genes (5 genes).

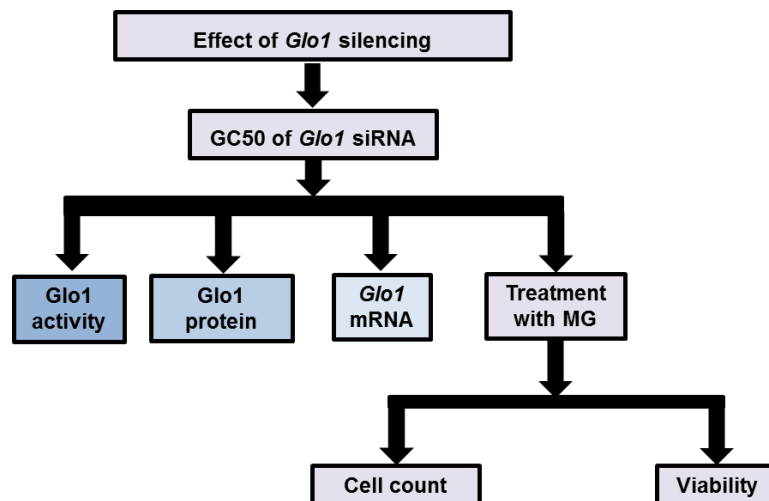


Figure 2.7: Summary of *in vitro* experiments of ESCs transfection with *Glo1* siRNA.

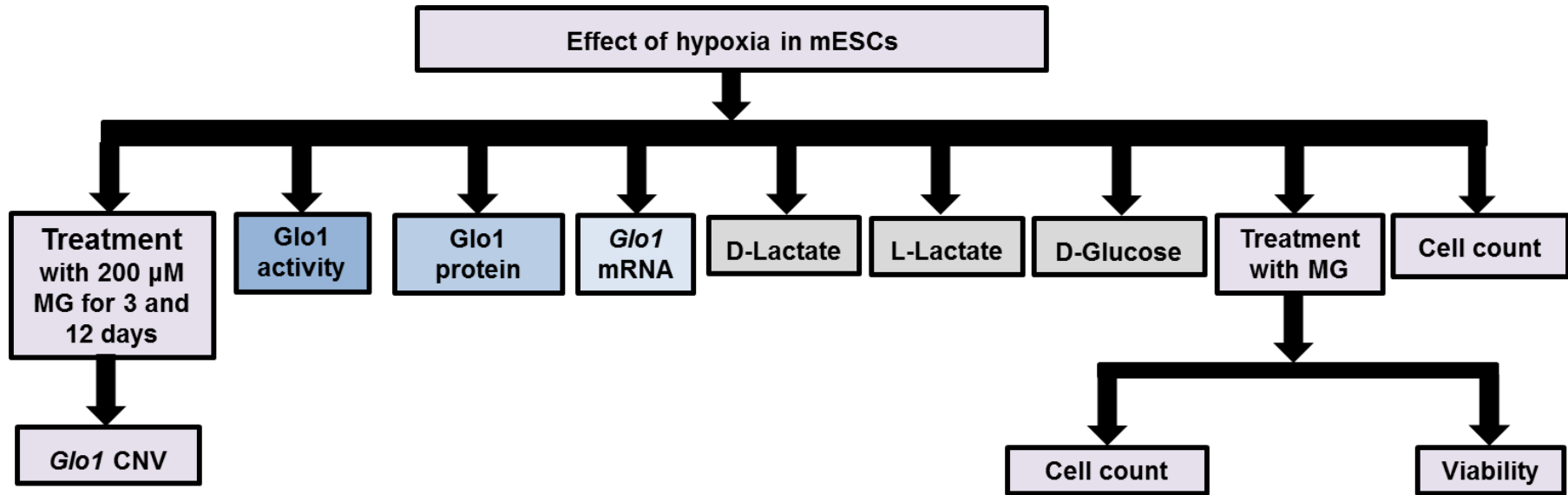


Figure 2.8: Summary of *in vitro* experiments of embryonic stem cells grown under 3% oxygen environment.

2.2.2.4. Collection of cell samples

After incubation, ESCs were removed by StemPro accutase solution, counted and cells sedimented by centrifugation (250 g, 5 min at room temperature). Cell pellets were washed thrice with PBS. Cell pellets were re-suspended in 50 - 200 μ l complete lysis-M buffer for 10 min at room temperature or used directly for DNA or RNA extraction. Cells were then sonicated (100 W, 30 s) and membranes were sedimented by centrifugation (20,000 x g, 30 min, 4°C). Supernatant was removed and stored at -80°C.

2.2.2.5. Cell viability measurement

Cell viability was assessed by Trypan blue dye exclusion technique (Strober, 2001). Cell suspension (20 μ l) containing 1 - 2 x 10⁶ cells per ml was mixed with 0.4% solution of Trypan blue (20 μ l) in PBS. Viability was then determined using haemocytometer ensuring that a total count of 100 - 200 cells. The number of cells excluding Trypan blue gives the viable cell count (V) and the number of cells stained with Trypan blue gives the non-viable cell count (NV). Percentage cell viability is given by $V/(V+NV) \times 100$. All experiments were performed with cell viability of $\geq 92\%$.

2.2.3. Glyoxalase 1 copy number alteration in clinical dicarbonyl stress - end stage renal disease

To study Glo1 copy number in clinical exposure to increased MG of renal failure, GLO1 copy number was determined in peripheral blood leukocytes of patients with ESRD - stage 5 chronic kidney disease on haemodialysis. These patients suffer the most clinically severe dicarbonyl stress and increased MG exposure (Agalou et al., 2005, Rabbani and Thornalley, 2012b, Rabbani and Thornalley, 2012a). Whole blood samples were collected with EDTA as anticoagulant from healthy human subjects and patients with ESRD with written informed consent. Clinical characteristics of the participants are given - Table 2.1. Healthy human subjects and ESRD patients were recruited at the University Hospitals Coventry & Warwickshire NHS Trust (Coventry, UK). Ethical approval was sought and gained from the National Research Ethics Service (NRES)

Committee West Midlands - Coventry & Warwickshire; project number 05/Q2802/26. Samples were stored at -80°C until analysis.

Table 2.1: Characteristics of end stage renal failure patients and healthy controls.

	Healthy subjects	Patients with ESRD
N	20	20
Gender (M/F)	10/10	10/10
Age (years)	53.7 ± 10.3	53.8 ± 9.4
BMI (kg/m ²)	26.3 ± 3.3	26.2 ± 3.3
Ethnicity (Caucasian/Asian)	18/2	20/0
Alcohol consumption (Yes/No)	17/3	12/8
Alcohol consumption (Unit)	3.5 (0 – 40)	1.0 (0 -18)
Smoking (Ex/Current/Never)	6/4/10	4/2/14
Systolic blood pressure (mmHg)	124 ± 14	139 ± 27
Diastolic blood pressure (mmHg)	76.0 ± 8.9	77.2 ± 13.2
Haemoglobin (g/dL)	13.5 ± 1.5	11.5 ± 1.5
Glucose (mmol/L)	5.49 ± 1.44	6.13 ± 1.53
HbA1c (mmol/mol)	39.9 ± 6.8	36.3 ± 4.9
Creatinine (µmol/L)	89.6 ± 17.1	621.9 ± 242.4

Data are mean ± SD. For alcohol consumption (Units), data are median (minimum – maximum).

2.2.4. Analytical Methods

2.2.4.1. Assay of total protein by the Bradford method

The concentration of protein in tissue extracts or cells lysate was measured by Bradford protein assay (Bradford, 1976, Compton and Jones, 1985). Concentrated standard stock solutions of bovine serum albumin (BSA) was calibrated by UV absorption spectrophotometry using the extinction coefficient at 279 nm for a 1% (10 mg/ml) solution; ϵ_{279} (1%) = 6.9 cm⁻¹ (Peters, 1962). Protein samples were diluted in the range 0.05 to 0.3 mg/ml. Test samples, BSA standards and blanks in triplicate (20 µl per well) were mixed with 200 µl of diluted Bradford reagent in a 96-well clear microplate. Absorbance at 595 nm was read 10 min after addition. The concentration of protein in test samples was deduced by interpolation of the calibration curve.

2.2.4.2. Activity of glyoxalase 1

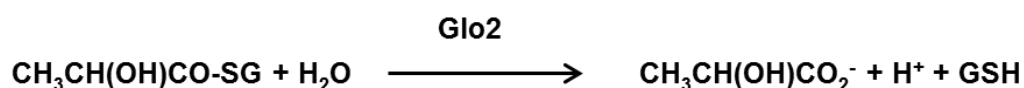
The activity of Glo1 was determined by measuring the initial rate of formation of S-D-lactoylglutathione from the MG-GSH hemithioacetal which is formed non-enzymatically from MG and reduced glutathione (GSH). The reaction was conveniently determined by following the increase in absorbance at 240 nm for which $\Delta\epsilon_{240} = 2.86 \text{ mM}^{-1} \text{ cm}^{-1}$.



Hemithioacetal was prepared by pre-incubation of 2 mM MG with 2 mM GSH for 10 min in 50 mM sodium phosphate buffer, pH 6.6 and 37°C (980 μl). The tissue extract or cell lysate (20 μl) was added and the absorbance at 240 nm was monitored with time for 5 min. The activity of Glo1 is deduced from the initial increase in absorbance, corrected for homogenization buffer blank. Glo1 activity is given in units per mg protein where one unit of Glo1 activity is the amount of enzyme which catalyses the formation of 1 μmol SLG per min under assay conditions (Arai et al., 2014).

2.2.4.3. Activity of glyoxalase 2

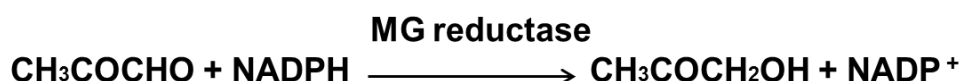
The activity of Glo2 was determined by measuring the initial rate of hydrolysis of SLG to D-lactate and GSH, followed spectrophotometrically at 240 nm; $\Delta\epsilon_{240} = -3.10 \text{ mM}^{-1}\text{cm}^{-1}$ (Clelland and Thornalley, 1991, Allen et al., 1993).



SLG (0.3 mM) was incubated in 50 mM Tris/HCl, pH 7.4 at 37°C and the tissue extract, cell lysate or lysate buffer for the blank was added at a 50-fold dilution to a final volume of 1 ml. The reaction was monitored for absorbance at 240 nm for 5 min at 37°C. The initial rate of change in absorbance was deduced. One unit of Glo2 activity is the amount of enzyme which catalyses the hydrolysis of 1 μmol SLG per min under assay conditions (Allen et al., 1993).

2.2.4.4. Assay of methylglyoxal reductase activity

The activity of MG reductase was determined by measuring the initial rate of reduction of MG to hydroxyacetone (major product) and lactaldehyde (minor product), conveniently followed by measuring the rate of oxidation of NADPH, followed spectrophotometrically at 340 nm; $\Delta\epsilon_{340} = 6.2 \text{ mM}^{-1}\text{cm}^{-1}$ (Murata et al., 1985).



NADPH (0.1 mM) and MG (1 mM) was incubated in 50 mM sodium phosphate buffer, pH 7.4 at 37°C and the tissue extract or lysate buffer for the blank was added to a final volume of 1 ml. The reaction monitored for absorbance at 340 nm for 5 min at 37°C. The initial rate of change in absorbance was deduced. One unit of MG reductase activity is the amount of enzyme which catalyses the hydrolysis of 1 μmol of NADPH per minute under assay conditions (Murata et al., 1985).

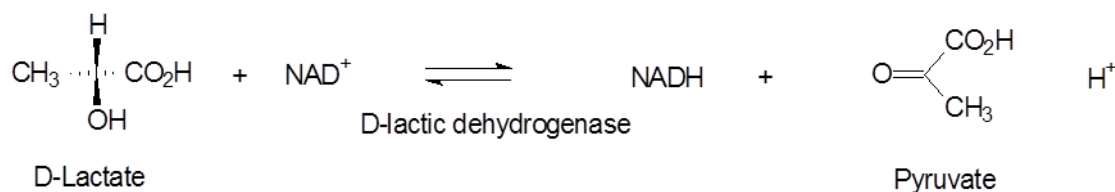
2.2.4.5. Western Blot

Tissue protein extract or cell lysate (20 μg) was mixed with 4x Laemmli sample buffer and separated using 8–16% Mini-PROTEAN® TGX™ gel in Tris/glycine/SDS electrophoresis buffer. The separated proteins were transferred from the gel to nitrocellulose membrane by Trans-Blot® Turbo™ RTA midi nitrocellulose transfer kit using PowerPac™ basic power supply electrophoresis unit (semi-dry transfer at 2.5 Ampere and 25 volt) for 3 min. The sandwich layer of semi-dry transfer consisted of filter paper, gel and membrane, immersed in transfer buffer. Membranes were blocked with 5% dried milk protein in Tris-buffered saline with tween-20 (TBS-T buffer; 500 mM NaCl, 20 mM Tris; pH 7.5 and 0.05% Tween-20) for 1 hour. Membranes were then probed with primary antibody using pre-determined concentrations of anti-Glo1 antibody or ESCs markers including SOX2, NANOG and OCT4 overnight at 4°C. After blotting with primary antibody, the membranes were washed with 3 x TBS-T buffer. Membranes were then probed with secondary antibody (anti-rabbit) at room temperature for 1 h. Membranes were rinsed with 3 x TBS-T and developed with ECL reagent and photographic films.

Glo1 blotting results were normalised to β -actin (protein loading control). Membranes were scanned and quantified with ImageQuant densitometry software.

2.2.4.6. Assay of D-lactate

The concentration of D-lactate in the media or tissue extract was assayed by endpoint enzymatic assay, modified for microplate techniques, with D-lactic dehydrogenase using fluorescence (McLellan et al., 1992).



Inclusion of hydrazine in the assay cocktail removes pyruvate from the equilibrium as pyruvyl-hydrazone and drives the forward reaction to completion and endpoint. The amount of D-lactate in the sample is deduced from the amount of NADH formed, determined by microplate fluorimetry with fluorescence detection at excitation wavelength 340 nm and emission wavelength 460 nm.

Media samples (500 μ l) were deproteinised with perchloric acid (PCA, 0.6 M; 1.0 ml), incubated on ice for 10 min, vortex-mixed and centrifuged (7000 g, 5 min, 4°C). The supernatant (700 μ l) was neutralised with potassium bicarbonate (175 μ l, 2 M) and centrifuged to sediment the resulting potassium perchlorate precipitate. For the tissue extracts, tissue samples (10 mg) were homogenized with PCA (0.6 M; 250 μ l), incubated on ice for 10 min, vortex-mixed and centrifuged (4000 g, 5 min, 4°C). The supernatant (200 μ l) was neutralised with potassium bicarbonate (80 μ l, 2 M) and centrifuged to sediment the resulting potassium perchlorate precipitate. Solutions were placed in a centrifugal evaporator and vacuum applied (20 mmHg) to remove dissolved CO_2 formed during the neutralisation. The neutralised PCA extract from tissue or media (100 μ l, pH 7) was assayed for D-lactate by incubating with glycine-hydrazine buffer (1.2 M glycine, 0.5 M hydrazine dihydrochloride, 2.5 mM DETAPAC, pH 9.2; 100 μ l), NAD^+ (25 μ l, 4 mM) and D-lactic dehydrogenase (25 μ l, 250 U/ml) for 2 h. Control samples were run in parallel without D-lactic dehydrogenase. A calibration curve was constructed in the range 0 - 6 nmol D-lactate for media samples (Figure 2.9) and the curve was constructed in the range 0 - 3 nmol D-lactate for tissue samples.

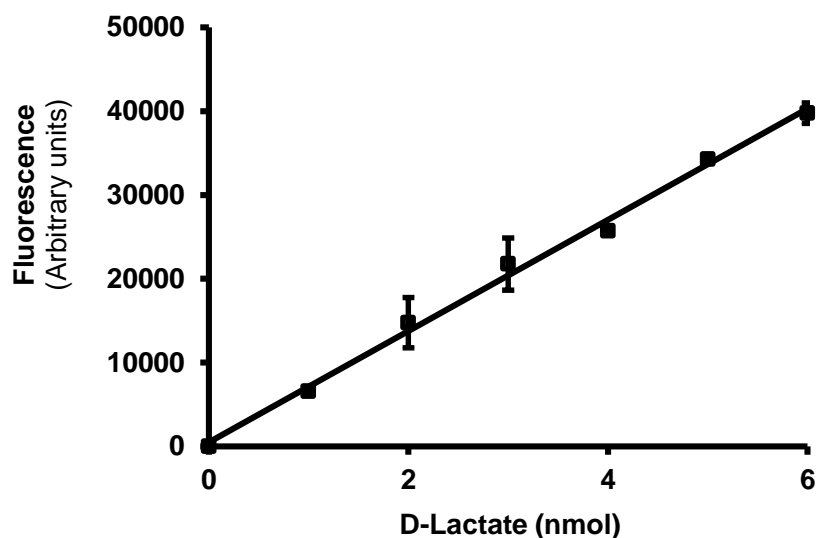


Figure 2.9: Typical calibration curve for assay of D-lactate. Linear regression equation: Fluorescence (arbitrary units) = $(6632 \pm 508) \times \text{D-lactate (nmol)}$; $R^2 = 0.995$ (data are mean \pm SD; $n = 3$).

2.2.4.7. Assay of L-lactate

The concentration of L-lactate in cell culture medium was determined similarly as the D-lactate method described in section 2.2.4.6. A standard curve was constructed using L-lactate standards in range 0 - 10 nmol and L-lactate dehydrogenase was used instead of D-lactate dehydrogenase used for the D-lactate assay. Since the cellular levels of L-lactate are 50-100 fold higher than D-lactate, media samples were first diluted with water to ensure that concentrations measured were within the standard curve range. Figure 2.10 shows a calibration curve for L-lactate.

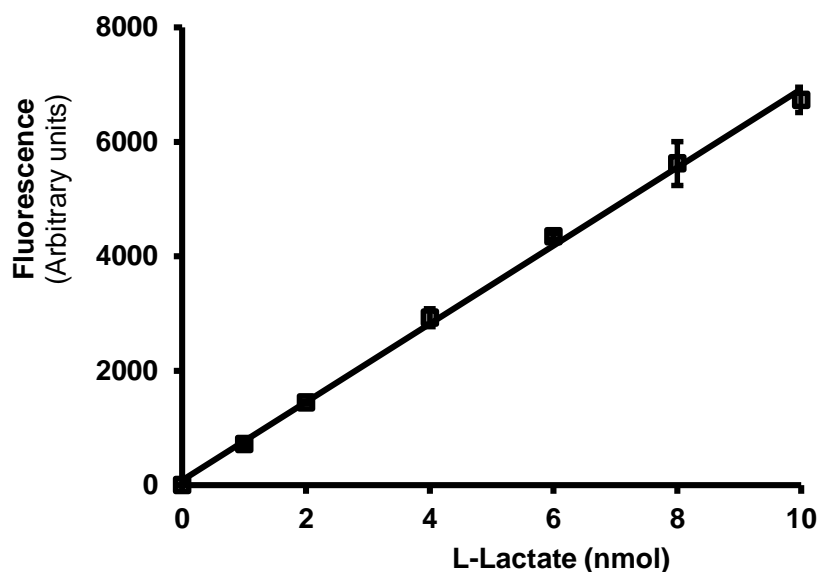


Figure 2.10: Typical calibration curve for assay of L-lactate. Linear regression equation: Fluorescence (arbitrary units) = $(683 \pm 87) \times$ L-lactate (nmol); $R^2 = 0.998$ (data are mean \pm SD; n = 3).

2.2.4.8. Assay of D-glucose

The concentration of glucose in cell culture media was determined using an end-point enzymatic assay using a commercial assay reagent (containing 1.5 mM NAD^+ , 1 mM ATP, 1 unit/ml hexokinase and 1 unit/ml glucose-6-phosphate (G6P) dehydrogenase) and 1 mg/ml D-glucose standard. The enzymatic basis of the assay is illustrated in Figure 2.11.

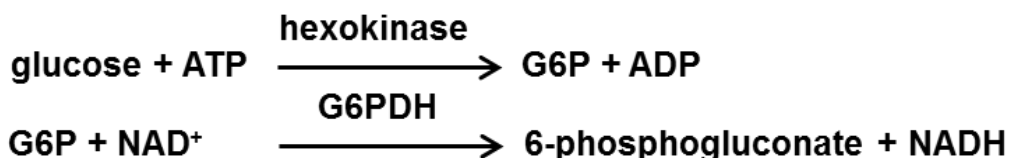


Figure 2.11: The coupled enzyme reactions of the glucose assay.

The formation of NADH was measured by spectrophotometrically at 340 nm. Since equimolar amounts of glucose are phosphorylated to G6P and NAD^+ reduced to NADH in this reaction, the increase in absorbance at 340 nm is directly proportional to the concentration of glucose. A standard curve was constructed in the range of 0 - 1.5 mM D-glucose - Figure 2.12.

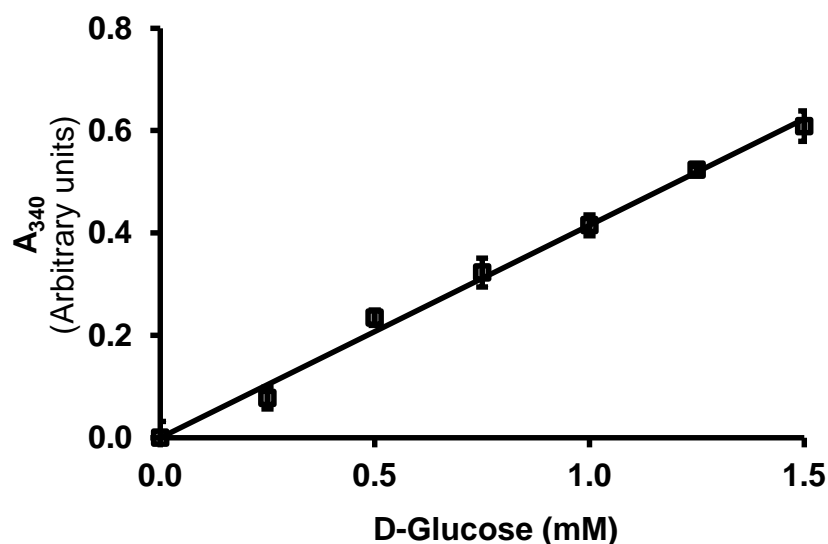


Figure 2.12: Typical calibration curve for assay of D-glucose. Linear regression equation: A_{340} (A.U.) = $(0.414 \pm 0.0142) \times$ D-glucose (mM); $R^2 = 0.994$ (data are mean \pm SD; n = 3).

Media samples at baseline and after treatment were collected and diluted with water appropriate for estimates to fall within the range of the calibration curve. Aliquot of standards and diluted samples (25 μ l) was added to a clear 96-well plate with 225 μ l of the assay reagent. The microplate was then incubated at room temperature for 15 min and absorbance was measured at 340 nm using FLUOstar optima microplate reader. The concentration of D-glucose was deduced from the standard curve and D-glucose levels were expressed in mM. The consumption of D-glucose was also calculated by subtracting the D-glucose levels after experimental incubations from baseline media concentrations and expressed in nmol/day/ 10^6 cells.

2.2.5. LC-MS/MS methods

2.2.5.1. Protein glycation, oxidation and nitration adducts

Protein glycation, oxidation and nitration adducts residues in the liver protein of Glo1 mutant mice and their WT sibling were quantified by stable isotopic dilution analysis LC-MS/MS after exhaustive enzymatic hydrolysis as described (Thornalley et al., 2003b) - see section 2.2.1.2.

Analytes determined were: early glycation adduct FL; AGEs – (CEL, CML, G-H1, MG-H1, 3DG-H, CMA and MOLD); oxidation adducts - methionine sulfoxide (MetSO), dityrosine (DT) and N-formylkynurenine (NFK); and nitration adduct 3-nitrotyrosine (3-NT).

The liver protein was delipidified by extraction three times with an equal volume of water-saturated ether. Residual ether was removed by a centrifugal evaporator. The protein (5 mg/ml) was diluted 5-fold with water and washed by 4 cycles of concentration to 50 μ l and dilution to 500 μ l with water over a microspin ultrafilter (10 kDa cut-off) at 4°C. The protein content was determined by Bradford assay. The diluted samples were further diluted to 100 μ g of protein in 20 μ l to be used for enzymatic hydrolysis.

An aliquot of washed protein sample containing 100 μ g of protein was diluted to 25 μ l with water in a glass vial and flushed with argon in preparation for enzymatic hydrolysis. The reagents and test samples were placed in a robotic processor (PAL HTS9, CTC Analytics, Switzerland) ready for automated enzymatic hydrolysis. Samples and reagents were made aseptic by microspin filtration in aseptic microspin filters. The processor was programmed to perform series of additions as follows and summarised in Table 2.2: 100 mM HCl (10 μ l), pepsin solution (2 mg/ml in 20 mM HCl; 5 μ l), and thymol solution (2 mg/ml in 20 mM HCl; 5 μ l) were added, and the samples were incubated at 37°C for 24 h. The samples were then neutralized and buffered at pH 7.4 by the addition of 12.5 μ l 100 mM potassium phosphate buffer, pH 7.4, and 5 μ l 260 mM KOH. Pronase E solution (2 mg/ml in 10 mM $\text{KH}_2\text{PO}_4/\text{K}_2\text{HPO}_4$, pH 7.4; 5 μ l) and penicillin/streptomycin (1000 units/ml and 1 mg/ml respectively; 5 μ l) were added, and the samples were incubated at 37°C for 24 h. Finally, aminopeptidase solution (2 mg/ml in 10 mM $\text{KH}_2\text{PO}_4/\text{K}_2\text{HPO}_4$, pH 7.4; 5 μ l) and prolidase solution (2 mg/ml in 10 mM $\text{KH}_2\text{PO}_4/\text{K}_2\text{HPO}_4$, pH 7.4; 5 μ l) were added, and the samples were incubated at 37°C for 48 h - Table 2.2. This gave the final enzymatic hydrolysate (77.5 μ l) for the LC-MS/MS assay. Hydrolysed sample (5 μ l) and water (20 μ l) was mixed with internal standard mixture (25 μ l) in HPLC vials to be analysed for protein glycation, oxidation and nitration adducts and related amino acids by LC-MS/MS.

Table 2.2: Protocol for enzymatic hydrolysis using CTC-PAL automated sample processor. Adapted from (Rabbani et al., 2014a).

Addition	Volume added (μ l)
Day 0	
100 mM HCl	10.0
Pepsin solution (2 mg/ ml)	5.0
Thymol (1 mg/ml)	5.0
Incubate for 24 h at 37°C	
Day 1	
100 mM KH ₂ PO ₄ /K ₂ HPO ₄ buffer, pH 7.4	12.5
260 mM KOH	5.0
Pronase E solution (2 mg/ml)	5.0
Penicillin (100 units/ml) and streptomycin (1 mg/ml)	5.0
Incubate for 24 h at 37°C	
Day 2	
Aminopeptidase solution (2 mg/ml)	5.0
Prolidase solution (2 mg/ml)	5.0
Incubate for 48 h at 37°C	

Standard curves for LC-MS/MS analysis were prepared as described in Table 2.3, using a cocktail of normal and isotopic standards prepared as described in Tables 2.4. Figure 2.13 shows typical calibration curves for arginine and MG-H1.

Table 2.3: Protocol for preparation of calibration standard solutions from cocktails of normal and stable isotopic standards for assay of protein glycation, oxidation and nitration adduct residues of liver protein extracts.

Cal no	Normal standards solution (μ l)	Water (μ l)	Stable isotopic standard solution (μ l)	Total volume (μ l)
0	0.00	25.00	25	50
1	1.25	23.75	25	50
2	2.50	22.75	25	50
3	6.25	18.75	25	50
4	12.50	12.50	25	50
5	18.75	6.25	25	50
6	25.00	0.00	25	50

Table 2.4: Analyte content of calibration standard solutions for assay of protein glycation, oxidation and nitration adduct residues of liver protein extracts.

Normal standards (nmol)								Internal standard (nmol)	
Cal no	0	1	2	3	4	5	6		
Lys	0	0.05	0.10	0.25	0.50	0.75	1.0	[¹³ C ₆]Lys	0.25
Arg	0	0.05	0.10	0.25	0.50	0.75	1.0	[¹⁵ N ₂]Arg	0.25
Met	0	0.05	0.10	0.25	0.50	0.75	1.0	[² H ₃]Met	0.25
Tyr	0	0.01	0.02	0.05	0.10	0.15	0.2	[² H ₄]Tyr	0.10
Trp	0	0.01	0.02	0.05	0.10	0.15	0.2	[¹⁵ N ₂]Trp	0.05
Normal standards (pmol)								Internal standard (pmol)	
Cal no	0	1	2	3	4	5	6		
FL	0	0.250	0.50	1.250	2.50	3.750	5.00	[² H ₄]FL	0.30
Orn	0	0.125	0.25	0.625	1.25	1.875	2.50	[² H ₆]Orn	2.50
G-H1	0	0.025	0.05	0.125	0.25	0.375	0.50	[¹⁵ N ₂]G-H1	0.25
MG-H1	0	0.125	0.25	0.625	1.25	1.875	2.50	[¹⁵ N ₂]MG-H1	1.25
3DG-H	0	0.125	0.25	0.625	1.25	1.875	2.50	[¹⁵ N ₂]3DG-H	1.25
CML	0	0.125	0.25	0.625	1.25	1.875	2.50	[¹³ C ₆]CML	0.25
CEL	0	0.025	0.05	0.125	0.25	0.375	0.50	[¹³ C ₆]CEL	0.25
CMA	0	0.025	0.05	0.125	0.25	0.375	0.50	[¹³ C ₂]CMA	0.25
MOLD	0	0.025	0.05	0.125	0.25	0.375	0.50	[² H ₈]MOLD	0.25
MetSO	0	0.125	0.25	0.625	1.25	1.875	2.50	[² H ₃]MetSO	1.25
DT	0	0.025	0.05	0.125	0.25	0.375	0.50	[² H ₆]DT	0.25
3-NT	0	0.025	0.05	0.125	0.25	0.375	0.50	[³ H ₂]3-NT	0.25
NFK	0	0.025	0.05	0.125	0.25	0.375	0.50	[¹⁵ N ₂]NFK	0.25

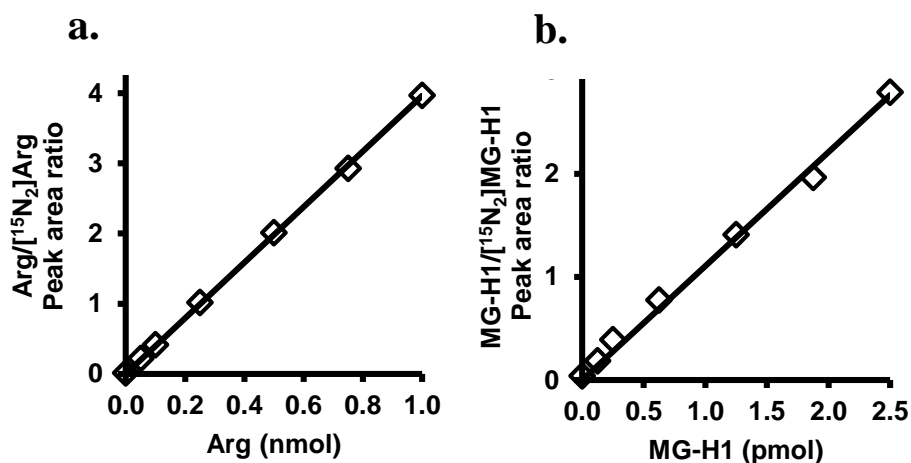


Figure 2.13: Typical calibration curves for arginine and MG-H1 in stable isotopic dilution analysis LC-MS/MS. a. Calibration curve of arginine. Linear regression equation: $\text{arg}/[^{15}\text{N}_2]\text{arg peak area ratio} = (3.93 \pm 0.03) \times \text{arg (nmol)} + 0.024 \pm 0.013$; $R^2 = 0.999$ ($n = 7$). **b.** Calibration curve of MG-H1. Linear regression equation: $\text{MG-H1}/[^{15}\text{N}_2]\text{MG-H1 peak area ratio} = (1.06 \pm 0.03) \times \text{MG-H1 (pmol)} + 0.073 \pm 0.035$; $R^2 = 0.994$ ($n = 7$).

Protein glycation, oxidation and nitration free adducts in urine samples from the Glo1 mutant and WT mice were also quantified by LC-MS/MS. Analytes determined were: early glycation adduct FL; AGEs - CEL, CML, G-H1, MG-H1 and 3DG-H and related structural isomers, CMA, MOLD and oxidation adducts - MetSO, DT and NFK; and nitration adducts 3-NT. Urine samples were collected from Glo1 mutant and WT mice by a metabolic cage. Ultrafiltrate was prepared from urine (50 μ l) by microspin ultrafiltration (3 kDa cut-off, 14,000 x g, 4°C). An aliquot of ultrafiltrate (5 μ l) was added to 0.1% TFA (20 μ l) and stable isotopic standard cocktail (25 μ l). This was then analyzed by LC-MS/MS. Standard curve was prepared as described in Tables 2.5. The calibration curve was prepared as shown in Tables 2.6. Figure 2.13 shows typical calibration curves for arginine and MG-H1.

Table 2.5: Protocol for preparation of calibration standard solutions from cocktails of normal and stable isotopic standards for assay of protein glycation, oxidation and nitration free adducts of urine.

Cal no	Normal standards solution (μ l)	Water (μ l)	Stable isotopic standard solution (μ l)	Total volume (μ l)
0	0.00	25.00	25.00	50
1	1.25	23.75	25.00	50
2	2.50	22.75	25.00	50
3	6.25	18.75	25.00	50
4	12.50	12.50	25.00	50
5	18.75	6.25	25.00	50
6	25.00	0.00	25.00	50

Table 2.6: Analyte content of calibration standard solutions for assay of protein glycation, oxidation and nitration free adducts of urine.

Normal standards (nmol)										Internal standard (nmol)	
Analyte	Calibration no										
	0	1	2	3	4	5	6	7	8		
Lys	0	1.0	2.0	5.0	10.0	15.0	20.0	40.0	-	[¹³ C ₆]Lys	5.0
Arg	0	1.0	2.0	5.0	10.0	15.0	20.0	-	-	[¹⁵ N ₂]Arg	5.0
Met	0	1.0	2.0	5.0	10.0	15.0	20.0	-	-	[² H ₃]Met	5.0
Tyr	0	0.2	0.4	1.0	2.0	3.0	4.0	20.0	30.0	[² H ₄]Tyr	2.0
Trp	0	0.2	0.4	1.0	2.0	3.0	4.0	-	-	[¹⁵ N ₂]Trp	1.0
Normal standards (pmol)										Internal standard (pmol)	
Analyte	Calibration no										
	0	1	2	3	4	5	6				
FL	0	5.00	10.0	25.0	50.0	75.0	100	[² H ₄]FL	6.0		
Ornithine	0	2.50	5.0	12.5	25.0	37.5	50.0	[² H ₆]Orn	50.0		
G-H1	0	2.50	5.0	12.5	25.0	37.5	50.0	[¹⁵ N ₂]G-H1	5.0		
MG-H1	0	2.50	5.0	12.5	25.0	37.5	50.0	[¹⁵ N ₂]MG-H1	25.0		
3DG-H	0	2.50	5.0	12.5	25.0	37.5	50.0	[¹⁵ N ₂]3DG-H	25.0		
CML	0	1.25	2.5	6.25	12.50	18.75	25.0	[¹³ C ₆]CML	5.0		
CEL	0	0.50	1.0	2.5	5.0	7.5	10.0	[¹³ C ₆]CEL	5.0		
CMA	0	0.50	1.0	2.5	5.0	7.5	10.0	[¹³ C ₂]CMA	5.0		
MOLD	0	0.50	1.0	2.5	5.0	7.5	10.0	[² H ₈]MOLD	5.0		
Pentosidine	0	0.05	0.10	0.25	0.50	0.75	1.00				
MetSO	0	2.50	5.0	12.5	25.0	37.5	50.0	[² H ₃]MetSO	25		
DT	0	0.50	1.0	2.5	5.0	7.5	10.0	[² H ₆]DT	5		
3-NT	0	0.50	1.0	2.5	5.0	7.5	10.0	[³ H ₂]3-NT	5		
NFK	0	0.50	1.0	2.5	5.0	7.5	10.0	[¹⁵ N ₂]NFK	10		

For pentosidine there was no isotopic standard as this is determined by in-line fluorescence detection.

For chromatographic conditions in LC-MS/MS analyses, two 5 µm particle size Hypercarb columns were used in series (column 1: 2.1 x 50 mm; and column 2: 2.1mm x 250 mm). The mobile phase was: solvent A - 0.1% TFA in water, and solvent B - 0.1% TFA in 50% acetonitrile (MeCN). Solvents for the post-run method for washing were: solvent A - 0.1% TFA in water, and solvent B - 0.1% TFA in 50% THF. The elution profiles for assay run and column washing and re-equilibration are given in Table 2.7. Flow from the column in the interval 4 to 35 min was directed to the MS/MS detector. Electrospray positive ion mass spectrometric multiple reaction monitoring (MRM) was used to detect all protein damage analytes. The ionisation source temperature and desolvation temperature were 120°C and 350°C, respectively. The cone gas and desolvation gas flow were 99 l/h and 901 l/h,

respectively. Optimised molecular ion and fragment ion masses and collision energies for MRM detection are given in Table 2.8. Masslynx software was used to integrate the chromatographic peaks. Analyte amounts in urine were normalised to amount of creatinine in urine. Analyte amounts in liver were normalised to amount of related unmodified amino acid in protein hydrolysates to deduce content of glycation, oxidation and nitration adduct residues in tissue protein and to creatinine to deduce fluxes of glycation, oxidation and nitration free adduct excretion in urine.

Table 2.7: Elution profile for LC-MS/MS analysis of protein glycation, oxidation and nitration adducts (Acquity-Xevo-TQS™ system).

Time (min)	Flow rate (ml/min)	Solvent A (%)	Solvent B (%)	Gradient
0	0.2	100	0	----
5	0.2	100	0	Linear
8	0.2	97	3	Linear
12	0.2	97	3	Linear
15	0.2	83	17	Linear
18	0.2	83	17	Linear
24	0.2	20	80	Linear
24	0.2	97	3	Linear
35	0.2	97	3	Linear
Post-run				
0	0.4	0	100	-----
10	0.4	0	100	Isocratic
20	0.2	0	100	Isocratic
20	0.2	100	0	Immediate
25	0.2	100	0	Isocratic
40	0.4	100	0	Isocratic

A similar elution profile was used for the Acquity-Quattro Premier™ LC-MS/MS system.

Table 2.8: Chromatographic retention times and MRM detection conditions for detection of glycation, oxidation and nitration adducts by stable isotopic dilution analysis tandem mass spectrometry (Acquity-Xevo-TQS™ system).

Analyte	Rt (min)	Molecular ion (Da)	Fragment ion (Da)
Lys	5.6	147.1	84.1
[¹³ C ₆]Lys	5.6	153.1	89.1
Val	8.6	117.8	72.0
[² H ₈]Val	8.6	125.8	80.0
MetSO	8.7	166.1	56.2
[² H ₃]MetSO	8.7	169.1	56.2
3DG-H	11.7	319.1	70.1
[¹⁵ N ₂]3DG-H	11.7	321.1	70.1
MG-H1	11.9	229.2	114.1
[¹⁵ N ₂]MG-H1	11.9	231.2	116.1
CMA	12.3	233.1	70.1
[¹³ C ₂]CMA	12.3	235.1	70.1
G-H1	12.7	215.2	100.1
[¹⁵ N ₂]G-H1	12.7	217.2	102.1
MOLD	15.0	341.2	83.9
[² H ₈]MOLD	15.0	349.2	87.9
Tyr	18.4	182.9	137.0
[² H ₄]Tyr	18.4	186.9	141
NFK	23.7	237.1	191.1
[¹⁵ N ₂]NFK	23.7	239.1	193.1
3-NT	23.4	227.1	181.1
[² H ₃]3-NT	23.4	230.1	184.1
Trp	23.7	205.1	158.8
[¹⁵ N ₂]Trp	23.7	205.1	160.8
CML	32.1	205.1	84.1
[¹³ C ₆]CML	32.1	211.1	89.1
FL	32.1	291.1	84.1
[² H ₄]FL	32.1	295.1	88.1
CEL	32.2	219.2	130.0
[¹³ C ₆]CEL	32.2	225.2	136.0
Arg	32.2	176.2	70.1
[¹⁵ N ₂]Arg	32.2	178.2	70.1
Met	32.2	150.0	104.0
[² H ₃]Met	32.2	153.0	107.0

2.2.5.2. Creatinine

Creatinine levels of urine were determined by stable isotopic dilution analysis LC-MS/MS using [*N*-methyl-²H₃] creatinine as internal standard. Creatinine stock solution was prepared in water and calibrated by UV spectrometry at λ_{\max} 234 nm with extinction coefficient of 6900 M⁻¹cm⁻¹ (Dawson et al., 1986, p11). Creatinine was detected and quantified using an Acquity-Quattro PremierTM LC-MS/MS system with a Hypercarb column (2.1 x 150 mm, 3 μ m). The mobile phase was: solvent A - 0.1% formic acid (FA); and solvent B1 - 0.1% FA in 50% MeCN. An additional solvent, solvent B2 - 0.1% FA in 50% THF, was used to wash the column in the post-run elution protocol. The elution profile is shown in Table 2.9.

Table 2.9: Elution profile for creatinine assay.

Measurement run					
Time (min)	Flow rate (ml/min)	Solvent A (%)	Solvent B1 (%)	Solvent B2 (%)	Gradient
Initial	0.2	100	0	-	----
5.0	0.2	100	0	-	Linear
20.0	0.2	100	0	-	Linear
Post-run column wash and re-equilibration					
Initial	0.2	0	-	100	----
20.0	0.2	0	-	100	Isocratic
25.0	0.2	100	-	0	Isocratic
40.0	0.4	100	-	0	Immediate change

Flow from the column was directed to the MS/MS detector in the interval 5 to 20 minutes for data collection. Electrospray positive ionisation was used for the MRM detection of creatinine. The ionisation source temperature and desolvation temperature were 120°C and 350°C, respectively. The cone gas and desolvation gas flow rate were 286 l/hr and 898 l/hr, respectively. The capillary and cone voltage were 1.0 kV and 15.0 V, respectively. The MRM and retention time of creatinine are shown in Table 2.10.

Table 2.10: Detection of creatinine by positive ion multiple reaction monitoring.

Analyte	Retention time (min)	Parent ion (Da)	Fragment ion (Da)	Cone voltage (V)	Collision energy (eV)
Creatinine	11.1	114.0	44.3	29.0	12.0
[<i>N-methyl-²H₃</i>] creatinine	11.4	117.0	47.3	29.0	12.0

Creatinine standard solution (5 μ M) was prepared in water. Standards were prepared in the range of 10 to 200 pmol, with addition of 100 pmol [*N-methyl-²H₃*] creatinine as an internal standard. Ultrafiltrate of urine samples were prepared as described above - section 2.2.5.1, and an aliquot (5 μ l) diluted 1000 fold. Each sample (10 μ l) was mixed with 100 pmol of [*N-methyl-²H₃*] creatinine and 0.1% FA added to make the final volume of 50 μ l and analysed by LC-MS/MS – Table 2.11.

Table 2.11: Preparation of calibration standards for creatinine assay.

Cal no	Analyte (pmol)	5 μ M Creatinine (μ l)	10 μ M [<i>N-methyl-²H₃</i>] creatinine (μ l)	Volume of 0.1% FA (μ l)
0	0	0	10	40
1	10	2	10	38
2	25	5	10	35
3	50	10	10	30
4	100	20	10	20
5	150	30	10	10
6	200	40	10	0

LC-MS/MS data for creatinine assay was integrated with MassLynx software. The calibration curve was plotted: peak area ratio of creatinine/[*N-methyl-²H₃*] creatinine against the amount of creatinine standard- Figure 2.14. The amount of creatinine in samples was deduced accordingly with the calibration curve.

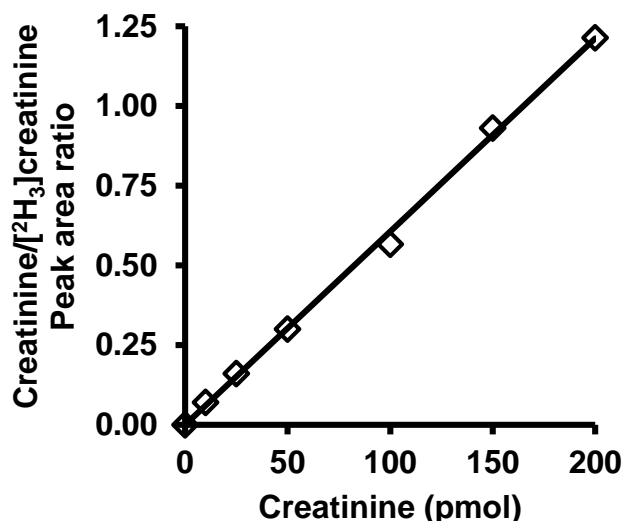


Figure 2.14: Calibration curve of creatinine. Linear regression equation: creatinine/ [²H³]creatinine peak area ratio = (0.0072 ± 0.0018) x creatinine (pmol); R² = 0.998 (n = 7).

2.2.5.3. Assay of methylglyoxal

The concentration of methylglyoxal in liver homogenate of Glo1 mutant mice was determined by derivatisation with 1,2-diaminobenzene and quantification of the resulting quinoxaline adducts - Figure 2.15, by stable isotopic dilution analysis LC-MS/MS.

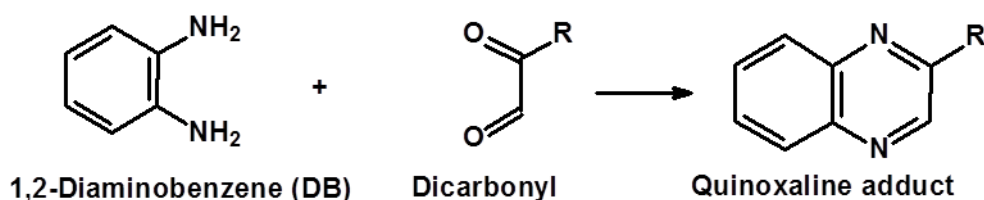


Figure 2.15: Derivatization used in the dicarbonyl assay.

Tissue samples (*ca.* 10 mg wet weight) of each sample were homogenized in 5 % ice-cold TCA-saline (50 µl). The tissue was homogenised by MULTI-GEN 7 homogenizer for 30 s to 60 s on ice. Isotopic standard, 2 pmol [¹³C₃]methylglyoxal (5 µl), was then added and the homogenate was mixed well. The homogenate was then centrifuged (20,000 g, 30 min, 4°C) to sediment membranes and fibrous material. The supernatant was removed and used in the analysis. For analysis, the supernatant (35 µl) was mixed with 3% (w/v) sodium azide (5 µl) and vortex-mixed. Finally, 10 µl 0.5 mM 1,2-diaminobenzene (DB) solution containing 0.5 mM DETAPAC and 0.2 M HCl was added to each sample. The samples were incubated in the dark for 4 h.

Calibration standards were prepared and derivatized concurrently containing 2 pmol isotopic standard and 0 - 20 pmol methylglyoxal - Tables 2.12 and 2.13.

Table 2.12: Calibration standards for dicarbonyl assay.

Cal no	MG (pmol)	Isotopic standard (pmol)
0	0	2
1	2	2
2	4	2
3	8	2
4	12	2
5	16	2
6	20	2

Table 2.13: Preparation of calibration standards from stock solutions. Adapted from (Rabbani and Thornalley, 2014c).

Cal no	5%TCA-0.9% saline (µl)	Water (µl)	3% Sodium azide (µl)	800 nM MG standard (µl)	400 nM IS (µl)	0.5 mM DB (µl)
0	10	25.0	5.0	0.0	5.0	10.0
1	10	22.5	5.0	2.5	5.0	10.0
2	10	20.0	5.0	5.0	5.0	10.0
3	10	15.0	5.0	10.0	5.0	10.0
4	10	10.0	5.0	15.0	5.0	10.0
5	10	5.0	5.0	20.0	5.0	10.0
6	10	0.0	5.0	25.0	5.0	10.0

Samples were assayed by LC-MS/MS using a Waters Acquity-Quattro Premier™ LC-MS/MS system. The column used was a BEH C18, 1.7 µm particle size column (100 x 2.1 mm) fitted with a 5 x 2.1 mm pre-column. The mobile phase was 0.1% TFA in water with a linear gradient of 0 - 50% MeCN over 10 min. The flow rate was 0.2 min/ml. The elution profile is shown in Table 2.14.

Table 2.14: Chromatographic elution profile in the MG assay.

Method phase	Time (min)	Flow rate (ml/min)	Solvent A (%)	Solvent B (%)	Curve
	Analysis	0	0.2	100	
	10	0.2	0	100	Linear
Column wash	15	0.2	0	100	Isocratic
Re-equilibration	15	0.2	100	0	Immediate change
	30	0.2	100	0	Isocratic

For mass spectrometric detection, the capillary voltage was 0.6 kV, ionisation temperature 120°C and desolvation temperature 350°C. The cone gas and desolvation gas flow were 149 l/h and 901 l/h, respectively. Optimised molecular ion and fragment ion masses and collision energies for MRM detection are given in Table 2.15.

Table 2.15: Mass-spectrometric multiple reaction monitoring detection of dicarbonyls.

Analyte	Parent ion (Da)	Fragment ion (Da)	Cone voltage (V)	Collision energy (eV)
MG	145.1	77.1	24	24
[¹³ C ₃]MG	148.1	77.1	24	24

2.2.6. Molecular biology methods

2.2.6.1. DNA extraction and purification

DNA extraction was performed using the Qiagen DNeasy blood & tissue kit according to the manufacturer's instructions. Briefly, samples of 1×10^6 cells, ≤ 25 mg of tissue or 200 μ l of whole blood were first lysed using proteinase K. Buffering conditions were adjusted to provide optimal DNA binding conditions and the lysate was loaded onto the DNeasy mini spin column. During centrifugation, DNA was selectively bound to the DNeasy membrane as contaminants including cell debris, proteins and other nucleic acids pass through. Remaining contaminants and enzyme inhibitors were removed in two washing steps and DNA was then eluted in AE buffer from the kit.

The quality and concentration of DNA was determined spectrophotometrically using a NanoDrop 1000 spectrophotometer. Extracted and purified DNA sample (2 μ l) was used to determine the concentration of DNA at A_{260} . The A_{260} is used to calculate the concentration of nucleic acids. At a concentration of 1 μ g/ml and a 1 cm path length, dsDNA has A_{260} equivalent to 50. The quality of the DNA was determined by ratio between A_{260} and A_{280} . DNeasy purified DNA has A_{260}/A_{280} ratios of 1.7–1.9 and absorbance scans show a symmetric peak at 260 nm confirming high purity.

2.2.6.2. RNA extraction and purification

Total RNA was extracted using the Qiagen RNeasy mini kit according to the manufacturer's instructions. Briefly, the samples were lysed by addition of a lysis buffer (350 μ l) containing β -mercaptoethanol and were pipetted up and down (10 times). The lysis buffer contained high concentration of guanidine-thiocyanate which acted as a chaotropic agent and helped in cell lysis. Lysed samples were mixed with 70% ethanol to enhance binding conditions to the silica-based spin-column. The sample was washed with multiple buffers to remove impurities and finally RNA was eluted by addition of RNase-free water.

The quality and concentration of RNA was determined spectrophotometrically using a NanoDrop 1000 spectrophotometer. RNA sample (2 μ l) was used to determine the concentration of RNA at A_{260} , given that value of 1 at A_{260} is equivalent to 40 μ g/ml of RNA. The quality of the RNA was determined by ratio between A_{260} and A_{280} . Pure RNA was expected to give a ratio of 1.9 - 2.1. Each sample was diluted to 50 ng nucleic acid and concentration confirmed using NanoDrop 1000.

2.2.6.3. Reverse transcription

cDNA was synthesised from the extracted RNA using reverse transcription. A total of 0.2 μ g RNA (11 μ l in 20 μ l reaction) from either animal tissue or cells was annealed with oligo (dT) (1 μ l) at 70°C for 5 min before chilling on ice. Subsequently, 8 μ l of mixture containing 10 U/ μ l RNase inhibitor (1 μ l), 10 mM dNTPs (1 μ l), 5x bioscript reaction buffer (4 μ l) and bioscript reverse transcriptase (1 μ l) were added to each sample. Samples were heated at 42°C for 60 min. The reaction was stopped by heating to 70°C for 10 min. cDNA formed was mixed with 40 μ l (3x dilution) of nuclease free water and stored at -20°C. Repeated freeze-thawing was avoided before analysis.

2.2.6.4. Mutant mice genotyping

Two methods were used for genotyping of Glo1 mutant mice including qualitative conventional PCR and semi-quantitative real time PCR.

2.2.6.4.1. Polymerase chain reaction

The PCR identifies the presence and the absence of a particular location in the DNA sample due to the attachment of the forward and reverse primers to the specific location. The PCR products were then identified by 2% agarose gel electrophoresis. For PCR, the primers used were that suggested by Lexicon – see Appendix A. Three pairs of primers were used to differentiate between wild-type, heterozygote and homozygote Glo1 mutant mice. First pair of primers was used to genotype the wild-type gene, while the second and third pairs were used to detect both ends of the inserted vector and the insertion loci - Figure 2.16.

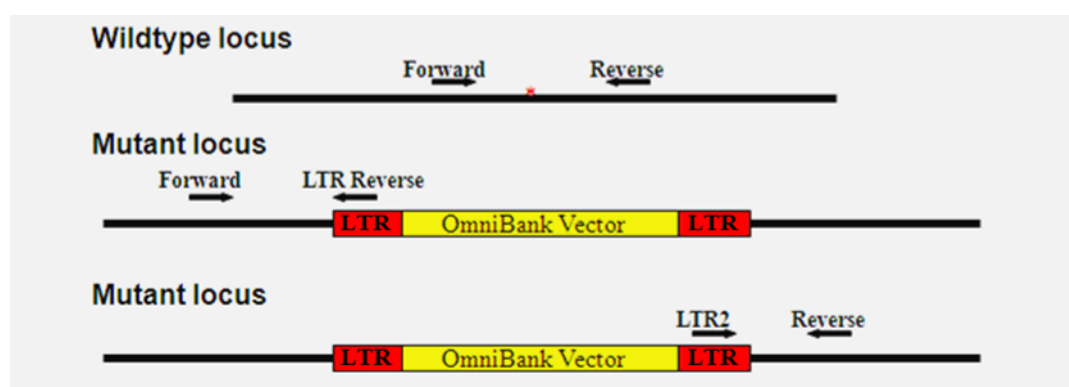


Figure 2.16: Genotyping of wild-type and knockout gene. The figure shows that the wild-type locus can be genotyped by using forward and reverse primers. The knockout locus can be genotyped by using forward and LTR reverse and/or LTR2 and reverse primer.

The reaction mixture contains the extracted DNA, Biomix red, water, forward primer and reverse primer. Each reaction contained 1 mM: dNTPs, 1.5 mM: Mg^{+2} , 0.2 pmol/ μ l: forward primer, 0.2 pmol/ μ l: reverse primer, 2 μ l of 100 ng/ μ l DNA sample, Taq polymerase, stabilizer and buffer to the final volume of 20 μ l. The protocol used for PCR is shown in Table 2.16.

Table 2.16: PCR programme used for genotyping.

Step	Process	Temperature	Time (min)
1	Initial denaturation	94°C	4:30
2	Denaturation	94°C	0:30
3	Annealing	58°C	0:30
4	Elongation	72°C	0:30
Repeat steps no 2 to 4 30 times (30 cycles)			
5	Final elongation	72°C	7:00
6	Hold	4°C	Overnight

Gel electrophoresis

The PCR product (5 μ l) was electrophoresed using 2% agarose gel stained with 0.5 μ g/ml ethidium bromide. The marker used was hyperladder V. The voltage used in gel electrophoresis was 100 volts for 90 min. After the electrophoresis, the gel was photographed using ultraviolet light by Chemi Genins².

2.2.6.4.2. Quantitative real time PCR (qPCR)

Three pairs of primers used for real time PCR are same as mentioned above. Real time PCR was used to quantify the products of each allele and to estimate number of copies present of each locus.

The qPCR reaction mixture containing DNA sample (4 μ l of 5 ng/ μ l stock solution), SensiMix Low-ROX (10 μ l), DNase/RNase free water (5 μ l), forward primer (0.5 μ l of 10 pmol/ μ l stock solution, final concentration was 0.25 pmol/ μ l) and reverse primer (0.5 μ l of 10 pmol/ μ l stock solution, final concentration was 0.25 pmol/ μ l) were added in a clear MicroAmp® optical 96-well reaction plate and sealed with MicroAmp® optical adhesive film. The plate was centrifuged for few seconds and genotyping was performed using a 7500 Fast-Real time PCR machine. The protocol used for PCR is shown in Table 2.17.

Table 2.17: qPCR protocol.

Repetitions	Temperature	Time (min)
1	95°C	10:00
40	95°C	00:15
	60°C	01:00
Hold	4°C	Overnight

Samples with the highest DNA concentration were used to construct the standard curve. The DNA was used to form standards 0 – 1,000,000 pg using serial dilutions. The reference gene was *Rn 18s*, which was used for the standards and for the samples as a housekeeping gene to normalize any experimental variation between the samples. A typical standard curve is shown in Figure 2.17.

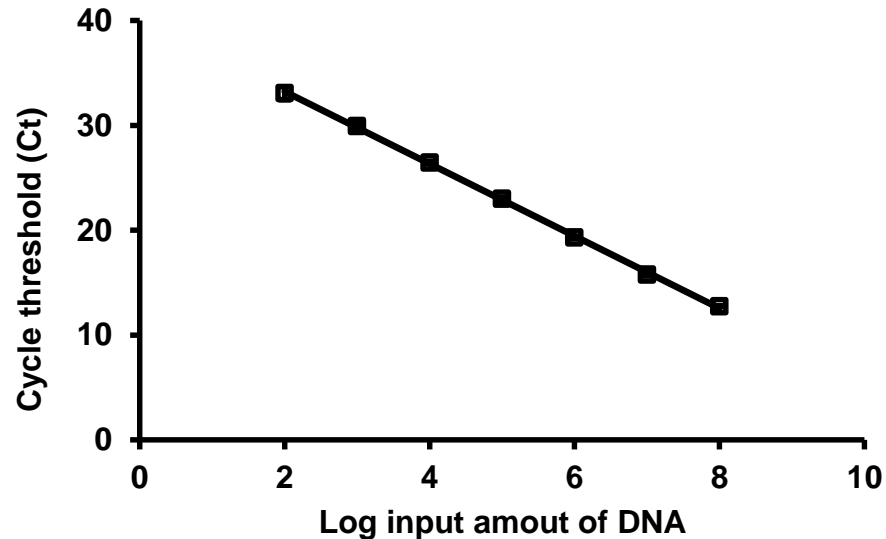


Figure 2.17: Typical calibration curve for qPCR. Linear regression equation: Cycle threshold = $(-3.23 \pm 0.037) \times \log \text{ input mRNA} + 40.16 \pm 0.20$; $R^2 = 0.999$ (data are mean \pm SD; n = 3).

2.2.6.5. Analysis of gene mRNA expression

Two methods were used for determination of gene mRNA expression including SYBR green and Taqman.

2.2.6.5.1. Gene mRNA expression analysis by SYBR green

This method was used to determine the expression of mRNA of specific genes and normalised to housekeeping gene. The mRNA was firstly transcript to cDNA as described in 2.2.6.3. The synthesised cDNA was used for standard curve construction and for analyses.

In this experiment, primers spanning exon-exon junctions were designed and chosen when possible; this acted as an additional quality control to avoid any genomic DNA contaminant which might act as a template for amplification (Appendix A). Dissociation plots were performed for all primers to test specificity. Dissociation plots were routinely performed for each PCR plate; this ensured that the primers perform consistently - Figure 2.18.

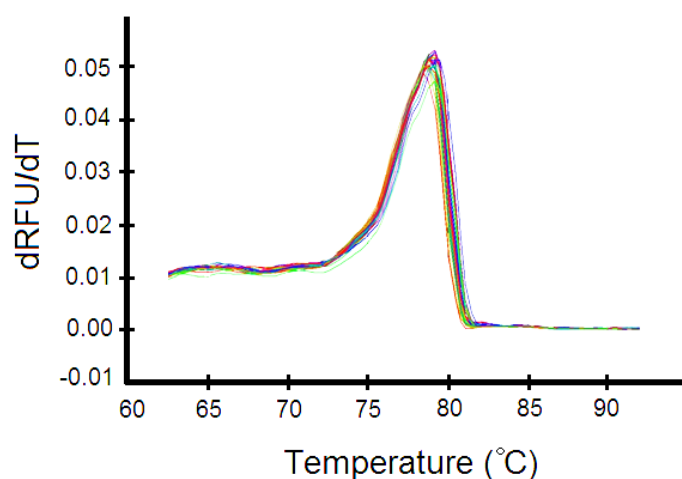


Figure 2.18: Dissociation curve of *Glo1* primers. The figure shows the specificity of *Glo1* primers represented in one peak in the curve. X axis represents the change in the temperature and Y axis represents the derivative of relative fluorescence divided by the derivative of temperature (dRFU/dT).

2.2.6.5.2. Gene mRNA expression analysis by Taqman method

This was performed using the Taqman gene expression assay protocol (PN 4333458) according to the manufacturer’s instructions. Briefly, in a clear 96 well MicroAmp® optical 96-well reaction plate, cDNA (4 µl, 10 ng/µl) was used from 2.2.6.3 and mixed with the target Taqman gene expression assay (1 µl of 20x), 2x TaqMan universal master mix II (10 µl) with UNG and 5 µl RNase-free water to make a total of 20 µl in a single well. Same mixture was used for the housekeeping gene (endogenous control) of either *Actb* or *Rn18s* using the gene specific 20x Taqman gene expression assay (1 µl) in another well - Table 2.18. After loading PCR reaction mix component for all samples, the plate was sealed with MicroAmp® optical adhesive film, centrifuged for few seconds, and loaded in a 7500 Fast-Real time PCR machine. The protocol used for PCR is shown in Table 2.19.

Table 2.18: Taqman PCR reaction mix component.

PCR reaction mix component	Single reaction	Three replicates
20x Taqman gene expression assay	1	3
2x Taqman universal master mix II, with UNG	10	30
cDNA template (10 ng/µl)	4	12
RNase-free water	5	15

Table 2.19: PCR protocol of Taqman gene expression assay.

Repetitions	Temperature	Time (min)
1	50°C	2:00
1	95°C	10:00
40	95°C	00:15
	60°C	01:00
Hold	4°C	Overnight

After the completion of the PCR reaction, the cycle threshold data was collected for each sample and endogenous control. Cycle threshold (Ct) is the cycle number at which the fluorescence for the reaction crosses the threshold value (definable parameter). Delta Ct is the difference in Ct between the target gene (Ct_(t)) and the endogenous control (Ct_(endl)) for a given sample.

$$dCt = Ct_{(t)} - Ct_{(endl)}$$

Delta delta Ct is the difference between the dCt of a particular gene for an experimental sample and the dCt of that same gene for the calibrator sample (control sample).

$$ddCt = dCt_{(exp)} - dCt_{(cal)}$$

The linear fold change in gene expression between the experimental and calibrator sample is:

$$\text{Fold change} = 2^{(-ddCt)}$$

This fold change value was used to compare between different samples.

2.2.6.6. Gene copy number analysis by Taqman method

Taqman® copy number assays employed Taqman® minor groove binding probe chemistry to evaluate the copy number of genomic DNA targets. Taqman® copy number assays are run together with a Taqman® copy number reference assay, which have a pair of specific primers and specific probe to hybridize to the complementary sequence in the DNA sample. Both run in a duplex real-time PCR using 7500 Fast-Real time PCR machine and CopyCaller™ software.

It was performed using the Taqman copy number assay protocol (PN 4397425) according to the manufacturer's instructions. Briefly, in a clear 96 well MicroAmp® optical 96-well reaction plate, 4 µl (5 ng/µl) DNA was used from 2.2.6.1. and mixed with 20x target Taqman copy number assay (1 µl), 20x reference Taqman copy number assay (1 µl), 2x Taqman genotyping master Mix (10 µl) and RNase-free water (4 µl) to make a total of 20 µl in a single well - Table 2.20. After

loading the components of the PCR reaction mixture for all samples, the plate was sealed with MicroAmp® optical adhesive film, centrifuged for few seconds, and then loaded in a 7500 Fast-Real time PCR machine. The protocol used for PCR is shown in Table 2.21.

Table 2.20: Component of Taqman copy number assay PCR reaction mix.

PCR reaction mix component	Single reaction	Three replicates
20x target Taqman copy number assay	1	3
20x reference Taqman copy number assay	1	3
2x Taqman genotyping master mix	10	30
DNA template (5 ng/μl)	4	12
RNase-free water	4	12

Table 2.21: PCR protocol of Taqman copy number assay.

Repetitions	Temperature	Time (min)
1	95°C	10:00
40	95°C	00:15
	60°C	01:00
Hold	4°C	Overnight

After the completion of the PCR reaction, the cycle threshold data was exported for each sample and control with setting of 0.2 threshold and autobaseline. The result was imported in CopyCaller™ Software where the software used Ct values of the target gene and reference gene of the samples and compares it to the data of the calibrator sample to calculate the copy number of the target gene.

2.2.6.7. Microarray-based comparative genomic hybridisation

Array-CGH was performed using SurePrint G3 mouse CGH microarrays 1x1M according to the manufacturer's instructions protocol no (G4410-90010: version 7.2 July 2012). In array-CGH, test and reference DNAs are differentially fluorescent labelled and hybridized together to the array. The resulting fluorescent ratio is then measured, clone by clone, and plotted relative to each clone's position in the genome. In this experiment, the reference samples were selected from C57BL/6 mouse strain according to the sex of the animal whose DNA was used as a sample.

Briefly, genomic DNA (0.5 μg in 20.2 μl AE buffer) of the samples and the corresponding reference derived from 2.2.6.1. were digested by BSA, Alu I and Rsa I enzymes from SureTaq complete DNA labelling kit according to the supplier's instructions - Table 2.22. The master mix was added to each reaction tube containing

gDNA to make total volume of 26 μ l. The tubes were loaded in a thermal cycler and incubated for 2 hours at 37°C, 20 minutes at 65°C and then at 4°C. The digested DNA (2 μ l) was loaded to 0.8% agarose gel to insure that most of the products were between 200 and 500 bp - Figure 2.19.

Table 2.22: Components of the digestion master mix.

Component	Volume per reaction (μ l)
Nuclease free water	2.0
10x Restriction enzyme buffer	2.6
BSA	0.2
Alu I	0.5
Rsa I	0.5
Final volume of digestion master mix	5.8

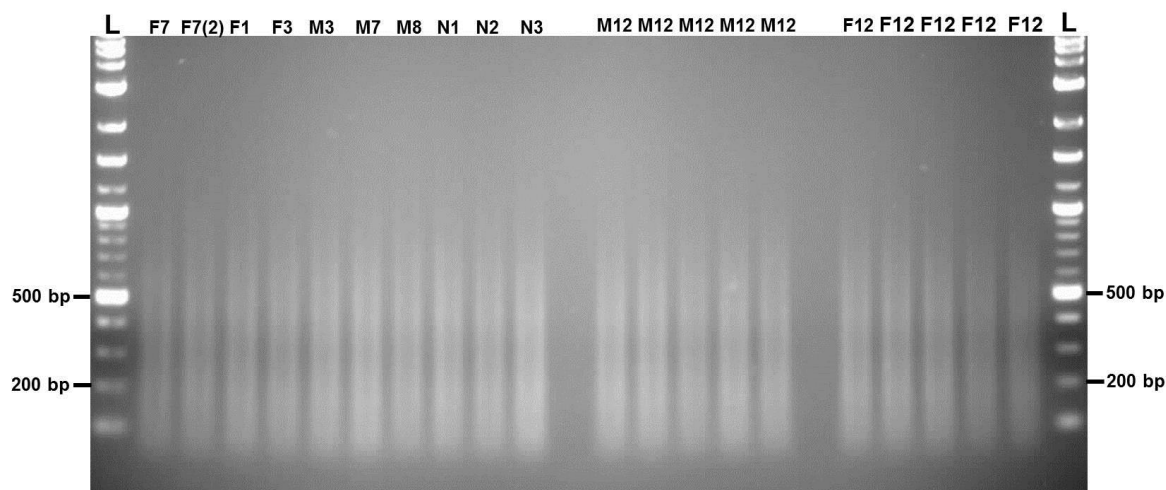


Figure 2.19: Determination of the digested DNA size in 0.8% agarose gel.

The digested DNA was amplified by random primers (5 μ l) (supplied in SureTaq complete DNA labelling kit) and heated to 95°C for 3 minutes and then at 4°C. The amplified DNA was labelled with labelling master mix (21 μ l) (Table 2.23) where the test samples were labelled with cyanine 5-dUTP and the reference samples were labelled with cyanine 3-dUTP. Then, the tubes were loaded in a thermal cycler and incubated for 2 hours at 37°C, 10 minutes at 65°C and then at 4°C.

Table 2.23: Components of the labelling master mix.

Component	Volume per reaction (μ l)
Nuclease free water	2.0
5x reaction buffer	10.0
10x dNTPs	5.0
Cyanine 3-dUTP or Cyanine 5-dUTP	3.0
Exo (-) Klenow	1.0
Final volume of labelling master mix	21.0

Labelled DNA was mixed with TE buffer (430 µl; pH 8.0) and purified with purification column provided in the SureTaq DNA labelling kit and spin for 10 min at 14,000 x g. The wash step was repeated with TE buffer (430 µl; pH 8.0) using same column and then the column was inverted in a new tube and spin for 1 min at 1,000 x g to make a total of 80.5 µl. From the mixture, 1.5 µl was used for determination of yield, degree of labelling and specific activity by using NanoDrop 1000 spectrophotometer and the following formulas:

$$\text{Degree of Labelling} = \frac{340 \times \text{pmol per } \mu\text{l dye}}{\text{ng per } \mu\text{l gDNA} \times 1000} \times 100$$

$$\text{Specific activity (pmol dyes per } \mu\text{g gDNA)} = \frac{340 \times \text{pmol per } \mu\text{l dye}}{\text{ng per } \mu\text{l gDNA} \times 1000}$$

$$\text{Yield } (\mu\text{g}) = \frac{\text{DNA concentration (ng/}\mu\text{l)} \times \text{Sample volume } (\mu\text{l})}{1000 \text{ ng/}\mu\text{g}}$$

The result was compared with the expected values in the following Table 2.24.

Table 2.24: Expected yield and specific activity after labelling and purification with the SureTag complete DNA labelling kit.

Input gDNA (µg)	Yield (µg)	Specific activity of cyanine-3 labelled Sample (pmol/µg)	Specific Activity of cyanine-5 labelled Sample (pmol/µg)
0.2	3 to 5	20 to 25	15 to 25
0.5	8 to 11	20 to 35	20 to 30
1	9 to 12	25 to 40	20 to 35

After insuring that all the values were fitted within the expected value range, the rest of the DNA sample and corresponding reference were mixed in nuclease free tube (158 µl). The hybridisation master mix (Table 2.25) was add to the tubes and heated to 95°C for 3 min then 37°C for 30 min.

Table 2.25: Hybridization master mix for microarray.

Component	Volume (µl) per hybridization
Cot-1 DNA (1.0 mg/ml)	5
10× aCGH blocking agent	11
2× HI-RPM hybridization buffer	55
Final volume of hybridization master mix	71

The mixture was hybridized to 1M array using the Oligo aCGH/ChIP-on-chip hybridization kit by loading 490 µl of the mixture to the gasket slide and covered with the active side of the microarray. The sandwich slides were loaded to Agilent microarray hybridization chamber which were all loaded to the hybridization oven heated to 60°C and rotate at 20 rpm for 40 h.

Following hybridization, the array was washed with Oligo aCGH/ChIP-on-chip wash buffer 1 and 2 and scanned using Surescan microarray slide holder and Surescan microarray scanner. All data was processed and collected by Agilent's feature extraction software. Agilent's feature extraction software finds and places microarray grids, accurately determines feature intensities and ratios, flags outlier pixels and calculates statistical confidences. Data analysis was performed with Agilent genomic workbench edition 7.0 which is a powerful visualization tool for the analysis of key microarray applications. The following settings were used in the analysis: ADM-2, threshold 6.0, with at least 3 consecutive oligos with an absolute log ratio of 0.25. For amplified DNA the algorithm ADM-2, threshold 6.0 was used with at least 3 consecutive probes with an absolute log ratio of 0.25.

2.2.6.8. PCR–restriction fragment length polymorphism

PCR–restriction fragment length polymorphism (PCR–RFLP) is a classic and relatively inexpensive method of genotyping that is based on endonuclease cleavage. A SNP that alters a restriction sequence can be genotyped by PCR–RFLP. The C to A (C419A) substitution in exon 4 of *GLO1*, which changes Ala111Glu in the encoded protein, leads to the loss of a recognition site for the SfaNI restriction enzyme.

The extracted DNA from whole blood of the clinical subject was PCR. The reaction mixture contains 200 ng/µl DNA sample, Biomix red, water, C419A genotyping forward primer and reverse primer. Each reaction contained 1 mM: dNTPs, 1.5 mM: Mg²⁺, 0.2 pmol/µl: forward primer, 0.2 pmol/µl: reverse primer, Taq polymerase, stabilizer and buffer to the final volume of 20 µl. The protocol used for PCR is shown in Table 2.26. The PCR products were digested with SfaNI digestive enzyme for 1 hour at 37°C. The digested product were resolved by 2% agarose gel electrophoresis and the fragments were visualized under UV light after staining with ethidium bromide to identify the single base pair change. The

restriction digest reveals 453 bp and 260 bp fragments in the presence of A 111 allele, and 713 bp fragment in the presence of E allele (Rinaldi et al., 2014).

Table 2.26: PCR protocol for A111E genotyping.

	Process	Temp.	Time (min)
1	Initial denaturation	94°C	5:00
2	Denaturation	94°C	0:40
3	Annealing	55°C	0:30
4	Elongation	72°C	0:40
Repeat steps no. 2 to 4 30 times (30 cycles)			
5	Final elongation	72°C	10:00
6	Hold	4°C	Overnight

2.2.7. Statistical analysis

Data was tested for normality of distribution (Kolmogorov-Smirnov test). Parametric data of independent samples (two groups) were analysed for significance of difference of means by Student's *t*-test with or without modification for difference of variance. Difference in variance was determined by the F-test. Parametric data of independent samples of (> 2 groups) was analysed by analysis of variance ANOVA. Non-parametric data were analysed using Mann Whitney-U test (2 groups) or by Kruskal-Wallis test (> 2 groups). Correlation analysis was performed with Pearson's test for parametric data and Spearman's test for non-parametric data.

3. Results

3.1. Glyoxalase 1 mutant mice

3.1.1. Genotyping

Forty-four offspring of Glo1 mutant mice were genotyped according to the method described in section 2.2.6.4. DNA extracted from liver tissue was used in PCR analysis with genotyping primer pairs 1, 2 and 3. Each of these pairs was run with DNA in a separate reaction - Figure 3.1. The amplified DNA PCR product size with each primer was 237 bp, 223 bp and 241 bp respectively. The extracted DNA from most of the Glo1 mutant mice showed a band with all 3 primers – for example, Figure 3.1, Primers 1 - 3 analyses, sample no 1 – 9 and 11. This indicates that these mice had both WT and mutant alleles and were therefore Glo1 (+/-) heterozygotes. Extracted DNA from some of the mice showed a band with primer pair 1 only - Figure 3.1, sample no 10. This indicates the presence of only the WT alleles and absence of mutant allele. This mouse is a WT sibling. Analysis of 44 offspring from mating of Glo1 mutant mice showed that 9 mice were WT and 35 were mutant heterozygote Glo1 (+/-). Mutant homozygote Glo1 (-/-) mice are expected to show reactivity with only primers 2 and 3. On this basis, there were no homozygote Glo1 (-/-) mouse offspring produced.

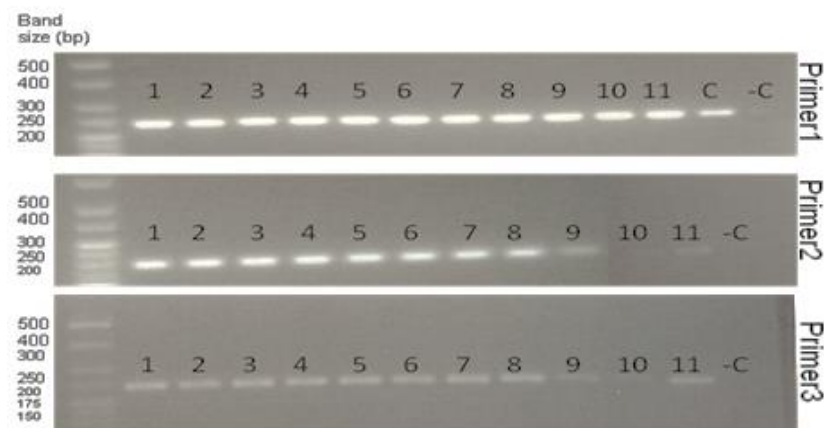


Figure 3.1: Electrophoresis results for PCR analysis of Glo1 mutant and wild-type control mice. The figure shows three agarose gels stained with ethidium bromide. The first lane on the left-hand side, Hyperladder V, shows electrophoresis of DNA size calibrators. On the right-hand side, a positive control was used in primer 1 (penultimate lane, labelled “C”) and a negative control (last lane, PCR water, labelled “-C”). Sample no 1 - 9 and 11 gave bands with all three pairs of primers with the expected band size - WT and *Glo1* mutant loci. Sample no 10 gave bands with primer pair 1 only - WT locus only.

3.1.2. **Glo1 activity of tissues of Glo1 (+/-) mutant mice and C57BL/6-UoW wild-type controls at 3 months of age**

C57BL/6-UoW and Glo1 mutant mice were sacrificed when 3 months old and Glo1 activity was measured in cytosolic extracts of tissues – as described in Section 2.2.4.2. Glo1 activity was highest in the liver and lowest in pancreas and spleen of both C57BL/6-UoW and Glo1 mutant mice. Glo1 activity of C57BL/6-UoW and Glo1 mutant mice were not significantly different in the liver, kidney, heart and pancreas whereas there was increased Glo1 activity in the brain (+58%), skeletal muscle (+19%) and spleen (+23%) of Glo1 (+/-) versus C57BL/6-UoW controls - Table 3.1.

Table 3.1: Glo1 activity in brain, heart, kidney, pancreas, skeletal muscle, spleen and liver tissue of C57BL/6-UoW and Glo1 (+/-) and mice.

Tissue	C57BL/6-UoW (unit/mg protein)	Glo1(+/-) (unit/mg protein)
Liver	3.45 ± 0.39	4.08 ± 0.91
Kidney	1.19 ± 0.15	1.36 ± 0.17
Brain	1.12 ± 0.25	1.77 ± 0.44*
Heart	1.12 ± 0.42	1.20 ± 0.19
Skeletal muscle	0.81 ± 0.07	0.96 ± 0.12*
Spleen	0.53 ± 0.04	0.65 ± 0.07**
Pancreas	0.50 ± 0.12	0.57 ± 0.07

Mice were sacrificed at 3 months. Data are mean ± SD (n = 6). Significance: *, p<0.05 and **, p<0.01; Student's t-test.

3.1.3. **Glo1 activity of tissues of Glo1 (+/-) mutant mice and wild-type controls at 7 months of age**

The activity of Glo1 was measured in the tissues of 12 Glo1 mutant and 12 wild-type control mice at 7 months old. In this experiment, there were two types of WT controls: WT siblings of Glo1 mutant mice, shown as “WT” and WT C57BL/6 mice from UoW breeding stock, shown as “C57BL/6-UoW”.

3.1.3.1. Liver

The Glo1 activity of liver of WT sibling mice of Glo1 mutant mice at 7 months was 4.44 ± 0.80 U/mg protein ($n = 7$). This was decreased 13% in Glo1 mutant (+/-) heterozygotes but not significantly. The Glo1 activity of C57BL/6-UoW mice was decreased 32 % with respect to WT sibling mice of Glo1 mutant mice ($P < 0.01$) and 26 % with respect to Glo1 mutant (+/-) heterozygote mice ($P < 0.05$) – Figure 3.2. This indicates that C57BL/6-UoW mice has significantly lower activity of Glo1 than Glo1 (+/-) and also than WT siblings. The WT sibling mice have the same origin and genetic background as the Glo1 (+/-) mice and are therefore the appropriate non-mutant controls for Glo1 (+/-) mice. The different origin and different genetic background of C57BL/6-UoW and WT mice likely explains the differences in Glo1 activity found. The appropriate wild-type strain origin is critical for correct comparisons of Glo1 activity in this study. Comparing mutant Glo1 (+/-) heterozygote mice and WT siblings, therefore, it can be concluded there is no change in Glo1 activity in the live and hence there is compensation in Glo1 activity for the mutant Glo1 allele.

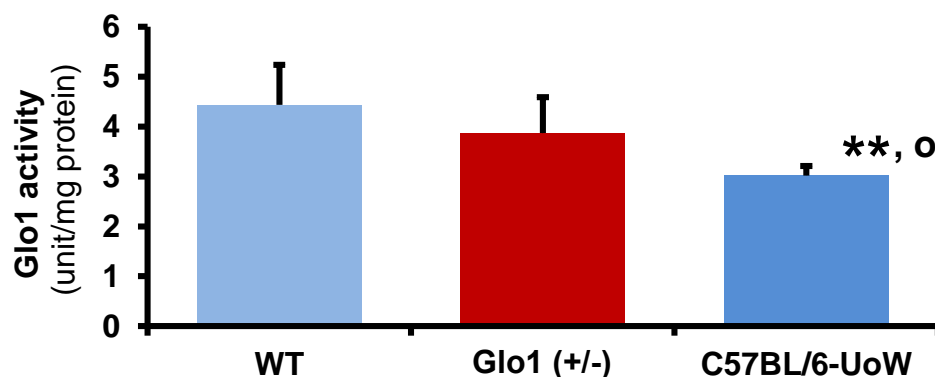


Figure 3.2: Glo1 activity of liver of Glo1 (+/-) mutant mice, wild-type sibling mice (WT) and wild-type “C57BL/6-UoW” mice. Data are mean \pm SD (Glo1 (+/-), $n = 7$; WT, $n = 12$; and C57BL/6-UoW, $n = 5$). Significance: **, $p < 0.01$ with respect to WT and °, $p < 0.05$ with respect to Glo1 (+/-); Student’s t-test.

3.1.3.2. Other tissues

Glo1 activity was measured in brain, heart, kidney, pancreas and spleen of Glo1 (+/-) mutant heterozygote mice and wild-type siblings at 7 months old - Table 3.2. There was no difference in Glo1 activity in liver, brain, skeletal muscle, heart, kidney, pancreas and spleen of Glo1 (+/-) mutant mice and wild-type siblings at 7 months old. It can be concluded there is compensation in Glo1 activity for the mutant Glo1 allele in these tissues.

Table 3.2: Glo1 activity in liver, brain, skeletal muscle, heart, kidney, pancreas and spleen of Glo1 (+/-) mutant mice and wild-type siblings at 7 months of age.

Tissue	Wild-type (units/mg protein)	Glo1 (+/-) (units/mg protein)
Liver	4.44 ± 0.80	3.87 ± 0.72
Brain	1.98 ± 0.20	2.10 ± 0.43
Skeletal muscle	1.88 ± 0.36	1.89 ± 0.33
Heart	0.95 ± 0.12	0.95 ± 0.09
Kidney	0.73 ± 0.10	0.77 ± 0.12
Pancreas	0.56 ± 0.09	0.65 ± 0.06
Spleen	0.39 ± 0.08	0.49 ± 0.14

Mice were sacrificed at 7 months. Data are mean ± SD (Glo1 (+/-) mutant, n = 12 and wild-type, n = 7). Significance: Student's t-test.

All tissues of Glo1 (+/-) mutant mice have normal, WT levels of Glo1 activity. They are therefore unsuitable for a model of Glo1 deficiency in functional genomics studies of the role of Glo1 in diabetic nephropathy and related diabetic complications. Consequently, at this point my plan of investigation changed from study of an experimental model of diabetic nephropathy to investigation of how and why the Lexicon Glo1 had maintained WT levels of Glo1 activity in all tissues tested. A first step in the investigation was to examine levels of Glo1 expression in tissues of these mice.

3.1.4. *Glo1* mRNA of kidney and liver of Glo1 (+/-) mutant mice and wild-type sibling controls at 7 months of age

Glo1 mRNA expression was analysed in RNA extracted from liver and kidney tissue samples of Glo1 (+/-) mutant mice and sibling WT control mice at 7 months of age. The mRNA expression of *Glo1* was normalized to *Rn18s* mRNA expression. There was no significant difference between these two genotypes in both tissues – Table 3.3. It can be concluded there is a mechanism compensating for the mutant Glo1 allele maintaining an unchanged level of *Glo1* mRNA in these tissues of Glo1 (+/-) mutant mice.

Table 3.3: Relative mRNA content of *Glo1* in liver and kidney tissue of *Glo1* (+/-) mutant mice and wild-type sibling controls at 7 months of age.

Tissue	WT	<i>Glo1</i> (+/-)
Liver	0.406 (0.393 – 0.415)	0.432 (0.411 – 0.436)
Kidney	0.540 (0.519 – 0.579)	0.531 (0.502 – 0.558)

Glo1 mRNA expression was normalized to *Rn18s* mRNA. Data are median (lower – upper quartile); (*Glo1* (+/-) mutant, n = 11 and WT, n = 7). Significance: Mann Whitney-U test.

3.1.5. *Glo1* protein of liver of *Glo1* (+/-) mutant mice and wild-type sibling controls at 7 months of age.

Glo1 protein in the liver cytosolic extract of *Glo1* (+/-) mutant mice and WT sibling controls at 7 months of age was measured and normalised to β -actin. The protein expression was analysed by Western blotting. There was no significant difference between both genotypes - Figure 3.3. It can be concluded there is a mechanism compensating for the mutant *Glo1* allele maintaining an unchanged level of *Glo1* protein in these tissues of *Glo1* (+/-) mutant mice.

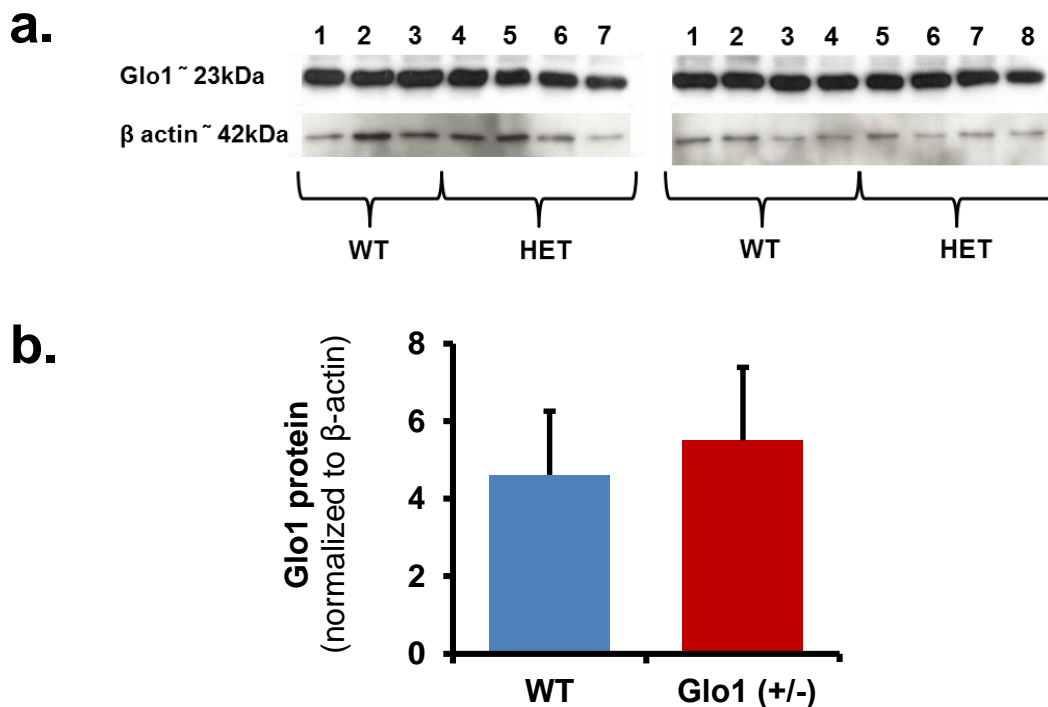


Figure 3.3: *Glo1* protein in liver tissue of *Glo1* (+/-) mutant mice and wild-type controls at 7 months of age. a. *Glo1* and β -actin immunoblotting bands for 15 samples of WT and *Glo1* (+/-). **b.** Quantification of *Glo1* protein, normalised to housekeeping protein, β -actin. Data are mean \pm SD (*Glo1* (+/-), n = 8 and WT mice, n = 7). Significance: Student's t-test. P>0.05 (not significant).

3.1.6. Glyoxalase 2 activity of liver of Glo1 (+/-) mutant mice and wild-type controls at 7 months of age.

Glo2 activity in the liver cytosolic extract of Glo1 (+/-) mutant mice and WT controls at 7 months of age was determined – see Section 2.2.4.3. There was no significant difference in Glo2 activity between Glo1 (+/-) mutant mice and WT sibling controls - Table 3.4. It can be concluded that the activity of Glo2 has not been changed by mutation of Glo1 allele in Glo1 (+/-) mutant mice.

Table 3.4: Glyoxalase 2 activity, D-lactate and MG content and methylglyoxal reductase activity in liver of Glo1 (+/-) mice and wild-type sibling control mice at 7 months of age.

Analyte	wild-type	Glo1 (+/-)
Glyoxalase 2 activity (U/mg protein)	0.109 ± 0.020	0.105 ± 0.012
Methylglyoxal reductase activity (mU/mg protein)	4.34 ± 0.65	4.32 ± 1.02
Methylglyoxal (pmol/mg wet weight)	3.26 ± 0.65	2.82 ± 0.80
D-Lactate (nmol/mg wet weight)	0.343 ± 0.063	0.360 ± 0.068

Data are mean ± SD (wild-type, n = 8 and Glo1 (+/-) mutant, n = 8 except for MG content for which n = 7). Significance: Student's t-test. P>0.05 (not significant).

3.1.7. Methylglyoxal and D-lactate contents of liver tissue of Glo1 (+/-) mutant mice and wild-type controls at 7 months of age.

MG is the major physiological substrate of Glo1. Assay of MG content of liver samples revealed there was no significant difference of MG content between Glo1 (+/-) mutant mice and WT sibling controls - Table 3.4. D-Lactate content of liver tissue of Glo1 (+/-) mutant mice and WT controls at 7 months of age were measured – see Section 2.2.4.6. There was no significant difference of D-lactate content between Glo1 (+/-) mutant mice and WT sibling controls - Table 3.4. D-Lactate is a surrogate marker of metabolic flux of MG formation. It can be concluded that the concentration and flux of MG formation in the liver is unchanged in Glo1 (+/-) mutant mice, with respect to WT controls.

3.1.8. Methylglyoxal reductase activity in liver cytosolic extract of Glo1 (+/-) mutant mice and wild-type controls at 7 months of age

Methylglyoxal reductase provides an alternative fate for MG metabolism when Glo1 activity is decreased. I therefore investigated if this alternative pathway

had been increased in Glo1 (+/-) mutant mice to compensate for the expected deficiency of Glo1 activity. Methylglyoxal reductase activity was measured in the cytosolic extracts of liver tissues of Glo1 (+/-) mutant mice and WT controls at 7 months of age – see section 2.2.4.4. There was no significant difference in methylglyoxal reductase activity between Glo1 (+/-) mutant mice and WT sibling controls - Table 3.4. It can be concluded that metabolism of MG by methylglyoxal reductase is unchanged in Glo1 (+/-) mutant mice.

Characterisation of glyoxalase- and MG-related variables in tissues of Glo1 (+/-) mutant mice showed that they were unchanged with respect to WT siblings. This suggests there was a compensatory mechanism maintaining normal Glo1 expression in Glo1 (+/-) mutant mice characterised by WT levels of mRNA, protein and activity. This suggests compensatory mechanism for the Glo1 mutant allele is at the transcriptional level. This was investigated further below.

It was also of interest to assess the effect of gender on expression and activity of Glo1 in mice.

3.1.9. Effect of gender on glyoxalase-related variables in pooled Glo1 (+/-) mutant mice and wild-type controls

Data collected on glyoxalase-related variables of WT and Glo1 (+/-) mutant mice indicated no significant difference with genotype. Data were then pooled and re-analysed for gender effects by comparing values for male and female mice. For mice of age 3 months, Glo1 activity of the liver and pancreas was increased 31% and 30%, respectively, in male mice compared to female mice; whereas, Glo1 activity of the heart was decreased 26% in male mice compared to female mice. For mice of age 7 months, Glo1 activity of the liver was increased 44% in male mice compared to female mice; and at this age, Glo1 activity of the spleen was increased by 40% in male mice compared to female mice – Table 3.5. For the liver, there was no similar increase in Glo1 protein or mRNA in male with respect to female mice, suggesting that the difference in Glo1 activity may be due to functional post-translational modification of Glo1 protein. Conversely, there was a 10% decrease of Glo1 mRNA in the kidney of male mice with respect to female mice but no similar change in Glo1 activity. Other glyoxalase-related variables of the liver - activity of Glo2 and MG reductase and contents of D-lactate and MG – were unchanged in male mice versus female mice.

Table 3.5: Summary of comparison between male and female mice for glyoxalase-related variables.

	Age (months)	N (male/female)	Tissue	Male	Female
Glo1 activity (U/mg protein)	3	6/6	Brain	1.53 ± 0.55	1.36 ± 0.44
			Heart	1.03 ± 0.22	1.40 ± 0.29*
			Kidney	1.25 ± 0.22	1.30 ± 0.13
			Liver	4.27 ± 0.74	3.27 ± 0.28*
			Pancreas	0.607 ± 0.056	0.467 ± 0.087**
			Skeletal muscle	0.880 ± 0.154	0.881 ± 0.101
			Spleen	0.621 ± 0.094	0.561 ± 0.060
	7	12/8	Brain	2.05 ± 0.29	1.91 ± 0.42
			Heart	0.969 ± 0.144	0.968 ± 0.107
			Kidney	0.796 ± 0.155	0.718 ± 0.512
			Liver	4.70 ± 0.49	3.27 ± 0.46***
			Pancreas	0.599 ± 0.097	0.632 ± 0.058
			Skeletal muscle	2.12 ± 0.49	1.73 ± 0.26
			Spleen	0.529 ± 0.143	0.379 ± 0.074*
Glo1 mRNA (<i>Glo1/18sRn</i>)	7	11/7	Kidney	0.505 (0.499 – 0.535)	0.570 (0.555 – 0.579)**
			Liver	0.416 (0.403 – 0.432)	0.414 (0.410 – 0.426)
Glo1 protein (Glo1/ β -actin)	7	12/8	Liver	5.25 ± 1.89	4.74 ± 1.69
Glo2 activity (U/mg protein)	7	8/8	Liver	0.111 ± 0.010	0.100 ± 0.019
D-Lactate (nmol/mg wet weight)	7	8/8	Liver	0.841 ± 0.133	0.861 ± 0.132
MG reductase activity (mu/mg protein)	7	8/8	Liver	3.46 ± 1.64	5.40 ± 1.15
MG content (pmol/mg wet weight)	7	8/7	Liver	3.22 ± 0.84	2.87 ± 0.60

Data are mean ± SD. Significance: Student's t-test except of mRNA analysis data are median (lower – upper quartile); Significance: Mann Whitney-U test. Significance: *, **, and ***, p<0.05, p<0.01 and p<0.001 respectively.

3.1.10. Urinary excretion of protein glycation free adducts, oxidation free adducts and related amino acids of Glo1 (+/-) mutant mice and wild-type sibling controls at 3 months of age

Urine was collected from Glo1 (+/-) mice and WT siblings and analysed for protein glycation and oxidation free adducts – see Sections 2.2.5.1 and 2.2.5.2. The flux of urinary excretion of glycation and oxidation free adducts is given in Table 3.6. For urinary excretion of amino acids, there was a 46% decrease in urinary excretion of lysine in Glo1 (+/-) mutant mice, with respect to WT controls. The urinary excretion of glycation adducts FL, CML, CEL, MG-H1 and CMA were unchanged whereas the urinary excretion of G-H1 was decreased 59% in Glo1 (+/-) mutant mice, with respect to WT controls – Table 3.6. Lack of change in urinary excretion of the major glycation adducts derived from MG, MG-H1 and CEL, suggests there is likely no increase in total body exposure to MG in Glo1 (+/-) mutant mice, with respect to WT controls.

Table 3.6: Urinary excretion of protein glycation and oxidation free adducts of Glo1 (+/-) mutant mice and wild-type sibling controls at 3 months of age.

Analyte	wild-type (n = 5)	Glo1 (+/-) (n = 7)
Amino acids (nmol/mg creatinine)		
Lys	0.249 (0.243 – 0.389)	0.134 (0.110 – 0.144)*
Arg	95.7 (69.8 – 123.1)	68.1(62.9 – 96.6)
Met	67.4 (58.3 – 71.7)	46.5 (37.6 – 66.1)
Tyr	65.0 (51.3 – 72.9)	50.6 (46.6 – 69.8)
Trp	8.48 (8.26 – 9.14)	5.52 (4.76 – 6.86)
Lysine-derived glycation adducts (nmol/mg creatinine)		
FL	723 (720 – 803)	656 (545 – 748)
CML	105.1 (79.5 – 107.2)	77.9 (75.2 – 98.2)
CEL	53.7 (47.3 – 82.8)	49.2 (47.3 – 60.2)
Arginine-derived glycation adducts residues (nmol/mg creatinine)		
MG-H1	47.8 (39.1 – 55.6)	17.8 (11.4 – 39.8)
G-H1	4.07 (3.38 – 4.48)	1.66 (1.46 – 2.49)**
CMA	6.66 (6.44 – 8.52)	7.15 (6.32 – 7.44)

Data are median (lower – upper quartile); wild-type, n = 5 and mutant Glo1 (+/-), n = 7. Significance: * and **, p<0.05 and p<0.01 respectively; Mann Whitney-U test.

3.1.11. Protein glycation and oxidation adduct residue contents of cytosolic protein extracts of mouse liver of mutant Glo1 (+/-) mice and wild-type sibling controls

Liver tissues were collected and cytosolic extracts prepared and analysed for protein glycation and oxidation adduct residue contents – see Section 2.2.5.1. The glycation and oxidation adduct residue contents of liver protein extracts are given in Table 3.7. There was no significant difference in the liver cytosolic protein contents of glycation and oxidation adduct residues except for a 45% increase of DT residues of mutant Glo1 (+/-) mice, with respect to WT controls - Table 3.7. Lack of change in liver protein residue content of the major glycation adducts derived from MG, MG-H1 and CEL, is consistent with there being no increase in MG content of Glo1 (+/-) mutant mice, with respect to WT controls – as determined directly (see above).

Comparison was also made of protein glycation and oxidation adduct residue contents of liver protein by gender. Glucosepane, CMA and NFK residue contents were higher and AASA residue content was lower in female mice compared with male littermates – Table 3.8. In all samples, pentosidine content was lower than the detection limit (20 fmol, equivalent to 0.006 mmol/mol lys).

Table 3.7: Protein glycation and oxidation adduct residue contents of liver protein of mutant Glo1 (+/-) mice and wild-type sibling controls.

Analyte	wild-type	Glo1 (+/-)
Lysine-derived glycation adduct residues (mmol/mol lys)		
FL	2.97 (2.54 – 3.52)	3.03 (2.31 – 3.37)
CML	0.134 (0.099 – 0.241)	0.096 (0.047 – 0.141)
Glucosepane	0.086 (0.061 – 0.1321)	0.055 (0.019 – 0.072)
Pentosidine	< detection limit	< detection limit
Arginine-derived glycation adduct residues (mmol/mol arg)		
MG-H1	0.447 (0.327 – 0.507)	0.382 (0.317 – 0.423)
3DG-H	0.132 (0.113 – 0.162)	0.073 (0.061 – 0.112)
G-H1	0.161 ± 0.067	0.174 ± 0.066
CMA	0.083 ± 0.024	0.077 ± 0.027
Oxidation adduct residues (mmol/mol amino acid residue modified)		
ASAA (mmol/mol lys)	0.057 (0.042 – 0.094)	0.070 (0.064 – 0.080)
GSA (mmol/mol arg)	0.039 (0.027 – 0.051)	0.050 (0.030 – 0.074)
Dityrosine (mmol/mol tyr)	1.00 (0.74 – 1.24)	1.45 (1.31 – 1.68)**
NFK (mmol/mol trp)	1.97 (1.72 – 2.28)	1.99 (1.75 – 2.08)
3-NT (mmol/mol tyr)	0.031 (0.022 – 0.044)	0.051 (0.025 – 0.087)

Data are mean ± SD or median (lower – upper quartile); n = 10. Significance: **, p<0.01; Mann Whitney-U test.

Table 3.8: Protein glycation and oxidation adduct residue contents of liver protein of male and female mice.

Analyte	Male	Female
Lysine-derived glycation adduct residues (mmol/mol lys)		
FL	2.97 (2.09 – 3.05)	3.14 (2.58 – 3.70)
CML	0.111 (0.059 – 0.206)	0.109 (0.066 – 0.176)
Glucosepane	0.061 ± 0.046	0.090 ± 0.051*
Pentosidine	< detection limit	< detection limit
Arginine-derived glycation adduct residues (mmol/mol arg)		
MG-H1	0.332 (0.316 – 0.429)	0.463 (0.371 – 0.563)
3DG-H	0.095 (0.063 – 0.116)	0.144 (0.086 – 0.188)
G-H1	0.151 ± 0.072	0.184 ± 0.056
CMA	0.070 ± 0.023	0.096 ± 0.022*
Oxidation adduct residues (mmol/mol amino acid residue modified)		
AASA (mmol/mol lys)	0.083 (0.069 – 0.094)	0.054 (0.042 – 0.064)**
GSA (mmol/mol arg)	0.051 (0.033 – 0.078)	0.035 (0.027 – 0.049)
Dityrosine (mmol/mol tyr)	1.23 (0.93 – 1.46)	1.36 (0.918 – 1.54)
NFK (mmol/mol trp)	1.72 (1.63 – 1.80)	2.27 (2.07 – 2.44)***
3-NT (mmol/mol tyr)	0.028 (0.019 – 0.038)	0.060 (0.026 – 0.087)

Data are mean ± SD or median (lower – upper quartile); n = 10. Significance: *, ** and ***, p<0.05, p<0.01 and p<0.001; Student's t-test or Mann Whitney-U test.

3.1.12. *Glo1* copy number of liver, kidney, brain and pancreas in *Glo1 (+/-)* mutant mice and wild-type controls at 7 months of age

A possible mechanism for compensatory transcription of *Glo1* in *Glo1 (+/-)* mutant mice is induction of increased copy number of the WT allele during mouse line generation by gene trapping with somatic retention of increased CNV in subsequent progeny to avoid embryonic dicarbonyl stress. The copy number of *Glo1* gene was measured by quantifying *Glo1* DNA - see Section 2.2.6.6. Two locations within the murine *Glo1* gene were chosen for DNA quantification by specific pairs of primers and Taqman probe for each location: the 3'-end of exon 1 and the 5'-end of exon 6. DNA of *Glo1 (+/-)* mutant mice and WT controls was extracted from tissues samples of liver, kidney, brain and pancreas and analysed for CNV - Figures 3.4 - 3.7. WT control siblings were assumed to have two copies of *Glo1*. CNV of *Glo1* was quantified by Taqman copy number assay and contents were normalized to Transferrin receptor protein 1 (*Tfrc*) as internal reference gene. *Tfrc* is known to be present in two copies in a diploid genome and located at chromosome 16 and is therefore at a remote genetic local from *Glo1* in a duplex PCR reaction.

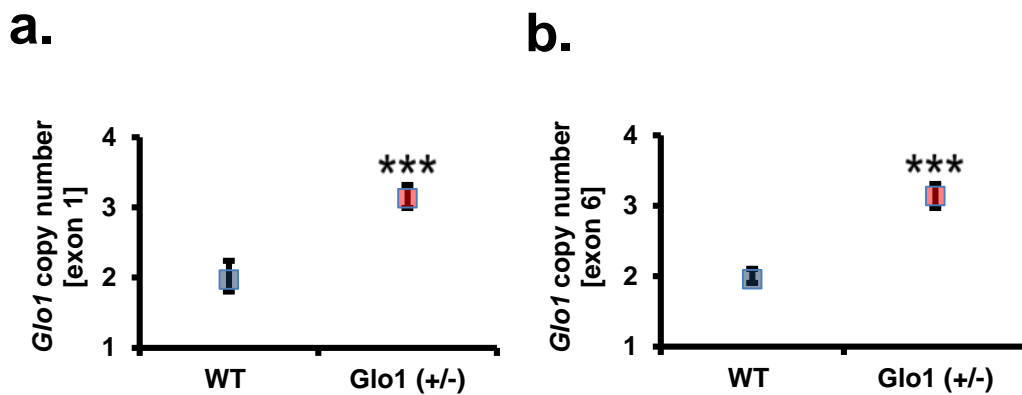


Figure 3.4: Assay of *Glo1* copy number by the Taqman method in liver tissue of *Glo1 (+/-)* mutant and sibling wild-type control mice at 7 months of age. a. Copy number of exon 1 of *Glo1*, and **b.** Copy number of exon 6 of *Glo1*. Data are median (lower – upper quartile); (*Glo1 (+/-)*, n = 9; and WT, n = 7). Significance: ***, p<0.001; Mann Whitney-U test.

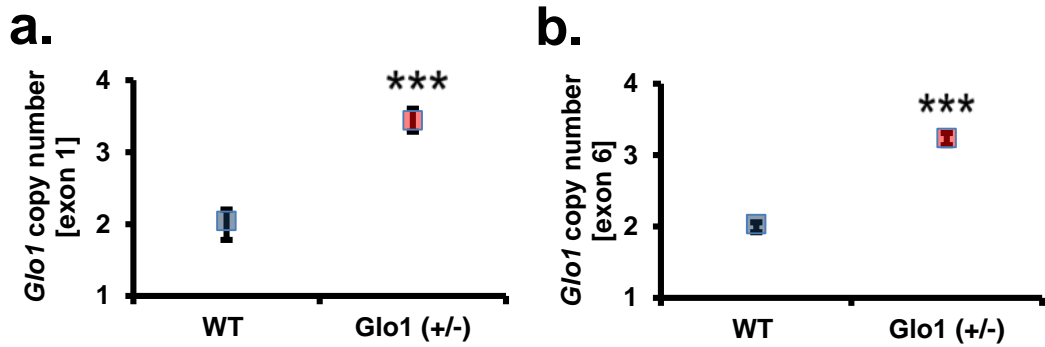


Figure 3.5: Assay of *Glo1* copy number by the Taqman method in kidney tissue of *Glo1 (+/-)* mutant and sibling wild-type control mice at 7 months of age. a. Copy number of exon 1 of *Glo1*, and **b.** Copy number of exon 6 of *Glo1*. Data are median (lower – upper quartile); *Glo1 (+/-)*, n = 9; and WT, n = 7. Significance: ***, p<0.001; Mann Whitney-U test.

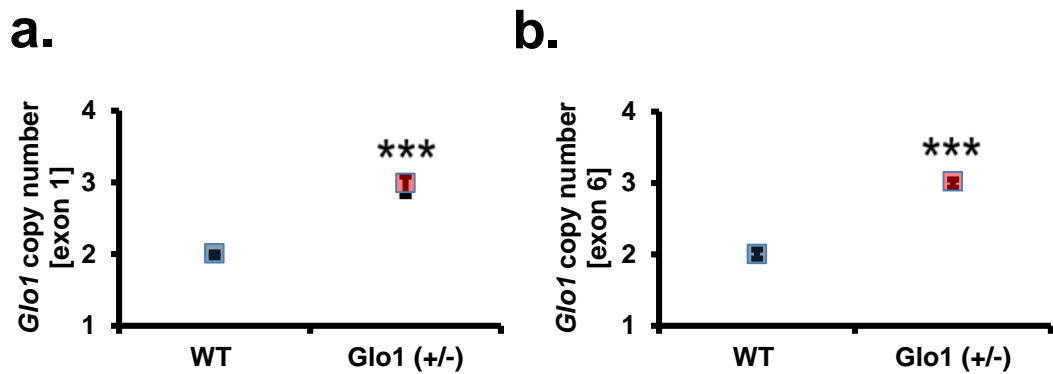


Figure 3.6: Assay of *Glo1* copy number by the Taqman method in brain tissue of *Glo1 (+/-)* mutant and sibling wild-type control mice at 7 months of age. a. Copy number of exon 1 of *Glo1*, and **b.** Copy number of exon 6 of *Glo1*. Data are median (lower – upper quartile); *Glo1 (+/-)*, n = 9; and WT, n = 7. Significance: ***, p<0.001; Mann Whitney-U test.

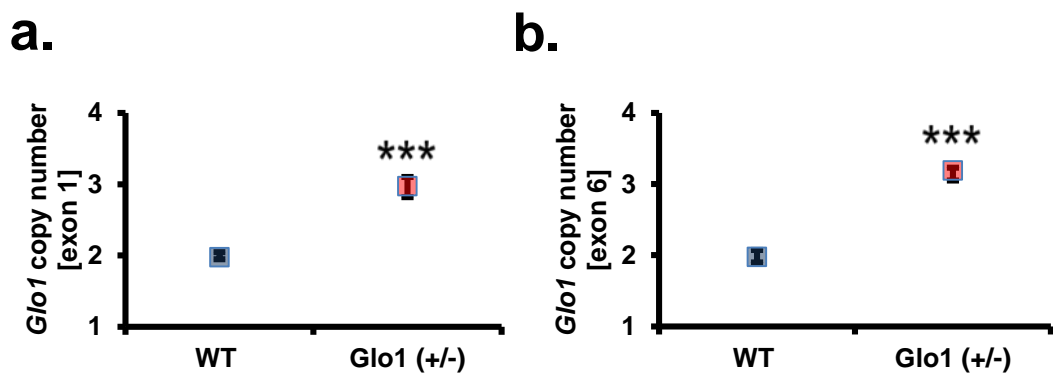


Figure 3.7: Assay of *Glo1* copy number by the Taqman method in pancreas tissue of *Glo1 (+/-)* mutant and sibling wild-type control mice at 7 months of age. a. Copy number of exon 1 of *Glo1*, and **b.** Copy number of exon 6 of *Glo1*. Data are median (lower – upper quartile); *Glo1 (+/-)*, n = 9; and WT, n = 7. Significance: ***, p<0.001; Mann Whitney-U test.

The data show that all *Glo1* (+/-) mice have *ca.* 3 copies of *Glo1* in all tissues analysed. In addition, the increased CNV occurred at both ends of *Glo1*, 3'-end of exon 1 and at the 5'-end of exon 6. It is likely, therefore, that the increase copy number extends across the entire *Glo1* gene. The increased copy number of *Glo1* in *Glo1* (+/-) mutant mice may explain the levels of mRNA, protein and activity of *Glo1* being similar to that of WT siblings if the additional copy of *Glo1* is of the WT gene.

To investigate the transfer of increased *Glo1* CNV through generations and to gain insight into the chromosomal location of the WT allele with respect to the mutant alleles of *Glo1*, I then investigated inheritance of mutant and WT alleles in genetic inheritance studies.

3.1.13. Inheritance study of the *Glo1* duplication in *Glo1* (+/-) mutant mice and wild-type controls

To study the inheritance pattern of *Glo1* mutation, DNA was extracted from blood samples of offspring of mating of different 3 pairs of WT and *Glo1* (+/-) mutant mice. Qualitative assessment of *Glo1* copy number in the *Glo1* (+/-) mutant and WT mice was made by qPCR with primers that distinguish between WT and mutated *Glo1* alleles. The following applies: (i) copy number is integer valued and (ii) total copy number is known from Taqman copy number assay. qPCR detects DNA domains with increased copy number earlier in the PCR than of DNA in WT controls with the normal 2 copies. Combination of copy number assay by the Taqman method and qPCR genotyping enabled assessment of the number of mutant and non-mutant, WT copies - Figure 3.8.

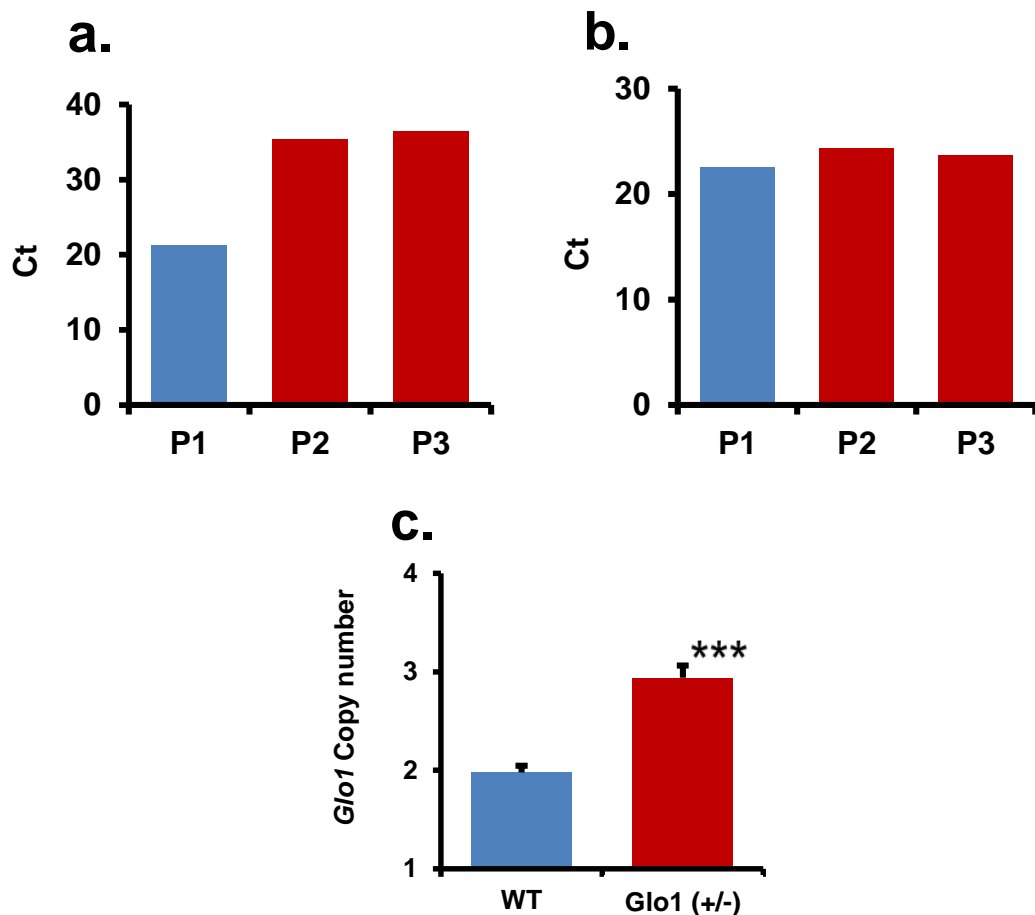


Figure 3.8: qPCR and Taqman copy number assay for inheritance studies.
a. qPCR results of genotyping of the wild-type mouse showing the detection of wild-type allele and no detection of the mutant allele (P1 primer pair 1 for wild-type allele, P2, P3 primer pair 2 and 3 respectively for heterozygote allele detection).
b. qPCR results of genotyping of the heterozygote mouse showing the detection of wild-type allele and detection of the mutant allele almost at same PCR cycle.
c. Taqman copy number assay for *Glo1* gene in blood sample of *Glo1 (+/-)* mutant mice and wild-type. Data are mean \pm SD (*Glo1 (+/-)*, n = 3; and WT, n = 3). Significance: ***, p<0.001; Student's t-test.

3.1.13.1. Inheritance study – mouse mating and family offspring, no 1

Breeding of WT female and *Glo1 (+/-)* male produced four pups. Ear punches were collected from all family for genotyping and quantification of mutant and WT copies of *Glo1* - Table 3.9. The analyses showed that the inheritance of *Glo1* mutated allele, *Glo1*^{Gt(OSTGST_4497-D9)Lex} – abbreviated to *Glo1 (+/+)*^{Gt(./.)Lex}, was simple Mendelian inheritance as the pups were two *Glo1 (+/-)* and two WT. This is expected in simple Mendelian inheritance - Figure 3.9. The heterozygote had a non-mutated *Glo1* allele on each chromosome and a targeted mutated allele on one chromosome – given nomenclature *Glo1 (+/+)*^{Gt(./.)Lex}.

Table 3.9: Summary of the qPCR genotyping and Taqman copy number assays for mouse breeding pair 1.

Mouse no.	Total <i>Glo1</i> copies (Taqman copy number assay)	Mutant allele	WT allele	Genotype
1	2	0	2	<i>Glo1</i> (+/+)
2	3	1	2	<i>Glo1</i> (+/+) ^{<i>Gt(·)1Lex</i>}
3	3	1	2	<i>Glo1</i> (+/+) ^{<i>Gt(·)1Lex</i>}
4	3	1	2	<i>Glo1</i> (+/+) ^{<i>Gt(·)1Lex</i>}
5	2	0	2	<i>Glo1</i> (+/+)
6	2	0	2	<i>Glo1</i> (+/+)

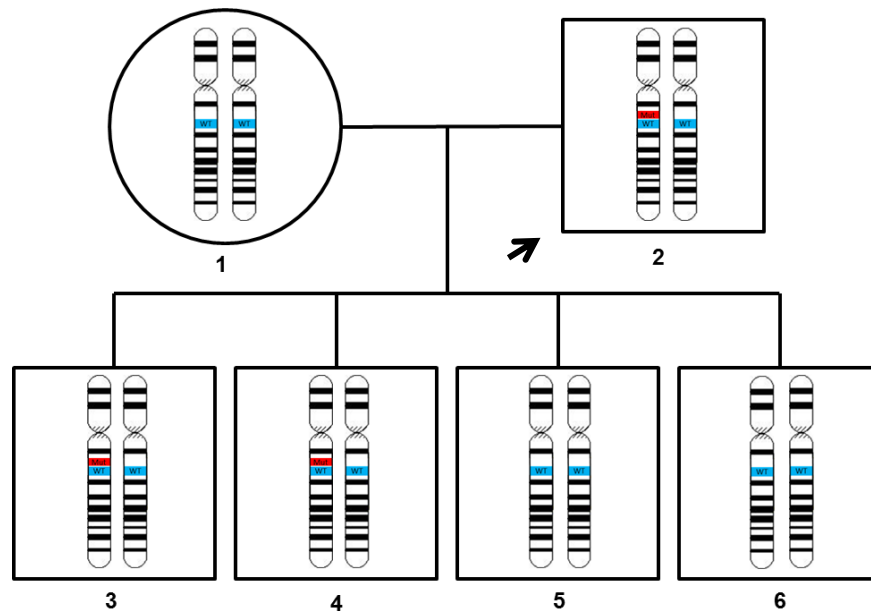


Figure 3.9: Pedigree of inheritance study - mouse mating and family offspring, no 1. The figure shows the paternal and maternal chromosome 17 in each mouse. The blue band represents the WT allele of *Glo1*. The red band represents the mutant allele of *Glo1*. The female parent has two WT *Glo1* alleles and no *Glo1* mutant allele. The male parent has two WT *Glo1* alleles and one *Glo1* mutant allele. Two of the pups have two WT *Glo1* alleles and no *Glo1* mutant allele and the other two have two WT *Glo1* alleles and one *Glo1* mutant allele.

3.1.13.2. Inheritance study – mouse mating and family offspring, no 2

Breeding of $Glo1(+/+)^{Gt(..)1Lex}$ female and $Glo1(+/+)^{Gt(..)1Lex}$ male produced six pups. Ear punches were collected from all family for genotyping and quantification of mutant and WT copies of $Glo1$ - Table 3.10. The analyses showed that the inheritance of $Glo1^{Gt(..)Lex}$ mutant allele was simple Mendelian inheritance as two pups had the $Glo1^{Gt(..)Lex}$ mutant allele and two siblings had only non-mutated alleles - expected in simple Mendelian inheritance - Figure 3.10. A new genotype with a non-mutated and a $Glo1^{Gt(..)Lex}$ mutant allele on each chromosome, denoted by $Glo1(+/+)^{Gt(..)2Lex}$, appeared in pup number 4 which had the maternal and paternal $Glo1$ mutant copy. The total copies of the new genotype were 4 copies in total - Figure 3.11.

To confirm the genotype of the pup number 4, a new Taqman copy number assay was designed (Glo1-Vec). The assay primers and probe detect the connection point between the inserted vector and insertion location in $Glo1$. It distinguishes between WT allele and mutant allele by quantifying the mutant allele - Figure 3.12. The result of this assay confirmed that the mice which were genotyped as WT have no mutant allele. In addition, it was able to differentiate between the mice which have 1 or 2 copies of mutant $Glo1$ allele.

Table 3.10: Summary of the qPCR genotyping results and Taqman copy number assay for the second family.

Mouse no.	Total $Glo1$ copies (from Taqman copy number assay results)	Mutant allele	WT allele	Genotype
1	3	1	2	$Glo1(+/+)^{Gt(..)1Lex}$
2	3	1	2	$Glo1(+/+)^{Gt(..)1Lex}$
3	3	1	2	$Glo1(+/+)^{Gt(..)1Lex}$
4	4	2	2	$Glo1(+/+)^{Gt(..)2Lex}$
5	2	0	2	$Glo1(+/+)$
6	3	1	2	$Glo1(+/+)^{Gt(..)1Lex}$
7	2	0	2	$Glo1(+/+)$
8	2	0	2	$Glo1(+/+)$

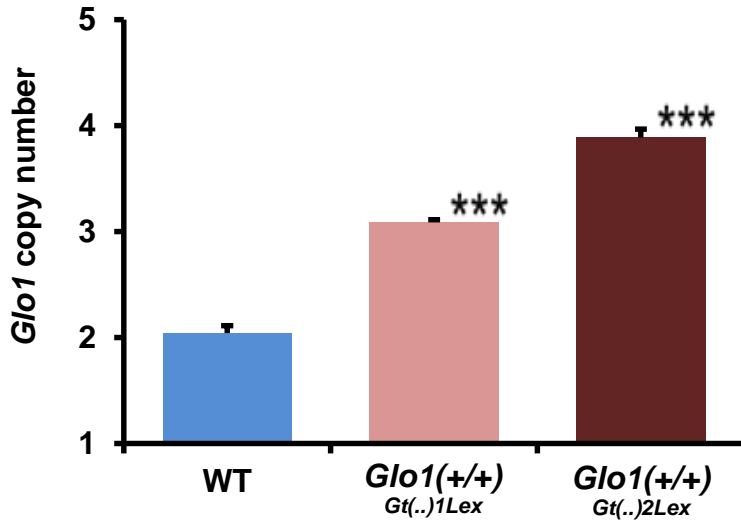


Figure 3.10: Taqman copy number assay for *Glo1* gene in wild-type, $Glo1(+/+)^{Gt(..)1Lex}$ and $Glo1(+/+)^{Gt(..)2Lex}$ mutant mice. The figure shows quantification of *Glo1* copy number in the three genotypes. Data are mean ± SD (n = 3; WT, n = 3; $Glo1(+/+)^{Gt(..)1Lex}$ and n = 3; and $Glo1(+/+)^{Gt(..)2Lex}$ mice). Significance: ***, p<0.001 compared to WT control; Student's t-test.

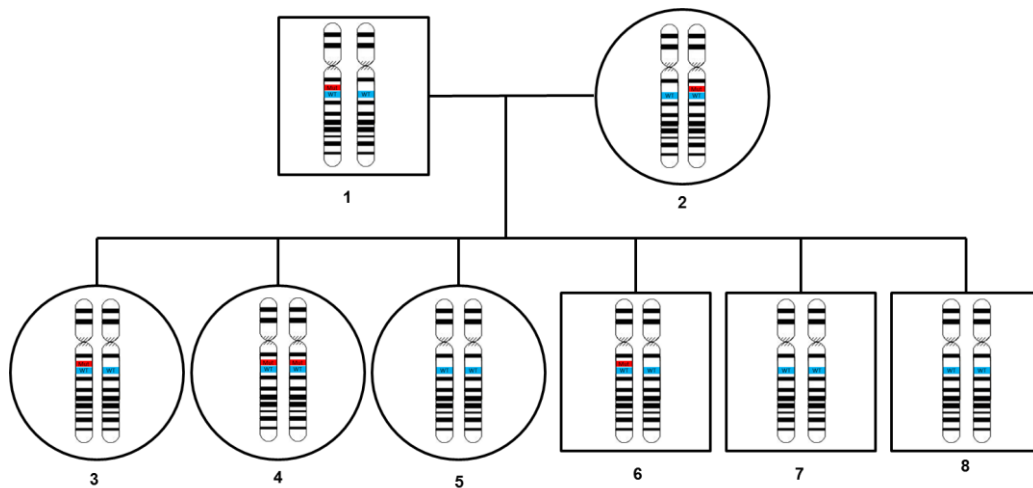


Figure 3.11: Pedigree of inheritance study - mouse mating and family offspring, no 2. The figure shows the paternal and maternal chromosome 17 in each mouse. The blue band represents the WT allele of *Glo1*. The red band represents the mutant allele of $Glo1^{Gt(..)1Lex}$. Both parents have two WT *Glo1* alleles and one *Glo1* mutant allele ($Glo1(+/+)^{Gt(..)1Lex}$). Three of the pups have two WT *Glo1* alleles and no *Glo1* mutant allele and the two have two WT *Glo1* alleles and one *Glo1* mutant allele. Pup number 4 has two chromosomes 17 and each chromosome has one WT *Glo1* alleles and one *Glo1* mutant allele. This pup (no. 4) is a new genotype which has in total of four copies of *Glo1* gene.

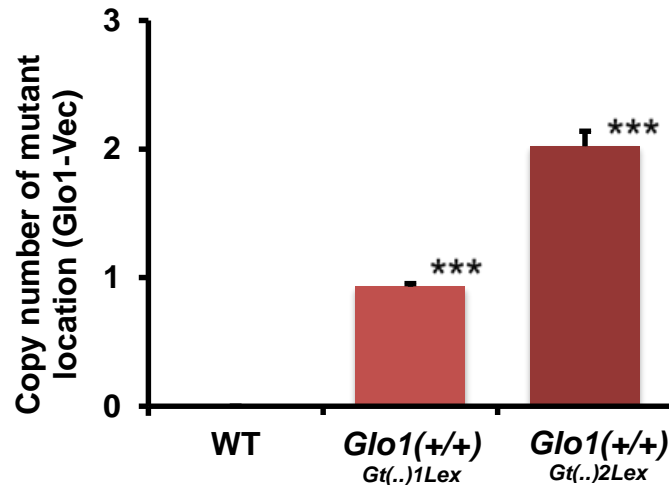


Figure 3.12: Taqman copy number assay for *Glo1* mutant allele in offspring of breeding of $Glo1(+/+)^{Gt(..)1Lex}$ mutant mice. The figure shows quantification of mutant *Glo1* copy number in the three genotypes. Data are mean \pm SD (WT, n = 3; $Glo1(+/+)^{Gt(..)1Lex}$ n = 3; and $Glo1(+/+)^{Gt(..)2Lex}$, n = 3). Significance: ***, p<0.001 compared to WT control; Student's t-test.

3.1.13.3. Inheritance study – mouse mating and family offspring, no 3

Breeding of $Glo1(+/+)^{Gt(..)1Lex}$ female and $Glo1(+/+)^{Gt(..)1Lex}$ male produced six pups in the second family. Pup number 4, $Glo1(+/+)^{Gt(..)2Lex}$, with four copies of *Glo1*, was bred with WT male. This breeding produced 7 pups with $Glo1(+/+)^{Gt(..)1Lex}$ genotype. All pups in this family have three copies of *Glo1* including two WT *Glo1* alleles and one $Glo1^{Gt(..)Lex}$ mutant allele - Table 3.11. Analyses showed that the inheritance of *Glo1* mutation was simple Mendelian inheritance - Figure 3.13. This confirms the genotyping of the second family; specifically pup number 4 in the second family.

Table 3.11: Summary of the qPCR genotyping results and Taqman copy number assay for the third family.

Mouse no.	Total <i>Glo1</i> copies	Mutant allele	WT allele	Genotype
Grandparents				
1	3	1	2	<i>Glo1</i> (+/+) ^{<i>Gt(..)1Lex</i>}
2	3	1	2	<i>Glo1</i> (+/+) ^{<i>Gt(..)1Lex</i>}
Parents				
3	2	0	2	<i>Glo1</i> (+/+)
4	4	2	2	<i>Glo1</i> (+/+) ^{<i>Gt(..)2Lex</i>}
Offspring				
5	3	1	2	<i>Glo1</i> (+/+) ^{<i>Gt(..)1Lex</i>}
6	3	1	2	<i>Glo1</i> (+/+) ^{<i>Gt(..)1Lex</i>}
7	3	1	2	<i>Glo1</i> (+/+) ^{<i>Gt(..)1Lex</i>}
8	3	1	2	<i>Glo1</i> (+/+) ^{<i>Gt(..)1Lex</i>}
9	3	1	2	<i>Glo1</i> (+/+) ^{<i>Gt(..)1Lex</i>}
10	3	1	2	<i>Glo1</i> (+/+) ^{<i>Gt(..)1Lex</i>}
11	3	1	2	<i>Glo1</i> (+/+) ^{<i>Gt(..)1Lex</i>}

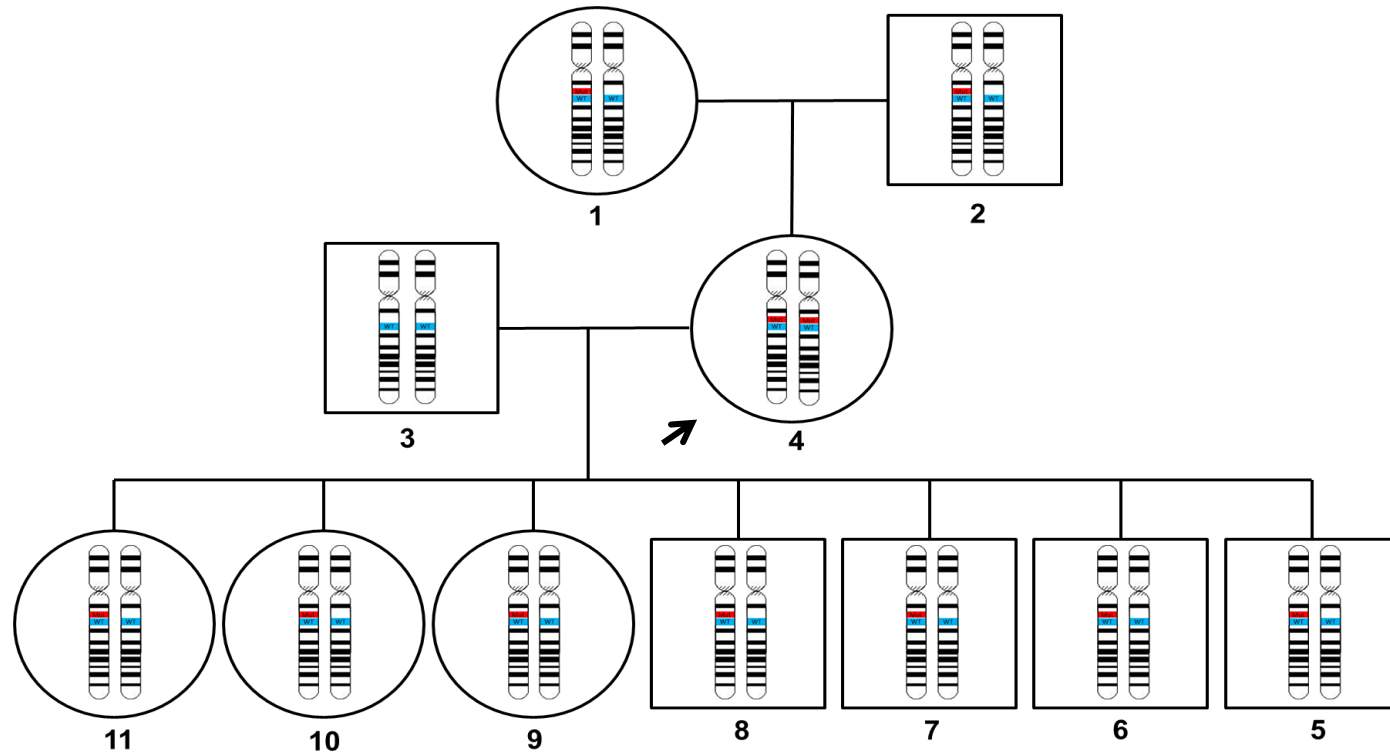
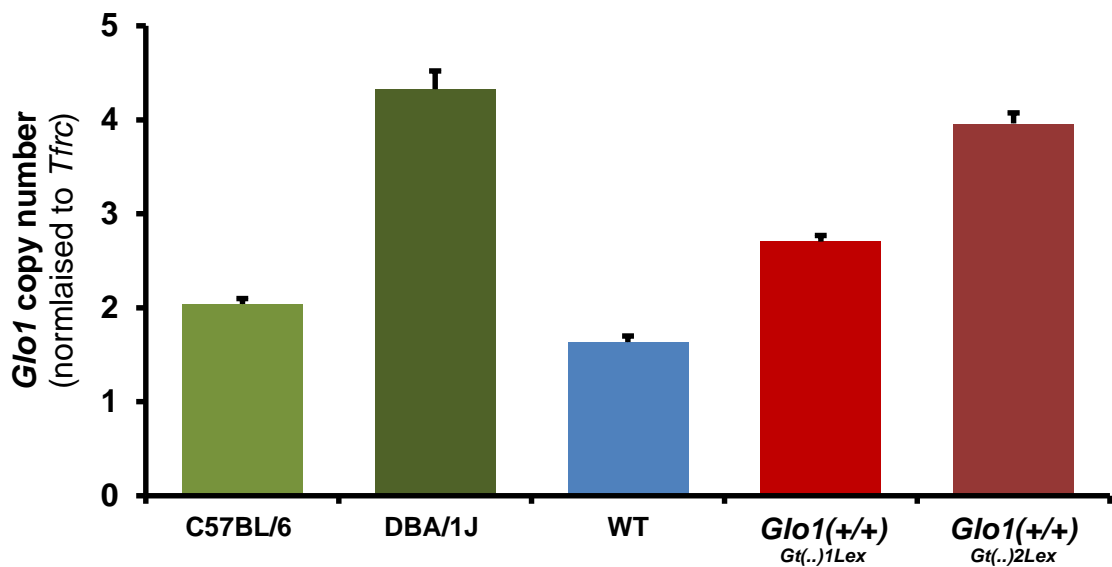


Figure 3:13: Pedigree of inheritance study - mouse mating and family offspring, no 3. The figure shows the paternal and maternal chromosome 17 in each mouse. The blue band represents the WT allele, *Glo1*. The red band represents the mutant allele, *Glo1^{Gt(·)1Lex}*. Both grandparents have two WT *Glo1* alleles and one mutant allele, *Glo1*(+/+)^{*Gt(·)1Lex*} genotype. The female parent was *Glo1*(+/+)^{*Gt(·)2Lex*} genotype bred with a WT mouse. This breeding produced 7 pups. Each of the 7 pups had two WT *Glo1* alleles and one *Glo1* mutant, *Glo1*(+/+)^{*Gt(·)1Lex*} genotype.

3.1.14. Evaluation of Taqman copy number assay for *Glo1* gene

The three genotypes including WT, *Glo1*(+/+)^{Gt(·)1Lex} and *Glo1*(+/+)^{Gt(·)2Lex} were analysed for *Glo1* copy number assay against two commercial DNA controls - C57BL/6 and DBA/1J strains. The C57BL/6 strain has 2 copies of *Glo1* and the DBA/1J strain has *Glo1* duplication and hence 4 copies of *Glo1* (Williams et al., 2009). In addition, the analysis includes two different reference gene assays including *Tfrc* and *Tert*. The quantification of *Glo1* copy number was by Taqman copy number assay and showed: 2 copies in WT, 3 copies in *Glo1*(+/+)^{Gt(·)1Lex} mutant mice and 4 copies in *Glo1*(+/+)^{Gt(·)2Lex} mutant mice, 2 copies in C57BL/6 mice and 4 copies in DBA/1J mice. There was no significant difference between the results when referenced to *Tfrc* or *Tert* - Figure 3.14.

a.



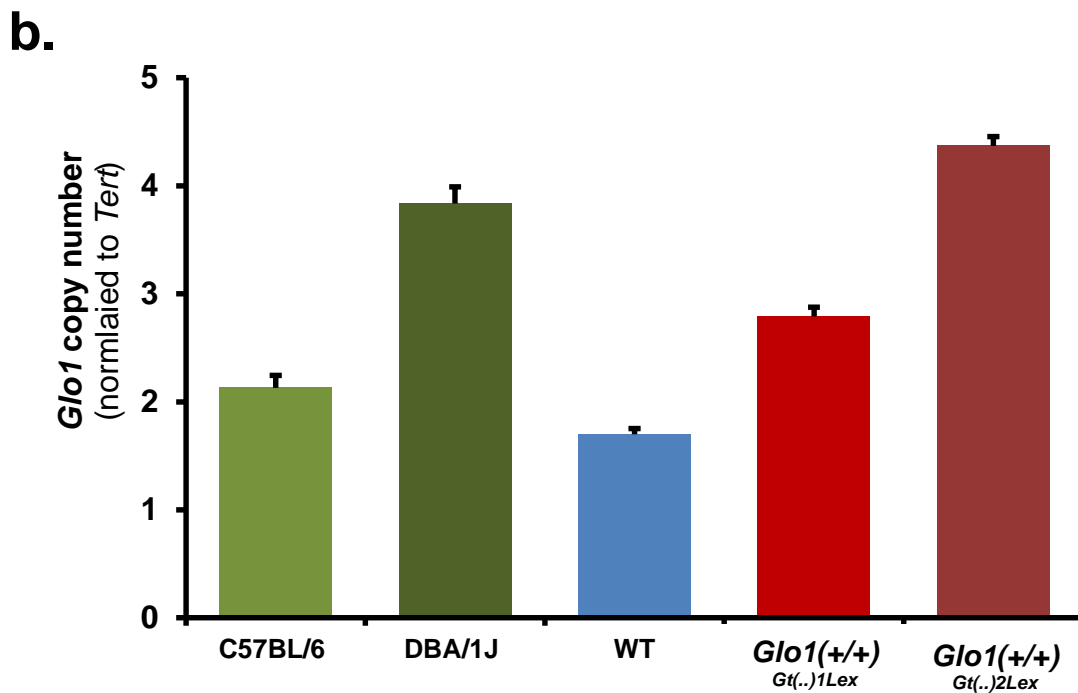


Figure 3.14: Evaluation of Taqman copy number assay for *Glo1* gene.

The figure shows *Glo1* copy number results obtained from WT, *Glo1*^{Gt(·)1Lex} and *Glo1*^{Gt(·)2Lex} mutant mice, C57BL/6 and DBA/1J mice. **a.** Quantification of *Glo1* copy number was referenced to *Tfrc* gene. **b.** Quantification of *Glo1* copy number was referenced to *Tert* gene. Data are mean ± SD (WT, n = 3; *Glo1*^{Gt(·)1Lex} n = 3; *Glo1*^{Gt(·)2Lex}, n = 3; C57BL/6, n = 3; and DBA, n = 3).

3.1.15. Characterization of *Glo1* mutation in *Glo1* mutant mice

My previous studies showed the presence and inheritance of increased copies of WT and mutant *Glo1* alleles in the *Glo1* mutant mice and their offspring – assessed by qPCR. The length of the DNA of increased CNV and genes completely or partially within it are unknown. To characterize the sequence of the *Glo1* duplication, I next performed a quantitative assessment of the range and domains of DNA CNV increase by high intensity DNA microarray. CNV quantitation at the domains of PCR primers was known from Taqman copy number assay and qPCR studies.

3.1.15.1. Comparative genomic hybridisation microarray of *Glo1* mutant mice and sibling wild-type controls

High intensity DNA microarray SurePrint G3 unrestricted CGH 1x1M was used for three mice of each genotype of the *Glo1* mutant mice. The three genotypes are: (i) WT control, (ii) *Glo1*^{Gt(·)1Lex}, and (iii) *Glo1*^{Gt(·)2Lex}. Reference DNA was extracted from wild-type C57BL/6 male mouse for male samples and wild-type C57BL/6 female mouse for female samples. The analysis was performed according to the method described in Section 2.2.6.7. Data analysis was by Agilent genomic work bench software which showed the expected different outcomes for each study group (Figure 3.15):

- A. In WT controls there was no increased CNV detected at the *Glo1* locus, confirming that these WTs have two copies of *Glo1*. In this DNA microarray, the result was referenced to the whole genome.
- B. In *Glo1*^{Gt(·)1Lex}, one copy of duplicated DNA domain was found which was detected by 300 DNA oligomer probes covering a sequence of 473,479 bp. This included a partial duplication of *Btbd9* and *Glp1r* genes and complete duplication of *Glo1* and *Dnahc8* genes.
- C. In *Glo1*^{Gt(·)2Lex}, two copies of duplicated DNA domain as detected in B was found - also detected by 300 probes covering the same sequence of 473,479 bp include partial duplication of *Btbd9* and *Glp1r* genes and complete duplication of *Glo1* and *Dnahc8* genes.

Chr17: 30381522-31276041, 896kb

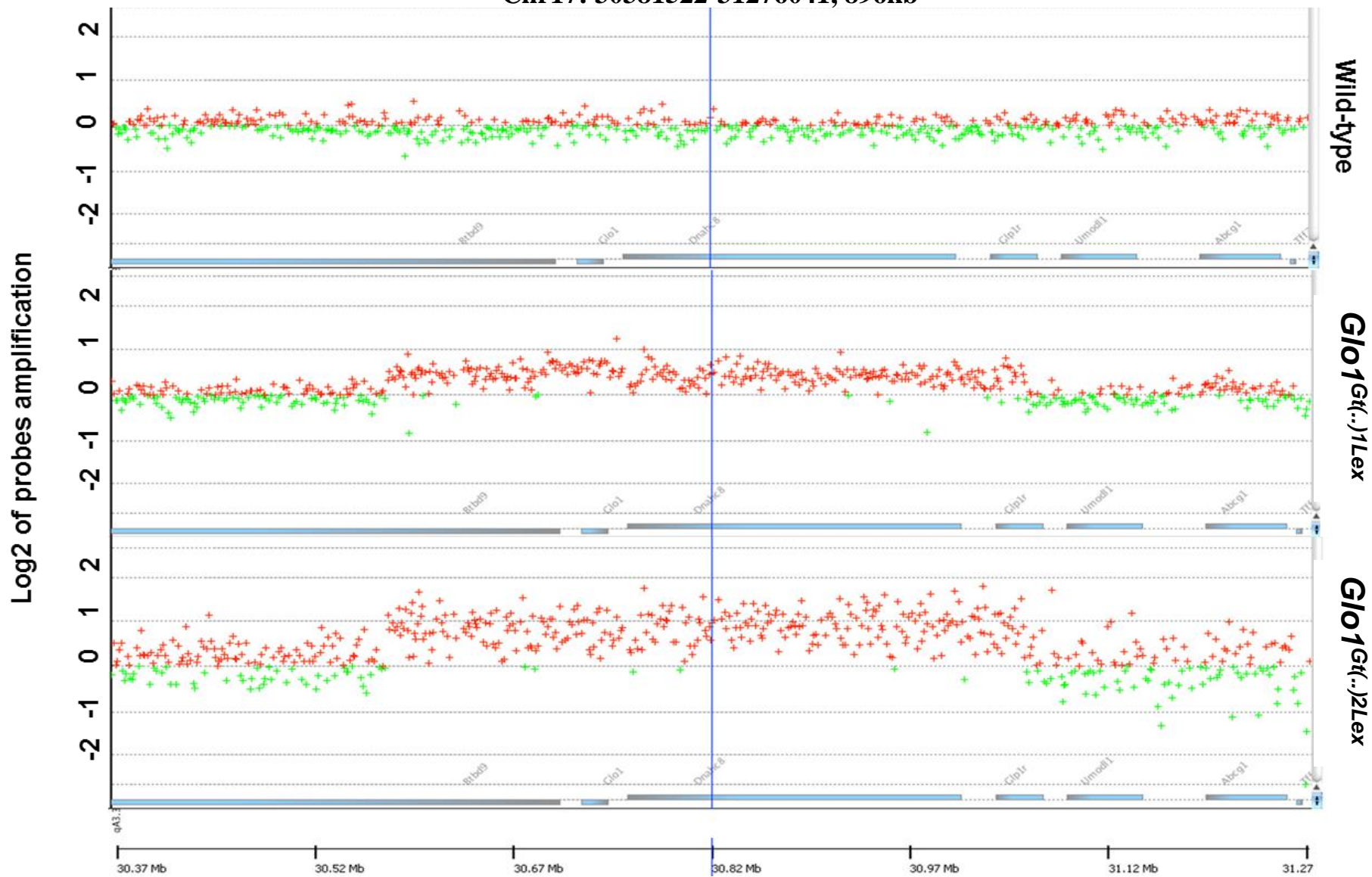


Figure 3.15: SurePrint G3 aCGH results of one mouse of each genotype.

This shows 894 kb of chromosome 17 of mouse genome starting from base number 30379127 to 31273646. The sample probes are in red and the probes of the reference samples are in green. The reference DNA was extracted from wild-type C57BL/6 male mouse for male samples and wild-type C57BL/6 female mouse for female samples. The duplicated area in the mouse genome reacted with 300 probes covering an area of 473,479 bp and includes a partial duplication of *Btbd9* and *Glp1r* genes and complete duplication of *Glo1* and *Dnahc8* genes. The results were analysed by Agilent genomic work bench software. Log₂ R is the logarithm (base 2) of the ratio of the probe intensity to that of the average in reference DNA.

The analysis of the other parts of the mice genome showed random amplifications in different areas which are not linked to *Glo1* mutation genotype. However, two genes were duplicated only in the *Glo1*^{Gt(·)1Lex} and *Glo1*^{Gt(·)2Lex} mice. These two genes are *Vmn2r111*, *Vmn2r112*. This duplication is in chromosome 17 from base number 22673192 to 22797105. These genes were detected by 26 DNA oligomer probes.

3.1.15.2. Expression of duplicated genes in Glo1 mutant mice

High density DNA microarray analysis revealed the extent of the DNA domains duplicated in *Glo1* mutant mice. It was now of interest to assess if this increased copy number was functional and had related increased expression. Gene expression was assessed by quantitation of related mRNA level was analysed using extracted RNA from liver tissue of the three genotypes: WT control, *Glo1*^{Gt(·)1Lex} and *Glo1*^{Gt(·)2Lex}. The analysis was performed for the genes which are fully or partly located in the duplication area. These genes were: *Btbd9*, *Dnahc8*, and *Vmn2r112*. The data are given in Figure 3.16, A, B and C.

Part of the *Btbd9* gene was within the DNA domain duplicated in *Glo1* mutant mice. The relative mRNA level of *Btbd9* showed a 36% decrease in *Glo1*^{Gt(·)1Lex} mice which just failed to reach significance and a 51% decrease in *Glo1*^{Gt(·)2Lex} which was significant (P<0.05, t-test), with respect to WT controls. The relative mRNA level of *Btbd9* in *Glo1*^{Gt(·)1Lex} and *Glo1*^{Gt(·)2Lex} mutant mice was not significantly different. Combining expression data from *Glo1*^{Gt(·)1Lex} and *Glo1*^{Gt(·)2Lex} mutant mice, the level of *Btbd9* in *Glo1* mutant mice was decreased by 44% (P<0.01, t-test). This suggests that the presence of the DNA duplication in *Glo1* mutant mice decreased expression of *Btbd9* - Figure 3.16 A.

Dnahc8 was a gene that was completely duplicated within the DNA domain duplicated in *Glo1* mutant mice. The relative mRNA level of *Dnahc8* showed an increase of 254% in *Glo1^{Gt(·)1Lex}* mutant mice, compared to WT controls. In *Glo1^{Gt(·)2Lex}* mutant mice, however, the relative mRNA level of *Dnahc8* returned to levels of WT controls - Figure 3.16 B. The expression of *Dnahc8* was influenced differently by increased copy number of the duplicated DNA domain, increasing with one additional copy and then unchanged by 2 additional copies.

Vmn2r112 is a gene increased in copy number in *Glo1* mutant mice but outside of the main DNA duplicated domain. The relative expression of mRNA of *Vmn2r112* was 27% in *Glo1^{Gt(·)1Lex}* mutant mice and 94% in *Glo1^{Gt(·)2Lex}* mutant mice, with respect to WT. The relative expression of mRNA of *Vmn2r112* was 67% lower in *Glo1^{Gt(·)2Lex}* mutant mice, with respect to *Glo1^{Gt(·)1Lex}* mutant mice. Increased copy number of the duplicated DNA domain therefore decreased expression of *Vmn2r112* progressively with increased copy number - Figure 3.16 C.

These findings show differential expression of genes partly or completely duplicated with *Glo1* in *Glo1* mutant mice where there is increase or decrease in expression with increased *Glo1* copy number. Similar effects have been found previously where increase copy number of a gene of interest has effects in expression of unrelated genes (Teng et al., 2013).

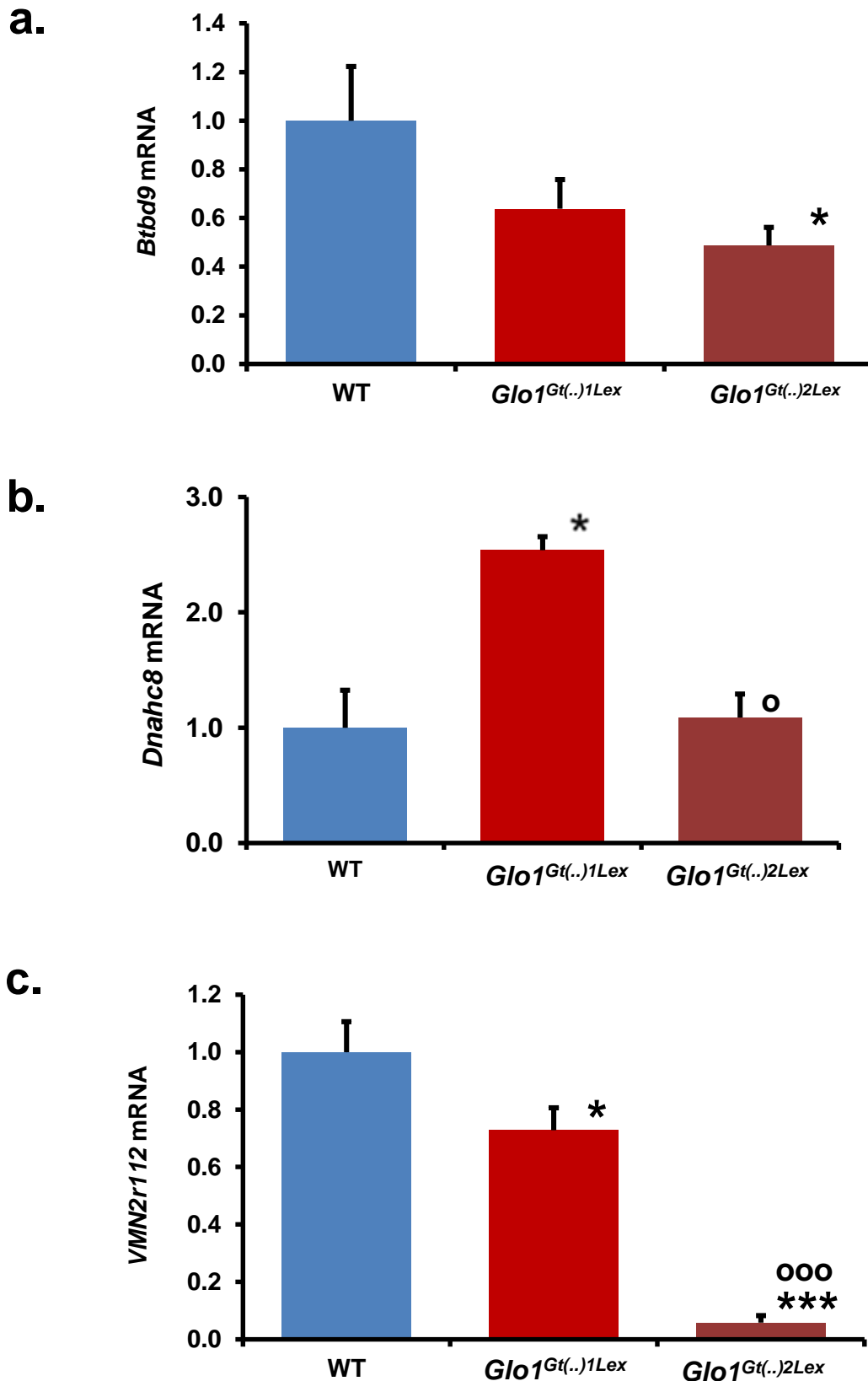


Figure 3.16: Relative mRNA level of genes duplicated in liver tissue of wild-type mice and *Glo1^{Gt(..)1Lex}* and *Glo1^{Gt(..)2Lex}* genotypes. a. *Btbd9*. b. *Dnahc8*. c. *VMN2r112*. Data are mean \pm SD (n = 3). Significance: * and *, $p < 0.05$ and $P < 0.001$ with respect to WT control; o and ooo, $P < 0.05$ and $P < 0.001$ with respect to *Glo1^{Gt(..)1Lex}* mutant mice; Student's t-test.**

The experimental studies so far indicated how the Lexicon *Glo1* mutant mice had maintained normal, WT expression of *Glo1* – by inducing increased *Glo1* CNV. This has occurred such that a non-mutant, normal *Glo1* allele is inherited on each homolog of the chromosome where the *Glo1* mutant allele is co-inherited and therefore mutant mice containing one or two copies of the mutant *Glo1* allele retain two copies of the non-mutant, functional *Glo1* allele and maintain normal *Glo1* expression in all tissue. An outstanding question is why this has occurred in response to *Glo1* gene trapping. I hypothesised that a likely explanation is that gene trapping of *Glo1* induces dicarbonyl stress and *Glo1* copy number alteration (CNA) is an adaptive survival response of ESCs to counter dicarbonyl stress. To test this hypothesis, I initiated a series of experiments to culture mouse ESCs and impose dicarbonyl stress experimentally with exogenous MG or cell permeable *Glo1* inhibitor and examine if *Glo1* CNA occurs.

3.2. Mouse embryonic stem cells (ESCs)

Mouse ESCs were obtained from a commercial supplier and grown *in vitro*. To ensure the ESCs phenotype on receipt and that it was maintained under undifferentiated status, a set of specific markers for mouse ESCs were identified after each experiment. These markers include SOX2, NANOG and OCT4 with a band size of 34 kDa, 35 kDa and 39 kDa respectively. All experiments were performed after maintaining ESCs growing without feeder layer.

3.2.1. Characterisation of the glyoxalase system in ESCs under normal and low oxygen conditions

The glyoxalase system in ESCs was characterised under conventional aerobic conditions and under 3% oxygen which is typical of physiologic environment of ESCs (Powers et al., 2008). The ESCs were cultured under low oxygen conditions for physiological relevance and as these conditions change the metabolic environment under which the glyoxalase system operates. Under 3% oxygen environment ESCs have increased anaerobic glycolysis (Ito and Suda, 2014) and thereby potential increased flux of MG formation – although this has not previously been measured. There is also the potential for decrease in *Glo1* expression under 3%

oxygen environment as Glo1 expression is suppressed by activation of hypoxia-related transcription factor, HIF1- α (Zhou et al., 2012) .

3.2.1.1. Growth and viability of mouse ESCs *in vitro*

Mouse ESCs were plated and grown under an atmosphere of 5% carbon dioxide, 20% or 3% oxygen and nitrogen – see Section 2.2.2. ESCs were plated with the same density in both conditions and cultured for 6 days. The growth and viability of ESCs was assessed by measuring viable cell number. ESCs maintain high cell viability (>95%) and increase in viable cell number was *ca.* 3-fold higher in 20% oxygen compared to 3% oxygen atmosphere - Figure 3.17.

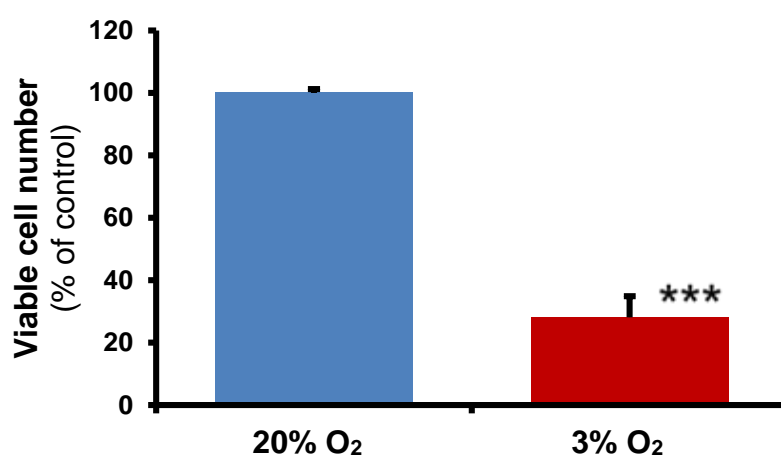


Figure 3.17: Growth of murine ESCs under 20% oxygen and 3% oxygen atmosphere *in vitro*. Data are mean \pm SD (n = 3). Significance: ***, p<0.001; Student's t-test.

In studies of dicarbonyl stress in murine ESCs, it is important to characterise the endogenous enzymatic defence provided by the glyoxalase system in murine ESCs. This has not been done previously and therefore I performed studies to do this.

3.2.1.2. Activity and expression of glyoxalase 1 in murine ESCs *in vitro*

The activity of Glo1 was assayed in cytosolic extracts of murine ESCs grown under atmospheres of 20% and 3% oxygen. The activity of Glo1 was decreased by *ca.* 25% in ESCs grown under 3% oxygen atmosphere, with respect to 20% oxygen, normoxia control - Figure 3.18. There was a similar 28% decrease in Glo1 protein in ESCs grown under an atmosphere of 3% oxygen, compared to normoxia control cultures - Figure 3.19.

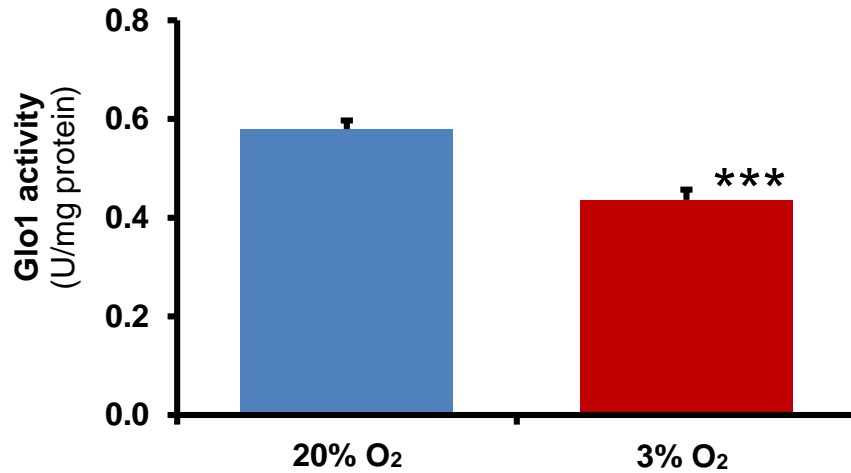


Figure 3.18: Activity of glyoxalase 1 of ESCs cultured under 20% oxygen and 3% oxygen atmosphere *in vitro*. Data are mean \pm SD (n = 3). Significance: ***, p<0.001; Student's t-test.

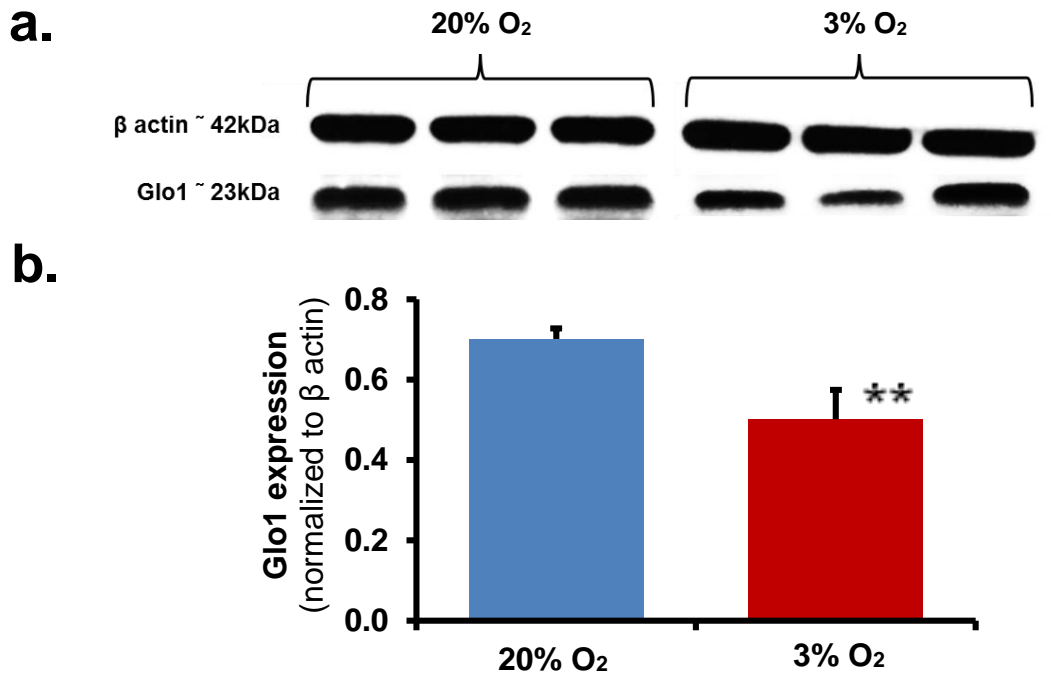


Figure 3.19: Glo1 protein content of ESCs cultured under 20% oxygen and 3% oxygen atmosphere *in vitro*. **a.** Glo1 and β -actin protein bands for 6 samples of ESCs under 20% oxygen and 3% oxygen atmosphere. **b.** Relative content of Glo1 protein. Data are mean \pm SD (n = 3). Significance: **, p<0.01; Student's t-test.

3.2.1.3. Flux of formation of D-lactate in ESC cultures under 20% oxygen and 3% oxygen atmosphere *in vitro*

D-Lactate was determined in the culture media at baseline and 3 days in ESC cultures under 20% oxygen and 3% oxygen atmosphere. The flux of D-lactate formation was deduced as a surrogate measure of flux of formation of MG. The production of D-lactate in ESCs cultured in 3% oxygen was increased 60%, with respect to cultures under normoxia: 4.47 ± 0.15 versus 2.80 ± 0.12 nmol/million cells/day ($P < 0.001$, Student's t-test) - Figure 3.20.

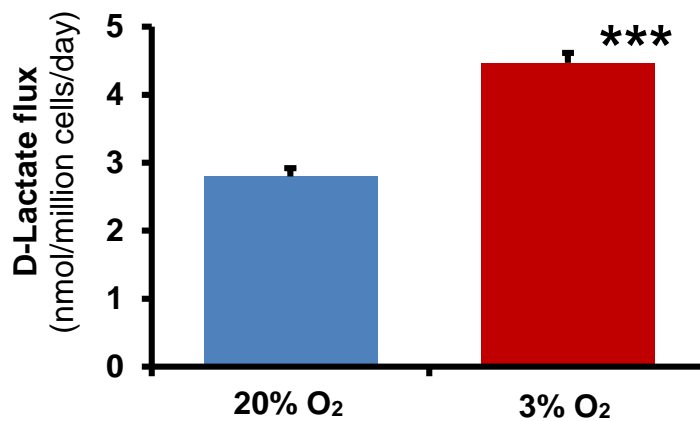


Figure 3.20: Flux of D-lactate formation by ESCs cultured under 20% oxygen and 3% oxygen atmosphere *in vitro*. Data are mean \pm SD (n = 3). Significance: ***, $p < 0.001$; Student's t-test.

3.2.1.4. Net flux of formation of L-Lactate by murine ESCs cultured under 20% oxygen and 3% oxygen atmosphere *in vitro*

L-Lactate was determined in cell culture media of ESCs cultured under 20% oxygen and 3% oxygen atmosphere *in vitro*. ESCs were cultured for 6 days. The media was sampled at day 4 and day 6 and the net flux of formation of L-lactate over days 4 – 6 deduced. Since L-lactate is efficiently metabolised in ESCs, the absolute flux of formation of L-lactate cannot be estimated - Figure 3.21. The net flux of L-lactate by ESCs cultured under normoxia conditions was > 100 fold higher than the flux of formation of D-lactate; *cf.* Figures 3.20 and 3.21. The net flux of formation of L-lactate in ESCs cultured in 3% oxygen was *ca.* 3-fold higher than for cultures under normoxia - Figure 3.21.

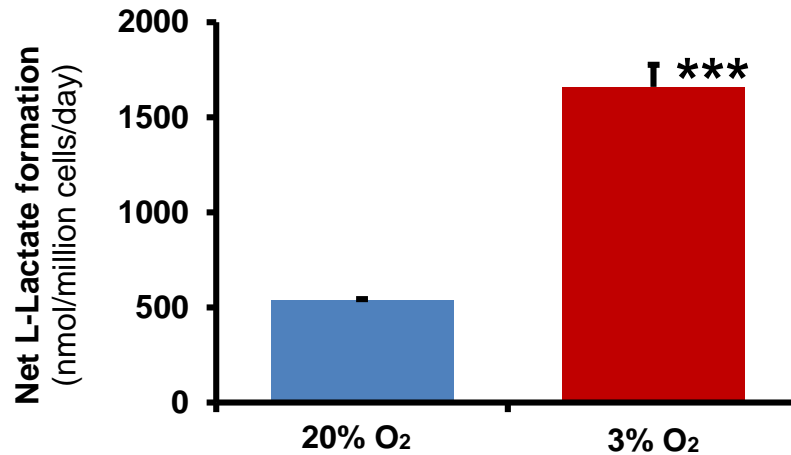


Figure 3.21: Net formation of L-lactate by ESCs cultured under 20% oxygen and 3% oxygen atmosphere *in vitro*. Data are mean \pm SD (n = 3). Significance: ***, P<0.001; Student's t-test.

3.2.1.5. Consumption of D-glucose by murine ESCs cultured under 20% oxygen and 3% oxygen atmosphere *in vitro*

The rate of D-glucose consumption by ESCs cultured under 20% oxygen and 3% oxygen atmosphere *in vitro* was determined in the culture media over day 4 – day 6 of a 6 day culture. The flux of D-glucose consumption by ESCs cultured under normoxia conditions was *ca.* 1000 fold higher than the flux of formation of D-lactate; *cf.* Figures 3.20 and 3.22. This suggests that the rate of formation of MG in murine ESCs under normoxia is *ca.* 0.1% of glucose metabolism or *ca.* 0.05% of flux of glucotriose – which is similar in most human cells where these flux measurements have been made. The flux of glucose consumption in ESCs cultured in 3% oxygen was *ca.* 3-fold higher than that cultured under normoxia - Figure 3.22; *cf.* similar increase of net flux of formation of L-lactate - Figure 3.21.

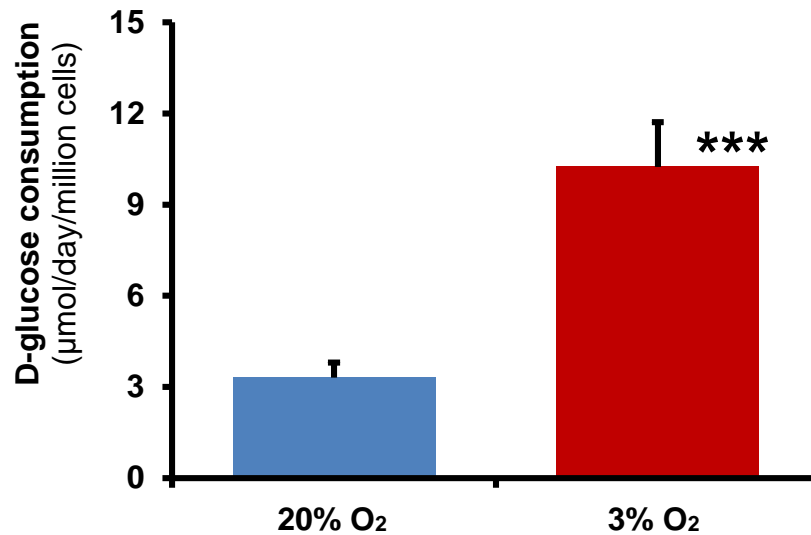


Figure 3.22: Glucose consumption of ESCs cultured under 20% oxygen and 3% oxygen atmosphere *in vitro*. Data are mean \pm SD (n = 3). Significance: **, p<0.001; Student's t-test.

In summary, characteristics of the glyoxalase system in murine ESCs revealed flux of formation of MG from glucose metabolism similar to that found in other cells – Table 3.12 – *ca.* 0.1% glucose metabolism or *ca.* 0.05% flux of glucotriose (assuming flux of glucotriose formation is 2 x flux of glucose metabolism). The Glo1 activity was relatively high – *ca.* twice that found in human BJ fibroblasts in primary culture which was *ca.* 0.3 U/mg protein (Xue et al., 2012).

Table 3.12: Characterization of ESCs under under 20% oxygen and 3% oxygen atmosphere *in vitro*.

	20% O ₂	3% O ₂
Cell Count (x1,000,000)	29.3 \pm 0.4	8.26 \pm 0.56***
Glo1 protein expression (normalized to β -actin expression)	0.701 \pm 0.026	0.501 \pm 0.073**
Glo1 activity (unit/mg protein)	0.579 \pm 0.018	0.436 \pm 0.211***
D-Lactate formation (nmol/million cells/day)	2.80 \pm 0.12	4.47 \pm 0.15***
D-glucose (µmol/day/million cells)	3.30 \pm 0.50	10.20 \pm 1.48***
Net flux of formation of L-lactate (nmol/million cells/day)	538 \pm 6	1660 \pm 116***

Data are mean \pm SD (n = 3) and t-test was used as statistical test. Significance: **, p<0.01, ***, p<0.001.

I next designed experiments to impose dicarbonyl stress in ESCs *in vitro* by: (i) addition of cell permeable Glo1 inhibitor, BrBzGSHCP₂, which induces dicarbonyl stress by accumulation of endogenous MG, and (ii) addition of a high concentration of exogenous MG.

3.2.2. Effect of cell permeable Glo1 inhibitor on cell growth and *Glo1* copy number of ESCs *in vitro*

3.2.2.1. Effect of cell permeable Glo1 inhibitor on ESCs growth *in vitro*

ESCs were cultured for 24 h for culture flask surface attachment. Thereafter, the ESCs were incubated with and without 1 – 100 μ M BrBzGSHCP₂ and the effect on cell growth assessed after incubation for a further 48 h. The growth of ESCs was inhibited with 5 - 100 μ M of BrBzGSHCP₂. Viable cell number data (% of untreated control) were fitted to a dose response curve and solved for the median growth inhibitory concentration (GC₅₀) and logistic regression coefficient *n*. For BrBzGSHCP₂, GC₅₀ = 25.5 \pm 1.8, and *n* = 4.00 \pm 0.86 (N = 21) – Figure 3.23a. Cell viability of ESCs decreased with increasing concentration of BrBzGSHCP₂ – Figure 3.23b, suggesting the inhibition of cell growth by BrBzGSHCP₂ was likely due to both growth arrest and toxicity. This indicates that murine ESCs are susceptible to growth arrest by dicarbonyl stress induced by 20 – 50 μ M BrBzGSHCP₂ and also cytotoxicity at 50 – 100 μ M; the median cytotoxic concentration (TC₅₀) was > 100 μ M. The cytotoxicity of BrBzGSHCP₂ was relatively low and murine ESCs appear resistant to dicarbonyl stress: *cf*, BrBzGSHCP₂ was cytotoxic to human neutrophils *ex vivo* where the TC₅₀ concentration was 40 μ M (Lo and Thornalley, 1992).

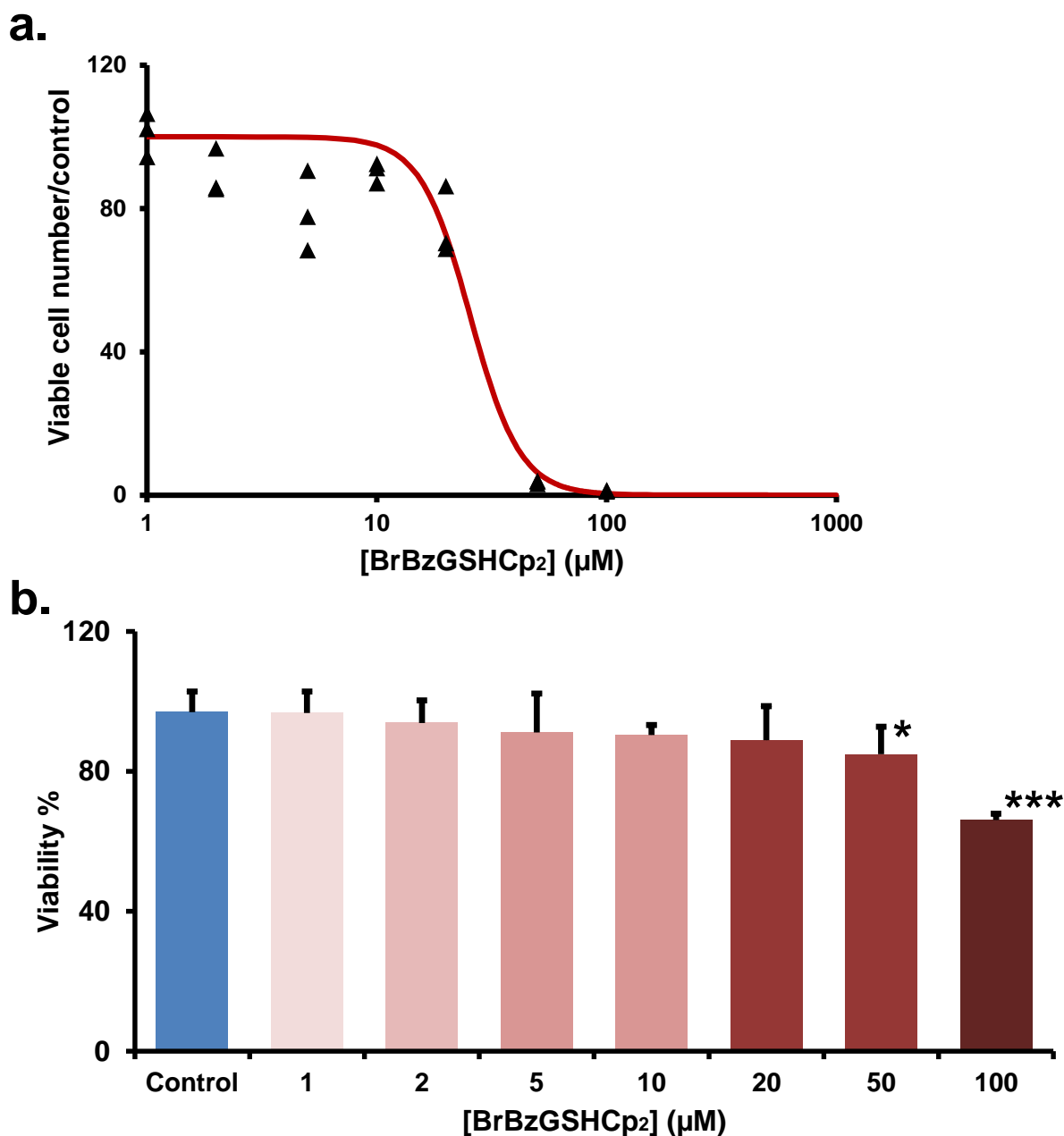


Figure 3.23: Effect of BrBzGSHCP₂ on ESCs growth and viability *in vitro*.
a. BrBzGSHCP₂ concentration – cell growth curve for 48 h treatment. For BrBzGSHCP₂, GC₅₀ = 25.5 ± 1.8 µM, and n = 4.00 ± 0.86 (N = 21). **b.** Effect of BrBzGSHCP₂ on cell viability. Data are mean ± SD (n = 3). Significance: *, p<0.05, ***, p<0.001 compared to control; Student's t-test.

3.2.2.2. Effect of cell permeable Glo1 inhibitor on *Glo1* copy number of ESCs *in vitro*

ESCs were cultured for 24 h after passage and then incubated for a further 3 days with and without 10 μ M of BrBzGSHCp₂. The viable cell number and *Glo1* copy number was then determined. The treatment with 10 μ M BrBzGSHCp₂ decreased cell growth by *ca.* 50%. However, there was no effect on *Glo1* copy number - Figure 3.24. This may be due to increase in expression of Glo1 or MG reductase when ESCs go into growth arrest and therefore protection against dicarbonyl stress and related *Glo1* CNA. In addition, three days may not have been long enough sustained increased levels of MG to increase *Glo1* copy number.

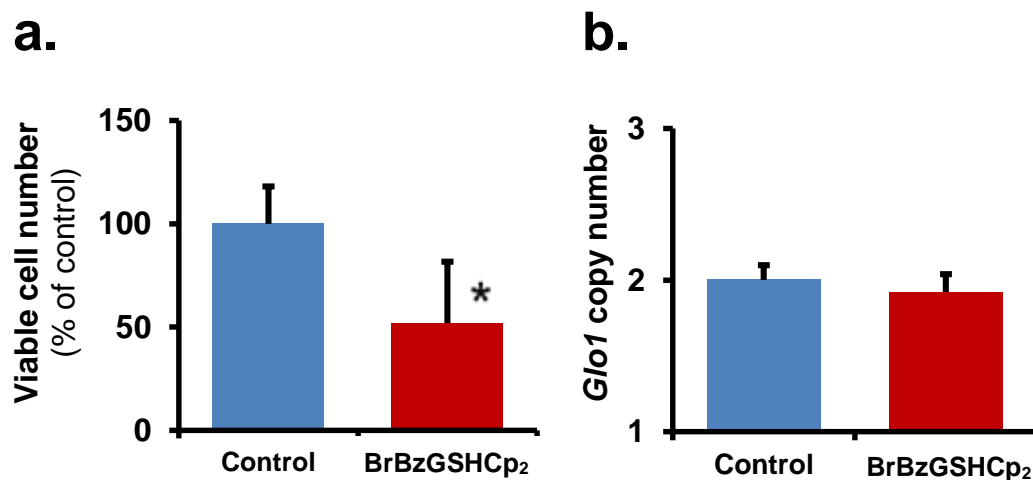


Figure 3.24: Effect of BrBzGSHCp₂ on murine ESCs growth and *Glo1* copy number *in vitro*. a. Viable cell number. b. *Glo1* copy number. Data are mean \pm SD (n = 3). Significance: *, p<0.05; Student's t-test.

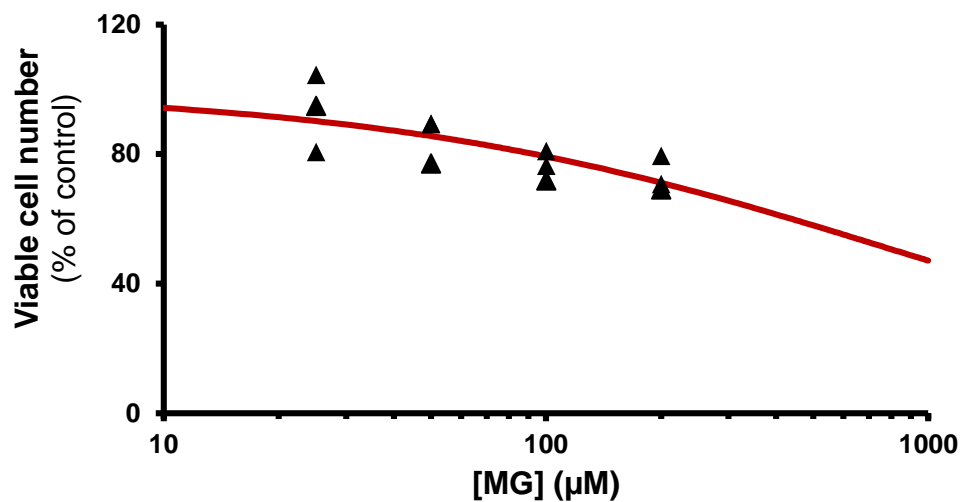
Following the failure of dicarbonyl stress imposed by BrBzGSHCp₂ to induce increased *Glo1* CNV in murine ESCs *in vitro*, I next designed and implemented a series of experiments imposed dicarbonyl stress by addition of exogenous MG.

3.2.3. Effect of MG on growth and *Glo1* copy number of ESCs *in vitro*

3.2.3.1. Effect of MG on growth of ESCs *in vitro*

ESCs were cultured for 24 h for culture flask surface attachment and then incubated with and without 25 – 200 μM methylglyoxal for 48 h. The median growth inhibitory concentration (GC_{50}) of MG was deduced by non-linear regression of viable cell number, expressed as a percentage of control cultures, on MG concentration - fitting to a concentration-response curve and solving for GC_{50} and logistic regression coefficient n . For MG, $\text{GC}_{50} = 831 \pm 5 \mu\text{M}$, and $n = 0.635 \pm 0.002$ ($N = 12$) – Figure 3.25. In addition, viability of ESCs decreased with increasing concentration of MG when cultured under 20% oxygen and 3% oxygen atmospheres (Figures 3.25b and 3.26) suggesting the inhibition of cell growth by MG was likely due to both growth arrest and toxicity.

a.



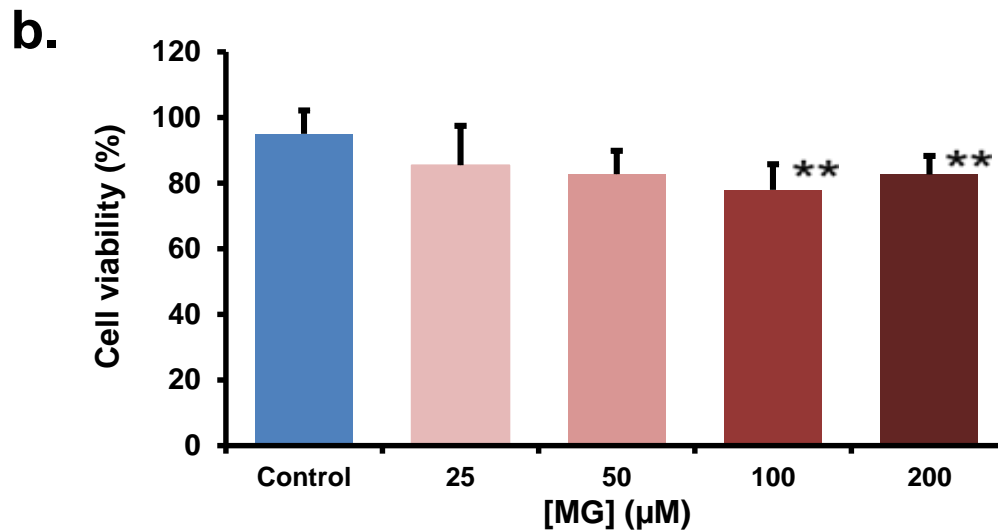


Figure 3.25: Effect of MG on ESCs growth and viability *in vitro* cultured under 20% oxygen atmosphere. a. MG concentration – cell growth curve for 48 h treatment. For MG, $GC_{50} = 813 \pm 5 \mu\text{M}$, and $n = 0.635 \pm 0.002$ ($N = 12$). **b.** Effect of MG on cell viability. Data are mean \pm SD ($n = 3$). Significance: **, $P < 0.01$, compared to control; Student's t-test.

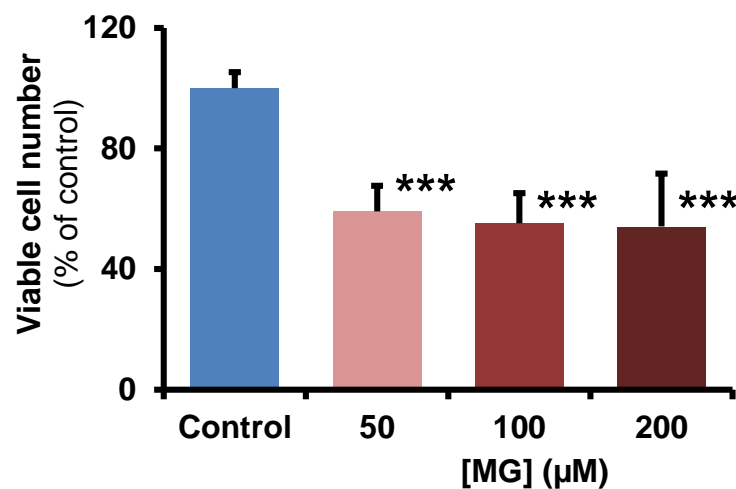


Figure 3.26: Effect of MG on ESCs growth and viability *in vitro* cultured under 3% oxygen atmosphere. Data are mean \pm SD ($n = 3$). Significance: ***, $P < 0.001$ compared to control; Student's t-test.

3.2.3.2. Effect of MG on *Glo1* copy number of murine ESCs *in vitro*

ESCs were cultured for 24 h for attachment to cell culture flasks and thereafter they were treated with and without 200 μM MG. The cells were treated with one dose daily over 3, 6 and 12 days. After each period, the cells were collected and DNA extracted for CNV analysis. The DNA was analysed for copy number of *Btbd9*, *Glo1* - exon 1 and 6, *1700097n02rik* and *Dnahc8* by Taqman copy number assay.

After 3 days, treatment with 200 μ M MG decreased the copy number of *Btbd9* by 13.0% ($P < 0.01$) whereas the copy number of *Glo1* was increased by 5.5 % at exon-1 ($P < 0.05$) and 9.5% at exon-6 ($P < 0.01$). There was no significant change in the copy number of *1700097n02rik* and *Dnahc8* - Figure 3.27. After 6 days, the treatment with 200 μ M MG increased the copy number of *Glo1* at exon-1 and exon-6 by 7.5 % ($P < 0.01$) but did not change the copy number of *Btbd9*, *1700097n02rik* nor *Dnahc8* - Figure 3.28. After 12 days treatment with 200 μ M MG increased copy number of *Glo1* at exon 1 and 6 by 16.0% and 8.0%, respectively ($P < 0.001$), and increased copy number of *1700097n02rik* by 7.0% ($P < 0.05$). There was no change in copy number of *Btbd9* and *Dnahc8* after treatment with MG for 12 days - Figure 3.29. A summary of all of the effect of 200 μ M MG for 3, 6, 12 days on *Glo1* copy number is given in Table 3.13.

Table 3.13: Effect of treatment of murine ESCs with 200 μ M MG for 3, 6 and 12 days *in vitro* on copy number of *Glo1* and surrounding genes.

Gene	Copy number		
	Control	+ MG	% Change
3 Days			
<i>Btbd9</i>	2.00 \pm 0.10	1.74 \pm 0.22**	-13.0
Exon-1 of <i>Glo1</i>	2.00 \pm 0.06	2.09 \pm 0.09*	4.5
Exon-6 of <i>Glo1</i>	2.00 \pm 0.14	2.19 \pm 0.09**	9.5
<i>1700097n02rik</i>	2.00 \pm 0.09	2.09 \pm 0.15	
<i>Dnahc8</i>	2.00 \pm 0.11	1.98 \pm 0.12	
6 Days			
<i>Btbd9</i>	2.00 \pm 0.06	1.79 \pm 0.29	
Exon-1 of <i>Glo1</i>	2.00 \pm 0.07	2.15 \pm 0.11**	7.5
Exon-6 of <i>Glo1</i>	2.00 \pm 0.08	2.15 \pm 0.11**	7.5
<i>1700097n02rik</i>	2.00 \pm 0.08	2.01 \pm 0.08	
<i>Dnahc8</i>	2.00 \pm 0.07	2.00 \pm 0.06	
12 Days			
<i>Btbd9</i>	2.00 \pm 0.10	1.94 \pm 0.20	
Exon1 of <i>Glo1</i>	2.00 \pm 0.09	2.32 \pm 0.09***	16.0
Exon6 of <i>Glo1</i>	2.00 \pm 0.09	2.16 \pm 0.05***	8.0
<i>1700097n02rik</i>	2.00 \pm 0.10	2.14 \pm 0.16*	7.0
<i>Dnahc8</i>	2.00 \pm 0.07	2.04 \pm 0.09	

Analyses were performed using Taqman copy number assay. Data are mean \pm SD (n = 9). Significance: *, ** and ***, $P < 0.05$, $P < 0.01$ and $P < 0.001$, respectively; Student's t-test.

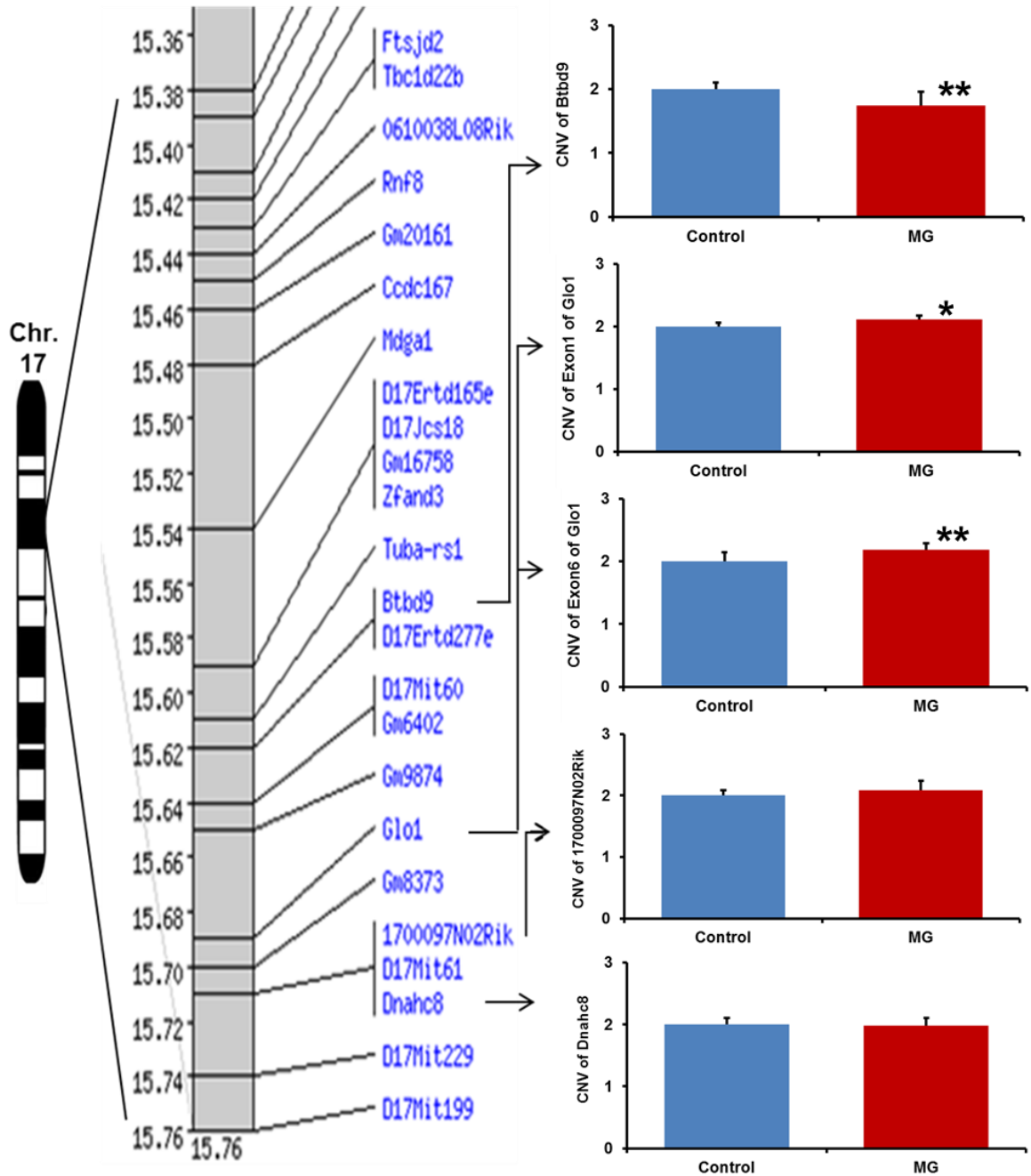


Figure 3.27: Effect of treatment of 200 μ M MG for 3 days on copy number of *Glo1* and the surrounding genes in ESCs *in vitro*. The figure shows mouse chromosome 17 with amplified allele which has *Glo1* gene and other surrounding genes. Three genes surrounding *Glo1* were chosen for checking the stability of the *Glo1* surrounding area including *Btbd9*, *1700097n02rik*, *Dnahc8* and beginning and the end of *Glo1*. All experiments were performed using Taqman copy number assay. Data are mean \pm SD (n = 9). Significance: * and **, P<0.05 and P<0.01, respectively; Student's t-test.

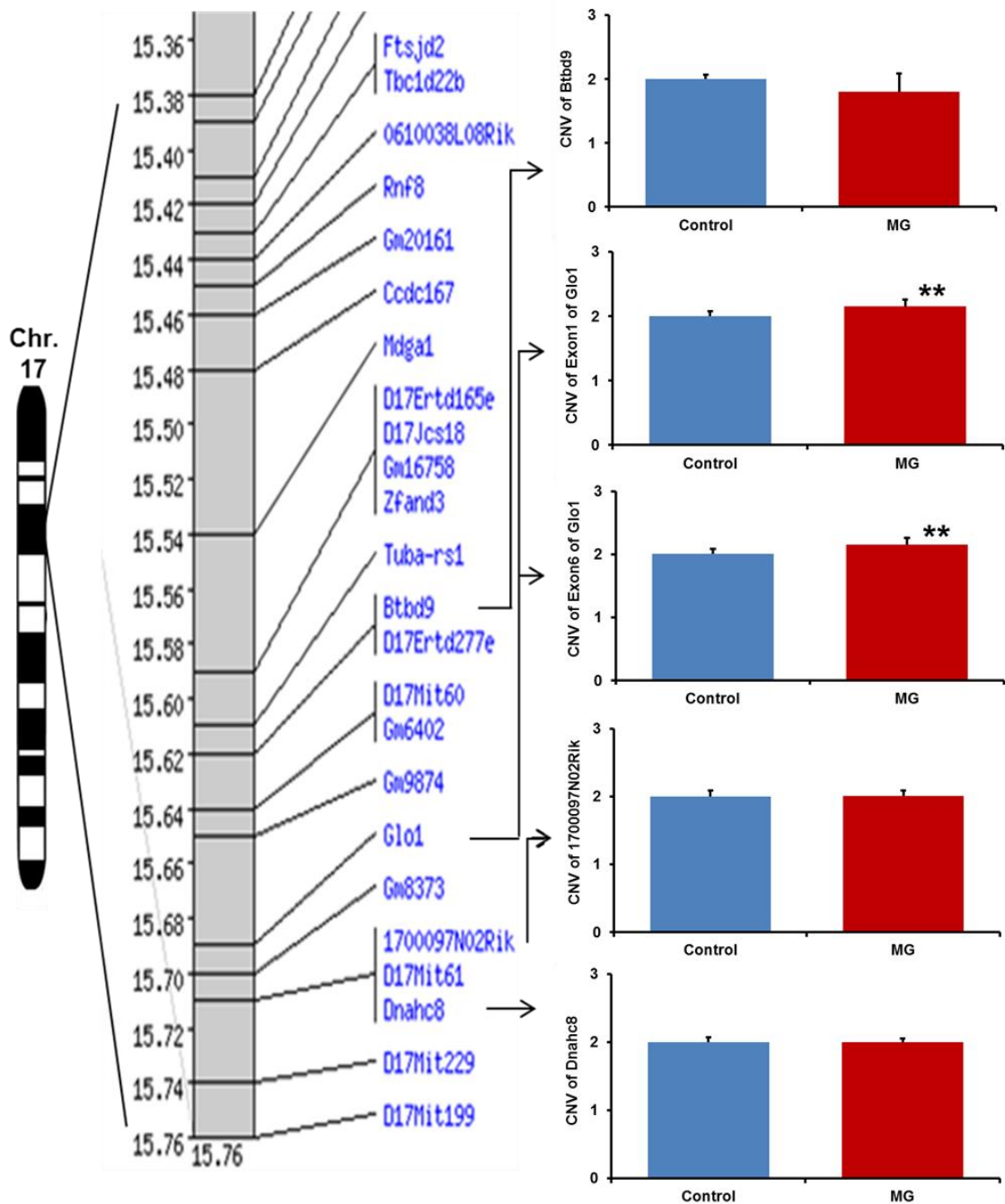


Figure 3.28: Effect of treatment of 200 μ M MG for 6 days on copy number of *Glo1* and the surrounding genes in ESCs *in vitro*. The figure shows mouse chromosome 17 with amplified allele which has *Glo1* gene and others. Three genes surrounding *Glo1* were chosen for checking the stability of the *Glo1* surrounding area including *Btd9*, *1700097n02rik*, *Dnahc8* and beginning and the end of *Glo1*. All experiments were performed using Taqman copy number assay. Data are mean \pm SD (n = 9). Significance: **, P<0.01; Student's t-test.

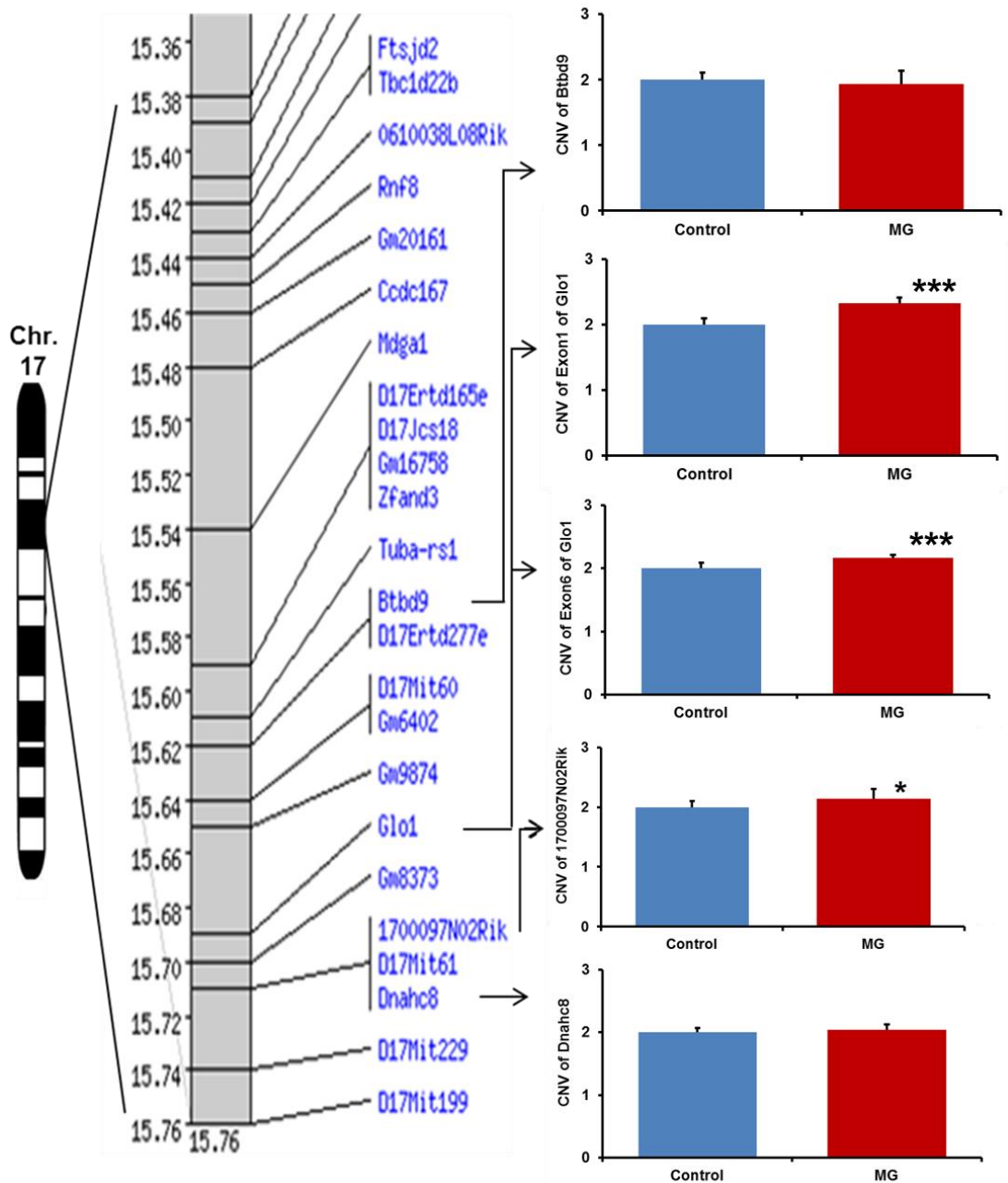


Figure 3.29: Effect of treatment of 200 μ M MG for 12 days on copy number of *Glo1* and the surrounding genes in ESCs *in vitro*. The figure shows mouse chromosome 17 with amplified allele which has *Glo1* gene and others. Three genes surrounding *Glo1* were chosen for checking the stability of the *Glo1* surrounding area including *Btd9*, *1700097n02rik*, *Dnahc8* and beginning and the end of *Glo1*. All experiments were performed using Taqman copy number assay. Data are mean \pm SD (n = 9). Significance: * and ***, P<0.05 and P<0.001, respectively; Student's t-test.

These studies suggest that dicarbonyl stress imposed on murine ESCs *in vitro* by exposure to exogenous MG induces increased CNV of *Glo1*. This may be increased copy number of DNA fragments of the *Glo1* gene or complete replication of the *Glo1* gene with increasing functional copy number and increased expression of Glo1. To examine if the increased *Glo1* copy number was functional, I next assessed the effect of exposure of murine ESCs to exogenous MG for 3, 6 and 12 days on Glo1 expression – judged by the level of *Glo1* mRNA, Glo1 protein and activity.

3.2.3.3. Effect of treatment of murine ESCs with 200 μ M MG for 3, 6 and 12 days *in vitro* on *Glo1* mRNA

Murine ESCs were incubated for 3, 6 and 12 days with 200 μ M MG as described above and mRNA extracted to determine the relative *Glo1* mRNA levels. The analysis showed that there was no significant change of *Glo1* mRNA levels from control levels by treatment with MG - Table 3.14.

Table 3.14: Effect of treatment of ESCs *in vitro* with 200 μ M MG for 3, 6 and 12 days on *Glo1* mRNA content

Duration (days)	<i>Glo1</i> mRNA (normalized to <i>Rn18s</i> mRNA)	
	Control	200 μ M MG
3	0.816 \pm 0.023	0.816 \pm 0.031
6	0.864 \pm 0.005	0.855 \pm 0.015
12	0.828 \pm 0.014	0.821 \pm 0.006

Data are mean \pm SD (n = 3). Significance: Student's t-test. All comparisons of +200 μ M MG versus control gave P>0.05.

3.2.3.4. Effect of treatment of murine ESCs with 200 μ M MG for 3, 6 and 12 days *in vitro* on Glo1 protein

Murine ESCs were incubated for 3, 6 and 12 days with 200 μ M MG as described above, cell protein extracted and Glo1 protein determined by quantitative immunoblotting. There was no change of Glo1 protein content of ESCs at 3 and 6 days of treatment with 200 μ M MG. After treatment of ESCs with 200 μ M MG for 12 days, however, there was 25% increase in Glo1 protein content, compared to controls - Figure 3.30.

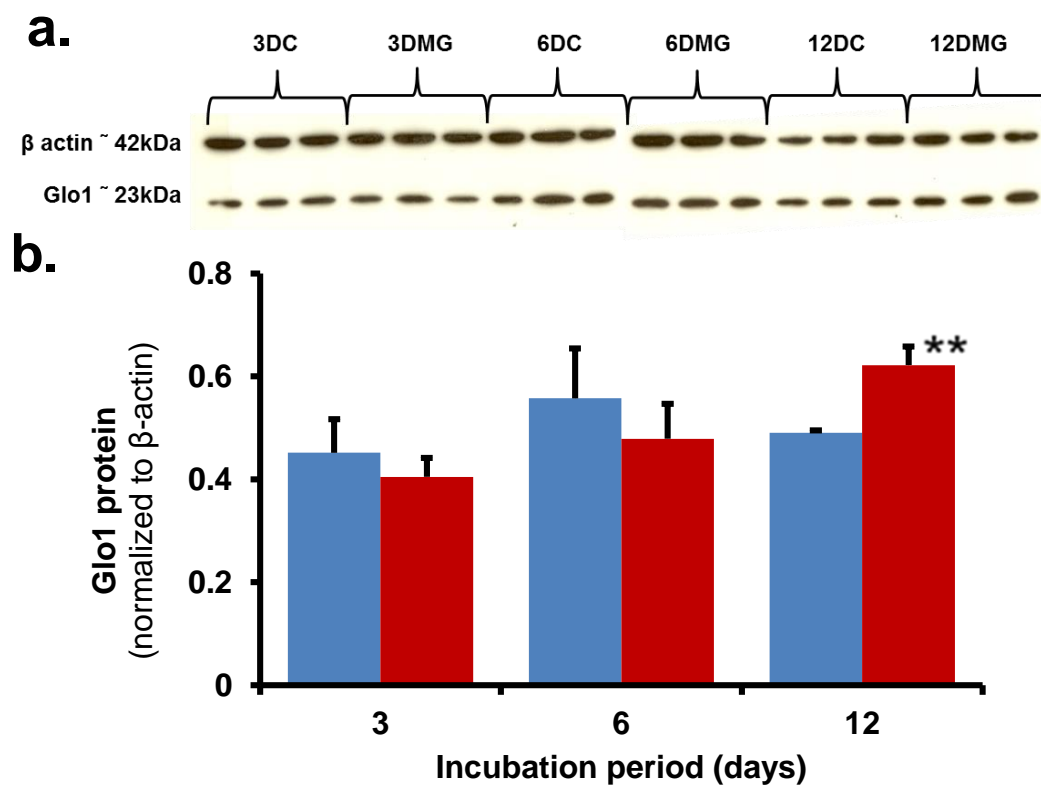


Figure 3.30: Effect of treatment of 200 μM MG for 3, 6 and 12 days on Glo1 protein content in ESCs *in vitro*. **a.** Immunoblotting of Glo1 and β-actin. **b.** Quantification of the blots. Key: blue bars – control, red bars – + 200 μM MG. Data are mean ± SD (n = 3). Significance: **, P<0.01; Student's t-test.

3.2.3.5. Effect of treatment of murine ESCs with 200 μM MG for 3, 6 and 12 days *in vitro* on Glo1 activity

ESCs were incubated for 3, 6 and 12 days with 200 μM MG as described above, cell cytosolic protein extracts prepared and Glo1 activity determined. There was no significant difference in Glo1 activity of ESCs treated with 200 μM MG and controls over 3 days. There was a significant decrease in Glo1 activity in the ESCs treated with 200 μM MG over 6 days when compared to the controls, but there was a significant increase in Glo1 activity in the ESCs treated with 200 μM MG over 12 days, compared to the controls - Figure 3.31.

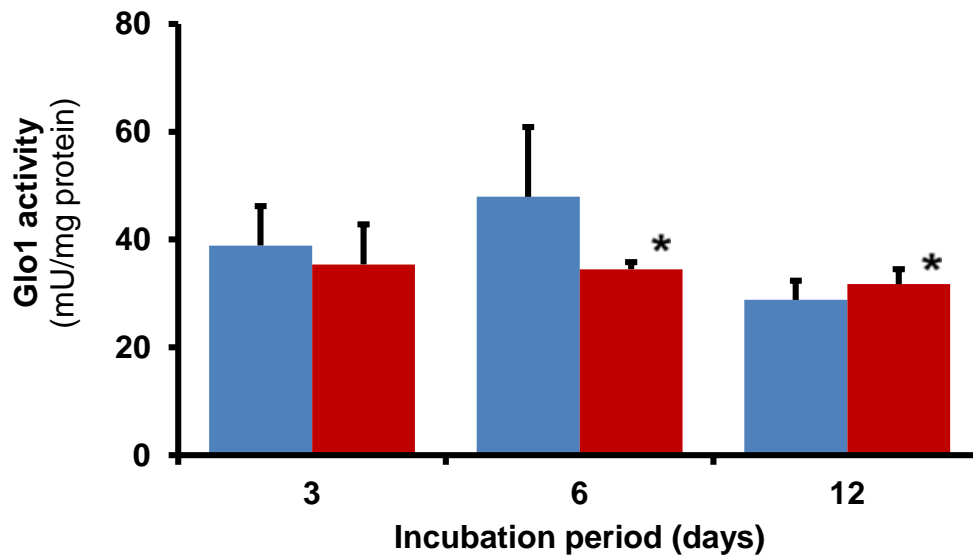


Figure 3.31: Effect of treatment of 200 μM MG for 3, 6 and 12 days on Glo1 activity in ESCs *in vitro*. Key: blue bars – control, red bars – + 200 μM MG. Data are mean ± SD (n = 3). Significance: *, P<0.05; Student’s t-test.

The studies on markers of Glo1 expression in ESCs treated with exogenous MG gave support for functionality of *Glo1* copy number increase after 12 days treatment from the findings of increase Glo1 protein and activity. *Glo1* CNV increase appears to require sustained exposure to exogenous MG. This may be due to repair of *Glo1* copy number increase in subsequent DNA replication after mitosis occurring during ESC proliferation. Increased functional copies of *Glo1* are expected to give rise to increase *Glo1* mRNA, Glo1 protein and Glo1 activity. The detection of increased levels will depend on how stable these markers of expression are. Since measurements were made 24 h after the last addition of exogenous MG, relatively-short-lived markers may relax back to the control values. Estimates of the half-lives of *Glo1* mRNA and protein are 15 h (HepG2 cells) and 63 h (MCF7 cells), respectively (Yang et al., 2003, Kristensen et al., 2008). Failure to detect increased *Glo1* mRNA whereas increased Glo1 protein and Glo1 activity were detected after exogenous MG treatment may have been due to the relative instability of *Glo1* mRNA compared to Glo1 protein. The precision of measurement of Glo1 protein and activity were also relatively low compared to the precision of copy number measurement which also makes assessment of functionality of small changes in gene copy number difficult to assess. In studies of functional *GLO1* copy number increase in human tumours, for example, the most reliable marker of copy number increase was *GLO1* DNA (Santarius et al., 2010).

Glo1 copy number increase induced by exogenous MG may be corrected in DNA replication occurring in the S-phase of the ESC growth cycle. ESC growth cycle time is *ca.* 12 h (Li et al., 2012). Therefore, increase in *Glo1* copy number may suffer repair between treatments with exogenous MG made only once every 24 h. More frequent additions of MG may avoid this and increase *Glo1* copy number further. To test this, I designed and implemented a study where treatment with exogenous MG was made more frequently.

3.2.3.6. Effect of treatment of ESCs *in vitro* with 200 μ M MG every 6 h for 24 h on cell viability and *Glo1* copy number

ESCs were incubated for 24 h with and without addition of 200 μ M MG with additions made every 6 h for 24 h. At 24 h cell viability and *Glo1* copy number were determined. There was no significant effect of MG treatment on cell viability - Table 3.15. Extracted DNA was analysed by Taqman copy number assay for *Glo1* copy number. The analyses showed that there was no significant difference in the *Glo1* copy number between the ESCs treated with 200 μ M MG over 24 hours and the control - Table 3.15.

Table 3.15: Effect of treatment of 200 μ M MG for 1 day with dose every 6 hours on ESCs *in vitro*

	Control	+ 200 μ M MG
Cell viability (%)	96.1 \pm 10.6	87.9 \pm 7.4
Copy number of <i>Glo1</i>	2.00 \pm 0.06	2.07 \pm 0.10

Data are mean \pm SD (n = 3). Student's t-test. P>0.05 (not significant).

These findings suggest that the frequency of additions of exogenous MG every 24 h in previous studies were probably not a limiting factor for induction of increased *Glo1* copy number.

A further factor that may influence potency of MG to increase *Glo1* copy number in ESCs is the oxygen environment. To test this, I designed and performed a study where treatment with exogenous MG of ESCs was made every 24 h for 3 and 12 days with cultures under an atmosphere of 3% oxygen.

3.2.3.7. Effect of treatment of ESCs *in vitro* with 200 μ M MG for 3 and 12 days on *Glo1* copy number under 3% oxygen atmosphere

ESCs were incubated for 3 and 12 days with 200 μ M MG as described above but under 3% oxygen atmosphere and *Glo1* copy number determined. Over three days, the treatment with 200 μ M MG had no effect on *Glo1* copy number, compared to control. However, there was 3% decrease of *Glo1* copy number in the cells treated with 200 μ M MG under 3% oxygen atmosphere, compared with the cells grown under 3% oxygen atmosphere without MG treatment - Figure 3.32.

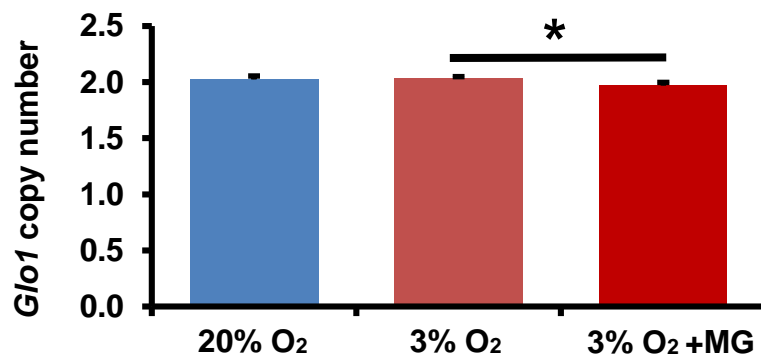


Figure 3.32: Effect of treatment of 200 μ M MG for 3 days on *Glo1* copy number of ESCs *in vitro* under 3% oxygen atmosphere. Data are mean \pm SD (n = 3). Significance: *, p<0.01; Student's t-test.

Over twelve days, incubation under 3% oxygen atmosphere and under 3% oxygen atmosphere with 200 μ M MG increased the *Glo1* copy number by 8% and 5% respectively, compared to untreated cells control in normoxia - Figure 3.33.

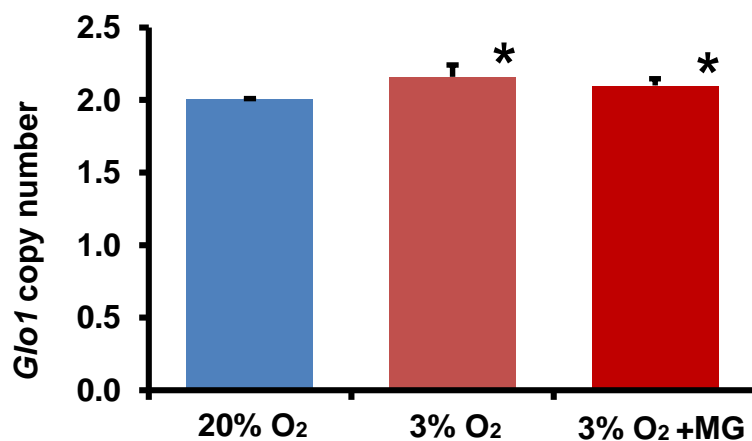


Figure 3.33: Effect of treatment of 200 μ M MG for 12 days on *Glo1* copy number of ESCs *in vitro* under 3% oxygen atmosphere. Data are mean \pm SD (n = 3). Significance: *, P<0.01; Student's t-test.

These findings suggest that ESC metabolism under low, physiological oxygen concentration pre-disposes to *Glo1* copy number increase. This may be due to the continual increased formation and decreased metabolism of endogenous MG in ESCs. The continual exposure to increased cellular MG may be the explanation as to why 3% oxygen atmosphere was a relatively good inducer of increased *Glo1* copy number.

A further strategy to increase dicarbonyl stress in ESCs is to decrease *Glo1* expression by siRNA gene silencing. Accordingly, I performed a series of experiments to decrease *Glo1* expression in ESCs and study the effect on copy number of *Glo1*.

3.2.4. Effect of silencing of *Glo1* on the cell growth and *Glo1* expression and activity of ESCs *in vitro*

3.2.4.1. Effect of silencing of *Glo1* on the cell growth of ESCs *in vitro*

ESCs were cultured for 24 h after passage for attachment to culture flask wall. Cells were then transfected with 5 nM, 10 nM, 25 nM, 50 nM, 100 nM and 200 nM of SMART pool: ON-TARGET plus *Glo1* siRNA for two days. Controls used were ESCs treated with ON-TARGET plus non-targeting pool siRNA and ESCs treated with Lipofectamine 2000 transfection reagent only. The viability of the ESCs was assessed after the two days. After the two days, the cells were counted, collected and RNA extracted for measurement of *Glo1* mRNA.

Cell growth and viability assessment showed that there was no significant difference in the viability between the ESCs transfected with any of the concentrations of SMART pool: ON-TARGET plus *Glo1* siRNA and the controls - Figure 3.34.

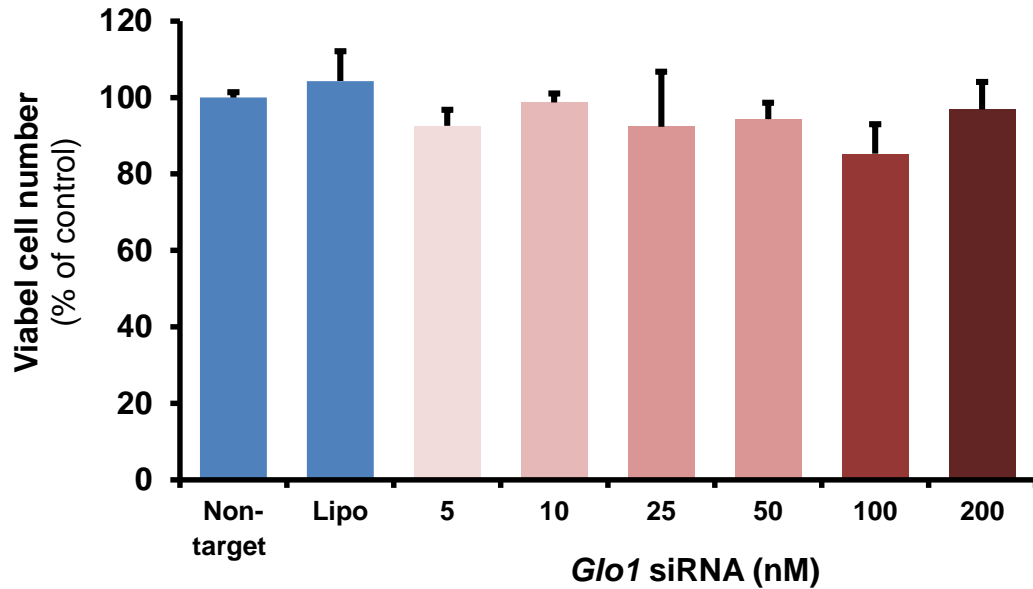


Figure 3.34: Effect of silencing of *Glo1* on the growth of ESCs *in vitro*. The figure shows the change in the ESCs viability after *Glo1* knockdown by different concentrations of SMART pool: ON-TARGET plus *Glo1* siRNA for 2 days. The controls used were ESCs treated with ON-TARGET plus non-targeting pool siRNA and ESCs treated with Lipofectamine 2000 transfection reagent only. Data are mean \pm SD (n = 3).

To assess of silencing of *Glo1* had decreased *Glo1* expression, the relative level of *Glo1* mRNA in ESCs with *Glo1* siRNA silencing was assessed. This showed that there was a significant decrease in *Glo1* mRNA in all transfected cells with SMART pool: ON-TARGET plus *Glo1* siRNA when compared to the controls - Figure 3.35. The use of ON-TARGET plus non-targeting pool siRNA as a control proved the specificity of this application, that is there was no decrease of *Glo1* mRNA in the controls.

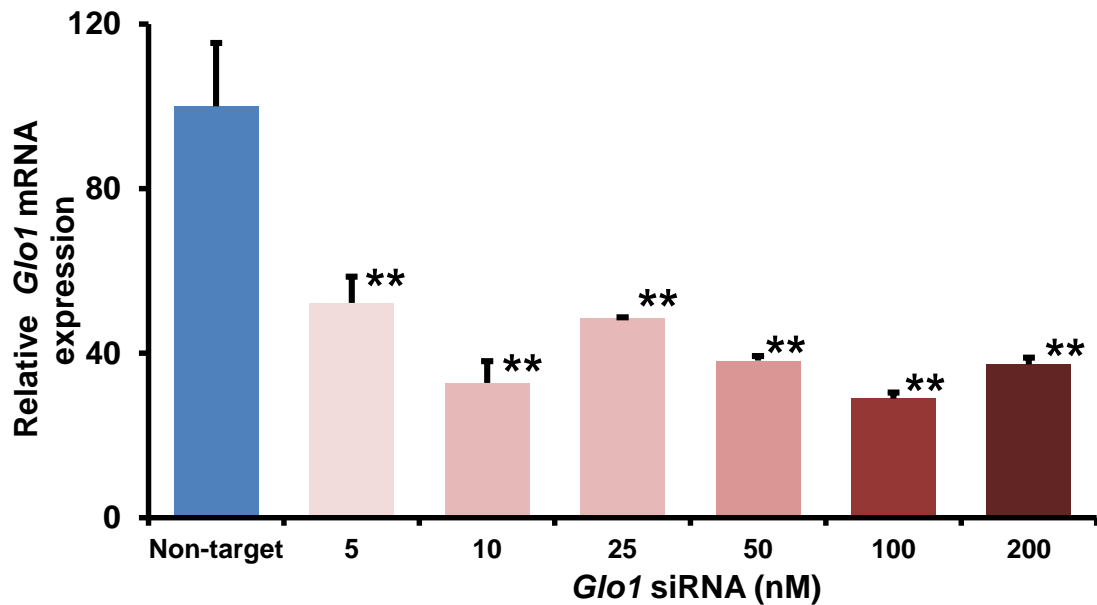


Figure 3.35: Effect of silencing of *Glo1* on *Glo1* mRNA of ESCs *in vitro*. The figure shows the change in *Glo1* mRNA expression in the ESCs after *Glo1* knockdown by different concentrations of SMART pool: ON-TARGET plus *Glo1* siRNA for 2 days. The control used is ESCs treated with ON-TARGET plus non-targeting pool siRNA. Data are mean \pm SD (n = 3). Significance: **, p<0.01; Student's t-test.

There was a lack of dose response *Glo1* siRNA concentration on the level of *Glo1* mRNA and *ca.* 40% residual *Glo1* mRNA at the highest level of *Glo1* siRNA used. This raises doubts on the specificity and potency of *Glo1* siRNA in silencing of *Glo1* in ESCs. To assess the effect of *Glo1* silencing further, I examined the effect on *Glo1* protein and activity.

3.2.4.2. Effect of silencing of *Glo1* on *Glo1* protein of ESCs *in vitro*

ESCs were cultured as described above with 100 nM and 200 nM of SMART pool: ON-TARGET plus *Glo1* siRNA for two days. The *Glo1* protein expression and activity of the ESCs was assessed. *Glo1* protein was decreased by 85% and 88% in the ESCs transfected with 100 nM and 200 nM *Glo1* siRNA, respectively - Figure 3.36, a. and b. *Glo1* activity was also decreased by 86% and 89% in the ESCs transfected with 100 nM and 200 nM *Glo1* siRNA respectively - Figure 3.37.

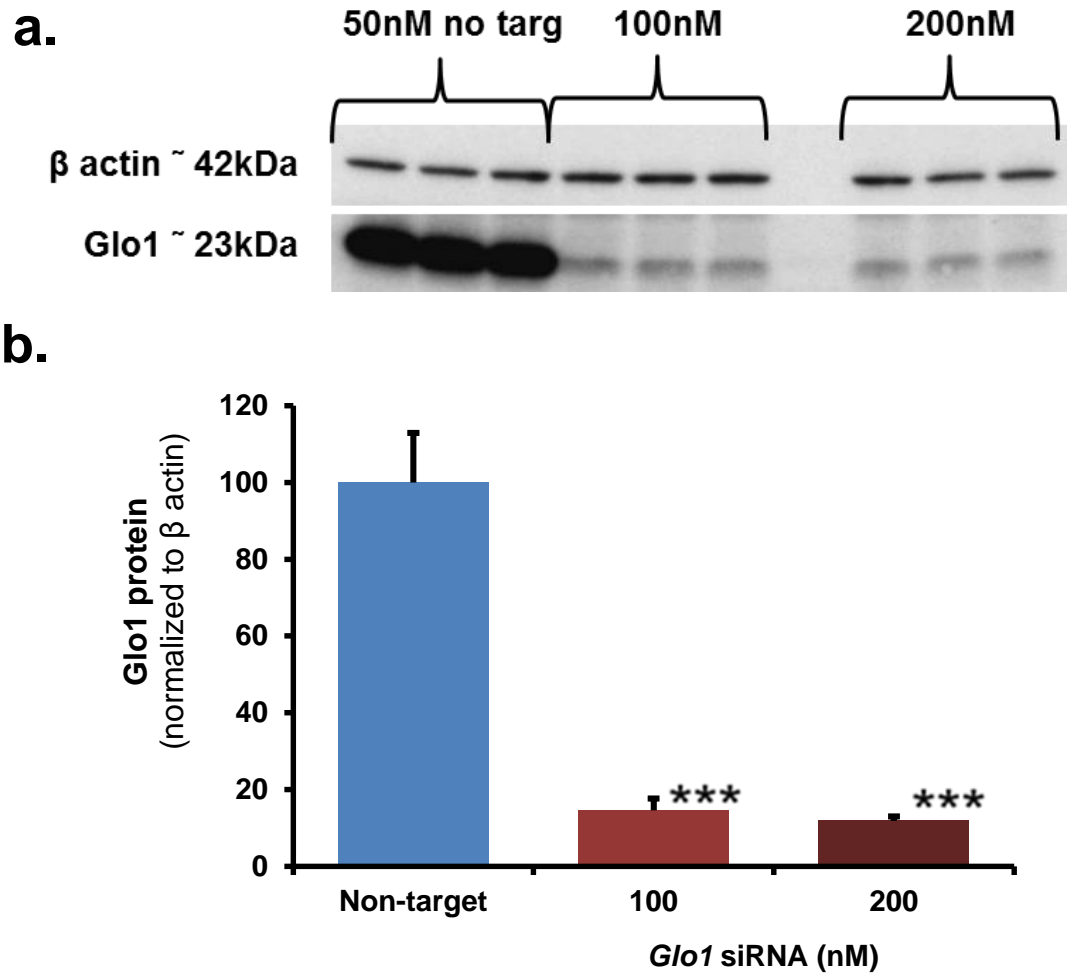


Figure 3.36: Effect of silencing of *Glo1* on Glo1 protein of ESCs *in vitro*.
a. Western blotting of Glo1 and β -actin. **b.** Quantification of Glo1 protein. The control used is ESCs treated with ON-TARGET plus non-targeting pool siRNA. Data are mean \pm SD (n = 3). Significance: ***, p<0.001; Student's t-test.

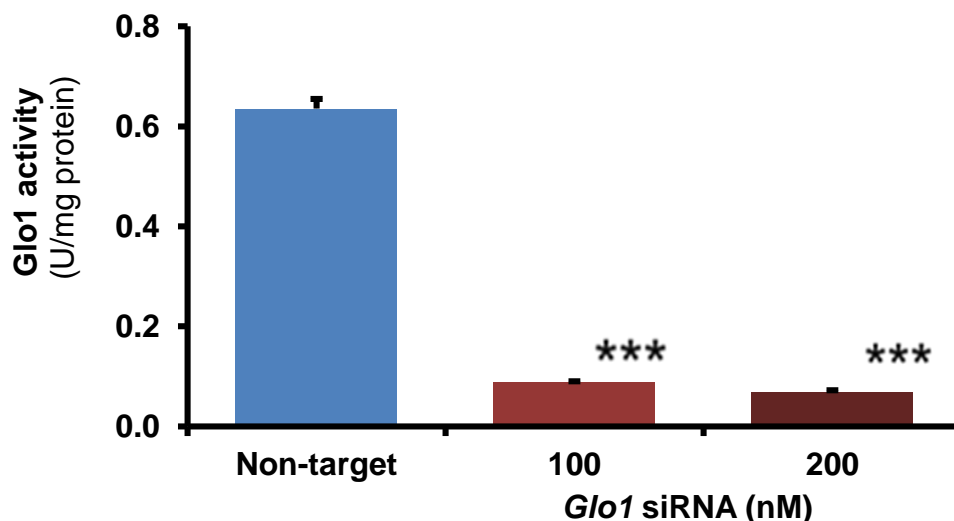


Figure 3.37: Effect of silencing of *Glo1* on *Glo1* activity of ESCs *in vitro*. The control used is ESCs treated with ON-TARGET plus non-targeting pool siRNA. Data are mean \pm SD (n = 3). Significance: ***, p<0.001; Student's t-test.

These findings indicate potent decrease in *Glo1* protein and activity in ESCs by *Glo1* silencing with relatively high levels of *Glo1* siRNA. This would be expected to increase the growth inhibitory effects of exogenous MG on ESCs *in vitro*. This was now assessed.

3.2.4.3. Effect of MG and silencing of *Glo1* on the growth of ESCs *in vitro*

ESCs were cultured and *Glo1* silenced by incubation with 100 nM of SMART pool: ON-TARGET plus *Glo1* siRNA for three days. The transfected cells were then treated with 10, 50 and 100 μ M MG. The dose of MG was added on the fourth day and another dose was added in the fifth day. The cells were collected and counted on the sixth day. The control was ESCs treated with 50 nM of ON-TARGET plus non-targeting pool siRNA for three days and then treated without MG for two days. Growth of ESCs was decreased 41%, 38 % and 57% due to the silencing of *Glo1* and subsequent treatment with 10, 50 and 100 μ M of MG respectively - Figure 3.38. This indicates that the GC₅₀ of MG is now <100 μ M and hence *Glo1* silencing has decreased the GC₅₀ of MG by > 8-fold; *cf.* Figure 3.25.

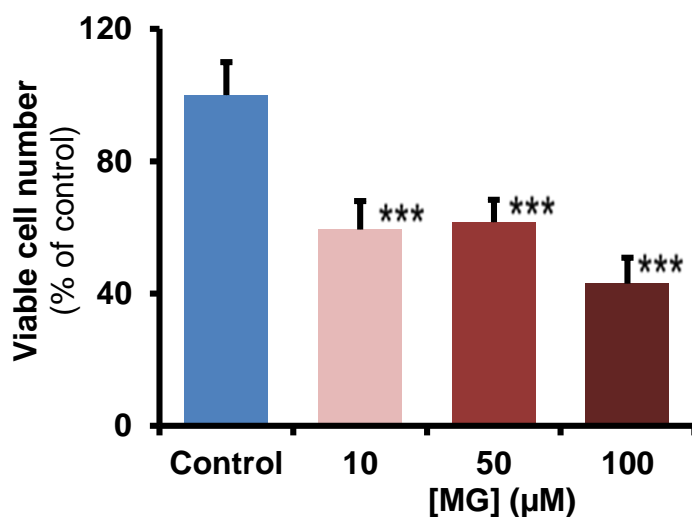


Figure 3.38: Effect of MG with on the growth ESCs *in vitro* with prior silencing of *Glo1*. *Glo1* expression was knocked down by 100 nM of SMART pool: ON-TARGET plus *Glo1* siRNA for 3 days. Then, the transfected cells were treated with 10, 50 and 100 µM of MG, at 0 and 24 h. Cell growth and viability was assessed at 48 h. The control used is ESCs treated with 50 nM ON-TARGET plus non-targeting pool siRNA. Data are mean ± SD (n = 3). Significance: ***, P<0.001; Student's t-test.

Increased *GLO1* copy number was found in human tumours (Santarius et al., 2010). I assessed if this may be induced by exogenous MG using the human leukaemia 60 (HL60) cell line.

3.3. Effect of MG on the growth and *GLO1* copy number of human leukaemia cells *in vitro*

HL60 cells were cultured according to method given in Section 2.2.2.2. HL60 cells were treated for three days with 238 µM MG – the median growth inhibitor concentration by single dose treatment (Kang et al., 1996). Herein, there were additional treatments with 238 µM MG at 24 and 48 h. This treatment regime decreased the growth of HL60 cells by 77%, with respect to control HL60 cells - Figure 3.39. Analysis of cellular DNA analysis showed a significant decrease of *GLO1* copy number by 15% when compared to *GLO1* copy number of the control - Figure 3.40.

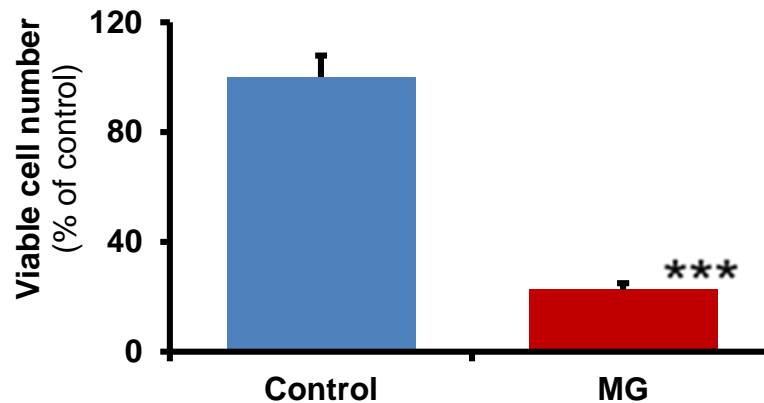


Figure 3.39: Effect of MG on the growth of HL60 cells *in vitro*. HL60 cells were incubated with and without 238 μ M MG at 0, 24 and 48 h for 3 days. Data are mean \pm SD (n = 3). Significance: ***, P<0.001; Student's t-test.

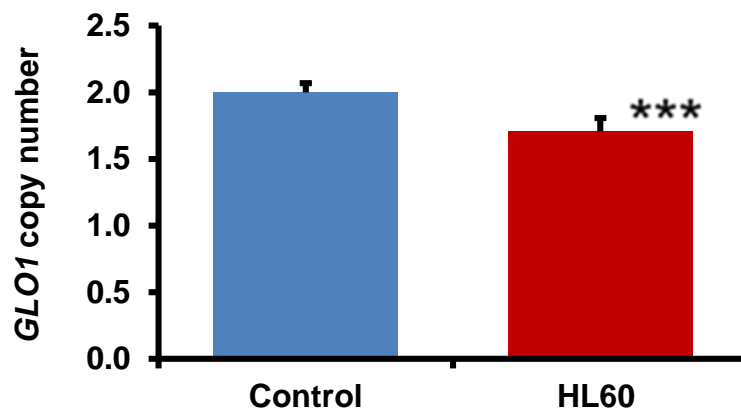


Figure 3.40: Effect of MG on the *GLO1* copy number of HL60 cells *in vitro*. HL60 cells were incubated with and without 238 μ M MG at 0, 24 and 48 h for 3 days. Data are mean \pm SD (n = 3). Significance: ***, P<0.001; Student's t-test

This finding indicates that induction of dicarbonyl stress by exogenous MG decreased *GLO1* DNA. This may be due to DNA damage induced by MG modification. MG modification of DNA occurs in HL60 treatment by the concentration of MG and induction of apoptosis (Kang et al., 1996).

The physiological relevance of *GLO1* copy number alternation may be assessed by examining *GLO1* copy number in clinical condition of dicarbonyl stress. Severe dicarbonyl stress occurs in ESRD (Agalou et al., 2005, Rabbani and Thornalley, 2012b, Rabbani and Thornalley, 2012a). I therefore initiated a clinical collaboration to acquire and analyse blood samples of healthy human subjects and ESRD patients. *GLO1* copy number can be conveniently analysed in peripheral blood mononuclear cells.

3.4. *GLO1* copy number in clinical end stage renal disease

The *GLO1* gene copy number was quantified in DNA extracted from blood samples of healthy human subjects and patients at stage 5 of chronic kidney disease. *GLO1* copy number was determined in peripheral blood mononuclear cells of patients with stage 5 chronic kidney disease and healthy controls. In addition, NCL-H522 human lung carcinoma cells were used as positive control of increased *GLO1* copy number. These cells have *ca.* 6 copies of *GLO1* (Santarius et al., 2010).

There was no significant difference in *GLO1* copy number of healthy subjects and patients with ESRD – Figure 3.41. In addition, these samples and cells were genotyped for C419A SNP in *GLO1* gene according to method no 2.2.6.8. The genotyping shows 6 subjects are homozygote A/A, 18 subjects heterozygote A/E and 13 subjects are homozygote E/E. These genotypes were equally distributed in the study groups. Three subjects were not genotyped due to the limitation of the DNA samples. Furthermore, NCL-H522 human lung carcinoma cells are heterozygote A/E. sample of the genotyping results is shown in Figure 3.42.

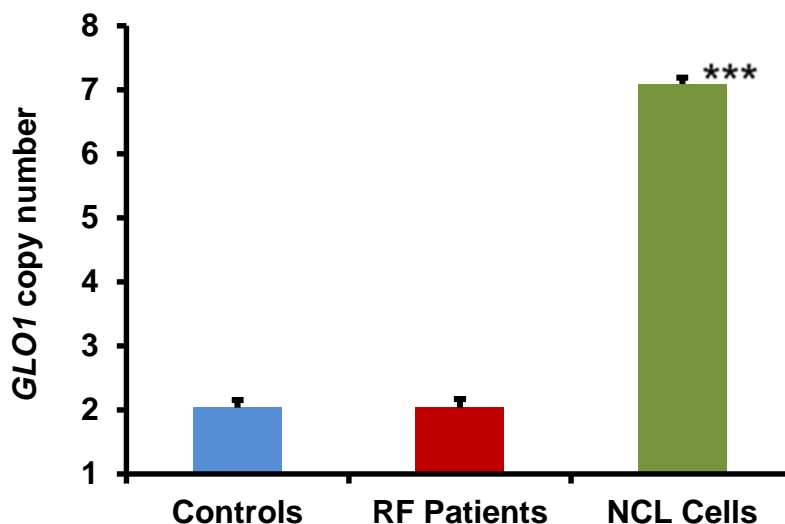


Figure 3.41: Taqman copy number assay for *GLO1* gene in the DNA of end stage renal failure patients, controls and NCL-H522 cell line. Data are mean \pm SD (controls, n = 20; RF, n = 20; and NCL-H522 cell line, n = 3). Significance: ***, $p < 0.001$ compared to controls; Student's t-test.

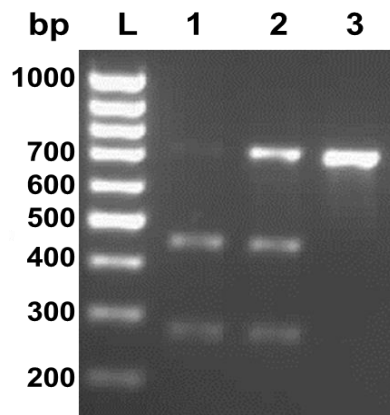


Figure 3.42: Specimen genotyping results for C419A SNP in *GLO1* gene. The figure shows two bands reveals 453 bp and 260 bp fragments in the presence of A 111 allele in sample no.1. In sample no. 2, there are three bands reveals 713 bp, 453 bp and 260 bp fragments in the presence of A 111 allele and E 111 allele. In sample no. 3, there is one band reveals 713 bp fragment in the presence of E 111 allele.

4. Discussion

CNV is a source of substantial diversity of gene expression and phenotype (Zarrei et al., 2015). It occurs at chromosomal fragile sites, with defects in DNA replication or telomere dysfunction. This may be linked to endogenous and exogenous mechanisms mediating DNA damage and endogenous mechanisms of DNA damage repair, particularly non-homologous repair of broken replication forks increasing likelihood of CNV (Hastings et al., 2009b). Genome-wide CNV increases were observed with chemical agents that inhibit enzymes of DNA metabolism, aphidicolin and hydroxyurea (Arlt et al., 2012). MG modification is a major cause of endogenous DNA damage and this may drive *Glo1* CNA cytoprotective response revealed herein. It does not account for, however, how duplication of the *Glo1* gene is selectively retained. This may be linked to the DNA damage response such that retention of *Glo1* copy number increase is retained to dampen this response. The cytoprotective and survival advantage may also account for why duplication of the *Glo1* gene is selectively retained.

4.1. Importance of advancing understanding of the glyoxalase system in biomedical research

The glyoxalase system is an important protective system found throughout biological life. It is the key enzymatic system protecting against glycation by reactive dicarbonyl metabolites (Xue et al., 2012, Rabbani et al., 2014b). Its fundamental importance is highlighted by its implication in many diseases such as diabetes, obesity, cardiovascular complications in diabetes and aging in human tissues, mouse tissues and cells (Thornalley, 1988, Wilson et al., 1991, Lo et al., 1994a, McLellan and Thornalley, 1989, Dunn et al., 1989, Dunn et al., 1991, Haik Jr et al., 1994, Ahmed et al., 1997, Sharma-Luthra and Kale, 1994). The essential importance of this role is highlighted by the null mutation of *GLO1* is embryonically lethal in humans (Arai et al., 2010). Studies of malignant transformation of liver progenitor cells in mice lacking p53 and overexpressing proto-oncogene *Myc* suggested *Glo1* is a tumour suppressor gene- one of only 13 genes in genome-wide analysis (Zender et al., 2008). When malignancy is established, however, *Glo1* promotes the development of tumours (Hosoda et al., 2014) – although as *Glo1* does

not mediate malignant transformation itself, nor is mutated into a form that does. This indicates GLO1 is neither an oncogene nor proto-oncogene by conventional definitions (Futreal et al., 2004). Increased expression of GLO1 may be permissive of rapid growth of some tumours, however, sustained by high glycolytic rates by suppressing the risk of toxicity of associated high fluxes of MG formation (Thornalley et al., 2010). Inhibitors of GLO1 are prospective anti-cancer drugs – reviewed in (Thornalley and Rabbani, 2011). GLO1 overexpression by increased gene amplification in tumours is associated with MDR (Santarius et al., 2010). *GLO1* amplification, where functional, may be a marker of sensitivity to cell permeable GLO1 inhibitors (Santarius et al., 2010). Metabolic modelling of the GLO1 pathway suggests this may not be generally correct as a high flux of MG formation with high expression of GLO1, and absence of other pathways for MG metabolism (for example, aldoketo reductases) are conditions required for sensitivity to GLO1 inhibition through accumulation of MG to toxic levels (Rabbani et al., 2014b).

The regulatory promoter region of *GLO1* gene is a hotspot of copy number variation in the human and mouse genomes although the prevalence of multiple *GLO1* promoter copies and related increased GLO1 expression in the human population is unknown (Williams et al., 2009, Redon et al., 2006). In addition, there is increased evidence regarding the involvement of glyoxalase system in cell senescence and aging as the accumulation of protein glycation adducts is associated with enzyme inactivation, protein denaturation and a cellular mediated immune response (Ikeda et al., 2011). Excessive nucleotide glycation is associated with mutagenesis and apoptosis (Thornalley, 1999).

The glyoxalase system was discovered in the early 20th century. Since then, many cellular and animal models have been developed to improve the understanding of this system under different physiological condition. *Glo1* deficient mice and transgenic mice overexpressing *Glo1* provide valuable models to study control of change in extent of dicarbonyls glycation in mammalian systems. *Glo1* knockout might produce further understanding about the importance of the glyoxalase system and how the physiological system may react with increased MG.

To date, only one *Glo1* deficient mouse model has been developed and produced through expression of *Glo1* siRNA. There was a 45–65% decrease in tissue *Glo1* activity in the heterozygous offspring of the founder (Queisser et al., 2010). In

addition, Lexicon Pharmaceuticals produced a Glo1 mutant mouse from C57BL/6 species. The mouse produced by gene trapping method and the modification was in the chromosome 17 of the mice embryonic stem cells. Lexicon evaluated the expression of Glo1 in several tissue and they claimed that mRNA of *Glo1* was completely absent. Surprisingly and unexpectedly there was no pathogenic phenotype. There is requirement to understand how Glo1 in Lexicon Glo1 mutant mouse has apparently null mutation of *Glo1* without any health effect. This conundrum has been addressed in this project and caused a major shift in the hypothesis, aim and objectives.

The main hypothesis of this project was: *the accumulation of MG in the glomerular endothelium in diabetes leads to cell dysfunction and development of diabetic nephropathy*. The aim of this study was to test this hypothesis by studying the effect of decreasing Glo1 activity by genetic silencing in Lexicon Glo1 mutant mouse on the development of diabetic nephropathy. This would be achieved by studying the effect of Glo1 knockout on the development of nephropathy (DN) in STZ-induced diabetes. To test if increased *in situ* exposure to glyoxal and MG accelerates the development of DN, the development of DN in Glo1 knockout mouse and C57BL/6J wild-type control mice with STZ-induced diabetes would be studied. STZ-induced diabetes, a model of type 1 diabetes, does not consistently show albuminuria nor severe glomerular mesangial expansion in C57BL/6J mice (Qi et al., 2005, Nakagawa et al., 2007). In addition, increased renal MG-modified mitochondrial proteins is expected to induce oxidative stress and metabolic dysfunction and accelerate DN (Rosca et al., 2005).

However, the aim was redeveloped to characterise the Lexicon Glo1 mutant mouse after completion of the first objective where a compensatory mechanism of Glo1 expression in the Lexicon Glo1 mutant mouse was discovered. For this reason, proceeding with the previous aim was re-evaluated as both genotypes including Lexicon Glo1 mutant mouse and WT controls have a similar phenotype which negated the use of Lexicon Glo1 mutant mouse as a Glo1 deficient mouse and a model of accelerated diabetic complication. In addition, it is interesting and likely fruitful to further investigate the potential genetic causes behind the phenotype of Lexicon Glo1 mutant mouse. This includes examining the mechanism of escape from Glo1 silencing and assessing if such mechanisms are active elsewhere – particularly clinically. Therefore, the hypothesis of this study was redeveloped to be:

Gene trapping of Glo1 in ESCs leads to compensatory expression of Glo1 to counter dicarbonyl stress by a mechanism which may operate in other circumstances of dicarbonyl stress. The aim of this study is to test this hypothesis by characterising the mechanism of compensatory expression of Glo1 in the Lexicon mutant mouse, modelling similar induction of Glo1 expression in experimental dicarbonyl stress in murine ESCs *in vitro* and exploring if a similar response occurs in clinical dicarbonyl stress *in vivo*.

Initial examination characterised compensatory expression of Glo1 in all tissues tested of the Lexicon Glo1 mutant mouse. In this project, I attempted to understand how gene targeting of *Glo1* can produce precise compensatory expression of Glo1.

There is a requirement still for the field of glyoxalase research to produce a stable Glo1 deficient mouse where Glo1 deficiency is produced in maturity onset – see Conclusions. My findings indicate that the commissioned requirement of Lexicon to produce a Glo1 deficient mouse was not fulfilled.

4.2. Lexicon Glyoxalase 1 mutant mouse

4.2.1. Genotyping and evidence for Glo1 copy number alteration induced by gene trapping

The evaluation and characterization of Lexicon Glo1 mutant mouse was expected to show ablation of Glo1 expression and, as a consequence, increased tissue concentrations of MG and MG-modified proteins (Thornalley et al., 1989). Initially, Lexicon Glo1 mutant mouse colony was analysed for the inserted mutation. The mutation was successfully inserted in the *Glo1* gene and the mutation was detected in mutant mice. Initial genotyping showed that of 44 offspring from Lexicon Glo1 mutant mice colony, there was no off-spring with mutated *Glo1* allele only, 79.5% had both mutant and wild-type alleles and 20.5% contained wild-type alleles only. Assuming this initial genotyping reflected homozygotes, heterozygotes and wild-type offspring, respectively, this represented a significant disturbance from the Hardy Weinberg distribution. This would be consistent with embryonic lethality of homozygous inheritance of the *Glo1* mutant allele. It seemed appropriate as lack of Glo1 or inhibition of Glo1 impairs cell survival and induces apoptosis (Morcos et al.,

2008, Lo and Thornalley, 1992). A similar finding was noted in human subjects where the null mutation of *GLO1* is embryonically lethal (Arai et al., 2010).

In breeding of the Lexicon *Glo1* mutant mice there was, however, no indication of decreased litter size – suggesting that the assumed embryonic lethality of putative homozygous *Glo1* mutant mice may not be correct. It was also noted that Lexicon claimed to have produced viable homozygous *Glo1* mutant mice with normal phenotype (Lexicon, 2007). This was, however, based on inappropriate genotyping – assessing genotype by measurement of *Glo1* mRNA only.

In the studies herein, expression of *Glo1* mRNA, protein and activity in several tissues was not significantly different between groups containing the mutant allele and wild-type controls. This suggested that compensatory *Glo1* regulation was not at the level of increased *Glo1* protein stability or increased *Glo1* mRNA translation but rather at the level of *Glo1* gene transcription. Some gene expression compensatory mechanisms in mutant mice are at translational level: for example, in heterozygous knockout of cardiac troponin T (Ahmad et al., 2008) and kidney-specific NaK2Cl cotransporter, BSC1/NKCC2 (Takahashi et al., 2002). The compensatory mechanism to maintain normal expression on Lexicon mutant mice however is at the transcriptional level and may occur through change in *Glo1* copy number.

I established qPCR Taqman methods to quantify copies of both the *Glo1* wild-type and mutant alleles. This revealed that Lexicon mutant mice has increased copy number of total *Glo1* alleles and the “heterozygotes” were of two types: one with one copy of the mutant *Glo1* allele and one with two copies of the mutant allele. Appropriate genotypic nomenclature was therefore *Glo1*^{Gt(OSTGST_4497-D9)1Lex} and *Glo1*^{Gt(OSTGST_4497-D9)2Lex}, respectively. All offspring had two copies of the wild-type *Glo1* allele, explaining the normal, wild-type expression of *Glo1* in all tissues. This explains the compensatory mechanism of *Glo1* expression in Lexicon *Glo1* mutant mice and the absence of any differences between *Glo1* expressions in both groups. The lack of pathogenic phenotype in the Lexicon characterisation studies is explained by the apparent heterozygotes and homozygotes having the normal 2 wild-type copies of the *Glo1* allele. The unusual genotyping by Lexicon by measurement mRNA appears to have been unreliable and the additional copy number of the wild-type allele was not detected by Lexicon.

The *Glo1* copy number was analysed in several tissues and all analysed tissues showed three copies in *Glo1*^{Gt(OSTGST_4497-D9)1Lex} and two copies in WTs. This indicates that the origin of the extra *Glo1* copy is the mouse ESC where the mutation was induced by insertion of vector VECTOR48. The replication of wild-type *Glo1* in the ESC mutated by gene trapping provided the founder of this colony. The produced *Glo1*^{Gt(OSTGST_4497-D9)1Lex} mice was maintained through breeding and crossing with wild-type controls in the Lexicon mutant mouse colony. This was confirmed by the stability of the mutation and the mode of the inheritance in this colony. It is possible that there were *Glo1* gene duplication prior to the induction of the VECTOR48, however, according to (Williams et al., 2009, Liang et al., 2008, Bryk and Tautz, 2014) *Glo1* duplication presents in multiple strains of mice such as A/J, DBA/2J and in ESCs of 129/C57 strain but not in C57Bl/6 strain which is the background of the Lexicon *Glo1* mutant mouse. This might exclude the possibility of the presence of the duplication prior to the VECTOR48 induction.

There remains a minor possibility of *de novo Glo1* duplication. It has been suggested that *de novo* germ-line CNVs can occur within mouse strains, leading to inter-individual variation (Liang et al., 2008). The analyses of the genome of clonal isolates of mouse ESCs derived from common parental lines revealed that there are extensive and recurrent CNVs. This variation arises during mitosis and can be co-transmitted into the mouse germ line along with engineered alleles, contributing to genetic variability. The frequency and extent of these genomic changes in ESCs suggests that all somatic tissues in individuals will be mosaics composed of variants of the zygotic genome. CNV of *Glo1* has not been found, however, in ESCs in culture but rather only associated with strain-specific *Glo1* duplication (Liang et al., 2008). The stability of the mutation in *Glo1*^{Gt(OSTGST_4497-D9)1Lex} during the mutation inheritance as well as the presence of constant number of *Glo1* copies in all analysed tissues, the absence of *Glo1* copy number increase in the C56BL/6 strain and ESC cultures suggest that *Glo1* copy number increase was not present before mutation and was likely induced as copy number alteration in response to dicarbonyl stress induced by *Glo1* mutation.

The inheritance of *Glo1* mutation showed that it is inherited in a simple Mendelian manner. In the inheritance study, each parent passes one allele in chromosome 17 to the offspring. In the cases of *Glo1*^{Gt(OSTGST_4497-D9)1Lex} parent, some offspring have the parental WTs chromosome and the remainder have the

parental mutated chromosome. This produces WT ($Glo1^{Gt(OSTGST_4497-D9)0Lex}$) and mutant ($Glo1^{Gt(OSTGST_4497-D9)1Lex}$) offspring, respectively. However, when two $Glo1^{Gt(OSTGST_4497-D9)1Lex}$ were crossed, a new genotype, $Glo1^{Gt(OSTGST_4497-D9)2Lex}$, was produced. This new genotype has the mutant chromosome 17 from each heterozygote parent. The activity and the expression of *Glo1* in this new genotype were similar to heterozygote and WT's siblings. In addition, there was no significant difference in all *Glo1* analytes in these three genotypes. This confirms that glyoxalase system performs with same efficiency in all genotypes analysed. This likely explains how Lexicon were able to report “heterozygote” and “homozygote” mutant mice with a normal healthy phenotypes.

Taqman copy number assay was the main analytical method used in the CNV quantification in this study. This assay produced an accurate and precise quantification. The used of controls including liver DNA from C57BL/6 and DBA/1J strains proved the accuracy and the specificity of this assay. C57BL/6 and DBA/1J have 2 and 4 copies of *Glo1* respectively (Williams et al., 2009). DNA from liver of each strain was used as negative and positive control for *Glo1* duplication. In addition, the PCR reaction of Taqman copy number assay is a duplex reaction where the signal strength of the target compared to the signal strength of the of the internal standard (Ponchel et al., 2003). In order to evaluate the efficiency and the accuracy of this duplex assay, *Tfrc* and *Tert* genes were used as internal standard. *Tfrc* and *Tert* genes are located on chromosome 16 and 13 respectively. These reference genes are located on other chromosomes not chromosome 17 where *Glo1* is located. This was to avoid using reference gene located in the duplication area, which will give a false negative result. However, no other locus specific quantification has been used as this Taqman copy number assay produced accurate, precise and constant results with all used controls and internal controls. Furthermore, this assay is a locus specific assay which does not show the extent of the duplication. I studied this by genome-wide microarray analysis.

Microarray aCGH is the ideal assay for genome-wide scale identification. aCGH quantifies the CNV with extent of any duplication as well as provides information about any other duplication in the analysed genome (Carter, 2007). The quantification of *Glo1* copy number in the liver samples from the new genotype ($Glo1^{Gt(OSTGST_4497-D9)2Lex}$), $Glo1^{Gt(OSTGST_4497-D9)1Lex}$ and WT siblings using aCGH produced a similar quantification of *Glo1* copy number as indicated in the Taqman

assay. This provides a supporting evidence for *Glo1* copy number increase in the Lexicon mutant mice. In addition, the duplication of *Glo1* in all analysed samples was 473 kbp and included a partial duplication of *Btbd9* and *Glp1r* genes and complete duplication of *Glo1* and *Dnahc8* genes. This duplication is similar to the duplication reported in Fkbp5 knockout mice which carries a gene duplication of *Glo1* with similar break point of the *Glo1* duplication in Lexicon *Glo1* mutant mice (Kollmannsberger et al., 2013). In addition, the *Glo1* duplication of Lexicon *Glo1* mutant mice has a similar break point as the break points of *Glo1* duplication which was detected in 23 strains out of 71 inbred strains tested of various outbred and wild-caught mice (Williams et al., 2009). Furthermore, the genome-wide CNV analyses in individuals from two recently diverged natural populations of the house mouse showed a 0.5 Mb amplification that includes *Btbd9*, *Glo1* and *Dnahc8* which is similar to the duplication in Lexicon *Glo1* mutant mouse (Bryk and Tautz, 2014). This break point in mouse appears to be a hotspot for breakage and for copy number.

Microarray aCGH data genome showed random amplifications in different areas which are not linked to *Glo1* mutation genotype. However, in addition to *Glo1* duplication there were two genes duplicated only in *Glo1*^{Gt(OSTGST_4497-D9)1Lex} and *Glo1*^{Gt(OSTGST_4497-D9)2Lex} mice. These two genes are *Vmn2r111*, *Vmn2r112*. This duplication is in chromosome 17 from base number 22673192 to 22797105. This duplication might have arisen as a response for the deletion in a nearby gene, which is due to “flanking allele problem” which is a likely common phenomenon in gene knockout via homologous recombination (Crusio et al., 2009). By linking the duplication to the gene expression, it was expected to find an increased mRNA expression produced from the duplicated genes. However, the analyses of the mRNA expression for *Btbd9*, *Dnahc8* and *Vmn2r112* showed different panel of expression in each genotype. It was expected that this amplification results in a corresponding change in gene expression. In humans and mice, 85%–95% of CNVs are associated with changes in expression of the affected genes – reviewed by (Tang and Amon, 2013). However, this different panel of expression is likely due to incomplete duplication in the case of *Btbd9* and might be explained by the fact that the engineered CNV or mutation of single genes has previously been found to induce CNV of unrelated genes and mutations in secondary effect genes leading to impaired expression (Teng et al., 2013). This impaired mRNA expression is clearly demonstrated in the mRNA expression results.

It has been suggested that mutation of any single gene may cause a genomic imbalance, with consequences sufficient to drive adaptive genetic changes. This is a logical consequence of losing a functional unit originally acquired under pressure during evolution (Szamecz et al., 2014). Szamecz and colleagues showed that baker's yeast genome was able to compensate the complete loss of genes during evolution by 68% of the total 180 haploid baker's yeast genotypes. In addition, 68% of the genotypes reached near wild-type fitness through accumulation of adaptive mutations elsewhere in the genome (Szamecz et al., 2014). A similar acute adaptation to fitness or survival in ESCs when exposed to gene trapping of *Glo1* may explain the induction of the extra WT copy of *Glo1* in the Lexicon Glo1 mutant mouse. Furthermore, most gene knockout in yeast strains were found to have one additional mutant gene and independent knockouts of the same gene often evolved mutations in the same secondary gene (Teng et al., 2013). In mouse, knockout of an essential gene such as *CALBINDIN-D9K* and *LRP1b* was compensated with the expression of other genes from same family but may be with different splicing (Marschang et al., 2004, Lee et al., 2007). This might be not applicable in our case as the aCGH microarray result confirms the duplication of *Glo1* gene. In addition, the data obtained from Glo1-Vic Taqman assay confirmed that there are two WT copies of *Glo1* in all analysed genotypes.

4.2.2. Glyoxalase pathway metabolism - evidence for normal homeostasis

To complete the characterization of Lexicon Glo1 mutant mice, other components of glyoxalase system - MG, Glo2 activity and D-lactate production - were analysed. There was no significant difference noticed in any analyte between mutants and wild-type controls. A deficiency of Glo1 is expected to increase MG concentration and related MG-derived AGEs (McLellan and Thornalley, 1989, Dunn et al., 1989, Dunn et al., 1991, Haik Jr et al., 1994, Ahmed et al., 1997, Sharma-Luthra and Kale, 1994). Glycation and oxidation adducts were analysed in liver tissue and urine of Lexicon Glo1 mutant mice and WTs siblings. There was no significant difference in AGEs directly related to the glyoxalase system. This provides evidence that the glyoxalase system in both groups was performing with normal efficiency and normal dicarbonyl metabolism was maintained.

There are several pathways for the detoxification of MG, based on different enzymes that are able to convert MG to less toxic compounds. Methylglyoxal reductase is the second MG detoxifier after glyoxalase enzymes (Rabbani and Thornalley, 2012b). Methylglyoxal reductase activity was analysed in the liver tissue of Lexicon Glo1 mutant mice and their WT's siblings and no significant differences were found. This suggests no compensatory increased in activity of other MG metabolising enzymes were induced by Glo1 mutation – and indeed none was required as the wild-type *Glo1* copy number had been maintained in *Glo1*^{Gt(OSTGST_4497-D9)2Lex} and *Glo1*^{Gt(OSTGST_4497-D9)1Lex} mutant mice.

4.2.3. Glo1 activity – effect of ageing

The Glo1 activity for brain, skeletal muscle, spleen, heart, kidney, pancreas and liver of Lexicon Glo1 mutant mice at two time points (3 and 7 months) showed that Glo1 activity was not decreased with age in the heterozygote and wild type mice tissues except in the kidney tissue. In rats kidney, Glo1 activity of renal cortex lysate decreased in an age-dependent manner (Ikeda et al., 2011). On the other hand, the Glo1 activity increases with age in skeletal muscle, brain and liver when compare between three and seven month old mice. This changes match with the Glo1 activity changes which has been published by (Sharma-Luthra and Kale, 1994). Sharma-Luthra and Kale showed the range of Glo1 activity in multiple tissues from 2 months to 24 months where the activity of the liver increases up to 12 months of age and then it starts to decline.

At both time points of age used in this study, Glo1 activity was highest in liver and lowest in spleen and pancreas. The high Glo1 activity in liver comparing to the other tissues has been published previously by (Bierhaus et al., 2012). The Glo1 activity of the heterozygote does not defer significantly from wild-type Glo1 activity. Interestingly, Glo1 activity was lower in the WT's control strain maintained at University of Warwick (C57BL/6-UoW) when compared with WT's siblings of Glo1 mutant mice. Although, both mice groups are C57BL/6 strain, the origin and the environmental factor might have an effect (Williams et al., 2009). Importantly, Glo1 mutant mice have distribution in their genome due to the inserted vector which might have an influence on Glo1 expression and activity.

4.3. Glyoxalase 1 copy number alteration in mouse embryonic stem cells

Mouse ESCs are key tools for genetic engineering. These cells were employed in this project to understand the ability to induce *Glo1* copy number in relation to increased dicarbonyl stress. There are extensive and recurrent CNVs in ESCs (Liang et al., 2008). This variation arises during mitosis and can be co-transmitted into the mouse germ line contributing to genetic variability. The frequency and extent of these genomic changes in ESCs suggests that all somatic tissues in individuals will be mosaics composed of variants of the zygotic genome (Liang et al., 2008). However, In Lexicon *Glo1* mutant mouse, the increased *Glo1* copy number was distributed equally in all analysed tissues not mosaic and hence the extra *Glo1* copy was created more likely before the differentiation of the ESCs. Therefore, the cells were maintained under undifferentiated status by using LIF (Williams et al., 1988). It is important to start with characterisation of the metabolism and glyoxalase system under normal culturing condition and under 3% oxygen atmosphere condition. Culture of ESCs under a 3% oxygen atmosphere was important for relevance to physiologic oxygen concentration of embryonic development which takes place in a low oxygen concentration environment (Powers et al., 2008). The oxygen environment of ESCs *in vivo* is much lower and with a pO₂ of approximately 3% (Simon and Keith, 2008). The environmental pO₂ regulates energy metabolism and is intrinsic to the self-renewal of ESCs (Mohyeldin et al., 2010, Forristal et al., 2013).

ESCs were maintained in undifferentiated status using LIF and this was confirmed by determination of the ESCs markers (Williams et al., 1988). The proliferation of the cells was decreased *ca.* 3 fold in 3% oxygen atmosphere. In addition, culture under 3% oxygen atmosphere decreased *Glo1* activity and expression. This may be due to the presence of the HRE which is known to down regulate the expression of *Glo1* under hypoxic conditions (Zhang et al., 2012). However, there was an increase in the production of D-lactate and L-lactate, and D-glucose consumption. The increased production of L-lactate and consumption of D-glucose under 3% oxygen atmosphere in murine ESCs was reported previously by (Katsuda et al., 2013). This suggests that ESCs under 3% oxygen atmosphere depend more on anaerobic glycolysis compared to the cells under normoxia. It has been

published that under 3% oxygen atmosphere, stem cells have enhanced conversion of pyruvate to lactate by cytosolic NADH. The 3% oxygen atmosphere environment renders them dependent upon anaerobic glycolysis to produce ATP. The metabolic adaptation of stem cells from an oxidative phenotype to one dependent upon glycolytic metabolism represents specific advantages that promote stem cell homeostasis. Stem cells remain metabolically flexible, however, where they are able to rapidly change to an oxidative phenotype during differentiation to support the large amounts of ATP needed for this process (Ochocki and Simon, 2013). ESCs are more metabolically active under 3% oxygen atmosphere as the glucose consumption and L-lactate production was *ca.* 3.1 fold higher than the glucose consumption and L-lactate production in normoxia. The decreased *Glo1* expression and activity under 3% oxygen atmosphere with high metabolic activity is expected to increase AGE formation. This suggests that adverse effects of MG are more likely to be present under 3% oxygen atmosphere – and indeed, these are the lower range of usual oxygen concentration for ESCs *in vivo* (Powers et al., 2008).

The proliferation of ESCs was decreased by treatment with *Glo1* cell permeable inhibitor BrBzGSHCp₂. This cytotoxicity effect was reported using other cells as some tumour sensitive to BrBzGSHCp₂ (Thornalley et al., 1996, Sakamoto et al., 2000, Sakamoto et al., 2001). Although the *Glo1* inhibitor decreased the proliferation of ESCs *in vitro*, when the ESCs were treated with BrBzGSHCp₂ for three days there was no effect on the *Glo1* copy number. This may be due to the short incubation period which not has been long enough to increase *Glo1* copy number.

To examine the direct effect of dicarbonyl stress on *Glo1* copy number, a non-toxic but growth inhibitory concentration of exogenous MG was applied to ESCs for 2 days. The median growth inhibitor concentration of MG for ESCs in normoxia was 831 μM which is relatively high (*cf.* 238 μM for human leukaemia 60 cells (Kang et al., 1996)). ESCs growth was decreased by 27% with addition of 200 μM MG. A concentration of MG markedly higher than those in the physiological systems - human blood plasma, 100–120 nM, and cellular concentrations of 1–5 μM – was used (Dobler et al., 2006, Rabbani and Thornalley, 2014c, Kurz et al., 2011). Nevertheless, it was non-toxic and designed to impose dicarbonyl stress and test the hypothesis that such conditions induce *Glo1* copy number increase. Although the mRNA of *Glo1* was not significantly increased at any time point, there was a

significant increase in *Glo1* copy number by 16% at 12 days. In addition, there was a significant increase in Glo1 activity and protein expression in 12 days of treatment. In addition, the increased Glo1 protein expression in ESCs treated with 200 μ M MG over 12 days led to increased Glo1 activity in these cells. On the other hand, the decreased Glo1 protein expression in ESCs treated with 200 μ M MG over 3 and 6 led to decreased Glo1 activity. Although, there was an increased trend of Glo1 protein expression with time of treatment, Glo1 activity had a decreased trend of Glo1 activity with time of treatment, which might be due to inactivation of Glo1 protein with unknown mechanism. This induction indicates that *Glo1* copy number alteration may be induced modestly by dicarbonyl stress in ESCs. Unchanged *Glo1* mRNA expression might be due to the short life of *Glo1* mRNA in the cells or modification by MG and impaired detection (Schwanhäusser et al., 2011). The specificity of this induction was proven by the analyses of the copy number of the surrounding gene and finding that there was no significant increase of the copy number in of the surrounding gene in both sides.

Stress induced CNA to date has mainly be linked to replicative stress. This induces a high frequency of CNVs in normal human cells that resemble non recurrent CNVs in humans in all aspects. These agents include the polymerase inhibitor aphidicolin, the ribonucleotide reductase inhibitor and hydroxyurea which are commonly used in the treatment of sickle cell disease and other disorders. Such data provides an experimental support evidence for replication error models for the origins of CNVs (Arlt et al., 2012). The type of stress induced by these agents is similar to the stress induced by MG as both cause DNA breakage and hence increased errors in DNA replication (Kang, 2003). However, this is the first report of stress induced functional copy number increase of *Glo1* gene. Moreover, unlike features of replicative stress and irradiation induced stress, dicarbonyl stress linked CNA appears localised to the *Glo1* gene and not spread widely across the genome. Short periods of dicarbonyl stress, for example – one day, did not increase *Glo1* copy number. This suggests that the process of the *Glo1* copy number induction is not an acute response to high levels of MG but may be a response to high MG exposure during multiple consecutive cell growth cycles.

CNA may have effects on ESC function. In future studies stability of MG-induced CNA will be important to investigate further. It has long been known that changes in the copy number of specific genes can have a dramatic impact on

organismal and cellular fitness. For example, budding yeast cells harbouring an extra copy of the β -tubulin-encoding gene are inviable. Studies in humans suggest that as many as 15% of neurodevelopmental disorders and other diseases are due to rare, large CNVs resulting in the imbalance of a handful of genes. For example, duplication of *PMP22* leads to Charcot-Marie-Tooth 1A neuropathy. Duplication of *SNCA* is associated with Parkinson's disease, duplication of *GSK3b* with bipolar disorder, and low-copy amplification of the *C4* gene with lupus. Finally, amplifications and deletions of individual genes are major drivers of tumorigenesis. Amplification of the oncogene *MYC*, for example, is thought to be a driving factor in human acute myeloid leukaemia - reviewed by (Tang and Amon, 2013).

The treatment of ESCs with 200 μ M MG under 3% oxygen atmosphere showed decreased *Glo1* copy number within three days when compared to the cells grown under 3% oxygen atmosphere without treatment. This may indicate that these cells have lower ability to repair DNA breakage induced by MG under 3% oxygen atmosphere conditions and/or the continuous exposure to increased endogenous MG formation and decreased metabolism by *Glo1* are conditions required to most effectively increase *Glo1* copy number by CNA. Cells exposed to high MG concentration may be less able to repair the DNA breakage (Kang, 2003).

Knockdown of *Glo1* by ON-TARGET plus *Glo1* siRNA provided evidence that the ESCs can survive with *ca.* 13% of normal *Glo1* protein expression and activity. The specificity of the knockdown was proven by the use of ON-TARGET plus non-targeting pool siRNA as a control where no decrease of *Glo1* mRNA noticed. However, the treatment with lower concentration of MG, comparing to the previous experiments, had a strong effect on the proliferation of the cells. In low oxygen atmosphere or physiological condition, low *Glo1* expression and activity has been found (Zhang et al., 2012). This makes the cells more sensitive to increased MG comparing to the cells in normal cell culture condition.

4.4. Other studies of glyoxalase 1 copy number alteration

HL60 human leukaemia cells were used as another cells to examine the stress ability to induce *GLO1* copy number. The proliferation of the cells was strongly affected by MG treatment. Interestingly, the copy number of *GLO1* was decreased. This may be due to the decreased ability to repair DNA breakage in these cancerous

cells (Farzanch et al., 1987, Kang, 2003). This may suggest that ESCs have a higher ability to repair DNA breakage than HL60 cells. Also it may also contribute to the anti-proliferative effect of MG on HL60 cells *in vitro*.

Clinical translational study was performed to provide further evidence that the induction of *Glo1* copy number in the previous models was due to the increased concentration of MG. *GLO1* copy number was determined in peripheral blood leukocytes of patients with stage 5 chronic kidney disease on HD – patients suffering the most clinically severe dicarbonyl stress and increased MG exposure (Agalou et al., 2005, Rabbani and Thornalley, 2012b, Rabbani and Thornalley, 2012a) and normal healthy controls. This analysis showed that there was no significant difference between this patients and control subjects. This may be due to the small size of the sample (20 patients and 20 controls) and/or it might be due to the sample type as the leukocytes in general have a shorter lifespan than many other cells.

Strengths of this study can be summarised by in-depth characterization of glyoxalase system of Lexicon *Glo1* mutant mouse and explanation of the change of *Glo1* expression in this mouse. Also, it successfully characterised the compensatory mechanism of *Glo1* expression in the Lexicon *Glo1* mutant mouse, characterization of glyoxalase system in mouse ESCs under 20% and 3% oxygen atmosphere condition and induction of *Glo1* copy number under methylglyoxal stress. Weaknesses of this study were: not addressing the mechanism of the CNV in Lexicon *Glo1* mutant mouse as this needs further support from Lexicon by providing the original stem cells which were used for *Glo1* knockout. Although, mimicking the CNA was not up to the level determined in Lexicon *Glo1* mutant mouse, this is a novel example of stress induction of functional copy number specifically for *Glo1* gene.

5. Conclusion and Further work

5.1. Conclusion

The initial aim of this study was to study the exacerbation of diabetic nephropathy by Glo1 deficiency in streptozotocin-induced diabetic mice, with an initial objective to confirm Glo1 deficiency in the IMKC Glo1 mutant mouse and subsequent objectives contingent on this. Initial studies were unable to confirm Glo1 deficiency in this mouse model and so a revised aim was to characterise the mechanism of compensatory Glo1 expression in the mutant mouse and explore similar occurrence in similar precursor mouse ESCs and related clinical application. Therefore, this PhD project is comprised of four parts:

1. To evaluate the Lexicon Glo1 mutant mouse as Glo1 deficient mouse and the possibility of using this mouse to improve the understanding of the role of Glo1 in the development of diabetic nephropathy.
2. To characterise the compensatory mechanism of Glo1 expression in the Lexicon Glo1 mutant mouse.
3. To study the copy number alteration of *Glo1* in mouse embryonic stem cells.
4. To study the copy number alteration of *GLO1* in clinical samples.

The effect of gene trapping in the Lexicon Glo1 mutant mouse was evaluated. The mutation was successfully inserted to *Glo1* gene. However, related CNA of *Glo1* maintained the normal 2 wild-type copies of the *Glo1* gene in all offspring and a normal phenotype throughout. This indicates that the mutant mouse appears to have a compensatory mechanism of Glo1 expression in the Lexicon Glo1 mutant mouse and have been incorrectly genotyped in preliminary characterisation by the originator. Therefore, the normal phenotype of the Lexicon Glo1 mutant mouse limits the benefits of using this mouse as a Glo1 deficient mouse and a model of accelerated diabetic complication. Nevertheless, this phenotype directs the study to further investigate the potential genetic causes behind the phenotype of Lexicon Glo1 mutant mouse, also, applying these genetic causes in wider contexts.

The characterization of gene duplication in Lexicon Glo1 mutant mice confirms that the *Glo1* locus with the reported break points are hotspots for DNA breakage and CNA as same duplicated locus has been reported previously by

multiple research groups. In this duplication, *Glo1* was the main gene that produced increased protein expression. There was also increased expression of Dnahc8 in the *Glo1*^{Gt(OSTGST_4497-D9)1Lex} genotype. Thus indicating importance of maintaining the expression of *Glo1* to wild-type levels.

Murine ESC studies suggest that exposure to dicarbonyl stress may induce CNA of *Glo1* and thereby provide a precedent for the proposal that increased dicarbonyl stress by mutation of *Glo1* in mice produced *Glo1* CNA in the Lexicon *Glo1* mutant mouse. However, further investigation is required to confirm the mechanism of *Glo1* CNA in Lexicon *Glo1* mutant mice.

Finally, clinical translational study was performed to provide further evidence that the induction of *Glo1* copy number in the previous models was due to the increased concentration of MG. This study of *GLO1* copy number in peripheral blood leukocytes of patients with ESRD was performed but did not show a significant change comparing with control subject. This requires further investigation with bigger sample size and may be with other type of tissue.

5.2. Further work

In this project, characterization Lexicon *Glo1* mutant mouse confirmed that the method used to knockout *Glo1* was not successful. It is attractive to investigate the mechanism of *Glo1* copy induction using similar methods and cells with analysis of the *Glo1* copy number after the vector insertion. For *Glo1* knockout, other methods might be more successful such as inducible gene deletion by Cre-lox system, which provides tissue specific inducible knockout, avoids developmental effects and bypasses embryonic lethality of some gene deletions.

The reported finding in the murine ESC studies is a novel example of stress induction of functional copy number specifically for *Glo1* gene in ESCs which was investigated under undifferentiated status of ESCs. This was done to mimic the increase *Glo1* copy number in Lexicon *Glo1* mutant mouse. It is likely to have different result with using the same model but in differentiated state.

MG-induced CNA of *Glo1* is an important phenomenon to be addressed, which might be involved in induction of *GLO1* copy number due to increased MG concentration causing multidrug resistance in cancer chemotherapy as well as the resistance of bacteria to antibiotics.

Finally, my studies open the possibility that different types of metabolic stress may produce CNA and, for the first time, GLO1 may contribute to adaptive genomics effects in mammalian organisms.

6. Bibliography

- ABORDO, E. A., MINHAS, H. S. & THORNALLEY, P. J. 1999. Accumulation of α -oxoaldehydes during oxidative stress: a role in cytotoxicity. *Biochemical pharmacology*, 58, 641-648.
- AGALOU, S., AHMED, N., BABAEI-JADIDI, R., DAWNAY, A. & THORNALLEY, P. J. 2005. Profound mishandling of protein glycation degradation products in uremia and dialysis. *Journal of the American Society of Nephrology*, 16, 1471-1485.
- AGALOU, S., KARACHALIAS, N., THORNALLEY, P. J., TUCKER, B. & DAWNAY, A. B. Estimation of α -oxoaldehydes formed from the degradation of glycolytic intermediates and glucose fragmentation in blood plasma of human subjects with uraemia. International Congress Series, 2002. Elsevier, 181-182.
- AHMAD, F., BANERJEE, S. K., LAGE, M. L., HUANG, X. N., SMITH, S. H., SABA, S., RAGER, J., CONNER, D. A., JANCZEWSKI, A. M. & TOBITA, K. 2008. The role of cardiac troponin T quantity and function in cardiac development and dilated cardiomyopathy. *PLoS One*, 3, e2642.
- AHMED, M., BRINKMANN, F. E., DEGENHARDT, T., THORPE, S. & BAYNES, J. 1997. N ϵ -(Carboxyethyl) lysine, a product of the chemical modification of proteins by methylglyoxal, increases with age in human lens proteins. *Biochem. J*, 324, 565-570.
- AHMED, N., ARGIROV, O., MINHAS, H., CORDEIRO, C. & THORNALLEY, P. 2002. Assay of advanced glycation endproducts (AGEs): surveying AGEs by chromatographic assay with derivatization by 6-aminoquinolyl-N-hydroxysuccinimidyl-carbamate and application to N ϵ -carboxymethyl-lysine-and N ϵ -(1-carboxyethyl) lysine-modified albumin. *Biochem. J*, 364, 1-14.
- AHMED, N., BABAEI-JADIDI, R., HOWELL, S., BEISSWENGER, P. & THORNALLEY, P. 2005a. Degradation products of proteins damaged by glycation, oxidation and nitration in clinical type 1 diabetes. *Diabetologia*, 48, 1590-1603.
- AHMED, N., BABAEI-JADIDI, R., HOWELL, S. K., THORNALLEY, P. J. & BEISSWENGER, P. J. 2005b. Glycated and oxidized protein degradation products are indicators of fasting and postprandial hyperglycemia in diabetes. *Diabetes Care*, 28, 2465-2471.
- AHMED, N., DOBLER, D., DEAN, M. & THORNALLEY, P. J. 2005c. Peptide mapping identifies hotspot site of modification in human serum albumin by methylglyoxal involved in ligand binding and esterase activity. *J Biol Chem*, 280, 5724-32.
- AHMED, N. & THORNALLEY, P. J. 2007. Advanced glycation endproducts: what is their relevance to diabetic complications? *Diabetes Obes Metab*, 9, 233-45.

- AHMED, N., THORNALLEY, P. J., DAWCZYNSKI, J., FRANKE, S., STROBEL, J., STEIN, G. & HAIK, G. M. 2003. Methylglyoxal-derived hydroimidazolone advanced glycation end-products of human lens proteins. *Investigative ophthalmology & visual science*, 44, 5287-5292.
- AHMED, U., DOBLER, D., LARKIN, S. J., RABBANI, N. & THORNALLEY, P. J. 2008. Reversal of Hyperglycemia-Induced Angiogenesis Deficit of Human Endothelial Cells by Overexpression of Glyoxalase 1 In Vitro. *Annals of the New York Academy of Sciences*, 1126, 262-264.
- AHMED, U., THORNALLEY, P. J. & RABBANI, N. 2014. Possible role of methylglyoxal and glyoxalase in arthritis. *Biochemical Society transactions*, 42, 538-542.
- AITMAN, T. J., DONG, R., VYSE, T. J., NORSWORTHY, P. J., JOHNSON, M. D., SMITH, J., MANGION, J., ROBERTON-LOWE, C., MARSHALL, A. J. & PETRETTO, E. 2006. Copy number polymorphism in Fcgr3 predisposes to glomerulonephritis in rats and humans. *Nature*, 439, 851-855.
- ALLEN, R. E., LO, T. W. & THORNALLEY, P. J. 1993. Purification and characterisation of glyoxalase II from human red blood cells. *European Journal of Biochemistry*, 213, 1261-1267.
- AMICARELLI, F., DI ILIO, C., MASCIOTTO, L., BONFIGLI, A., ZARIVI, O., D'ANDREA, M. R., DI GIULIO, C. & MIRANDA, M. 1997. Aging and detoxifying enzymes responses to hypoxic or hyperoxic treatment. *Mechanisms of ageing and development*, 97, 215-226.
- ANTONARAKIS, S. E., KAZAZIAN, H. H., GITSCHIER, J., HUTTER, P., DE MOERLOOSE, P. & MORRIS, M. A. 1995. Molecular etiology of factor VIII deficiency in hemophilia A. *Hum Mutat.*, 5(1):1-22.
- ARAI, M., NIHONMATSU-KIKUCHI, N., ITOKAWA, M., RABBANI, N. & THORNALLEY, P. 2014. Measurement of glyoxalase activities. *Biochemical Society transactions*, 42, 491-494.
- ARAI, M., YUZAWA, H., NOHARA, I., OHNISHI, T., OBATA, N., IWAYAMA, Y., HAGA, S., TOYOTA, T., UJIKE, H. & ARAI, M. 2010. Enhanced carbonyl stress in a subpopulation of schizophrenia. *Archives of general psychiatry*, 67, 589-597.
- ARLT, M. F., MULLE, J. G., SCHAIBLEY, V. M., RAGLAND, R. L., DURKIN, S. G., WARREN, S. T. & GLOVER, T. W. 2009. Replication stress induces genome-wide copy number changes in human cells that resemble polymorphic and pathogenic variants. *The American Journal of Human Genetics*, 84, 339-350.
- ARLT, M. F., RAJENDRAN, S., BIRKELAND, S. R., WILSON, T. E. & GLOVER, T. W. 2014. Copy number variants are produced in response to low-dose ionizing radiation in cultured cells. *Environmental and molecular mutagenesis*, 55, 103-113.
- ARLT, M. F., WILSON, T. E. & GLOVER, T. W. 2012. Replication stress and mechanisms of CNV formation. *Current opinion in genetics & development*, 22, 204-210.
- ARMENGOL, L., VILLATORO, S., GONZÁLEZ, J. R., PANTANO, L., GARCÍA-ARAGONÉS, M., RABIONET, R., CÁCERES, M. & ESTIVILL, X. 2009. Identification of copy number variants defining genomic differences among major human groups. *PloS one*, 4, e7230.
- ATKINS, T. & THORNALLEY, P. 1989. Glyoxalase activity in tissues of lean (HO) and genetically obese diabetic (ob/ob) mice. *Med Sci Res*, 17, 777-8.

- ATKINS, T. & THORNALLY, P. 1989. Erythrocyte glyoxalase activity in genetically obese (ob/ob) and streptozotocin diabetic mice. *Diabetes research (Edinburgh, Scotland)*, 11, 125-129.
- AYOUB, F., ZAMAN, M., THORNALLEY, P. & MASTERS, J. 1992. Glyoxalase activities in human tumour cell lines in vitro. *Anticancer research*, 13, 151-155.
- BABA, S. P., BARSKI, O. A., AHMED, Y., O'TOOLE, T. E., CONKLIN, D. J., BHATNAGAR, A. & SRIVASTAVA, S. 2009. Reductive metabolism of AGE precursors: a metabolic route for preventing AGE accumulation in cardiovascular tissue. *Diabetes*, 58, 2486-2497.
- BABAEI-JADIDI, R., KARACHALIAS, N., KUPICH, C., AHMED, N. & THORNALLEY, P. 2004. High-dose thiamine therapy counters dyslipidaemia in streptozotocin-induced diabetic rats. *Diabetologia*, 47, 2235-2246.
- BAILEY, J. A. & EICHLER, E. E. 2006. Primate segmental duplications: crucibles of evolution, diversity and disease. *Nature Reviews Genetics*, 7, 552-564.
- BARATI, M. T., MERCHANT, M. L., KAIN, A. B., JEVANS, A. W., MCLEISH, K. R. & KLEIN, J. B. 2007. Proteomic analysis defines altered cellular redox pathways and advanced glycation end-product metabolism in glomeruli of db/db diabetic mice. *American Journal of Physiology-Renal Physiology*, 293, F1157-F1165.
- BEISSWENGER, P. J., HOWELL, S. K., NELSON, R. G., MAUER, M. & SZWERGOLD, B. S. 2003. Alpha-oxoaldehyde metabolism and diabetic complications. *Biochem Soc Trans*, 31, 1358-63.
- BEISSWENGER, P. J., HOWELL, S. K., TOUCHETTE, A. D., LAL, S. & SZWERGOLD, B. S. 1999. Metformin reduces systemic methylglyoxal levels in type 2 diabetes. *Diabetes*, 48, 198-202.
- BEJERANO, G., PHEASANT, M., MAKUNIN, I., STEPHEN, S., KENT, W. J., MATTICK, J. S. & HAUSSLER, D. 2004. Ultraconserved elements in the human genome. *Science*, 304, 1321-1325.
- BERNER, A., BROUWERS, O., PRINGLE, R., KLAASSEN, I., COLHOUN, L., MCVICAR, C., BROCKBANK, S., CURRY, J., MIYATA, T. & BROWNLEE, M. 2012. Protection against methylglyoxal-derived AGEs by regulation of glyoxalase 1 prevents retinal neuroglial and vasodegenerative pathology. *Diabetologia*, 55, 845-854.
- BIERHAUS, A., FLEMING, T., STOYANOV, S., LEFFLER, A., BABES, A., NEACSU, C., SAUER, S. K., EBERHARDT, M., SCHNÖLZER, M. & LASITSCHKA, F. 2012. Methylglyoxal modification of Nav1. 8 facilitates nociceptive neuron firing and causes hyperalgesia in diabetic neuropathy. *Nature medicine*, 18, 926-933.
- BIRKENMEIER, G., STEGEMANN, C., HOFFMANN, R., GÜNTHER, R., HUSE, K. & BIRKEMEYER, C. 2010. Posttranslational modification of human glyoxalase 1 indicates redox-dependent regulation. *PLoS One*, 5, e10399.
- BLACKBURN, N. J., VULESEVIC, B., AHMADI, A., MCNEILL, B., MILNE, R. W. & SUURONEN, E. J. 2013. Glyoxalase-1 Over-expression Preserves Cardiac Function Post-MI by Enhancing Vascularity and Reducing AGE Accumulation and Cardiomyocyte Apoptosis. *CIRCULATION*, 128: A14257.

- BONSIGNORE, A., LEONCINI, G., SIRI, A. & RICCI, D. 1972. Kinetic behaviour of glyceraldehyde 3-phosphate conversion into methylglyoxal. *The Italian journal of biochemistry*, 22, 131-140.
- BOOKCHIN, R. M. & GALLOP, P. M. 1968. Structure of hemoglobin A1c: nature of the N-terminal beta chain blocking group. *Biochem Biophys Res Commun*, 32, 86-93.
- BRADFORD, M. M. 1976. A rapid and sensitive method for the quantitation of microgram quantities of protein utilizing the principle of protein-dye binding. *Anal Biochem*, 72, 248-54.
- BRADLEY, A., ANASTASSIADIS, K., AYADI, A., BATTEY, J. F., BELL, C., BIRLING, M.-C., BOTTOMLEY, J., BROWN, S. D., BÜRGER, A. & BULT, C. J. 2012. The mammalian gene function resource: the international knockout mouse consortium. *Mammalian genome*, 23, 580-586.
- BRADLEY, A., HASTY, P., DAVIS, A. & RAMIREZ-SOLIS, R. 1992. Modifying the mouse: design and desire. *Nature Biotechnology*, 10, 534-539.
- BRANDT, R. B., SIEGEL, S. A., WATERS, M. G. & BLOCH, M. H. 1980. Spectrophotometric assay for D-(-)-lactate in plasma. *Analytical biochemistry*, 102, 39-46.
- BRENNDÖRFER, J., ALTMANN, A., WIDNER-ANDRÄ, R., PÜTZ, B., CZAMARA, D., TILCH, E., KAM-THONG, T., WEBER, P., REX-HAFFNER, M. & BETTECKEN, T. 2014. Connecting Anxiety and Genomic Copy Number Variation: A Genome-Wide Analysis in CD-1 Mice. *PloS one*, 10, e0128465-e0128465.
- BREYER, M. D., BÖTTINGER, E., BROSIUS, F. C., COFFMAN, T. M., HARRIS, R. C., HEILIG, C. W. & SHARMA, K. 2005. Mouse models of diabetic nephropathy. *Journal of the American Society of Nephrology*, 16, 27-45.
- BRIDGES, C. B. 1936. The bar" gene" a duplication. *Science*, 83, 210-211.
- BROUWERS, O., NIESSEN, P., HAENEN, G., MIYATA, T., BROWNLEE, M., STEHOUWER, C., DE MEY, J. & SCHALKWIJK, C. 2010. Hyperglycaemia-induced impairment of endothelium-dependent vasorelaxation in rat mesenteric arteries is mediated by intracellular methylglyoxal levels in a pathway dependent on oxidative stress. *Diabetologia*, 53, 989-1000.
- BROUWERS, O., NIESSEN, P. M., FERREIRA, I., MIYATA, T., SCHEFFER, P. G., TEERLINK, T., SCHRAUWEN, P., BROWNLEE, M., STEHOUWER, C. D. & SCHALKWIJK, C. G. 2011. Overexpression of glyoxalase-I reduces hyperglycemia-induced levels of advanced glycation end products and oxidative stress in diabetic rats. *Journal of Biological Chemistry*, 286, 1374-1380.
- BROUWERS, O., NIESSEN, P. M., MIYATA, T., ØSTERGAARD, J. A., FLYVBJERG, A., PEUTZ-KOOTSTRA, C. J., SIEBER, J., MUNDEL, P. H., BROWNLEE, M. & JANSSEN, B. J. 2014. Glyoxalase-1 overexpression reduces endothelial dysfunction and attenuates early renal impairment in a rat model of diabetes. *Diabetologia*, 57, 224-235.
- BROWNLEE, M. 2001. Biochemistry and molecular cell biology of diabetic complications. *Nature*, 414, 813-820.

- BRUDER, C. E., PIOTROWSKI, A., GIJSBERS, A. A., ANDERSSON, R., ERICKSON, S., DE STÅHL, T. D., MENZEL, U., SANDGREN, J., VON TELL, D. & POPLAWSKI, A. 2008. Phenotypically concordant and discordant monozygotic twins display different DNA copy-number-variation profiles. *The American Journal of Human Genetics*, 82, 763-771.
- BRYK, J. & TAUTZ, D. 2014. Copy number variants and selective sweeps in natural populations of the house mouse (*Mus musculus domesticus*). *Evolutionary and Population Genetics*, 5, 153.
- BUZZARD, J. J., GOUGH, N. M., CROOK, J. M. & COLMAN, A. 2004. Karyotype of human ES cells during extended culture. *Nature biotechnology*, 22, 381-382.
- CAHAN, P., LI, Y., IZUMI, M. & GRAUBERT, T. A. 2009. The impact of copy number variation on local gene expression in mouse hematopoietic stem and progenitor cells. *Nat Genet*, 41, 430-7.
- CAMERON, A. D., OLIN, B., RIDDERSTRÖM, M., MANNERVIK, B. & JONES, T. A. 1997. Crystal structure of human glyoxalase I—evidence for gene duplication and 3D domain swapping. *The EMBO journal*, 16, 3386-3395.
- CAMERON, A. D., RIDDERSTRÖM, M., OLIN, B. & MANNERVIK, B. 1999. Crystal structure of human glyoxalase II and its complex with a glutathione thiolester substrate analogue. *Structure*, 7, 1067-1078.
- CARTER, N. P. 2007. Methods and strategies for analyzing copy number variation using DNA microarrays. *Nature genetics*, 39, S16-S21.
- CERADINI, D. J., YAO, D., GROGAN, R. H., CALLAGHAN, M. J., EDELSTEIN, D., BROWNLEE, M. & GURTNER, G. C. 2008. Decreasing intracellular superoxide corrects defective ischemia-induced new vessel formation in diabetic mice. *Journal of Biological Chemistry*, 283, 10930-10938.
- CERAMI, A. 1986. Aging of proteins and nucleic acids: what is the role of glucose? *Trends in Biochemical Sciences*, 11, 311-314.
- CHEN, F., WOLLMER, M. A., HOERNDLI, F., MUNCH, G., KUHLA, B., ROGAEV, E. I., TSOLAKI, M., PAPASSOTIROPOULOS, A. & GOTZ, J. 2004. Role for glyoxalase I in Alzheimer's disease. *Proceedings of the National Academy of Sciences of the United States of America*, 101, 7687-7692.
- CHEN, Y., AHMED, N. & THORNALLEY, P. 2005. Peptide mapping of human hemoglobin modified minimally by methylglyoxal in vitro. *Annals of the New York Academy of Sciences*, 1043, 905-905.
- CHOUDHARY, C., KUMAR, C., GNAD, F., NIELSEN, M. L., REHMAN, M., WALTHER, T. C., OLSEN, J. V. & MANN, M. 2009. Lysine acetylation targets protein complexes and co-regulates major cellular functions. *Science*, 325, 834-840.
- CHOY, K. W., SETLUR, S. R., LEE, C. & LAU, T. K. 2010. The impact of human copy number variation on a new era of genetic testing. *BJOG: An International Journal of Obstetrics & Gynaecology*, 117, 391-398.
- CIAVARDELLI, D., SILVESTRI, E., DEL VISCOVO, A., BOMBA, M., DE GREGORIO, D., MORENO, M., DI ILIO, C., GOGLIA, F., CANZONIERO, L. & SENSI, S. 2010. Alterations of brain and cerebellar proteomes linked to A β and tau pathology in a female triple-transgenic murine model of Alzheimer's disease. *Cell death & disease*, 1, e90.

- CLELLAND, J. D. & THORNALLEY, P. J. 1991. S-2-hydroxyacylglutathione-derivatives: enzymatic preparation, purification and characterisation. *J. Chem. Soc., Perkin Trans. 1*, 3009-3015.
- CLUGSTON, S. L., BARNARD, J. F., KINACH, R., MIEDEMA, D., RUMAN, R., DAUB, E. & HONEK, J. F. 1998. Overproduction and characterization of a dimeric non-zinc glyoxalase I from *Escherichia coli*: evidence for optimal activation by nickel ions. *Biochemistry*, 37, 8754-8763.
- COMBES, P., BONNET-DUPEYRON, M.-N., GAUTHIER-BARICHARD, F., SCHIFFMANN, R., BERTINI, E., RODRIGUEZ, D., ARMOUR, J. A., BOESPFLUG-TANGUY, O. & VAURS-BARRIÈRE, C. 2006. PLP1 and GPM6B intragenic copy number analysis by MAPH in 262 patients with hypomyelinating leukodystrophies: identification of one partial triplication and two partial deletions of PLP1. *Neurogenetics*, 7, 31-37.
- COMPTON, S. J. & JONES, C. G. 1985. Mechanism of dye response and interference in the Bradford protein assay. *Anal Biochem*, 151, 369-74.
- CONBOY, C. M., SPYROU, C., THORNE, N. P., WADE, E. J., BARBOSA-MORAIS, N. L., WILSON, M. D., BHATTACHARJEE, A., YOUNG, R. A., TAVARÉ, S. & LEES, J. A. 2007. Cell cycle genes are the evolutionarily conserved targets of the E2F4 transcription factor. *PLoS One*, 2, e1061.
- CONNOR, H., WOODS, H. & LEDINGHAM, J. 1983. Comparison of the kinetics and utilisation of D (-)-and L (+)-sodium lactate in normal man. *Annals of nutrition and metabolism*, 27, 481-487.
- CONROY, P. J. 1979. Carcinostatic activity of methylglyoxal and related substances in tumour-bearing mice. *Submolecular biology and cancer*, 67, 271-298.
- COOK JR, E. H. & SCHERER, S. W. 2008. Copy-number variations associated with neuropsychiatric conditions. *Nature*, 455, 919-923.
- COPELAND, N. G., JENKINS, N. A. & COURT, D. L. 2001. Recombineering: a powerful new tool for mouse functional genomics. *Nature Reviews Genetics*, 2, 769-779.
- CORDELL, P. A., FUTERS, T. S., GRANT, P. J. & PEASE, R. J. 2004. The human hydroxyacylglutathione hydrolase (HAGH) gene encodes both cytosolic and mitochondrial forms of glyoxalase II. *Journal of Biological Chemistry*, 279, 28653-28661.
- CRUSIO, W., GOLDBOWITZ, D., HOLMES, A. & WOLFER, D. 2009. Standards for the publication of mouse mutant studies. *Genes, Brain and Behavior*, 8, 1-4.
- CZECHANSKI, A., BYERS, C., GREENSTEIN, I., SCHRODE, N., DONAHUE, L. R., HADJANTONAKIS, A.-K. & REINHOLDT, L. G. 2014. Derivation and characterization of mouse embryonic stem cells from permissive and nonpermissive strains. *Nature protocols*, 9, 559-574.
- D'AUTRÉAUX, B. & TOLEDANO, M. B. 2007. ROS as signalling molecules: mechanisms that generate specificity in ROS homeostasis. *Nature Reviews Molecular Cell Biology*, 8, 813-824.
- DAJANI, R., LI, J., WEI, Z., GLESSNER, J. T., CHANG, X., CARDINALE, C. J., PELLEGRINO, R., WANG, T., HAKOOZ, N. & KHADER, Y. 2015. CNV Analysis Associates AKNAD1 with Type-2 Diabetes in Jordan Subpopulations. *Scientific reports*, 5.
- DAKIN, H. & DUDLEY, H. 1913. An enzyme concerned with the formation of hydroxy acids from ketonic aldehydes. *Journal of Biological Chemistry*, 14, 155-157.

- DAWSON, R. M. C., C., E. D., H., E. W. & M., J. K. 1986. Data for biochemical research, *Oxford Science Publications*. p11
- DE HEMPTINNE, V., RONDAS, D., VANDEKERCKHOVE, J. & VANCOMPENOLLE, K. 2007. Tumour necrosis factor induces phosphorylation primarily of the nitric-oxide-responsive form of glyoxalase I. *Biochem. J*, 407, 121-128.
- DE VRESE, M. & BARTH, C. 1991. Postprandial plasma D-lactate concentrations after yogurt ingestion. *Zeitschrift für Ernährungswissenschaft*, 30, 131-137.
- DEL GAUDIO, D., FANG, P., SCAGLIA, F., WARD, P. A., CRAIGEN, W. J., GLAZE, D. G., NEUL, J. L., PATEL, A., LEE, J. A. & IRONS, M. 2006. Increased MECP2 gene copy number as the result of genomic duplication in neurodevelopmentally delayed males. *Genetics in Medicine*, 8, 784-792.
- DINKOVA-KOSTOVA, A. T., TALALAY, P., SHARKEY, J., ZHANG, Y., HOLTZCLAW, W. D., WANG, X. J., DAVID, E., SCHIAVONI, K. H., FINLAYSON, S. & MIERKE, D. F. 2010. An exceptionally potent inducer of cytoprotective enzymes elucidation of the structural features that determine inducer potency and reactivity with Keap1. *Journal of Biological Chemistry*, 285, 33747-33755.
- DISTECHE, C. M. 2006. Dosage compensation of the active X chromosome in mammals. *Nature genetics*, 38, 47-53.
- DISTLER, M. G., PLANT, L. D., SOKOLOFF, G., HAWK, A. J., ANEAS, I., WUENSCHHELL, G. E., TERMINI, J., MEREDITH, S. C., NOBREGA, M. A. & PALMER, A. A. 2012. Glyoxalase 1 increases anxiety by reducing GABAA receptor agonist methylglyoxal. *J Clin Invest*, 122, 2306-15.
- DOBLER, D., AHMED, N., SONG, L., EBOIGBODIN, K. E. & THORNALLEY, P. J. 2006. Increased dicarbonyl metabolism in endothelial cells in hyperglycemia induces anoikis and impairs angiogenesis by RGD and GFOGER motif modification. *Diabetes*, 55, 1961-1969.
- DOBLER, D. P. 2008. *Molecular pathology of glycated extracellular matrix in disease*. PhD, University of Essex.
- DRAGANI, B., COCCO, R., RIDDERSTRÖM, M., STENBERG, G., MANNERVIK, B. & ACETO, A. 1999. Unfolding and refolding of human glyoxalase II and its single-tryptophan mutants. *Journal of molecular biology*, 291, 481-490.
- DU, R., LONG, J., YAO, J., DONG, Y., YANG, X., TANG, S., ZUO, S., HE, Y. & CHEN, X. 2010. Subcellular quantitative proteomics reveals multiple pathway cross-talk that coordinates specific signaling and transcriptional regulation for the early host response to LPS. *Journal of proteome research*, 9, 1805-1821.
- DUNN, J. A., MCCANCE, D. R., THORPE, S. R., LYONS, T. J. & BAYNES, J. W. 1991. Age-dependent accumulation of N. epsilon.-(carboxymethyl) lysine and N. epsilon.-(carboxymethyl) hydroxylysine in human skin collagen. *Biochemistry*, 30, 1205-1210.
- DUNN, J. A., PATRICK, J. S., THORPE, S. R. & BAYNES, J. W. 1989. Oxidation of glycated proteins: age-dependent accumulation of N. epsilon.-(carboxymethyl) lysine in lens proteins. *Biochemistry*, 28, 9464-9468.
- EICHELBAUM, M., INGELMAN-SUNDBERG, M. & EVANS, W. E. 2006. Pharmacogenomics and individualized drug therapy. *Annu. Rev. Med.*, 57, 119-137.

- EKWALL, K. & MANNERVIK, B. 1973. The stereochemical configuration of the lactoyl group of *S*-lactoylglutathione formed by the action of glyoxalase I from porcine erythrocytes and yeast. *Biochimica et Biophysica Acta (BBA)-General Subjects*, 297, 297-299.
- EL-OSTA, A., BRASACCHIO, D., YAO, D., POCAI, A., JONES, P. L., ROEDER, R. G., COOPER, M. E. & BROWNLIE, M. 2008. Transient high glucose causes persistent epigenetic changes and altered gene expression during subsequent normoglycemia. *The Journal of experimental medicine*, 205, 2409-2417.
- EMANUEL, B. S. & SHAIKH, T. H. 2001. Segmental duplications: an expanding role in genomic instability and disease. *Nature Reviews Genetics*, 2, 791-800.
- EMBDEN, G., DEUTICKE, H. & KRAFT, G. 1933. Über die intermediären Vorgänge bei der Glykolyse in der Muskulatur. *Journal of Molecular Medicine*, 12, 213-215.
- EVANS, M. J. & KAUFMAN, M. H. 1981. Establishment in culture of pluripotential cells from mouse embryos. *nature*, 292, 154-156.
- EWASCHUK, J. B., NAYLOR, J. M. & ZELLO, G. A. 2005. D-lactate in human and ruminant metabolism. *The Journal of nutrition*, 135, 1619-1625.
- FARZANCH, F., FEON, S., LEBBY, R. A., BRILL, D., DAVID, J.-C. & SHALL, S. 1987. DNA repair in human promyelocytic cell line, HL-60. *Nucleic acids research*, 15, 3503-3513.
- FELLERMANN, K., STANGE, D. E., SCHAEFFELER, E., SCHMALZL, H., WEHKAMP, J., BEVINS, C. L., REINISCH, W., TEML, A., SCHWAB, M. & LICHTER, P. 2006. A chromosome 8 gene-cluster polymorphism with low human beta-defensin 2 gene copy number predisposes to Crohn disease of the colon. *The American Journal of Human Genetics*, 79, 439-448.
- FEUK, L., CARSON, A. R. & SCHERER, S. W. 2006. Structural variation in the human genome. *Nature Reviews Genetics*, 7, 85-97.
- FINOT, P. & MAURON, J. 1969. Le blocage de la lysine par la réaction de MAILLARD. I. Synthèse de N-(désoxy-1-D-fructosyl-1)-et N-(désoxy-1-D-lactulosyl-1)-L-lysines. *Helvetica Chimica Acta*, 52, 1488-1495.
- FORRISTAL, C. E., CHRISTENSEN, D. R., CHINNERY, F. E., PETRUZZELLI, R., PARRY, K. L., SANCHEZ-ELSNER, T. & HOUGHTON, F. D. 2013. Environmental oxygen tension regulates the energy metabolism and self-renewal of human embryonic stem cells. *PLoS ONE* e0062507
- FREEMAN, J. L., PERRY, G. H., FEUK, L., REDON, R., MCCARROLL, S. A., ALTSHULER, D. M., ABURATANI, H., JONES, K. W., TYLER-SMITH, C. & HURLES, M. E. 2006. Copy number variation: new insights in genome diversity. *Genome research*, 16, 949-961.
- FRIEDBERG, E. C., WALKER, G. C., SIEDE, W. & WOOD, R. D. 2005. DNA repair and mutagenesis, *American Society for Microbiology Press*.
- FRIEDEL, R. H., SEISENBERGER, C., KALOFF, C. & WURST, W. 2007. EUCOMM—the European conditional mouse mutagenesis program. *Briefings in functional genomics & proteomics*, 6, 180-185.

- FROYEN, G., CORBETT, M., VANDEWALLE, J., JARVELA, I., LAWRENCE, O., MELDRUM, C., BAUTERS, M., GOVAERTS, K., VANDELEUR, L. & VAN ESCH, H. 2008. Submicroscopic duplications of the hydroxysteroid dehydrogenase HSD17B10 and the E3 ubiquitin ligase HUWE1 are associated with mental retardation. *The American Journal of Human Genetics*, 82, 432-443.
- FUCHS, J., NILSSON, C., KACHERGUS, J., MUNZ, M., LARSSON, E.-M., SCHÜLE, B., LANGSTON, J., MIDDLETON, F., ROSS, O. & HULIHAN, M. 2007. Phenotypic variation in a large Swedish pedigree due to SNCA duplication and triplication. *Neurology*, 68, 916-922.
- FUJIMOTO, M., UCHIDA, S., WATANUKI, T., WAKABAYASHI, Y., OTSUKI, K., MATSUBARA, T., SUETSUGI, M., FUNATO, H. & WATANABE, Y. 2008. Reduced expression of glyoxalase-1 mRNA in mood disorder patients. *Neuroscience Letters*, 438, 196-199.
- FUTREAL, P. A., COIN, L., MARSHALL, M., DOWN, T., HUBBARD, T., WOOSTER, R., RAHMAN, N. & STRATTON, M. R. 2004. A census of human cancer genes. *Nature Reviews Cancer*, 4, 177-183.
- GALE, C. P. & GRANT, P. J. 2004. The characterisation and functional analysis of the human glyoxalase-1 gene using methods of bioinformatics. *Gene*, 340, 251-260.
- GEOFFRION, M., DU, X., IRSHAD, Z., VANDERHYDEN, B. C., COURVILLE, K., SUI, G., D'AGATI, V. D., OTT-BRASCHI, S., RABBANI, N. & THORNALLEY, P. J. 2014. Differential effects of glyoxalase 1 overexpression on diabetic atherosclerosis and renal dysfunction in streptozotocin-treated, apolipoprotein E-deficient mice. *Physiological reports*, 2, e12043.
- GHAZALPOUR, A., BENNETT, B., PETYUK, V. A., OROZCO, L., HAGOPIAN, R., MUNGRUE, I. N., FARBER, C. R., SINSHEIMER, J., KANG, H. M. & FURLOTTE, N. 2011. Comparative analysis of proteome and transcriptome variation in mouse. *PLoS genetics*, 7, e1001393.
- GIACCO, F., DU, X., D'AGATI, V. D., MILNE, R., SUI, G., GEOFFRION, M. & BROWNLEE, M. 2014. Knockdown of glyoxalase 1 mimics diabetic nephropathy in nondiabetic mice. *Diabetes*, 63, 291-299.
- GIRIRAJAN, S., CAMPBELL, C. D. & EICHLER, E. E. 2011. Human copy number variation and complex genetic disease. *Annual review of genetics*, 45, 203-226.
- GONZALEZ, E., KULKARNI, H., BOLIVAR, H., MANGANO, A., SANCHEZ, R., CATANO, G., NIBBS, R. J., FREEDMAN, B. I., QUINONES, M. P. & BAMSHAD, M. J. 2005. The influence of CCL3L1 gene-containing segmental duplications on HIV-1/AIDS susceptibility. *Science*, 307, 1434-1440.
- HAIK JR, G. M., LO, T. W. & THORNALLEY, P. J. 1994. Methylglyoxal concentration and glyoxalase activities in the human lens. *Experimental eye research*, 59, 497-500.
- HAMBSCH, B., CHEN, B. G., BRENNDÖRFER, J., MEYER, M., AVRABOS, C., MACCARRONE, G., LIU, R. H., EDER, M., TURCK, C. W. & LANDGRAF, R. 2010. Methylglyoxal-mediated anxiety involves increased protein modification and elevated expression of glyoxalase 1 in the brain. *J Neurochem*, 113, 1240-51.

- HAMMAD, S. M., HAZEN-MARTIN, D. J., SOHN, M., ELDRIDGE, L., POWELL-BRAXTON, L., WON, W. & LYONS, T. J. 2003. Nephropathy in a hypercholesterolemic mouse model with streptozotocin-induced diabetes. *Kidney and Blood Pressure Research*, 26, 351-361.
- HANSEN, N. M., BROUWERS, O., GIJBELS, M. J., WOUTERS, K., WIJNANDS, E., CLEUTJENS, J. P., DE MEY, J. G., MIYATA, T., BIESSEN, E. A. & STEHOUSER, C. D. 2014. Glyoxalase 1 overexpression does not affect atherosclerotic lesion size and severity in ApoE^{-/-} mice with or without diabetes. *Cardiovascular research*, 104, 160-170.
- HASTINGS, P. 2007. Adaptive amplification. *Critical Reviews in Biochemistry and Molecular Biology*, 42, 271-283.
- HASTINGS, P., IRA, G. & LUPSKI, J. R. 2009a. A microhomology-mediated break-induced replication model for the origin of human copy number variation. *PLoS genet*, 5, e1000327.
- HASTINGS, P., LUPSKI, J. R., ROSENBERG, S. M. & IRA, G. 2009b. Mechanisms of change in gene copy number. *Nature Reviews Genetics*, 10, 551-564.
- HENLE, T. & BACHMANN, A. 1996. Synthesis of pyrrolidine reference material. *Zeitschrift für Lebensmittel-Untersuchung und Forschung*, 202, 72-74.
- HENLE, T., WALTER, A. W., HAEBNER, R. & KLOSTERMEYER, H. 1994. Detection and identification of a protein-bound imidazolone resulting from the reaction of arginine residues and methylglyoxal. *Zeitschrift für Lebensmittel-Untersuchung und Forschung*, 199, 55-58.
- HENRICHSEN, C. N., CHAIGNAT, E. & REYMOND, A. 2009. Copy number variants, diseases and gene expression. *Human Molecular Genetics*, 18, R1-R8.
- HIMO, F. & SIEGBAHN, P. E. 2001. Catalytic mechanism of glyoxalase I: a theoretical study. *Journal of the American Chemical Society*, 123, 10280-10289.
- HOLLOX, E. J., HUFFMEIER, U., ZEEUWEN, P. L., PALLA, R., LASCORZ, J., RODIJK-OLTHUIS, D., VAN DE KERKHOF, P. C., TRAUPE, H., DE JONGH, G. & DEN HEIJER, M. 2008. Psoriasis is associated with increased β -defensin genomic copy number. *Nature genetics*, 40, 23-25.
- HOPKINS, F. G. & MORGAN, E. 1945. On the distribution of glyoxalase and glutathione. *Biochemical Journal*, 39, 320.
- HOSODA, F., ARAI, Y., OKADA, N., SHIMIZU, H., MIYAMOTO, M., KITAGAWA, N., KATAI, H., TANIGUCHI, H., YANAGIHARA, K. & IMOTO, I. 2014. Integrated genomic and functional analyses reveal glyoxalase I as a novel metabolic oncogene in human gastric cancer. *Oncogene*, 26;34(9):1196-206.
- HOVATTA, I., TENNANT, R. S., HELTON, R., MARR, R. A., SINGER, O., REDWINE, J. M., ELLISON, J. A., SCHADT, E. E., VERMA, I. M., LOCKHART, D. J. & BARLOW, C. 2005. Glyoxalase 1 and glutathione reductase 1 regulate anxiety in mice. *Nature*, 438, 662-6.
- HOVE, H. 1998. Lactate and short chain fatty acid production in the human colon: implications for D-lactic acidosis, short-bowel syndrome, antibiotic-associated diarrhoea, colonic cancer, and inflammatory bowel disease. *Danish medical bulletin*, 45, 15.

- HUETTEL, B., KREIL, D. P., MATZKE, M. & MATZKE, A. J. 2008. Effects of aneuploidy on genome structure, expression, and interphase organization in *Arabidopsis thaliana*. *PLoS Genet*, , e1000226
- HUGGINS, T. G., WELLS-KNECHT, M., DETORIE, N., BAYNES, J. & THORPE, S. 1993. Formation of o-tyrosine and dityrosine in proteins during radiolytic and metal-catalyzed oxidation. *Journal of Biological Chemistry*, 268, 12341-12347.
- IAFRATE, A. J., FEUK, L., RIVERA, M. N., LISTEWNIK, M. L., DONAHOE, P. K., QI, Y., SCHERER, S. W. & LEE, C. 2004. Detection of large-scale variation in the human genome. *Nature genetics*, 36, 949-951.
- IKEDA, Y., INAGI, R., MIYATA, T., NAGAI, R., ARAI, M., MIYASHITA, M., ITOKAWA, M., FUJITA, T. & NANGAKU, M. 2011. Glyoxalase I retards renal senescence. *The American journal of pathology*, 179, 2810-2821.
- INAGI, R., MIYATA, T., UEDA, Y., YOSHINO, A., NANGAKU, M., DE STRIHO, C. V. Y. & KUROKAWA, K. 2002. Efficient in vitro lowering of carbonyl stress by the glyoxalase system in conventional glucose peritoneal dialysis fluid. *Kidney international*, 62, 679-687.
- INOUE, K. & LUPSKI, J. R. 2002. Molecular mechanisms for genomic disorders. *Annual review of genomics and human genetics*, 3, 199-242.
- INTERNATIONAL-MOUSE-KNOCKOUT-CONSORTIUM 2007. A Mouse for All Reasons. *Cell*, 128, 9-13.
- IRSHAD Z, X. M., THORNALLEY PJ, RABBANI N 2014. Disturbance of the glyoxalase system in human vascular endothelial cells by high glucose in vitro and reversal by trans-resveratrol. *Diabetes*, 63, A9.
- ITO, K. & SUDA, T. 2014. Metabolic requirements for the maintenance of self-renewing stem cells. *Nature Reviews Molecular Cell Biology*, 15, 243-256.
- ITSARA, A., WU, H., SMITH, J. D., NICKERSON, D. A., ROMIEU, I., LONDON, S. J. & EICHLER, E. E. 2010. De novo rates and selection of large copy number variation. *Genome research*, 20, 1469-1481.
- JACK, M., RYALS, J. & WRIGHT, D. 2011. Characterisation of glyoxalase I in a streptozocin-induced mouse model of diabetes with painful and insensate neuropathy. *Diabetologia*, 54, 2174-2182.
- JACK, M., RYALS, J. & WRIGHT, D. 2012. Protection from diabetes-induced peripheral sensory neuropathy—A role for elevated glyoxalase I? *Experimental neurology*, 234, 62-69.
- JERZYKOWSKI, T., WINTER, R. & MATUSZEWSKI, W. 1973. gammadelta-Dioxoalate as a substrate for the glyoxalase enzyme system. *Biochem. J*, 135, 713-719.
- JO-WATANABE, A., OHSE, T., NISHIMATSU, H., TAKAHASHI, M., IKEDA, Y., WADA, T., SHIRAKAWA, J. I., NAGAI, R., MIYATA, T. & NAGANO, T. 2014. Glyoxalase I reduces glycative and oxidative stress and prevents age-related endothelial dysfunction through modulation of endothelial nitric oxide synthase phosphorylation. *Aging cell*, 13, 519-528.
- JONES, L., WEI, G., SEVCIKOVA, S., PHAN, V., JAIN, S., SHIEH, A., WONG, J. C., LI, M., DUBANSKY, J. & MAUNAKEA, M. L. 2010. Gain of MYC underlies recurrent trisomy of the MYC chromosome in acute promyelocytic leukemia. *The Journal of experimental medicine*, 207, 2581-2594.
- JOWETT, M. & QUASTEL, J. H. 1933. The glyoxalase activity of the red blood cell: The function of glutathione. *Biochemical Journal*, 27, 486.

- JUNAID, M. A., KOWAL, D., BARUA, M., PULLARKAT, P. S., SKLOWER BROOKS, S. & PULLARKAT, R. K. 2004. Proteomic studies identified a single nucleotide polymorphism in glyoxalase I as autism susceptibility factor. *American Journal of Medical Genetics Part A*, 131, 11-17.
- KAHLEM, P., SULTAN, M., HERWIG, R., STEINFATH, M., BALZEREIT, D., EPPENS, B., SARAN, N. G., PLETCHER, M. T., SOUTH, S. T. & STETTEN, G. 2004. Transcript level alterations reflect gene dosage effects across multiple tissues in a mouse model of down syndrome. *Genome research*, 14, 1258-1267.
- KALOUSOVÁ, M., GERMANOVÁ, A., JÁCHYMOVÁ, M., MESTEK, O., TESAŤ, V. & ZIMA, T. 2008. A419C (E111A) polymorphism of the glyoxalase I gene and vascular complications in chronic hemodialysis patients. *Annals of the New York Academy of Sciences*, 1126, 268-271.
- KANG, J. H. 2003. Oxidative damage of DNA induced by methylglyoxal in vitro. *Toxicology letters*, 145, 181-187.
- KANG, Y., EDWARDS, L. G. & THORNALLEY, P. J. 1996. Effect of methylglyoxal on human leukaemia 60 cell growth: Modification of DNA, G₁ growth arrest and induction of apoptosis. *Leukemia research*, 20, 397-405.
- KARACHALIAS N, B.-J. R., AHMED N, BAYNES K, THORNALLEY PJ 2005. Urinary d-lactate as a marker of biochemical dysfunction linked to the development of diabetic microvascular complications. *Diabet Med*, 22(Suppl.2), 21.
- KARACHALIAS, N., BABAEI-JADIDI, R., RABBANI, N. & THORNALLEY, P. J. 2010. Increased protein damage in renal glomeruli, retina, nerve, plasma and urine and its prevention by thiamine and benfotiamine therapy in a rat model of diabetes. *Diabetologia*, 53, 1506-1516.
- KATSUDA, T., TERATANI, T., CHOWDHURY, M. M., OCHIYA, T. & SAKAI, Y. 2013. Hypoxia efficiently induces differentiation of mouse embryonic stem cells into endodermal and hepatic progenitor cells. *Biochemical Engineering Journal*, 74, 95-101.
- KILE, B. T. & HILTON, D. J. 2005. The art and design of genetic screens: mouse. *Nature Reviews Genetics*, 6, 557-567.
- KIM, M. J., KIM, D. W., LEE, B. R., SHIN, M. J., KIM, Y. N., EOM, S., PARK, B.-J., CHO, Y. S., HAN, K. H. & PARK, J. 2013. Transduced Tat-glyoxalase protein attenuates streptozotocin-induced diabetes in a mouse model. *Biochemical and biophysical research communications*, 430, 294-300.
- KIM, N.-S., SEKINE, S., KIUCHI, N. & KATO, S. 1995. cDNA cloning and characterization of human glyoxalase I isoforms from HT-1080 cells. *Journal of biochemistry*, 117, 359-361.
- KINGSBURY, M., YUNG, Y., PETERSON, S., WESTRA, J. & CHUN, J. 2006. Aneuploidy in the normal and diseased brain. *Cellular and Molecular Life Sciences CMLS*, 63, 2626-2641.
- KIRK, J. 1960. The glyoxalase I activity of arterial tissue in individuals of various ages. *Journal of Gerontology*, 15, 139-141.
- KLEINJAN, D. A. & VAN HEYNINGEN, V. 2005. Long-range control of gene expression: emerging mechanisms and disruption in disease. *The American Journal of Human Genetics*, 76, 8-32.

- KNIGHT, M. A., HERNANDEZ, D., DIEDE, S. J., DAUWERSE, H. G., RAFFERTY, I., VAN DE LEEMPUT, J., FORREST, S. M., GARDNER, R. M., STOREY, E. & VAN OMMEN, G.-J. B. 2008. A duplication at chromosome 11q12. 2–11q12. 3 is associated with spinocerebellar ataxia type 20. *Human molecular genetics*, 17, 3847-3853.
- KOLLMANNBERGER, L. K., GASSEN, N. C., BULTMANN, A., HARTMANN, J., WEBER, P., SCHMIDT, M. V. & REIN, T. 2013. Increased Glyoxalase-1 Levels in Fkbp5 Knockout Mice Caused by Glyoxalase-1 Gene Duplication. *G3-Genes Genomes Genetics*, 3, 1311-1313.
- KONDOH, Y., KAWASE, M., KAWAKAMI, Y. & OHMORI, S. 1992a. Concentrations of d-lactate and its related metabolic intermediates in liver, blood, and muscle of diabetic and starved rats. *Research in experimental medicine*, 192, 407-414.
- KONDOH, Y., KAWASE, M. & OHMORI, S. 1992b. D-Lactate concentrations in blood, urine and sweat before and after exercise. *European journal of applied physiology and occupational physiology*, 65, 88-93.
- KONRADE, I., STOYANOV, S., HAAG, G., SEREGIN, Y., HUMPERT, P., MORCOS, M., THORPE, S., THORNALLEY, P., NAWROTH, P. & BIERHAUS, A. 2006. RAGE-dependent impairment of glyoxalase-1 contributes to functional deficits in diabetic neuropathy. *Diabetologia*, 49, 662-662.
- KOOLE, C., SAVAGE, E. E., CHRISTOPOULOS, A., MILLER, L. J., SEXTON, P. M. & WOOTTEN, D. 2013. Minireview: Signal Bias, Allosterism, and Polymorphic Variation at the GLP-1R: Implications for Drug Discovery. *Molecular Endocrinology*, 27, 1234-1244.
- KRISTENSEN, A. R., SCHANDORFF, S., HOYER-HANSEN, M., NIELSEN, M. O., JAATTELA, M., DENGJEL, J. & ANDERSEN, J. S. 2008. Ordered organelle degradation during starvation-induced autophagy. *Molecular & Cellular Proteomics*, 7(12):2419-28.
- KROEMER, S. A., KESSLER, M. S., MILFAY, D., BIRG, I. N., BUNCK, M., CZIBERE, L., PANHUYSSEN, M., PUETZ, B., DEUSSING, J. M., HOLSBOER, F., LANDGRAF, R. & TURCK, C. W. 2005. Identification of glyoxalase-I as a protein marker in a mouse model of extremes in trait anxiety. *Journal of Neuroscience*, 25, 4375-4384.
- KUHLA, B., BOECK, K., LÜTH, H.-J., SCHMIDT, A., WEIGLE, B., SCHMITZ, M., OGUNLADE, V., MÜNCH, G. & ARENDT, T. 2006. Age-dependent changes of glyoxalase I expression in human brain. *Neurobiology of aging*, 27, 815-822.
- KUHLA, B., BOECK, K., SCHMIDT, A., OGUNLADE, V., ARENDT, T., MÜNCH, G. & LÜTH, H.-J. 2007. Age- and stage-dependent glyoxalase I expression and its activity in normal and Alzheimer's disease brains. *Neurobiology of aging*, 28, 29-41.
- KUMAGAI, T., NANGAKU, M., KOJIMA, I., NAGAI, R., INGELFINGER, J. R., MIYATA, T., FUJITA, T. & INAGI, R. 2009. Glyoxalase I overexpression ameliorates renal ischemia-reperfusion injury in rats. *American Journal of Physiology-Renal Physiology*, 296, F912-F921.

- KUROTAKI, N., SHEN, J. J., TOUYAMA, M., KONDOH, T., VISSER, R., OZAKI, T., NISHIMOTO, J., SHIIHARA, T., UETAKE, K. & MAKITA, Y. 2005. Phenotypic consequences of genetic variation at hemizygous alleles: Sotos syndrome is a contiguous gene syndrome incorporating coagulation factor twelve (FXII) deficiency. *Genetics in Medicine*, 7, 479-483.
- KURZ, A., RABBANI, N., WALTER, M., BONIN, M., THORNALLEY, P., AUBURGER, G. & GISPERT, S. 2011. Alpha-synuclein deficiency leads to increased glyoxalase I expression and glycation stress. *Cellular and Molecular Life Sciences*, 68, 721-733.
- LACHMAN, H. M., PEDROSA, E., PETRUOLO, O. A., COCKERHAM, M., PAPOLOS, A., NOVAK, T., PAPOLOS, D. F. & STOPKOVA, P. 2007. Increase in GSK3 β gene copy number variation in bipolar disorder. *American Journal of Medical Genetics Part B: Neuropsychiatric Genetics*, 144, 259-265.
- LANDRO, J. A., BRUSH, E. J. & KOZARICH, J. W. 1992. Isomerization of (R)- and (S)-glutathiolactaldehydes by glyoxalase I: the case for dichotomous stereochemical behavior in a single active site. *Biochemistry*, 31, 6069-6077.
- LAPP, A. & DUNN, M. 1955. DL-Methionine sulphoxide. *Biochem. Prep*, 80-85.
- LARSEN, K., ARONSSON, A.-C., MARMSTÅL, E. & MANNERVIK, B. 1985. Immunological comparison of glyoxalase I from yeast and mammals and quantitative determination of the enzyme in human tissues by radioimmunoassay. *Comparative Biochemistry and Physiology Part B: Comparative Biochemistry*, 82, 625-638.
- LE MARÉCHAL, C., MASSON, E., CHEN, J.-M., MOREL, F., RUSZNIEWSKI, P., LEVY, P. & FÉREC, C. 2006. Hereditary pancreatitis caused by triplication of the trypsinogen locus. *Nature genetics*, 38, 1372-1374.
- LEE, C. & SCHERER, S. W. 2010. The clinical context of copy number variation in the human genome. *Expert Reviews in Molecular Medicine*, 12.
- LEE, G. S., LEE, K. Y., CHOI, K. C., RYU, Y. H., PAIK, S. G., OH, G. T. & JEUNG, E. B. 2007. Phenotype of a Calbindin-D9k Gene Knockout Is Compensated for by the Induction of Other Calcium Transporter Genes in a Mouse Model. *Journal of Bone and Mineral Research*, 22, 1968-1978.
- LEE, J.-Y., SONG, J., KWON, K., JANG, S., KIM, C., BAEK, K., KIM, J. & PARK, C. 2012. Human DJ-1 and its homologs are novel glyoxalases. *Human molecular genetics*, 21, 3215-3225.
- LEE, J. A., INOUE, K., CHEUNG, S. W., SHAW, C. A., STANKIEWICZ, P. & LUPSKI, J. R. 2006. Role of genomic architecture in PLP1 duplication causing Pelizaeus-Merzbacher disease. *Human molecular genetics*, 15, 2250-2265.
- LEXICON. 2007. *Lexicon phenotypic analysis* [Online]. Lexicon Pharmaceuticals. Available: https://beta.infracorner.eu/sites/infracorner.eu/files/upload/public/lexicon/WTL_October_2007/LEXKO-1493-treeFrame.html 2014].
- LI, J., FUNG, I., GLESSNER, J. T., PANDEY, R., WEI, Z., BAKAY, M., MENTCH, F. D., PELLEGRINO, R., WANG, T. & KIM, C. 2015. Copy Number Variations in CTNNA3 and RBFOX1 Associate with Pediatric Food Allergy. *The Journal of Immunology*, 195, 1599-1607.
- LI, V. C., BALLABENI, A. & KIRSCHNER, M. W. 2012. Gap 1 phase length and mouse embryonic stem cell self-renewal. *Proceedings of the National Academy of Sciences*, 109, 12550-12555.

- LI, Y., ZHENG, H., LUO, R., WU, H., ZHU, H., LI, R., CAO, H., WU, B., HUANG, S. & SHAO, H. 2011. Structural variation in two human genomes mapped at single-nucleotide resolution by whole genome de novo assembly. *Nature biotechnology*, 29, 723-730.
- LIANG, Q., CONTE, N., SKARNES, W. C. & BRADLEY, A. 2008. Extensive genomic copy number variation in embryonic stem cells. *Proceedings of the National Academy of Sciences*, 105, 17453-17456.
- LIFTON, R. P., DLUHY, R. G., POWERS, M., RICH, G. M., COOK, S., ULICK, S. & LALOUEL, J.-M. 1992. A chimaeric 11 β -hydroxylase/aldosterone synthase gene causes glucocorticoid-remediable aldosteronism and human hypertension. *Nature*, 16;355(6357):262-5.
- LIMPHONG, P., MCKINNEY, R. M., ADAMS, N. E., BENNETT, B., MAKAROFF, C. A., GUNASEKERA, T. & CROWDER, M. W. 2009. Human glyoxalase II contains an Fe (II) Zn (II) center but is active as a mononuclear Zn (II) enzyme. *Biochemistry*, 48, 5426-5434.
- LISKAY, R. M., LETSOU, A. & STACHELEK, J. L. 1987. Homology requirement for efficient gene conversion between duplicated chromosomal sequences in mammalian cells. *Genetics*, 115, 161-167.
- LIU, G.-H., QU, J. & SHEN, X. 2008. NF- κ B/p65 antagonizes Nrf2-ARE pathway by depriving CBP from Nrf2 and facilitating recruitment of HDAC3 to MafK. *Biochimica et Biophysica Acta (BBA)-Molecular Cell Research*, 1783, 713-727.
- LO, T. W., SELWOOD, T. & THORNALLEY, P. J. 1994a. The reaction of methylglyoxal with aminoguanidine under physiological conditions and prevention of methylglyoxal binding to plasma proteins. *Biochemical pharmacology*, 48, 1865-1870.
- LO, T. W. & THORNALLEY, P. J. 1992. Inhibition of proliferation of human leukaemia 60 cells by diethyl esters of glyoxalase inhibitors *in vitro*. *Biochemical pharmacology*, 44, 2357-2363.
- LO, T. W., WESTWOOD, M. E., MCLELLAN, A. C., SELWOOD, T. & THORNALLEY, P. J. 1994b. Binding and modification of proteins by methylglyoxal under physiological conditions. A kinetic and mechanistic study with N alpha-acetylarginine, N alpha-acetylcysteine, and N alpha-acetyllysine, and bovine serum albumin. *J Biol Chem*, 269, 32299-305.
- LOHMANN, K. 1932. A study of the enzymatic transformation of synthetic methylglyoxal to lactic acid. *Biochem. Ztschr*, 254, 332-354.
- LOVETT, S. T., HURLEY, R. L., SUTERA, V. A., AUBUCHON, R. H. & LEBEDEVA, M. A. 2002. Crossing over between regions of limited homology in Escherichia coli: RecA-dependent and RecA-independent pathways. *Genetics*, 160, 851-859.
- LUNDBY, A., LAGE, K., WEINERT, B. T., BEKKER-JENSEN, D. B., SECHER, A., SKOVGAARD, T., KELSTRUP, C. D., DMYTRIYEV, A., CHOUDHARY, C. & LUNDBY, C. 2012. Proteomic analysis of lysine acetylation sites in rat tissues reveals organ specificity and subcellular patterns. *Cell reports*, 2, 419-431.
- LUPSKI, J. & CHANCE, P. 2005. Hereditary motor and sensory neuropathies involving altered dosage or mutation of PMP22: the CMT1A duplication and HNPP deletion. *Peripheral neuropathy*, 2, 1659-80.

- LUPSKI, J. R. & STANKIEWICZ, P. 2005. Genomic disorders: molecular mechanisms for rearrangements and conveyed phenotypes. *PLoS Genet*, 1, e49.
- MACDONALD, J. R., ZIMAN, R., YUEN, R. K., FEUK, L. & SCHERER, S. W. 2014. The Database of Genomic Variants: a curated collection of structural variation in the human genome. *Nucleic acids research*, 42, D986-D992.
- MADSON, M. A. & FEATHER, M. S. 1981. An improved preparation of 3-deoxy-d-erythro-hexos-2-ulose via the bis (benzoylhydrazone) and some related constitutional studies. *Carbohydrate Research*, 94, 183-191.
- MAILANKOT, M., PADMANABHA, S., PASUPULETI, N., MAJOR, D., HOWELL, S. & NAGARAJ, R. H. 2009. Glyoxalase I activity and immunoreactivity in the aging human lens. *Biogerontology*, 10, 711-720.
- MÄKINEN, V.-P., CIVELEK, M., MENG, Q., ZHANG, B., ZHU, J., LEVIAN, C., HUAN, T., SEGRÈ, A. V., GHOSH, S. & VIVAR, J. 2014. Integrative genomics reveals novel molecular pathways and gene networks for coronary artery disease. *PLoS genetics*, 10, e1004502.
- MALHOTRA, D. & SEBAT, J. 2012. CNVs: harbingers of a rare variant revolution in psychiatric genetics. *Cell*, 148, 1223-1241.
- MANN, V., TUCKER, B., THOMALLEY, P. & DAYNAY, A. Elevated plasma methylglyoxal and glyoxal in uraemia: implications for advanced glycation end-product formation. 1999. *Kidney International*, 55(6):2582-2582.
- MAO, L., HARTL, D., NOLDEN, T., KOPPELSTÄTTER, A., KLOSE, J., HIMMELBAUER, H. & ZABEL, C. 2008. Pronounced alterations of cellular metabolism and structure due to hyper-or hypo-osmosis. *Journal of proteome research*, 7, 3968-3983.
- MARMSTAL, E., ARONSSON, A.-C. & MANNERVIK, B. 1979. Comparison of glyoxalase I purified from yeast (*Saccharomyces cerevisiae*) with the enzyme from mammalian sources. *Biochem. J*, 183, 23-30.
- MARSCHANG, P., BRICH, J., WEEBER, E. J., SWEATT, J. D., SHELTON, J. M., RICHARDSON, J. A., HAMMER, R. E. & HERZ, J. 2004. Normal development and fertility of knockout mice lacking the tumor suppressor gene LRP1b suggest functional compensation by LRP1. *Molecular and cellular biology*, 24, 3782-3793.
- MASUI, S., NAKATAKE, Y., TOYOOKA, Y., SHIMOSATO, D., YAGI, R., TAKAHASHI, K., OKOCHI, H., OKUDA, A., MATOBA, R. & SHAROV, A. A. 2007. Pluripotency governed by Sox2 via regulation of Oct3/4 expression in mouse embryonic stem cells. *Nature cell biology*, 9, 625-635.
- MCCANN, V., DAVIS, R., WELBORN, T., CONSTABLE, I. & BEALE, D. 1981. Glyoxalase phenotypes in patients with diabetes mellitus. *Australian and New Zealand journal of medicine*, 11, 380-382.
- MCLELLAN, A., PHILIPS, S. & THORNALLEY, P. 1993. The assay of SD-lactoylglutathione in biological systems. *Analytical biochemistry*, 211, 37-43.
- MCLELLAN, A. C., PHILLIPS, S. A. & THORNALLEY, P. J. 1992. Fluorimetric assay of D-lactate. *Anal Biochem*, 206, 12-6.
- MCLELLAN, A. C. & THORNALLEY, P. J. 1989. Glyoxalase activity in human red blood cells fractioned by age. *Mech Ageing Dev*, 48, 63-71.

- MCLELLAN, A. C. & THORNALLEY, P. J. 1992. Synthesis and chromatography of 1, 2-diamino-4, 5-dimethoxybenzene, 6, 7-dimethoxy-2-methylquinoxaline and 6, 7-dimethoxy-2, 3-dimethylquinoxaline for use in a liquid chromatographic fluorimetric assay of methylglyoxal. *Analytica chimica acta*, 263, 137-142.
- MCLELLAN, A. C. & THORNALLEY, P. J. 1994. Glyoxalase system in clinical diabetes mellitus and correlation with diabetic complications. *Clinical Science*, 87, 21-29.
- MCLELLAN, A. C., THORNALLEY, P. J., BENN, J. & SONKSEN, P. H. 1994. Glyoxalase system in clinical diabetes mellitus and correlation with diabetic complications. *Clin Sci (Lond)*, 87, 21-9.
- MELDAL, M. & KINDTLER, J. 1986. Synthesis of a proposed antigenic hexapeptide from Escherichia coli K88 protein fimbriae. *Acta chemica Scandinavica. Series B: Organic chemistry and biochemistry*, 40, 235.
- MEO, T., DOUGLAS, T. & RIJNBEEK, A. M. 1977. Glyoxalase-I polymorphism in mouse - new genetic-marker linked to H-2. *Science*, 198, 311-313.
- MEYERHOF, O. 1933. Intermediate products and the last stages of carbohydrate breakdown in the metabolism of muscle and in alcoholic fermentation. *Nature*, 132, 337-373.
- MILLER, A. G., TAN, G., BINGER, K. J., PICKERING, R. J., THOMAS, M. C., NAGARAJ, R. H., COOPER, M. E. & WILKINSON-BERKA, J. L. 2010. Candesartan attenuates diabetic retinal vascular pathology by restoring glyoxalase-I function. *Diabetes*, 59, 3208-3215.
- MISRA, K., BANERJEE, A. B., RAY, S. & RAY, M. 1995. Glyoxalase III from Escherichia coli: a single novel enzyme for the conversion of methylglyoxal into D-lactate without reduced glutathione. *Biochem. J*, 305, 999-1003.
- MITSUI, K., TOKUZAWA, Y., ITOH, H., SEGAWA, K., MURAKAMI, M., TAKAHASHI, K., MARUYAMA, M., MAEDA, M. & YAMANAKA, S. 2003. The homeoprotein Nanog is required for maintenance of pluripotency in mouse epiblast and ES cells. *cell*, 113, 631-642.
- MIYATA, T., DE STRIHOU, C. V. Y., IMASAWA, T., YOSHINO, A., UEDA, Y., OGURA, H., KOMINAMI, K., ONOGI, H., INAGI, R. & NANGAKU, M. 2001. Glyoxalase I deficiency is associated with an unusual level of advanced glycation end products in a hemodialysis patient. *Kidney international*, 60, 2351-2359.
- MOHYELDIN, A., GARZÓN-MUVDI, T. & QUIÑONES-HINOJOSA, A. 2010. Oxygen in stem cell biology: a critical component of the stem cell niche. *Cell stem cell*, 7, 150-161.
- MOORE, H., WINKELMANN, J., LIN, L., FINN, L., PEPPARD, P. & MIGNOT, E. 2013. Periodic Leg Movements during Sleep Are Associated with Polymorphisms in BTBD9, TOX3/BC034767, MEIS1, MAP2K5/SKOR1, and PTPRD. *Sleep*, 37, 1535-1542.
- MORCOS, M., DU, X., PFISTERER, F., HUTTER, H., SAYED, A. A., THORNALLEY, P., AHMED, N., BAYNES, J., THORPE, S. & KUKUDOV, G. 2008. Glyoxalase-1 prevents mitochondrial protein modification and enhances lifespan in Caenorhabditis elegans. *Aging cell*, 7, 260-269.

- MORTENSEN, P. B., HOVE, H., CLAUSEN, M. R. & HOLTUG, K. 1991. Fermentation to short-chain fatty acids and lactate in human faecal batch cultures intra-and inter-individual variations versus variations caused by changes in fermented saccharides. *Scandinavian journal of gastroenterology*, 26, 1285-1294.
- MURATA-KAMIYA, N., KAJI, H. & KASAI, H. 1999. Deficient nucleotide excision repair increases base-pair substitutions but decreases TGGC frameshifts induced by methylglyoxal in *Escherichia coli*. *Mutation Research/Genetic Toxicology and Environmental Mutagenesis*, 442, 19-28.
- MURATA-KAMIYA, N., KAMIYA, H., KAJI, H. & KASAI, H. 1998. Nucleotide Excision Repair Proteins May Be Involved in the Fixation of Glyoxal-Induced Mutagenesis in *Escherichia coli*. *Biochemical and biophysical research communications*, 248, 412-417.
- MURATA, K., FUKUDA, Y., SIMOSAKA, M., WATANABE, K., SAIKUSA, T. & KIMURA, A. 1985. Metabolism of 2-oxoaldehyde in yeasts. *European journal of biochemistry*, 151, 631-636.
- NAKAGAWA, T., SATO, W., GLUSHAKOVA, O., HEINIG, M., CLARKE, T., CAMPBELL-THOMPSON, M., YUZAWA, Y., ATKINSON, M. A., JOHNSON, R. J. & CROKER, B. 2007. Diabetic endothelial nitric oxide synthase knockout mice develop advanced diabetic nephropathy. *Journal of the American Society of Nephrology*, 18, 539-550.
- NANGIA-MAKKER, P., OCHIENG, J., CHRISTMAN, J. K. & RAZ, A. 1993. Regulation of the expression of galactoside-binding lectin during human monocytic differentiation. *Cancer Res*, 53, 5033-7.
- NATHANS, J., PIANTANIDA, T. P., EDDY, R. L., SHOWS, T. B. & HOGNESS, D. S. 1986. Molecular genetics of inherited variation in human color vision. *Science*, 232, 203-210.
- NEUBERG, C. 1913. The destruction of lactic aldehyde and methylglyoxal by animal organs. *Biochem Z*, 49, 502-506.
- NEUBERG, C. 1929. u. M. Kobel: Die Isolierung von Methylglyoxal bei der Milchsäuregärung. *Biochem. Z*, 207, 232-262.
- NGUYEN, D.-Q., WEBBER, C. & PONTING, C. P. 2006. Bias of selection on human copy-number variants. *PLoS genetics*, 2, e20.
- NIJHAWAN, D., ZACK, T. I., REN, Y., STRICKLAND, M. R., LAMOTHE, R., SCHUMACHER, S. E., TSHERNIAK, A., BESCHE, H. C., ROSENBLUH, J. & SHEHATA, S. 2012. Cancer vulnerabilities unveiled by genomic loss. *Cell*, 150, 842-854.
- NIWA, T., MIYAZAKI, T., KATSUZAKI, T., TATEMACHI, N. & TAKEI, Y. 1996. Serum levels of 3-deoxyglucosone and tissue contents of advanced glycation end products are increased in streptozotocin-induced diabetic rats with nephropathy. *Nephron*, 74, 580-5.
- NORTON, N., LI, D., RIEDER, M. J., SIEGFRIED, J. D., RAMPERSAUD, E., ZÜCHNER, S., MANGOS, S., GONZALEZ-QUINTANA, J., WANG, L. & MCGEE, S. 2011. Genome-wide Studies of Copy Number Variation and Exome Sequencing Identify Rare Variants in *BAG3* as a Cause of Dilated Cardiomyopathy. *The American Journal of Human Genetics*, 88, 273-282.
- O BRIEN, R., STREPER, R., AYALA, J., STADELMAIER, B. & HORNBUCKLE, L. 2001. Insulin-regulated gene expression. *Biochemical Society Transactions*, 29, 61-61.

- OCHOCKI, J. D. & SIMON, M. C. 2013. Nutrient-sensing pathways and metabolic regulation in stem cells. *The Journal of cell biology*, 203, 23-33.
- OH, M. S., URIBARRI, J., ALVERANGA, D., LAZAR, I., BAZILINSKI, N. & CARROLL, H. J. 1985. Metabolic utilization and renal handling of D-lactate in men. *Metabolism*, 34, 621-625.
- OHMORI, S. & IWAMOTO, T. 1988. Sensitive determination of D-lactic acid in biological samples by high-performance liquid chromatography. *Journal of Chromatography B: Biomedical Sciences and Applications*, 431, 239-247.
- OHMORI, S., NOSE, Y., OGAWA, H., TSUYAMA, K., HIROTA, T., GOTO, H., YANO, Y., KONDOH, Y., NAKATA, K. & TSUBOI, S. 1991. Fluorimetric and high-performance liquid chromatographic determination of D-lactate in biological samples. *Journal of Chromatography B: Biomedical Sciences and Applications*, 566, 1-8.
- OKADA, S., SHIKATA, K., MATSUDA, M., OGAWA, D., USUI, H., KIDO, Y., NAGASE, R., WADA, J., SHIKATA, Y. & MAKINO, H. 2003. Intercellular adhesion molecule-1-deficient mice are resistant against renal injury after induction of diabetes. *Diabetes*, 52, 2586-2593.
- ORSO, F., CORÀ, D., UBEZIO, B., PROVERO, P., CASELLE, M. & TAVERNA, D. 2010. Identification of functional TFAP2A and SP1 binding sites in new TFAP2A-modulated genes. *BMC genomics*, 11, 355.
- PADIATH, Q. S., SAIGOH, K., SCHIFFMANN, R., ASAHARA, H., YAMADA, T., KOEPPEN, A., HOGAN, K., PTÁČEK, L. J. & FU, Y.-H. 2006. Lamin B1 duplications cause autosomal dominant leukodystrophy. *Nature genetics*, 38, 1114-1123.
- PALSAMY, P. & SUBRAMANIAN, S. 2011. Resveratrol protects diabetic kidney by attenuating hyperglycemia-mediated oxidative stress and renal inflammatory cytokines via Nrf2-Keap1 signaling. *Biochimica et Biophysica Acta (BBA)-Molecular Basis of Disease*, 1812, 719-731.
- PAVELKA, N., RANCATI, G., ZHU, J., BRADFORD, W. D., SARAF, A., FLORENS, L., SANDERSON, B. W., HATTEM, G. L. & LI, R. 2010. Aneuploidy confers quantitative proteome changes and phenotypic variation in budding yeast. *Nature*, 468, 321-325.
- PERRY, G. H., DOMINY, N. J., CLAW, K. G., LEE, A. S., FIEGLER, H., REDON, R., WERNER, J., VILLANEVA, F. A., MOUNTAIN, J. L. & MISRA, R. 2007. Diet and the evolution of human amylase gene copy number variation. *Nature genetics*, 39, 1256-1260.
- PERRY, G. H., YANG, F., MARQUES-BONET, T., MURPHY, C., FITZGERALD, T., LEE, A. S., HYLAND, C., STONE, A. C., HURLES, M. E. & TYLER-SMITH, C. 2008. Copy number variation and evolution in humans and chimpanzees. *Genome research*, 18, 1698-1710.
- PETERS, T., JR. 1962. The biosynthesis of rat serum albumin. I. Properties of rat albumin and its occurrence in liver cell fractions. *J Biol Chem*, 237, 1181-5.
- PEZER, Ž., HARR, B., TESCHKE, M., BABIKER, H. & TAUTZ, D. 2015. Divergence patterns of genic copy number variation in natural populations of the house mouse (*Mus musculus domesticus*) reveal three conserved genes with major population-specific expansions. *Genome research*, 25, 1114-1124.
- PHILLIPS, S. A., MIRRLEES, D. & THORNALLEY, P. J. 1993. Modification of the glyoxalase system in streptozotocin-induced diabetic rats: effect of the aldose reductase inhibitor Statil. *Biochemical pharmacology*, 46, 805-811.

- PHILLIPS, S. A. & THORNALLEY, P. J. 1993. The formation of methylglyoxal from triose phosphates. Investigation using a specific assay for methylglyoxal. *Eur J Biochem*, 212, 101-5.
- PIEC, I., LISTRAT, A., ALLIOT, J., CHAMBON, C., TAYLOR, R. G. & BECHET, D. 2005. Differential proteome analysis of aging in rat skeletal muscle. *The FASEB Journal*, 19, 1143-1145.
- PIOTROWSKI, A., BRUDER, C. E., ANDERSSON, R., DE STÅHL, T. D., MENZEL, U., SANDGREN, J., POPLAWSKI, A., VON TELL, D., CRASTO, C. & BOGDAN, A. 2008. Somatic mosaicism for copy number variation in differentiated human tissues. *Human mutation*, 29, 1118-1124.
- PISCHETSRIEDER, M., SEIDEL, W., MÜNCH, G. & SCHINZEL, R. 1999. γ -(1-Carboxyethyl) deoxyguanosine, a Nonenzymatic Glycation Adduct of DNA, Induces Single-Strand Breaks and Increases Mutation Frequencies. *Biochemical and biophysical research communications*, 264, 544-549.
- POLLEX, R. L. & HEGELE, R. A. 2007. Genomic copy number variation and its potential role in lipoprotein and metabolic phenotypes. *Current opinion in lipidology*, 18, 174-180.
- PONCHEL, F., TOOMES, C., BRANSFIELD, K., LEONG, F. T., DOUGLAS, S. H., FIELD, S. L., BELL, S. M., COMBARET, V., PUISIEUX, A. & MIGHELL, A. J. 2003. Real-time PCR based on SYBR-Green I fluorescence: an alternative to the TaqMan assay for a relative quantification of gene rearrangements, gene amplifications and micro gene deletions. *BMC biotechnology*, 3, 18.
- POWERS, D. E., MILLMAN, J. R., HUANG, R. B. & COLTON, C. K. 2008. Effects of oxygen on mouse embryonic stem cell growth, phenotype retention, and cellular energetics. *Biotechnology and bioengineering*, 101, 241-254.
- PRAKASH, S. K., LEMAIRE, S. A., GUO, D.-C., RUSSELL, L., REGALADO, E. S., GOLABBAKHS, H., JOHNSON, R. J., SAFI, H. J., ESTRERA, A. L. & COSELLI, J. S. 2010. Rare copy number variants disrupt genes regulating vascular smooth muscle cell adhesion and contractility in sporadic thoracic aortic aneurysms and dissections. *The American Journal of Human Genetics*, 87, 743-756.
- QI, Z., FUJITA, H., JIN, J., DAVIS, L. S., WANG, Y., FOGO, A. B. & BREYER, M. D. 2005. Characterization of susceptibility of inbred mouse strains to diabetic nephropathy. *Diabetes*, 54, 2628-2637.
- QUEISSER, M. A., YAO, D., GEISLER, S., HAMMES, H.-P., LOCHNIT, G., SCHLEICHER, E. D., BROWNLEE, M. & PREISSNER, K. T. 2010. Hyperglycemia impairs proteasome function by methylglyoxal. *Diabetes*, 59, 670-678.
- RABBANI, N., SHAHEEN, F., ANWAR, A., MASANIA, J. & THORNALLEY, P. J. 2014a. Assay of methylglyoxal-derived protein and nucleotide AGEs. *Biochemical Society transactions*, 42, 511-517.
- RABBANI, N. & THORNALLEY, P. 2008. Dicarbonyls linked to damage in the powerhouse: glycation of mitochondrial proteins and oxidative stress. *Biochem Soc Trans*, 36, 1045-50.
- RABBANI, N. & THORNALLEY, P. J. 2012a. Advanced Glycation Endproducts (AGEs). *Uremic Toxins*, 293-304.

- RABBANI, N. & THORNALLEY, P. J. 2012b. Dicarbonyls (glyoxal, methylglyoxal, and 3-deoxyglucosone). *Uremic Toxins*, 177-192.
- RABBANI, N. & THORNALLEY, P. J. 2012c. Glycation research in amino acids: a place to call home. *Amino Acids*, 42, 1087-96.
- RABBANI, N. & THORNALLEY, P. J. 2012d. Methylglyoxal, glyoxalase 1 and the dicarbonyl proteome. *Amino acids*, 42, 1133-1142.
- RABBANI, N. & THORNALLEY, P. J. 2014a. The Critical Role of Methylglyoxal and Glyoxalase 1 in Diabetic Nephropathy. *Diabetes*, 63, 50-52.
- RABBANI, N. & THORNALLEY, P. J. 2014b. Glyoxalase Centennial: 100 Years of Glyoxalase Research and Emergence of Dicarbonyl Stress. *Biochemical Society Transactions*, 42.
- RABBANI, N. & THORNALLEY, P. J. 2014c. Measurement of methylglyoxal by stable isotopic dilution analysis LC-MS/MS with corroborative prediction in physiological samples. *Nature protocols*, 9, 1969-1979.
- RABBANI, N., XUE, M. & THORNALLEY, P. J. 2014b. Activity, regulation, copy number and function in the glyoxalase system. *Biochemical Society transactions*, 42, 419-424.
- RACKER, E. 1951. The mechanism of action of glyoxalase. *Journal of Biological Chemistry*, 190, 685-696.
- RACKER, E. Glutathione as a coenzyme in intermediary metabolism. Glutathione, a symposium, 1954. 165-183.
- RANGANATHAN, S., CIACCIO, P. J., WALSH, E. S. & TEW, K. D. 1999. Genomic sequence of human glyoxalase-I: analysis of promoter activity and its regulation. *Gene*, 240, 149-55.
- RAUH, D., FISCHER, F., GERTZ, M., LAKSHMINARASIMHAN, M., BERGBREDE, T., ALADINI, F., KAMBACH, C., BECKER, C. F., ZERWECK, J. & SCHUTKOWSKI, M. 2013. An acetylome peptide microarray reveals specificities and deacetylation substrates for all human sirtuin isoforms. *Nature communications*, 4.
- REDON, R., ISHIKAWA, S., FITCH, K. R., FEUK, L., PERRY, G. H., ANDREWS, T. D., FIEGLER, H., SHAPERO, M. H., CARSON, A. R. & CHEN, W. 2006. Global variation in copy number in the human genome. *nature*, 444, 444-454.
- REHNSTRÖM, K., YLISAUKKO-OJA, T., VANHALA, R., VON WENDT, L., PELTONEN, L. & HOVATTA, I. 2008. No association between common variants in glyoxalase 1 and autism spectrum disorders. *American Journal of Medical Genetics Part B: Neuropsychiatric Genetics*, 147, 124-127.
- REINIGER, N., LAU, K., MCCALLA, D., EBY, B., CHENG, B., LU, Y., QU, W., QUADRI, N., ANANTHAKRISHNAN, R., FURMANSKY, M., ROSARIO, R., SONG, F., RAI, V., WEINBERG, A., FRIEDMAN, R., RAMASAMY, R., D'AGATI, V. & SCHMIDT, A. M. 2010. Deletion of the Receptor for Advanced Glycation End Products Reduces Glomerulosclerosis and Preserves Renal Function in the Diabetic OVE26 Mouse. *Diabetes*, 59, 2043-2054.
- RHEE, H.-I., MURATA, K. & KIMURA, A. 1987. Molecular cloning of the Pseudomonasputida glyoxalase I gene in Escherichiacoli. *Biochemical and biophysical research communications*, 147, 831-838.

- RIBOULET-CHAVEY, A., PIERRON, A., DURAND, I., MURDACA, J., GIUDICELLI, J. & VAN OBBERGHEN, E. 2006. Methylglyoxal impairs the insulin signaling pathways independently of the formation of intracellular reactive oxygen species. *Diabetes*, 55, 1289-1299.
- RINALDI, C., D'ANGELO, R., RUGGERI, A., CALABRO, M. & SCIMONE, C. 2014. PON I and GLO I Gene Polymorphisms and Their Association with Breast Cancer: A Case-Control Study in a Population from Southern Italy. *J Mol Biomark Diagn*, 5, 2.
- ROSCA, M. G., MUSTATA, T. G., KINTER, M. T., OZDEMIR, A. M., KERN, T. S., SZWEDA, L. I., BROWNLEE, M., MONNIER, V. M. & WEISS, M. F. 2005. Glycation of mitochondrial proteins from diabetic rat kidney is associated with excess superoxide formation. *American Journal of Physiology-Renal Physiology*, 289, F420-F430.
- ROVELET-LECRUX, A., HANNEQUIN, D., RAUX, G., LE MEUR, N., LAQUERRIÈRE, A., VITAL, A., DUMANCHIN, C., FEUILLETTE, S., BRICE, A. & VERCELLETTO, M. 2005. APP locus duplication causes autosomal dominant early-onset Alzheimer disease with cerebral amyloid angiopathy. *Nature genetics*, 38, 24-26.
- ROVELET-LECRUX, A., HANNEQUIN, D., RAUX, G., LE MEUR, N., LAQUERRIÈRE, A., VITAL, A., DUMANCHIN, C., FEUILLETTE, S., BRICE, A. & VERCELLETTO, M. 2006. APP locus duplication causes autosomal dominant early-onset Alzheimer disease with cerebral amyloid angiopathy. *Nature genetics*, 38, 24-26.
- SAKAMOTO, H., MASHIMA, T., KIZAKI, A., DAN, S., HASHIMOTO, Y., NAITO, M. & TSURUO, T. 2000. Glyoxalase I is involved in resistance of human leukemia cells to antitumor agent-induced apoptosis. *Blood*, 95, 3214-3218.
- SAKAMOTO, H., MASHIMA, T., SATO, S., HASHIMOTO, Y., YAMORI, T. & TSURUO, T. 2001. Selective activation of apoptosis program by Sp-bromobenzylglutathione cyclopentyl diester in glyoxalase I-overexpressing human lung cancer cells. *Clinical cancer research*, 7, 2513-2518.
- SAMANT, S. A., OGUNKUA, O. O., HUI, L., LU, J., HAN, Y., ORTH, J. M. & PILDER, S. H. 2005. The mouse *Dnahc8* complex distorter/sterility candidate, *Dnahc8*, expresses a γ -type axonemal dynein heavy chain isoform confined to the principal piece of the sperm tail. *Developmental biology*, 285, 57-69.
- SANTARIUS, T., BIGNELL, G. R., GREENAN, C. D., WIDAA, S., CHEN, L., MAHONEY, C. L., BUTLER, A., EDKINS, S., WARIS, S., THORNALLEY, P. J., FUTREAL, P. A. & STRATTON, M. R. 2010. GLO1 - A novel amplified gene in human cancer. *Genes, Chromosomes and Cancer*, 49, 711-725.
- SARETZKI, G., ARMSTRONG, L., LEAKE, A., LAKO, M. & VON ZGLINICKI, T. 2004. Stress defense in murine embryonic stem cells is superior to that of various differentiated murine cells. *Stem Cells*, 22, 962-971.
- SCHIMANDLE, C. M. & VANDER JAGT, D. L. 1979. Isolation and kinetic analysis of the multiple forms of glyoxalase-I from human erythrocytes. *Archives of biochemistry and biophysics*, 195, 261-268.

- SCHÖLER, H., HATZOPOULOS, A. K., BALLING, R., SUZUKI, N. & GRUSS, P. 1989. A family of octamer-specific proteins present during mouse embryogenesis: evidence for germline-specific expression of an Oct factor. *The EMBO journal*, 8, 2543.
- SCHRIDER, D. R. & HAHN, M. W. 2010. Gene copy-number polymorphism in nature. *Proceedings of the Royal Society B: Biological Sciences*, 277, 3213-3221.
- SCHUSTER-BÖCKLER, B., CONRAD, D. & BATEMAN, A. 2010. Dosage sensitivity shapes the evolution of copy-number varied regions. *PloS one*, 5, e9474.
- SCHWANHÄUSSER, B., BUSSE, D., LI, N., DITTMAR, G., SCHUCHHARDT, J., WOLF, J., CHEN, W. & SELBACH, M. 2011. Global quantification of mammalian gene expression control. *Nature*, 473, 337-342.
- SEBAT, J., LAKSHMI, B., TROGE, J., ALEXANDER, J., YOUNG, J., LUNDIN, P., MÅNÉR, S., MASSA, H., WALKER, M. & CHI, M. 2004. Large-scale copy number polymorphism in the human genome. *Science*, 305, 525-528.
- SHAFIE, A., XUE, M., THORNALLEY, P. J. & RABBANI, N. 2014. Copy number variation of glyoxalase I. *Biochem. Soc. Trans*, 42, 500-503.
- SHAPIRO, L. J., YEN, P., POMERANTZ, D., MARTIN, E., ROLEWIC, L. & MOHANDAS, T. 1989. Molecular studies of deletions at the human steroid sulfatase locus. *Proceedings of the National Academy of Sciences*, 86, 8477-8481.
- SHARMA-LUTHRA, R. & KALE, R. 1994. Age related changes in the activity of the glyoxalase system. *Mechanisms of ageing and development*, 73, 39-45.
- SHIA, W.-C., KU, T.-H., TSAO, Y.-M., HSIA, C.-H., CHANG, Y.-M., HUANG, C.-H., CHUNG, Y.-C., HSU, S.-L., LIANG, K.-W. & HSU, F.-R. 2011. Genetic copy number variants in myocardial infarction patients with hyperlipidemia. *BMC genomics*, 12, S23.
- SHINOHARA, M., THORNALLEY, P., GIARDINO, I., BEISSWENGER, P., THORPE, S. R., ONORATO, J. & BROWNLEE, M. 1998. Overexpression of glyoxalase-I in bovine endothelial cells inhibits intracellular advanced glycation endproduct formation and prevents hyperglycemia-induced increases in macromolecular endocytosis. *Journal of Clinical Investigation*, 101, 1142.
- SHYH-CHANG, N., ZHENG, Y., LOCASALE, J. W. & CANTLEY, L. C. 2011. Human pluripotent stem cells decouple respiration from energy production. *The EMBO journal*, 30, 4851-4852.
- SIMON, M. C. & KEITH, B. 2008. The role of oxygen availability in embryonic development and stem cell function. *Nature reviews Molecular cell biology*, 9, 285-296.
- SIMSEK, T., KOCABAS, F., ZHENG, J., DEBERARDINIS, R. J., MAHMOUD, A. I., OLSON, E. N., SCHNEIDER, J. W., ZHANG, C. C. & SADEK, H. A. 2010. The distinct metabolic profile of hematopoietic stem cells reflects their location in a hypoxic niche. *Cell stem cell*, 7, 380-390.
- SINGLETON, A., FARRER, M., JOHNSON, J., SINGLETON, A., HAGUE, S., KACHERGUS, J., HULIHAN, M., PEURALINNA, T., DUTRA, A. & NUSSBAUM, R. 2003. α -Synuclein locus triplication causes Parkinson's disease. *science*, 302, 841-841.

- SOKOLOVSKY, M., RIORDAN, J. F. & VALLEE, B. L. 1966. Tetranitromethane. A Reagent for the Nitration of Tyrosyl Residues in Proteins*. *Biochemistry*, 5, 3582-3589.
- STINGELE, S., STOEHR, G., PEPOWSKA, K., COX, J., MANN, M. & STORCHOVA, Z. 2012. Global analysis of genome, transcriptome and proteome reveals the response to aneuploidy in human cells. *Molecular systems biology*, 8, 608.
- STONE, J. L., O'DONOVAN, M. C., GURLING, H., KIROV, G. K., BLACKWOOD, D. H., CORVIN, A., CRADDOCK, N. J., GILL, M., HULTMAN, C. M. & LICHTENSTEIN, P. 2008. Rare chromosomal deletions and duplications increase risk of schizophrenia. *Nature*, 455, 237-241.
- STRANGER, B. E., FORREST, M. S., DUNNING, M., INGLE, C. E., BEAZLEY, C., THORNE, N., REDON, R., BIRD, C. P., DE GRASSI, A., LEE, C., TYLER-SMITH, C., CARTER, N., SCHERER, S. W., TAVARE, S., DELOUKAS, P., HURLES, M. E. & DERMITZAKIS, E. T. 2007. Relative impact of nucleotide and copy number variation on gene expression phenotypes. *Science*, 315, 848-853.
- STROBER, W. 2001. Trypan blue exclusion test of cell viability. *Curr Protoc Immunol*, Appendix 3, Appendix 3B.
- SUDBERY, I., STALKER, J., SIMPSON, J. T., KEANE, T., RUST, A. G., HURLES, M. E., WALTER, K., LYNCH, D., TEBOUL, L. & BROWN, S. D. 2009. Deep short-read sequencing of chromosome 17 from the mouse strains A/J and CAST/Ei identifies significant germline variation and candidate genes that regulate liver triglyceride levels. *Genome Biol*, 10, R112.
- SUDMANT, P. H., MALLICK, S., NELSON, B. J., HORMOZDIARI, F., KRUMM, N., HUDDLESTON, J., COE, B. P., BAKER, C., NORDENFELT, S. & BAMSHAD, M. 2015. Global diversity, population stratification, and selection of human copy-number variation. *Science*, 349, aab3761.
- SZAMECZ, B., BOROSS, G., KALAPIS, D., KOVÁCS, K., FEKETE, G., FARKAS, Z., LÁZÁR, V., HRTYAN, M., KEMMEREN, P. & KOERKAMP, M. J. G. 2014. The genomic landscape of compensatory evolution. *PLoS biology*, 12, e1001935.
- SZENT-GYORGYI, A., HEGYELI, A. & MCLAUGHLIN, J. A. 1963. Cancer therapy: a possible new approach. *Science*, 140, 1391-1392.
- TAKAHASHI, K. 1977. Further studies on the reactions of phenylglyoxal and related reagents with proteins. *Journal of biochemistry*, 81, 403-414.
- TAKAHASHI, N., BROOKS, H. L., WADE, J. B., LIU, W., KONDO, Y., ITO, S., KNEPPER, M. A. & SMITHIES, O. 2002. Posttranscriptional compensation for heterozygous disruption of the kidney-specific NaK2Cl cotransporter gene. *Journal of the American Society of Nephrology*, 13, 604-610.
- TALASNIEMI, J. P., PENNANEN, S., SAVOLAINEN, H., NISKANEN, L. & LIESIVUORI, J. 2008. Analytical investigation: assay of D-lactate in diabetic plasma and urine. *Clinical biochemistry*, 41, 1099-1103.
- TANG, Y.-C. & AMON, A. 2013. Gene copy-number alterations: a cost-benefit analysis. *Cell*, 152, 394-405.
- TANG, Y.-C., WILLIAMS, B. R., SIEGEL, J. J. & AMON, A. 2011. Identification of aneuploidy-selective antiproliferation compounds. *Cell*, 144, 499-512.

- TATE, S. S. 1975. Interaction of γ -glutamyl transpeptidase with S-acyl derivatives of glutathione. *FEBS Lett.*, 54, 319-322.
- TENG, X., DAYHOFF-BRANNIGAN, M., CHENG, W.-C., GILBERT, C. E., SING, C. N., DINY, N. L., WHEELAN, S. J., DUNHAM, M. J., BOEKE, J. D. & PINEDA, F. J. 2013. Genome-wide consequences of deleting any single gene. *Molecular cell*, 52, 485-494.
- THORNALLEY, P. 1994. Methylglyoxal, glyoxalases and the development of diabetic complications. *Amino acids*, 6, 15-23.
- THORNALLEY, P. 1999. The clinical significance of glycation. *Clinical laboratory*, 45, 263-273.
- THORNALLEY, P. 2008. Protein and nucleotide damage by glyoxal and methylglyoxal in physiological systems--role in ageing and disease. *Drug Metabol Drug Interact*, 23, 125-50.
- THORNALLEY, P., BATTAH, S., AHMED, N., KARACHALIAS, N., AGALOU, S., BABAEI-JADIDI, R. & DAWNAY, A. 2003a. Quantitative screening of advanced glycation endproducts in cellular and extracellular proteins by tandem mass spectrometry. *Biochem. J*, 375, 581-592.
- THORNALLEY, P. & TISDALE, M. 1988. Inhibition of proliferation of human promyelocytic leukaemia HL60 cells by SD-lactoylglutathione in vitro. *Leukemia research*, 12, 897.
- THORNALLEY, P. J. 1988. Modification of the glyoxalase system in human red blood cells by glucose in vitro. *Biochem. J*, 254, 751-755.
- THORNALLEY, P. J. 1991. Population genetics of human glyoxalases. *Heredity*, 67, 139-42.
- THORNALLEY, P. J. 1993. The glyoxalase system in health and disease. *Molecular aspects of medicine*, 14, 287-371.
- THORNALLEY, P. J. 1998. Glutathione-dependent detoxification of α -oxoaldehydes by the glyoxalase system: involvement in disease mechanisms and antiproliferative activity of glyoxalase I inhibitors. *Chemico-biological interactions*, 111, 137-151.
- THORNALLEY, P. J. 2003a. The enzymatic defence against glycation in health, disease and therapeutics: a symposium to examine the concept. *Biochemical Society Transactions*, 31, 1341-1342.
- THORNALLEY, P. J. 2003b. Glyoxalase I--structure, function and a critical role in the enzymatic defence against glycation. *Biochem Soc Trans*, 31, 1343-8.
- THORNALLEY, P. J. 2005a. Dicarbonyl intermediates in the maillard reaction. *Ann N Y Acad Sci*, 1043, 111-7.
- THORNALLEY, P. J. 2005b. Measurement of protein glycation, glycated peptides, and glycation free adducts. *Peritoneal Dialysis International*, 25, 522-533.
- THORNALLEY, P. J. 2006. Unease on the role of glyoxalase 1 in high-anxiety-related behaviour. *Trends in molecular medicine*, 12, 195-199.
- THORNALLEY, P. J., BATTAH, S., AHMED, N., KARACHALIAS, N., AGALOU, S., BABAEI-JADIDI, R. & DAWNAY, A. 2003b. Quantitative screening of advanced glycation endproducts in cellular and extracellular proteins by tandem mass spectrometry. *Biochem J*, 375, 581-92.
- THORNALLEY, P. J., EDWARDS, L. G., KANG, Y. B., WYATT, C., DAVIES, N., LADAN, M. J. & DOUBLE, J. 1996. Antitumour activity of S-p-bromobenzylglutathione cyclopentyl diester in vitro and in vivo. Inhibition of glyoxalase I and induction of apoptosis. *Biochemical Pharmacology*, 51, 1365-1372.

- THORNALLEY, P. J., HOOPER, N. I., JENNINGS, P. E., FLORKOWSKI, C. M., JONES, A. F., LUNEC, J. & BARNETT, A. H. 1989. The human red blood cell glyoxalase system in diabetes mellitus. *Diabetes Res Clin Pract*, 7, 115-20.
- THORNALLEY, P. J. & RABBANI, N. Glyoxalase in tumourigenesis and multidrug resistance. *Seminars in cell & developmental biology*, 2011. Elsevier, 318-325.
- THORNALLEY, P. J. & RABBANI, N. 2014. Assay of methylglyoxal and glyoxal and control of peroxidase interference. *Biochem. Soc. Trans*, 42, 504-510.
- THORNALLEY, P. J., WARIS, S., FLEMING, T., SANTARIUS, T., LARKIN, S. J., WINKLHOFER-ROOB, B. M., STRATTON, M. R. & RABBANI, N. 2010. Imidazopurinones are markers of physiological genomic damage linked to DNA instability and glyoxalase 1-associated tumour multidrug resistance. *Nucleic Acids Res*. 38(16): 5432-5442
- THORNALLEY, P. J., YUREK-GEORGE, A. & ARGIROV, O. K. 2000. Kinetics and mechanism of the reaction of aminoguanidine with the α -oxoaldehydes glyoxal, methylglyoxal, and 3-deoxyglucosone under physiological conditions. *Biochemical pharmacology*, 60, 55-65.
- TIKELLIS, C., PICKERING, R. J., TSOROTES, D., HUET, O., COOPER, M. E., JANDELEIT-DAHM, K. & THOMAS, M. C. 2014. Dicarbonyl stress in the absence of hyperglycemia increases endothelial inflammation and atherogenesis similar to that observed in diabetes. *Diabetes*, DB_130932.
- TORRES, E. M., WILLIAMS, B. R. & AMON, A. 2008. Aneuploidy: cells losing their balance. *Genetics*, 179, 737-746.
- TRIPODIS, N., MASON, R., HUMPHRAY, S. J., DAVIES, A. F., HERBERG, J. A., TROWSDALE, J., NIZETIC, D., SENGER, G. & RAGOSSIS, J. 1998. Physical map of human 6p21. 2–6p21. 3: Region flanking the centromeric end of the major histocompatibility complex. *Genome research*, 8, 631-643.
- TYM A, J. T., ROSSMEISL M, KOPECKY J, SQUIRES P, RABBANI N, THORNALLEY PJ 2014. Increased pancreatic methylglyoxal in insulin resistance and beta cell detachment from the extracellular matrix. *Diabetes*, 63, A553-A554.
- UOTILA, L. 1973. Purification and characterization of S-2-hydroxyacylglutathione hydrolase (glyoxalase II) from human liver. *Biochemistry*, 12, 3944-3951.
- UPENDER, M. B., HABERMANN, J. K., MCSHANE, L. M., KORN, E. L., BARRETT, J. C., DIFILIPPANTONIO, M. J. & RIED, T. 2004. Chromosome transfer induced aneuploidy results in complex dysregulation of the cellular transcriptome in immortalized and cancer cells. *Cancer research*, 64, 6941-6949.
- VELAGALETI, G. V., BIEN-WILLNER, G. A., NORTHUP, J. K., LOCKHART, L. H., HAWKINS, J. C., JALAL, S. M., WITHERS, M., LUPSKI, J. R. & STANKIEWICZ, P. 2005. Position effects due to chromosome breakpoints that map ~ 900 kb upstream and ~ 1.3 Mb downstream of SOX9 in two patients with campomelic dysplasia. *The American Journal of Human Genetics*, 76, 652-662.
- VINCE, R. & WADD, W. B. 1969. Glyoxalase inhibitors as potential anticancer agents. *Biochemical and biophysical research communications*, 35, 593-598.
- VISHWANATH, V., FRANK, K. E., ELMETS, C. A., DAUCHOT, P. J. & MONNIER, V. M. 1986. Glycation of skin collagen in type I diabetes mellitus: correlation with long-term complications. *Diabetes*, 35, 916-921.

- VULESEVIC, B., MCNEILL, B., GEOFFRION, M., KURAITIS, D., MCBANE, J. E., LOCHHEAD, M., VANDERHYDEN, B. C., KORBUTT, G. S., MILNE, R. W. & SUURONEN, E. J. 2014. Glyoxalase-1 overexpression in bone marrow cells reverses defective neovascularization in STZ-induced diabetic mice. *Cardiovascular research*, 101, 306-316.
- WANG, J., ALEXANDER, P. & MCKNIGHT, S. 2011. Metabolic specialization of mouse embryonic stem cells. *Cold Spring Harbor symposia on quantitative biology, Cold Spring Harbor Laboratory Press*, 183-193.
- WANG, J., ALEXANDER, P., WU, L., HAMMER, R., CLEAVER, O. & MCKNIGHT, S. L. 2009. Dependence of mouse embryonic stem cells on threonine catabolism. *Science*, 325, 435-439.
- WANG, J., BAN, M. R. & HEGELE, R. A. 2005. Multiplex ligation-dependent probe amplification of LDLR enhances molecular diagnosis of familial hypercholesterolemia. *Journal of lipid research*, 46, 366-372.
- WEISS, L. A., SHEN, Y., KORN, J. M., ARKING, D. E., MILLER, D. T., FOSSDAL, R., SAEMUNDSEN, E., STEFANSSON, H., FERREIRA, M. A. & GREEN, T. 2008. Association between microdeletion and microduplication at 16p11. 2 and autism. *New England Journal of Medicine*, 358, 667-675.
- WILLIAMS, R., LIM, J. E., HARR, B., WING, C., WALTERS, R., DISTLER, M. G., TESCHKE, M., WU, C., WILTSHIRE, T., SU, A. I., SOKOLOFF, G., TARANTINO, L. M., BOREVITZ, J. O. & PALMER, A. A. 2009. A common and unstable copy number variant is associated with differences in Glo1 expression and anxiety-like behavior. *PLoS One*, 4, e4649.
- WILLIAMS, R. L., HILTON, D. J., PEASE, S., WILLSON, T. A., STEWART, C. L., GEARING, D. P., WAGNER, E. F., METCALF, D., NICOLA, N. A. & GOUGH, N. M. 1988. Myeloid leukaemia inhibitory factor maintains the developmental potential of embryonic stem cells. *Nature*, 336, 684-687.
- WILSON, A., ELSTON, R., TRAN, L. & SIERVOGEL, R. 1991. Use of the robust sib-pair method to screen for single-locus, multiple-locus, and pleiotropic effects: application to traits related to hypertension. *American journal of human genetics*, 48, 862.
- WOLMAN, S. R., GUNDAKER, H., APPELBAUM, F. R. & SLOVAK, M. L. 2002. Impact of trisomy 8 (+ 8) on clinical presentation, treatment response, and survival in acute myeloid leukemia: a Southwest Oncology Group study. *Blood*, 100, 29-35.
- WONG, K. K., DELEEuw, R. J., DOSANJH, N. S., KIMM, L. R., CHENG, Z., HORSMAN, D. E., MACAULAY, C., NG, R. T., BROWN, C. J. & EICHLER, E. E. 2007. A comprehensive analysis of common copy-number variations in the human genome. *The American Journal of Human Genetics*, 80, 91-104.
- WU, V.-Y. & STEWARD, L. A. 1991. Purification of glycated hemoglobin free of hemoglobin A1c and its use to produce monoclonal antibodies specific for deoxyfructosylsine residues in glycohemoglobin. *Biochemical and biophysical research communications*, 176, 207-212.
- XUE, M., RABBANI, N., MOMIJI, H., IMBASI, P., ANWAR, M. M., KITTERINGHAM, N., PARK, B. K., SOUMA, T., MORIGUCHI, T., YAMAMOTO, M. & THORNALLEY, P. J. 2012. Transcriptional control of glyoxalase 1 by Nrf2 provides a stress-responsive defence against dicarbonyl glycation. *Biochem J*, 443, 213-22.

- XUE, M., RABBANI, N. & THORNALLEY, P. J. 2011. Glyoxalase in ageing. *Seminars in cell & developmental biology, Elsevier*, 293-301.
- XUE, M., RABBANI, N. & THORNALLEY, P. J. 2014. Measurement of glyoxalase gene expression. *Biochemical Society Transactions*, 42.
- YAMAMOTO, Y., TAHARA, Y., CHA, T., NOMA, Y., FUKUDA, M., YAMATO, E., YONEDA, H., HASHIMOTO, F., OHBOSHI, C. & HIROTA, M. 1989. Radioimmunoassay of glycated serum protein using monoclonal antibody to glucitolysine and coomassie-brilliant-blue-coated polystyrene beads. *Diabetes research (Edinburgh, Scotland)*, 11, 45.
- YAMAZOYE, S. 1936. Glyoxalase and its co-enzyme. The Mechanism of the Action of Glutathione as the Co-Enzyme of Glyoxalase. *Journal of Biochemistry*, 23, 319-334.
- YAN, J., BI, W. & LUPSKI, J. R. 2007. Penetrance of craniofacial anomalies in mouse models of Smith-Magenis syndrome is modified by genomic sequence surrounding Rai1: not all null alleles are alike. *The American Journal of Human Genetics*, 80, 518-525.
- YANG, E., VAN NIMWEGEN, E., ZAVOLAN, M., RAJEWSKY, N., SCHROEDER, M., MAGNASCO, M. & DARNELL, J. E. 2003. Decay rates of human mRNAs: correlation with functional characteristics and sequence attributes. *Genome research*, 13, 1863-1872.
- YANG, Y., CHUNG, E. K., WU, Y. L., SAVELLI, S. L., NAGARAJA, H. N., ZHOU, B., HEBERT, M., JONES, K. N., SHU, Y. & KITZMILLER, K. 2007. Gene copy-number variation and associated polymorphisms of complement component C4 in human systemic lupus erythematosus (SLE): low copy number is a risk factor for and high copy number is a protective factor against SLE susceptibility in European Americans. *The American Journal of Human Genetics*, 80, 1037-1054.
- YANG, Y. X., CHEN, Z. C., ZHANG, G. Y., YI, H. & XIAO, Z. Q. 2008. A subcellular proteomic investigation into vincristine-resistant gastric cancer cell line. *Journal of cellular biochemistry*, 104, 1010-1021.
- YAO, D. & BROWNLEE, M. 2010. Hyperglycemia-induced reactive oxygen species increase expression of the receptor for advanced glycation end products (RAGE) and RAGE ligands. *Diabetes*, 59, 249-255.
- YOUNG, T. W., MEI, F. C., YANG, G., THOMPSON-LANZA, J. A., LIU, J. & CHENG, X. 2004. Activation of antioxidant pathways in ras-mediated oncogenic transformation of human surface ovarian epithelial cells revealed by functional proteomics and mass spectrometry. *Cancer research*, 64, 4577-4584.
- ZAIN, S. M., MOHAMED, Z., PIRMOHAMED, M., TAN, H. L., ALSHAWSH, M. A., MAHADEVA, S., CHAN, W.-K., MUSTAPHA, N. R. N. & MOHAMED, R. 2015. Copy number variation in exportin-4 (XPO4) gene and its association with histological severity of non-alcoholic fatty liver disease. *Scientific reports*, 5.
- ZARREI, M., MACDONALD, J. R., MERICCO, D. & SCHERER, S. W. 2015. A copy number variation map of the human genome. *Nature Reviews Genetics*, 16, 172-183.
- ZENDER, L., XUE, W., ZUBER, J., SEMIGHINI, C. P., KRASNITZ, A., MA, B., ZENDER, P., KUBICKA, S., LUK, J. M. & SCHIRMACHER, P. 2008. An oncogenomics-based in vivo RNAi screen identifies tumor suppressors in liver cancer. *Cell*, 135, 852-864.

- ZENG, S., ZHANG, Q. Y., HUANG, J., VEDANTHAM, S., ROSARIO, R., ANANTHAKRISHNAN, R., YAN, S. F., RAMASAMY, R., DEMATTEO, R. P. & EMOND, J. C. 2012. Opposing roles of RAGE and Myd88 signaling in extensive liver resection. *The FASEB Journal*, 26, 882-893.
- ZHANG, F., KHAJAVI, M., CONNOLLY, A. M., TOWNE, C. F., BATISH, S. D. & LUPSKI, J. R. 2009. The DNA replication FoSTeS/MMBIR mechanism can generate genomic, genic and exonic complex rearrangements in humans. *Nature genetics*, 41, 849-853.
- ZHANG, H., LI, H., XI, H. S. & LI, S. 2012. HIF1 α is required for survival maintenance of chronic myeloid leukemia stem cells. *Blood*, 119, 2595-2607.
- ZHOU, W., CHOI, M., MARGINEANTU, D., MARGARETHA, L., HESSON, J., CAVANAUGH, C., BLAU, C. A., HORWITZ, M. S., HOCKENBERY, D. & WARE, C. 2012. HIF1 α induced switch from bivalent to exclusively glycolytic metabolism during ESC-to-EpiSC/hESC transition. *The EMBO journal*, 31, 2103-2116.

Appendix

Appendix A: Primers sequences

Primer	Sequence (Sense, Antisense)
Glo1 Pair1	5'-TTGCTTGCTTGGCTTTGCCATTGC-3' 5'-GGACCACCACCTGAATGAGTCTTGC-3'
Glo1 Pair2	5'-TTGCTTGCTTGGCTTTGCCATTGC-3' 5'-TAAACCCTCTTGCAGTTGCATC-3'
Glo1 Pair3	5'-AAATGGCGTTACTTAAGCTAGCTTGC-3' 5'-GGACCACCACCTGAATGAGTCTTGC-3'
Rn 18s	Qiagen commercial stock (QT01036875)
C419A genotyping	5'-TCAGAGTGTGTGATTTTCGTG-3' 5'-CATGGTGAGATGGTAAGTGT-3'

Appendix B: Taqman Gene expression assay

Gene	Code of Taqman Gene expression assay
<i>Btbd9</i>	Mm00553921_m1
<i>Glo1</i>	Mm00844954_s1
<i>Dnah8</i>	Mm01299527_m1
<i>Glp1r</i>	Mm00445292_m1
<i>Vmn2r112</i>	Mm03647522_sH
<i>Actb</i>	Mm00607939_s1
<i>Rn18s</i>	Mm03928990_g1

Appendix C: TaqMan copy number assay

Gene	Code of Taqman copy number assay
Mouse <i>Glo1</i> (exon1)	Mm00470198_cn
Mouse <i>Glo1</i> (exon6)	Mm00470195_cn
Mouse <i>Btbd9</i>	Mm00460461_cn
Mouse <i>1700097N02Rik</i>	Mm00463219_cn
Mouse <i>Dnah8</i>	Mm00622696_cn
Mouse <i>Tert</i>	Catalogue number (4458368)
Mouse <i>Tfrc</i>	Catalogue number (4458366)
Human <i>GLO1</i>	Hs00127744_cn
Human <i>RNASE P</i>	Catalogue number (4403326)

List of presentations and publications derived from this project

Article

1. Shafie, A., Xue, M., Thornalley, P. J., & Rabbani, N. (2014). Copy number variation of glyoxalase 1. *Biochem. Soc. Trans*, 42, 500-503.
2. Shafie, A., Xue, M., Barker, G., Zehnder, D., Thornalley, P. J., & Rabbani, N. (2015). Metabolic stress-induced copy number alteration of glyoxalase 1. *The Scientific Reports*. Under review.

Oral presentation

Shafie, A., “Measurement of glyoxalase 1 copy number”. Glyoxalase Centennial: 100 Years of Glyoxalase Research and Emergence of Dicarbonyl Stress, 27-29 November 2013, University of Warwick, UK.

Posters

1. Shafie, A., Xue, M., Thornalley, P. J., & Rabbani, N. “Glo1 copy number increase in the Lexicon Glyoxalase 1 mutant mouse preserved the wild type phenotype”. 12th International Symposium on the Maillard Reaction, 8 – 11 September, 2015, Tokyo, Japan.
2. Shafie, A., Xue, M., Thornalley, P. J., & Rabbani, N. “Evaluation of a glyoxalase 1 mutant mouse”. The Eighth Saudi Students Conference, 31 January – 1 February, 2015, Imperial College London, UK.
3. Shafie, A., Xue, M., Thornalley, P. J., & Rabbani, N. “Evaluation of a glyoxalase 1 mutant mouse”. 50th European Association of the Study of Diabetes Annual Meeting, 15-19 September 2014, Vienna, Austria.
4. Shafie, A., Xue, M., Thornalley, P. J., & Rabbani, N. “Genotypic and phenotypic characterisation of a glyoxalase 1 mutant mouse”. The Seventh Saudi Scientific International Conference, 1-2 February, 2014, Edinburgh International Conference Centre, Edinburgh, UK.
5. Shafie, A., Xue, M., Thornalley, P. J., & Rabbani, N. “Difficulties in generating a Glo1 mutant mouse”. Glyoxalase Centennial : 100 Years of Glyoxalase Research and Emergence of Dicarbonyl Stress, 27-29 November 2013, University of Warwick, UK.

6. Shafie, A., Xue, M., Thornalley, P. J., & Rabbani, N. “Genotypic and phenotypic characterisation of a glyoxalase 1 mutant mouse”. The Sixth Saudi Scientific International Conference, 11-14 October 2012, Brunel University, UK.
7. Shafie, A., Xue, M., Thornalley, P. J., & Rabbani, N. “Genotypic and phenotypic characterisation of a glyoxalase 1 mutant mouse”. 11th International Symposium on the Maillard Reaction, 16 – 20 September, 2012, Nancy, France.

Award

Excellent poster award “Shafie, A., Xue, M., Thornalley, P. J., & Rabbani, N. Glo1 copy number increase in the Lexicon Glyoxalase 1 mutant mouse preserved the wild type phenotype”. 12th International Symposium on the Maillard Reaction, 8 – 11 September, 2015, Tokyo, Japan.

Excellent poster award certificate

*12th International Symposium
on the Maillard Reaction*

Presents this

Certificate of Congratulations

to

Alaa Shafie

For receipt of a

The excellent poster Award

in Tokyo, 2015

September 4th, 2015,

Teruo Miyazawa
Teruo Miyazawa, Ph.D
Chair, Organizing committee of 12th ISMR
IMARS President




Permission to reuse Figure 1.9

Do Not Reply Directly to This Email

To ensure that you continue to receive our emails,
please add rightslink@marketing.copyright.com to your address book.

RightsLink



Thank You For Your Order!

Dear Mr. Alaa Shafie,

Thank you for placing your order through Copyright Clearance Center's RightsLink service. Elsevier has partnered with RightsLink to license its content. This notice is a confirmation that your order was successful.

Your order details and publisher terms and conditions are available by clicking the link below:
<http://s100.copyright.com/CustomerAdmin/PLF.jsp?ref=a7aad0b3-19bc-48c1-88e9-ec90fdb6903b>

Order Details
Licensee: Alaa Shafie
License Date: Jun 30, 2015
License Number: 3658860265887
Publication: Structure
Title: Crystal structure of human glyoxalase II and its complex with a glutathione thiolester substrate analogue
Type Of Use: reuse in a thesis/dissertation
Total: 0.00 GBP


To access your account, please visit <https://myaccount.copyright.com>.

Please note: Online payments are charged immediately after order confirmation; invoices are issued daily and are payable immediately upon receipt.

To ensure that we are continuously improving our services, please take a moment to complete our [customer satisfaction survey](#).

B.1:v4.2

+1-855-239-3415 / Tel: +1-978-646-2777
customercare@copyright.com
<http://www.copyright.com>



This email was sent to: a.a-r.m.shafie@warwick.ac.uk

Please visit [Copyright Clearance Center](#) for more information.

This email was sent by Copyright Clearance Center
222 Rosewood Drive Danvers, MA 01923 USA